Regional Cerebral Blood Flow in Focal Epilepsy

Roderick Duncan, M.B., Ch.B., M.D., M.R.C.P.

A thesis submitted to the University of Glasgow in fulfillment of the requirements for the degree of Doctor of Philosophy

Department of Neurology, University of Glasgow
Wellcome Surgical Institute, University of Glasgow

August 1993.

ProQuest LLC.
789 East Eisenhower Parkway
P.O. Box 1346
Ann Arbor, MI 48106 – 1346

Acknowlegements

The author would like to thank the following for their help with this work:

The Department of Neurology, Institute of Neurological Sciences, for allowing a clinical Senior Registrar to take the time to carry this work out.

Professor PGE Kennedy for supervising, advising and supporting me during the work.

Professor J McCulloch for supervising this work, for the use of laboratory facilities at the Wellcome Surgical Institute, Garscube, and for the use of the SPECT imager at the Institute of Neurological Sciences.

The Department of Clinical Physics, Institute of Neurological Sciences, for help, advice and use of their facilities.

Dr M Macrae, Wellcome Surgical Institute, Garscube, for help and advice with the experimental work.

Dr Stig Hansen, Department of Clinical Physics, Institute of Neurological Sciences for computing and statistical help.

Dr R Roberts, Dundee Royal Infirmary, for carrying out correlative EEG studies.

Declaration

This thesis was composed by myself. The work it describes, including patient acquisition and selection, and gathering of clinical data, was carried out by myself, with the following necessary exceptions;

Mrs MT Hansen, Technician, Institute of Neurological Sciences, Glasgow carried out all SPECT acquisitions, and the injections for interictal scans. The majority of the injections for ictal and postictal SPECT scans were carried out by the residents and registrars on Neurology ward 62, Institute of Neurological Sciences, Glasgow (a minority were carried out by the author and by Mrs MT Hansen).

Dr J Patterson, Clinical Physicist, Institute of Neurological Sciences, Glasgow carried out independent visual interpretation of the SPECT images (the author being the other independent interpreter).

Dr IM Macrae, Lecturer, Wellcome Surgical Institute, Garscube Estate, Glasgow acted as second operator during the IAP procedures.

List of abbreviations used in this work

AHS - Ammon's horn sclerosis
AI - asymmetry index
CBF - cerebral blood flow
CMR - cerebral metabolic rate
CNS - central nervous system
CPS - complex partial seizures
CRGP - calcitonin gene-related peptide
CT - computerised tomography
EDRF - endothelium derived relaxation factor
EEG - electroencephalogram
FDG - fluorodeoxyglucose
FWHM - full width half maximum
HIDPM - N,N,N',-trimethyl-N'-(2-hydroxy-3-methyl-5-iodobenzyl)-1,3-propanediamine 2HCl
HMPAO - hexamethylpropyleneamine oxime
IAP - iodoantipyrine
IMP - N-isopropyl-p-iodoamphetamine
lCMR - local cerebral metabolic rate
lCMRGlc - local metabolic rate for glucose
lCMRO2 - local metabolic rate for oxygen
MTS - mesial temporal sclerosis
MRI - magnetic resonance imaging
OER - oxygen extraction ratio
PET - positron emission tomography
rCBF - regional cerebral blood flow
ROI - region of interest
SPECT - single photon emission computed tomography
VIP - vasoactive intestinal polypeptide

Table of contents

Page

Summary

The first systematic documentation of dynamic cerebral vascular changes associated with focal seizures was made by Penfield in the thirties. In recent years *in vivo* imaging techniques, principally single photon emission computed tomography (SPECT), have been used to study regional cerebral blood flow (rCBF) in patients with focal epilepsy. The main finding has been of focal hypoperfusion, the location in the brain differing according to the site of the focus. The incidence and clinical associations of this finding have varied, and few large studies have been carried out. Until the development of the blood flow tracer HMPAO (hexamethylpropyleneamine oxime) there was no practical way to study regional cerebral blood flow during or soon after seizures. When the present work was started no studies existed, although several have appeared during its course. Only complex partial seizures of temporal lobe origin have been systematically studied.

This work aims to define the incidence and clinical associations of interictal abnormalities of regional cerebral blood flow in patients with complex partial seizures, and to define the ictal and postictal patterns of regional rCBF seen in association with such seizures. The work is divided into three parts:

1. A study of interictal rCBF in patients with complex partial seizures;

HMPAO SPECT was used to determine rCBF in 92 patients suffering from complex partial seizures. rCBF was abnormal in 53% of the 81 patients with temporal lobe seizures, the abnormality most commonly taking the form of hypoperfusion of the temporal lobe. The principal clinical association of abnormal regional cerebral blood flow was early age at onset of epilepsy. The 11 patients with complex partial seizures originating outside the temporal lobe all had normal interictal regional cerebral blood flow.

2. A study of ictal and postictal regional cerebral blood flow in 42 of the above patients;

HMPAO SPECT was used to determine rCBF in 33 patients with complex partial seizures of temporal lobe origin. During the seizure, hyperperfusion of the whole temporal lobe was seen. Early in the postictal period, hyperperfusion of the hippocampus with lateral temporal hypoperfusion was seen, and in the late postictal period hypoperfusion of the whole temporal lobe was seen. Different patterns of rCBF were seen in the 9 patients with complex partial seizures originating elsewhere in the brain.

3. A study of regional cerebral blood flow, as determined both by the ^{14}C iodoantipyrine (IAP) and HMPAO methods, during focal motor seizures in the rat;

rCBF was determined during penicillin-induced focal motor seizures in 5 rats, and in 5 control animals, using a double label method which permitted the autoradiographic determination of IAP and HMPAO uptake at adjacent time points in the same animal. The two methods produced similar patterns of optic density on autoradiographs, with good correlation between optic densities obtained, at high as well as low flows. The data support the use of HMPAO as a blood flow tracer during seizures. The changes in regional cerebral blood flow seen were similar to changes seen in studies of local cerebral metabolic rate in the same model of epilepsy, and had obvious broad parallels with changes seen in humans.

It is concluded that in focal epilepsy a proportion of patients have focal hypoperfusion in the interictal period, the main association of which appears to be early onset of seizures. Peri-ictal changes have as their main features hyperperfusion at or around the focus, with more distant hypoperfusion, which becomes more prominent in the postictal period. These changes are in accord with early observations in humans, and with changes found in animal models of focal epilepsy.

Chapter 1

General Introduction

Epilepsy

Epilepsy is a common disease, with a prevalence of approximately 1:200 of the general population (Hauser & Kurland, 1975)). It comprises a group of disorders which have as their common pathophysiological theme an increase in cerebral neuronal excitability which leads to a tendency to recurrent paroxysmal discharges. These discharges are responsible for the common clinical theme of the epilepsies, the seizure.

Focal vs. generalised epilepsy

The epilepsies may be divided into generalised and focal disorders. Generalised epilepsies have as their basis a tendency to excitability throughout the grey matter of the brain. Most generalised epilepsies, such as juvenile myoclonic epilepsy, are thought to have a genetic basis (Delgado-Escueta & Greenberg, 1984; Noebels, 1984). Focal epilepsies have as their basis a tendency to excitability which is localised to one point or, more correctly, a specific volume of grey matter in the brain. This usually occurs in the grey matter at the margin of an area of tumor, or of scarring which results from a local injury of some kind, or in an area of cortical dysgenesis. The injury may be mechanical (head trauma), metabolic (local effects of hypoxia of ischaemia) or infective (meningitis, encephalitis)(Margerison & Corsellis, 1966; Corsellis & Meldrum, 1976; Robitaille et al., 1992).

Complex partial seizures

Focal seizures take a variety of forms, depending on the site of the focus and its anatomic connexions. The most common form of focal seizure in the adult human is the complex partial seizure, which is the main reason for it being chosen for study in this work. The clinical hallmark of the complex partial seizure is the absence (Baldy-Moulinier, 1990). This is characterised by an immobile stare, which typically lasts up to 1 minute. Temporal lobe absences may be accompanied by tonic posturing and

automatic movements, and may be preceded by an aura referrable to the area of origin of the seizure (e.g. deja vu feeling, hallucination of smell or taste). They are often followed by a period of confusion or somnolence, and sometimes headache. Frontal lobe absences are often brief, lasting a few seconds only, and may lack prodrome and postictal features. Onset and 'offset' are often abrupt. Automatisms tend to be more frenetic and bizarre than in temporal lobe seizures (Williamson et al., 1987). In both temporal and frontal epilepsies, secondary generalised seizures may also occur.

The majority of patients with complex partial seizures have foci in the temporal lobe, with a sizeable minority (10-15%) having foci in the frontal lobe (rarely complex partial seizures may originate in other areas) (Williamson et al., 1987).

The electrical and metabolic basis of focal seizures

The seizure is characterised by an electrical discharge. Recording from the surface, a typical series of electrical events may be seen (Baldy Moulinier, 1990; Binnie, 1990). They are illustrated in Figure 1.1. The initial event is usually a flattening of the trace, which may be preceded by a series of interictal-type spike-wave discharges. The flattening may last up to a few seconds, and is progressively replaced by a high frequency, low amplitude sinusoidal discharge (it may be that the flattening of the trace is simply due to the fact that the frequency of the discharge is at that point too high for the frequency sensitivity characteristics of current EEG technology). The discharge progressively augments in amplitude and, as it does so, diminishes in frequency. Clinically, this phase corresponds to the tonic (stiff) phase of the seizure (or to the stare phase of a complex partial seizure). This phase lasts from a few seconds to 1 minute or so. As frequency continues to diminish, the wave form becomes sharper, and spike or spike-wave activity supervenes. This corresponds to the clonic (jerking) phase of the seizure, and is variable in duration, lasting up to 1 minute typically. In the postictal period following this, there is a either slow wave activity or flattening of the trace, which gradually recovers to resting activity. This phase may be brief or absent, or may last many minutes. Clinically, the postictal period is characterised by drowsiness and/or variable levels of confusion.

Similar electrical changes may be seen during direct intracranial recordings (Figure 1.2). Direct intracranial recording removes problems of muscle artefact, better defines the topography of the discharge, and allows the detection of low-amplitude high frequency discharges which cannot be distinguished in surface recordings. The presently accepted relationship between macroscopic (surface or

depth) and cellular recordings was described using data from the penicillin model of epilepsy in the cat by Ayala et al. (1970), and is illustrated in Figure 1.3. The ictal discharge is manifested by a period of reduced membrane potential (paroxysmal depolarisation shift), during which there is a burst of action potentials (the macroscopic manifestation is the spike). Whereas the interictal spike discharge is followed by a period of hyperpolarisation (the macroscopic manifestation is the slow wave), the transition to an ictal discharge is attended by after-hypopolarisation of the membrane, resulting in repetitive and continuing action potentials (corresponding to the high-frequency discharge). As the seizure progresses, after-hyperpolarisation becomes progressively re-established, resulting in the action potentials becoming less continuous, again appearing in bursts. Macroscopically, this produces a reduction in the frequency of the discharge, and a change in morphology to spike-wave. Ayala et al. regarded the change from after-hyperpolarisation to after-hypopolarisation as important in the triggering of a seizure, and presented data to show that excitatory and inhibitory influences from other neurones were involved. This and other data (Sloviter, 1991) suggests that abnormal function of populations or networks of neurones, rather than single neurones is required for the triggering of seizures. Hence the concept of the 'epileptogenic zone', as opposed to the epileptic focus.

Intracranial EEG recording shows that ictal discharges may remain localised or may spread into other parts of the brain through normal neuronal pathways, disrupting normal function, and giving rise to abnormal function. As Jackson (1890) was the first to realise, the nature of the clinical manifestations of the seizure are therefore related to the site of origin of the discharge, and its anatomic connexions. All the electrical activity involved in the seizure requires energy, much of which goes to power the ion pumps which restore ionic gradients after depolarisation. This requires delivery of glucose and oxygen, as well as the removal of carbon dioxide and hydrogen ions, requiring in turn an increase in perfusion.

Clinical, electrical, metabolic and circulatory effects are all, therefore, intrinsic and essential components of the seizure.

The pathogenesis of focal epilepsy

In a simplistic way, one can understand the pathogenesis of focal epilepsy as a series of events and effects as depicted in Figure 1.4. A tissue abnormality gives rise to a change in neurotransmitter function. This causes the change in neuronal excitability, characterised by the 'paroxysmal depolarisation shift' (Ayala et al., 1970; Johnson & Brown, 1984 - see above), which in turn gives rise to the tendency for paroxysmal neuronal discharges, which causes the clinical manifestation known as

the seizure. The volume of tissue which gives rise to the seizure discharge is termed the 'epileptogenic zone'.

Seizures themselves may cause neuronal damage, probably by the 'excitotoxic' effects of excitatory neurotransmitters such as glutamate. This may apply either to the tissue around the primary focus, or to distant tissues. Where these tissues (e.g. the cerebellum (Duncan et al., 1990b)) are not potentially epileptogenic, then the effect is of loss of tissue and of function, which may manifest itself as cognitive impairment. Where damaged tissues are potentially epileptogenic (e.g. the hippocampus), the phenomenon of 'secondary epileptogenesis' may occur (McNamara, 1984).

The relevance of interictal and ictal regional cerebral blood flow (rCBF) to focal epilepsy

In the normal brain, rCBF is closely coupled to regional metabolic rate (see below). An alteration in rCBF therefore represents a change in the level of function of neurones in a given volume of brain, or a change in the number of neurones. The imaging of rCBF in the interictal state therefore provides a means by which localised functional alterations resulting from cell loss or other processes may be detected. The imaging of rCBF during seizures provides a means of showing the location and extent of ictal changes in the level of neuronal activity, whether reflecting primary involvement in the seizure discharge, secondary activation or inhibition.

The control of the cerebral circulation

Cerebral autoregulation

The term autoregulation refers to the intrinsic ability of an organ or a vascular bed to maintain a constant perfusion in the face of blood pressure changes. In the brain, autoregulation is effective over a wide range of arterial blood pressures. Under normal conditions cerebral perfusion is maintained constant between mean arterial pressures of 60 and 150mmHg (McHenry et al., 1974). Below the lower limit, vasodilatation continues although compensating increasingly inadequately for falling arterial pressure (MacKenzie et al., 1979a). Below the limit of autoregulation cerebral function is preserved to some extent by an increase in oxygen extraction from the blood. Above the upper limit of autoregulation, segmental forced dilatation of arterioles and blood-brain barrier damage occurs (Mackenzie et al., 1976; Skinhoj & Strandgaard, 1973).

Various mechanisms have been suggested to explain autoregulation. The myogenic hypothesis (Folkow, 1964) proposes that blood vessels constrict or dilate in response to changes in the transmural pressure gradient. Cerebral vascular smooth muscle and intact cerebral vessels do contract in response to increasing transmural pressure, but the mechanism of the effect is uncertain. It has been proposed that changes in intracellular membrane potential are involved (Harder & Lombard, 1985). There is also evidence that the vascular endothelium is involved; the constriction response of cerebral vessels to an increase in transluminal pressure has been observed to be abolished by disruption of the endothelium (Harder, 1984), while responses to direct stimulation by agonists such as 5HT are maintained. It has been suggested that there are endothelium-derived substances which relax and contract vascular smooth muscle (Furchgott et al., 1984; Rubanyi et al., 1986), and the endothelium serves as a transducer in the autoregulatory response to pressure.

The metabolic hypothesis proposes that metabolic changes in the cellular microenvironment resulting from neuronal energy metabolism give rise to autoregulatory vascular responses (Kuchinsky & Wahl, 1978). Many mediator molecules for a metabolic mechanism of autoregulation have been suggested, including CO_2, H^+, K^+, Ca^{2+} and adenosine (Kuchinsky, 1987). There is evidence against the involvement of some of these molecules, and it may be that an oxygen sensitive mechanism is also involved (Wei & Kontos, 1984). The coupling of cerebral metabolism and blood flow is further discussed below.

There is evidence that perivascular nerves play a role in autoregulation. Nerve fibres originating from the superior cervical ganglia and cranial ganglia such as the

sphenopalatine and otic ganglia provide sympathetic, parasympathetic and sensory innervations of the cerebral circulation (Edvinsson, 1975; Uddman & Edvinsson, 1989; Walters et al., 1986).

The sympathetic system has a small effect on resting blood flow, but has a marked effect on cerebral blood volume (via cerebral capacitance vessels (Edvinsson et al., 1971)), and stimulation shifts the limit of autoregulation upward (MacKenzie et al., 1979b). This is partly because its effect is predominantly on larger vessels (Harper et al., 1972), so constriction reduces the flow available to smaller vessels, which then have to use their vasodilatory capacity to compensate. Neuropeptide Y is colocalised with norepinephrine in sympathetic nerve endings in the CNS. It has a direct constrictor effect and potentiates the effect of exogenous norepinephrine and electrical stimulation (Edvinsson et al., 1987; Bevan, 1987).

Parasympathetic stimulation gives rise to an increase in cortical blood flow (Seylaz et al., 1988). Acetylcholine induced vasodilatation appears to result from activation of muscarinic receptors located on the endothelium of cerebral arteries, and the subsequent release of an endothelium-derived relaxing factor (Rosenblum, 1986). In some species, acetylcholine produces cerebral vasoconstriction, which appears to be mediated by prostanoids (Armstead et al., 1989a). Vasoactive intestinal polypeptide is associated with cholinergic systems (Hara et al., 1985) and produces vasodilatation via a prostanoid-dependent mechanism (Wei et al., 1980).

Sensory fibres from the trigeminal ganglion may also be involved in cerebral vascular reflexes (Goadsby & Duckworth, 1987), and there is evidence that dilation of cerebral blood vessels can result from activation of CNS neural pathways (Ishitsuka et al., 1984, see below): e.g. electrical stimulation of the fastigial nucleus of the cerebellum in the rat produces increases in cerebral blood flow unaccompanied by a rise in metabolic rate (Nakai et al., 1983)). These neurogenic systems act via vasoactive neurotransmitter substances such as vasoactive intestinal peptide (VIP), substance P, calcitonin gene-related peptide (CGRP) and others (Edvinsson et al, 1987; Edvinsson et al., 1980; Duckles & Said, 1982; Uddman & Edvinsson, 1989).

The endothelium contributes to the control of cerebral vessels by the realease of endothelium derived relaxant (EDRF) and contractile (EDCF) factors. EDRF is thought to be nitric oxide, or a nitric oxide-containing substance (Marshall & Kontos, 1990). Possible EDCF substances include prostanoids and a polypeptide substance called endothelin (Faraci, 1989). Endothelin causes vasoconstriction in the cerebral circulation, and decreases cerebral blood flow, an effect which is blocked by indomethacin suggesting that prostanoids mediate it (Sanchez-Ferrer & Marin, 1990; Armstead et al., 1989b).

The coupling of cerebral blood flow and cerebral metabolic rate

Barbiturate anaesthesia that produces EEG silence reduces oxidative catabolism of glucose in the brain to 40% of normal levels, and a further reduction to 20% reduction occurs with inhibition of Na^+K^+-ATPase. This suggests that up to 80% of the 20 Watts generated by the energy metabolism of the brain goes toward maintenance of ionic gradients (Edvinsson et al., 1993a), and that this is the proportion that will vary according to the level of neuronal activity. The brain derives its energy almost entirely from oxidative catabolism of glucose, so oxygen and glucose delivery by the cerebral circulation must be responsive to cerebral metabolic rate on a moment-to-moment basis.

Increased neuronal activity such as is seen during seizures is followed almost immediately by an increase in perfusion (see below). Roy & Sherrington (1890) originally postulated that some product of cerebral metabolism mediated vasodilatation in response to neuronal activity. It was originally thought that the effect was mediated directly by the CO_2 produced by oxidative metabolism of glucose (Sokoloff & Kety, 1960), but it now appears more likely that the effect is mediated through the resulting increase in hydrogen ion concentration and extracellular pH. (Edvinsson et al., 1993b). The effect may also be partly mediated through endothelium-derived factors such as nitric oxide (Wang et al., 1992).

Hypoxemia also causes cerebral vasodilatation and increases cerebral blood flow, but this mechanism only operates at low oxygen tensions (below 60mmHg)(Edvinsson et al., 1993b). There appears to be no influence on the response of the cerebral circulation to CO_2 of CNS or extrinsic neural influences (Skinhoj & Paulsson, 1969).

The extrinsic neural systems mentioned above under the heading of autoregulation may be involved in flow-metabolism coupling. Scopolamine, a cholinergic blocker with no direct vascular effect, can block rises in rCBF without affecting associated rises in metabolism (Pearce et al., 1981) and acetylcholine-induced vasodilatation occurs independently of rises in metabolic rate (Seylaz et al., 1988). There is also evidence for the involvement of adrenergic, serotonergic, dopaminergic and other systems (Lou et al., 1987).

Intrinsic neural mechanisms may also be involved. In animal studies, electrical stimulation of some brain areas, notably the dorsal medullary reticular formation and the cerebellar fastigial nucleus, can produce increases in rCBF which are independent of metabolism (McKee et al., 1976; Iadecola et al., 1983; Nakai et al., 1983), producing local or global uncoupling. Such data have been taken to indicate that an intrinsic neural system exists that is capable of influencing flow independently of metabolism in some situations. The neural pathways through which such a mechanism

might operate are unknown (Lou et al., 1987).

During somatosensory stimulation in humans it has been noted that rCBF may rise out of proportion to the local rise in metabolic rate (Fox et al., 1986). Whether this represents uncoupling or a change in coupling parameters remains unknown. The slope of the relationship between blood flow and metabolism may change under certain experimental circumstances which have pathophysiological counterparts (e.g. metabolic acidosis, K+ deficiency (Kuchinsky, 1987)), and changes in the relationship, rather than true uncoupling may be occurring. There appears to be little experimental evidence for true uncoupling (Kuchinsky, 1987; Lou et al., 1987).

Studies of cerebral blood flow, cerebral perfusion and cerebral metabolic rate in epilepsy

Changes in cerebral blood flow (CBF) and metabolic rate (CMR) in epilepsy have been of interest from the point of view of their part in the pathophysiology of epilepsy, and in particular their possible involvement in the development of seizure-related neurological damage. In recent years tomographic imaging methods (single photon emission computed tomography (SPECT) and positron emission tomography (PET)) have allowed the development of the clinical use of focal abnormalities of regional cerebral blood flow (rCBF) and local cerebral metabolic rate (lCMR) to localise epileptic foci prior to surgical resection. Many of the studies described below result from this.

The present work is concerned with blood flow rather than metabolism. Nonetheless, the two parameters are closely related and in most situations show parallel changes. This introductory review of the literature therefore includes studies of cerebral metabolic rate and studies of the relationship between metabolic rate and blood flow.

Early observations and studies of cerebral blood flow and metabolism in epilepsy

Cooper showed in 1836 that convulsions could be produced by carotid ligation, and suggested an ischaemic mechanism for epilepsy, but Penfield (1933; 1937) was the first to make systematic study of the dynamic vascular changes associated with seizures themselves. He pioneered the use of resective surgery for focal epilepsy and used intraoperative stimulation of the cerebral cortex in the area of the focus to induce seizures. He was therefore able to make direct observations of changes in the pial blood vessels. Because intraoperative induction of seizures is no longer carried out, no such observations have been made for many years. Penfield's were detailed and well documented, to the extent that an account of ictal changes in cerebral blood flow which is inconsistent with them should probably be regarded with circumspection.

He described a total of 49 examples of seizures in conscious patients whose cerebral cortex was open to direct observation on the operating table. He noted vascular changes in most of these cases, and categorised his findings as follows:

1. Cessation of arterial pulsation during a fit.

The almost invariable observation was arrest of visible pulsation of pial arteries. This was widespread in general seizures and focal where seizures were focal. It started and ended with the seizure, but pulsation might recur during the seizure if the latter were prolonged.

2. Postconvulsive hyperemia.

This was seen in a minority of patients, but was striking when it occurred. After the attack the cerebral arteries became bright red and highly pulsatile. The veins took on an arterial hue, and Penfield cited a remarkable observation of this. The patient had been stimulated, producing a unilateral focal motor seizure:

"One minute later my assistant, Dr. Thomas Hoen, called my attention to a curious stripe in some of the larger veins. An amazing change had taken place. The central portion of the parietal lobe was redder than the rest of the brain. This zone was bounded by large veins.

Into the tributaries of these large veins was flowing arterial blood from this reddened zone, while into tributaries from the outlying brain was flowing dark venous blood. The result was that the outer half of each vein was dark blue and the inner half dark red, the two streams maintaining their separation as when a muddy tributary joins aclear river and fails to mix for a long distance. ..... In such cases it must be concluded that the blood is passing rapidly through a widely opened capillary bed or that the tissues are for the time being incapable of taking up oxygen"

3. Focal blanching of the pia.

This might appear during the seizure, but more usually afterward.

4. Post convulsive arterial spasm.

This occurred from 15-30 min following the seizure, and was sufficiently marked to occlude the artery. The spasm was markedly segmental, and tended to appear at the same time as pial blanching. He noted that this observation was less common in later operations, attributing this to the fact that smaller currents were used to induce seizures, inducing localised more often than generalised seizures.

6. Cyanosis of the brain.

This was usually observed during major seizures, and accompanied systemic cyanosis.

7. Increase in local cerebral blood flow near the site of the focus.

Changes in blood flow were detected by means of a thermocouple heated above body temperature and inserted into brain tissue. The degree of cooling of the thermocouple was related to the flow of blood through the surrounding tissue. Rises in local blood flow were seen soon after the onset of the seizure, the time apparently depending of the distance between the site of origin of the seizure and the thermocouple In one case the thermocouple was 6cm from the focus, and the rise in blood flow was seen 1min after seizure onset. The increase lasted 4min after return of consciousness, and even then settled to a higher than basal level.

Penfield originally thought that these vasomotor changes produced ischemia which in turn caused the seizures, but Gibbs et al (1934) showed that there was no fall in cerebral blood flow preceding seizures, showing in fact that it increased, ruling out ischemia as a cause, and Penfield (1937) accepted this. His conclusions were:

1. That during a seizure there was increased blood flow through the involved cerebral cortex. The area involved remained local even when the seizure became generalised.

2. That vasodilatation might continue after seizure activity had ceased. Post convulsive hyperemia was characterised by the appearance of oxygenated blood in the cortical veins.

3. Cyanosis and bulging of the brain were due to respiratory embarrassment, and had nothing to do with the epileptogenic mechanism.

Penfield et al. (1939) later studied local cerebral blood flow in Monkeys and humans in which seizures were induced by local cerebral stimulation. They used the heated thermocouple method used by Gibbs et al., inserting the thermocouple into brain tissue. They found increases in blood flow in the cortex contralateral to focal seizures, but not ipsilateral. Where generalised seizures were produced, the rise in blood flow occurred on both sides. They also found rises in blood flow in the basal ganglia, of greater magnitude than those in the cortex. Changes in subcortical white matter were small and sluggish. The cortical rises in blood flow, were detected 4-10s after the first convulsive movement, continuing for some time after the convulsions

had ceased. Thermocouples placed distant from the focus showed either no increase in blood flow or a preliminary decrease.

They concluded that their observations showed that changes in blood flow were due to local, not systemic, factors and were secondary to the sudden increase in neuronal discharge during a seizure. They observed in one attack that cessation of pulsation was coincident with the increase in blood flow, concluding from this that cessation of pulsation, whatever the cause, was not due to a decrease in flow.

These observations established the basic principles that seizures were associated with changes in cerebral blood flow, local in the case of focal seizures, and (probably) generalised in generalised seizures, that these changes were secondary to the seizures rather than causal. and that they were to a great extent independent of systemic circulatory changes (though Mosier et al. (1957), White et al (1961), and Plum et al (1968) later showed that a rise in systemic blood pressure was necessary for the large rises in cerebral blood flow seen in generalised seizures). It was thought that blood flow followed the metabolic demand of brain tissue. This was consistent with the observations of Jasper & Erikson (1941), who noted decreases in cortical pH of cats during seizures, with those of Schmidt et al (1945) who used the nitrous oxide method to show increases in blood flow and metabolism in monkeys during seizures, and with those of Plum et al (1968) and Posner et al (1969) who showed that cerebral oxygen consumption rose substantially during induced generalised seizures in monkeys, and that oxygen supply kept pace with demand. Early studies of interictal cerebral blood flow in patients with seizures showed conflicting results. Gibbs et al (1946) and Grant et al. (1947) failed to find any difference in total CBF between normal patients and patients with epilepsy. Kennedy et al (1958) did find lower cerebral blood flow in a group of 12 children with epilepsy. However, this was a heterogenous group which included children with mental retardation and other forms of cerebral injury who may have had extensive cerebral damage. One might therefore expect low blood flow in such patients, whether epileptic or not.

Recent studies of cerebral blood flow (CBF and rCBF) and metabolic rate (CMR and LCMR) in epilepsy

In the last two decades there has been considerable study of cerebral metabolism and blood flow in seizure disorders, both in man and in animals. In man, PET and SPECT have allowed imaging and determination of regional cerebral blood flow and local cerebral metabolic rate for glucose (ICMRGlc) or cerebral oxygen consumption (ICMRO2). Autoradiographic techniques using 14C iodoantipyrine and

14C deoxyglucose have allowed similar studies in animals. Two major factors have shaped the course of these studies. Firstly, there has until very recently been no practicable way to image changes in metabolism and blood flow during or soon after seizures in man, so that most studies to date are of humans in the interictal state. Secondly, the lack of a suitable animal model of chronic epilepsy has meant that animal work has been largely confined to the study of blood flow and metabolism during seizures.

Generalised epilepsy - interictal studies of CBF, rCBF, CMR and lCMR

Theodore et al. (1984; 1985) found normal local and overall cerebral regional glucose metabolism (lCMRGlc) in a total of 17 patients with primary generalised epilepsy, and Sakai et al. (1978) found normal rCBF in 9 patients. Touchon et al (1986), using the 133 Xenon technique, found normal rCBF in 14 patients with primary generalised epilepsy. Engel et al (1983;1985) found normal interictal lCMRGlc in 4 patients with true petit mal epilepsy.

In summary, rCBF and lCMRGlc are normal in the interictal state in primary generalised epilepsy.

Generalised epilepsy - ictal and postictal studies of CBF, rCBF, CMR and lCMR

The early studies mentioned above suggested that there was a generalised increase in CBF during generalised seizures, and it was assumed that the same held for brain metabolism. Further studies in man and in animals using the nitrous oxide method (Schmidt et al., 1945; Grant et al., 1947; Kety et al., 1948; Meyer et al., 1965; Plum et al., 1968; Posner et al., 1969;) confirmed this, and showed postictal depression of CBF. The degree of the ictal rise in CBF varied between 140-500%, but the study of Meldrum and Nilsson (1976) found a rise early in generalised seizures in rats of 900%, by measuring venous outflow, and using the 133Xe desaturation method. They found also that the rise became less as seizure activity continued, to less than 300% after 2 hours of seizure activity.

The limited number of PET studies available in humans have tended to confirm that these changes also occur in cerebral metabolism (Engel et al., 1982b; 1983; Engel, 1983; 1984). The long time frame of fluorodeoxyglucose (FDG) PET measurement (approximately 10minutes) means that these studies encompass a relatively short period of ictal activity followed by several minutes of postictal

depression. This probably explains some studies which have shown 'ictal' hypometabolism. Interestingly, studies of generalised absence seizures have shown a greater rise in ICMRGlc (200-350%) than for tonic clonic seizures, probably because there is no depression of metabolism postictally. One study (Brodersen et al., 1973) of patients undergoing electroconvulsive therapy, using the Xe133 carotid method showed increases in rCBF averaging 111% during seizures, but failed to show depression of flow postictally.

Autoradiographic studies in animals have shown increases in blood flow which are greatest in the hippocampus, thalamus and neocortex (Horton et al., 1980). Rises in metabolic rate have been greatest in the hippocampus and amygdala (Evans & Meldrum, 1984).

Blood flow rises within seconds of the onset of seizure activity (Meldrum & Nillsen, 1976), and the rise is greatest in the first 4 minutes of seizure activity (<900%).

In summary, blood flow and metabolism rise several fold in the early part of a seizure, the rise becoming less if the seizure is prolonged, in animals at least. Human studies have shown post ictal depression of blood flow and metabolism.

Focal epilepsy - interictal studies of ICMR

Regional brain metabolism has been studied using PET, largely with O^{15} or ^{18}FDG. The most common finding is focal hypometabolism in the temporal lobe that is the site of a focus, with some patients showing more widespread or bilateral hypometabolism (Kuhl et al., 1980; Engel et al., 1982a; c; d; 1990; Bernardi et al., 1983; Franck et al., 1986; Abou Khalil et al., 1987; Theodore et al, 1983; 1984; 1986c; d; 1988). There may be a tendency for left hypometabolism to be greater than right (Theodore et al., 1986).

The proportion of patients in whom an abnormality is found appears to be higher using FDG PET, than using SPECT to image rCBF, in most series approximately 80%, as compared to 50-80% (see below). The reason for this difference is not clear. Kuhl et al (1980) studied a group of patients using 18FDG to image LCMR and 13NH3 to image rCBF, and found similar results with both, and Franck et al (1986) found no variation in oxygen extraction ratio (OER) in hypometabolic zones in patients with focal epilepsy. By contrast, some PET studies Yamamoto et al., 1983; Leiderman et al., 1989) have found that rCBF studies are less sensitive. Stefan et al (1987) used HMPAO SPECT and FDG PET to image rCBF and ICMRGlc in a group of patients and found that PET detected areas of hypometabolism that SPECT did not, albeit that the SPECT system was of relatively low resolution. Hypometabolism found using PET appears to

persist on retesting (Kuhl et al., 1980). As might be expected, changes in the basal ganglia and thalamus appear to mirror those in the cortex (Sakai et al, 1978; Bernardi et al., 1983; Henry et al., 1990; Sperling et al., 1990).

The site of PET abnormalities correlates well with EEG localisation of the epileptic focus, although the extent of hypometabolism tends to be much greater than the epileptogenic area (Kuhl et al., 1980; Engel et al., 1982c; d; 1990; Theodore et al., 1984; Abou Khalil et al., 1987). It does not correlate with the amount of spike activity detected during the scan (Engel et al., 1982d; Theodore et al., 1983). PET hypometabolism correlates well with the presence of anatomical lesions on CT and MRI, (Engel et al., 1982a; Theodore et al., 1984; 1986c; d; 1988; Stefan et al., 1985; Latack et al., 1986), although one study (Sperling et al., 1986) noted the reverse, i.e. a tendency for for patients with normal MRI to have abnormal PET and vice versa. As with interictal hypoperfusion, the hypometabolic area tends to be much larger than the anatomical lesion itself. The same holds for the finding of pathological abnormalities (usually mesial temporal sclerosis) in surgically resected specimens; in most studies the finding of temporal hypometablism is a good predictor of the finding of a pathological abnormality (Engel et al., 1982a; Theodore et al., 1984). Theodore et al (1988) found that the length of history of epilepsy in a group of 20 patients correlated inversely with their mean LCMRGlc, but that there was no correlation with the age of the patient or the age at onset of epilepsy. Anticonvulsant drugs such as barbiturate and phenytoin tend to reduce LCMRGlc, as does carbamazepine to a lesser extent (Theodore et al., 1983; 1986a; b; 1987; 1988).

Focal epilepsy - interictal studies of rCBF

Initially, rCBF was studied using 133Xe, inhaled, injected intravenously or into the carotid artery, in conjunction with multidetector scintillation cameras. Over the last decade, the principal methods used to study rCBF have been the carotid intra-arterial and intravenous xenon methods, SPECT (using either rotating gamma cameras or dedicated head imagers, with xenon, IMP (Holman et al., 1984), HIPDM (Holman et al., 1984) or latterly HMPAO (Neirinckx et al., 1987) as tracers), and PET, using the oxygen inhalation or intravenous ammonia techniques. One study (Fish et al., 1987) used the XeCT method.

The xenon mutidetector method did give quantitative results, but suffered the drawbacks of low spatial resolution and poor repeatability. They were non tomographic, essentially measuring only cortical blood flow. Results were expressed as raw figures over a relatively few areas of interest, rather than generating images. Studies of complex partial epilepsy found areas of reduced flow (Lavy et al., 1976;

Touchon et al., 1983; Valmier et al., 1987; 1989), while one study mainly of patients with focal motor epilepsy (Hougaard et al., 1976), by contrast showed focal increases in blood flow. Two studies (Touchon et al., 1983; Valmier et al, 1987) using the Xe methods have found, as well as focal reductions in rCBF in the temporal lobe, either generalised reductions in rCBF or lesser areas of reduced flow distant from the focus. There was also a tendency for the reduction to be greater when it was on the left (Valmier et al., 1987). Valmier et al. (1989) also used the Xe IV technique to investigate the effect of photic stimulation on rCBF in patients with complex partial seizures. The patients had no evidence of photic responses on EEG but appeared to show increases in rCBF around the sites of foci on stimulation. The patterns seen were different in lesional as opposed to non-lesional cases. Whether the phenomenon was anything to do with epilepsy rather than simple activation is uncertain. Tomographic imaging has the advantages of greater resolution and visualisation of deep structures. SPECT has been most widely used. Although its resolution is rather poorer than PET and it produces images which cannot be quatitated absolutely, it is vastly cheaper and easier to perform.

SPECT, using 133Xe, 131I IMP, 131I HIPDM or Tc99m HMPAO as tracers has been carried out on a large number of patients with focal epilepsy, in most cases temporal lobe epilepsy. In the majority of cases the main finding is of focal hypoperfusion, usually involving all or most of the temporal lobe. The area of hypoperfusion may be larger than this, extending into the ipsilateral frontal lobe or involving the whole hemisphere, and may occasionally be bilateral. Abnormalities have been found in between approximately 50% and 80% of patients in most series (Uren et al., 1983; Bonte et al., 1983; Podreka et al., 1988; Ryding et al., 1988, Grasso et al., 1989; Duncan et al., 1990a; c; d; Stefan et al., 1987; 1990). The little published data available (Jibiki et al., 1990) suggest that focal interictal hypoperfusion is a stable finding, although one study did find perfusion deficits in some patients in whom SPECT was repeated after an initially normal scan (Shen et al., 1990).

Some series (Uren et al., 1983; Grasso et al., 1989; Stefan et al., 1990; Duncan et al., 1990a; c; d) have found a proportion (up to 30%) of patients who showed focal hyperperperfusion interictally, or a combination of hypoperfusion and hyperperfusion in different areas or even contralateral to each other. In one study (Duncan et al. 1990a), 10 patients showing interictal hyperperfusion, were rescanned at a later date and the finding was then present in only 5. It has been suggested that 'interictal' hyperperfusion is due to subclinical seizure activity, but many of the patients with this finding (Duncan et al., 1990a; c; d) have had HMPAO injection with concurrent EEG monitoring, and showed no sign of ongoing seizure activity, at surface electrodes at least. Occasionally such areas of hyperperfusion are

large, and it is difficult to believe that they represent areas of increased neuronal activity when both behaviour and EEG are normal. Interictal hypermetabolism appears to be a less frequent finding in PET studies (Engel et al., 1982d).

The correlation between abnormalities of rCBF and EEG has been variable. In general, studies showing a high proportion of patients with localising abnormalities (Biersack et al., 1986; Valmier et al., 1987; Podreka et al., 1988) tend to have a proportion of patients in whom SPECT localisation disagrees with EEG, while studies showing a low abnormality rate tend to have few disagreements (Rowe et al., 1989b; 1990; 1991a; b; Newton et al., 1992). This would appear to suggest that only hypoperfusion of unequivocal degree is reliably localising, and that areas of hypoperfusion of lesser degree represent variations of normal or are epiphenomena. Where CT or MRI have shown a lesion in a patient with abnormal rCBF, the site correlates well but the area of hypoperfusion is usually much larger than the lesion. This is also true for abnormalities found pathologically in resected surgical specimens (Stefan et al., 1987; Rowe et al., 1989b).

The correlation between abnormalities of rCBF and clinical factors has also been variable. Valmier et al (1987) found that decreases in in rCBF correlated significantly with seizure frequency, but not with age at onset or duration of disease. Duncan et al (1990c) found a significant relationship between age at onset of epilepsy and abnormal rCBF, finding that patients with early onset disease were much more likely to have abnormal rCBF. No relationship was found with severity of disease or patient age. One study of the effect of the initiation of carbamazepine therapy on rCBF (Valmier et al., 1990) showed an initial generalised increase which fell back to basal levels at 4 months.

Focal epilepsy - ictal and postictal studies in ICMR and rCBF

PET may be used to study brain metabolism or blood flow during seizures, but suffers from the disadvantage that the patient must be scanned while the seizure is taking place. Despite this, a few patients have been studied, and have shown hypermetabolic zones around the site of epileptic foci (Engel, 1983; Engel et al., 1983; Franck et al., 1986; Theodore et al., 1983; 1984), in 1 case extending to involve the whole ipsilateral hemisphere (Engel, 1983). Engel et al (1983) also found an area of hypometabolism surrounding the hypermetabolic area. A further problem with the use of FDG PET to study ictal metabolism is its relatively long temporal resolution, making the interpretation of these changes difficult when metabolism may be changing from moment to moment (Engel et al., 1983).

Franck et al. (1986) studied 5 patients during status epilepticus, 2 with

epilepsia partialis continua, and 2 with continuous lateralised epileptic discharges. All showed focal increases in metabolism corresponding to the area of the discharge, and including the basal ganglia and thalamus ipsilaterally. The oxygen extraction ratioincreased in these areas suggesting that the increase in perfusion was adequate for metabolic demand.

SPECT has been used more widely to study blood flow during and soon after seizures. Amine tracers such as HIDPM (N,N,N'-trimethyl-N'-(2-hydroxy-3-methyl-5-123I-iodobenzyl)-1,3-propanediamine 2 HCL) and IMP (123I-N-isopropyl-p-iodoamphetamine) were used initially (Holman et al., 1984), and more recently HMPAO (Neirinckx et al., 1987). These tracers are distributed in brain according to regional perfusion and are then trapped for a period. Their pattern of distribution in the brain, and that of the isotope with which they are labelled, remains constant no matter what changes in rCBF subsequently take place. The patient need not therefore be in the scanner when the seizure takes place. Using HIPDM SPECT, Lee et al (1986; 1987a; b; 1988) and Shen et al.(1990) showed inreases in rCBF in the temporal lobes of patients during complex partial and partial onset tonic-clonic seizures. They noted that increases in rCBF persisted postictally. HIPDM is distributed in brain over a relatively long time frame (up to 10 minutes (Holman et al., 1984)), while HMPAO is distributed rapidly following injection, and therefore gives good temporal resolution, in the order of a minute or less. This allows more confident interpretation of images where, as during or soon after a seizure, the pattern of rCBF may be changing rapidly. Although the evidence is built up from a series of 'spot' measurements in different patients, data which have been published while this work was in progress have suggested that there is a sequence of 3 patterns of alteration of rCBF during and after seizures of temporal lobe origin (Rowe et al., 1989b; 1990; 1991b; Newton et al., 1992). During the seizure, there is hyperperfusion of the whole temporal lobe. In the immediate postictal period (up to 2 minutes after the end of the seizure) there is persisting hyperperfusion of the mesial temporal cortex, with hypoperfusion of the lateral cortex. Up to 15 minutes after the end of the seizure there is hypoperfusion only, which again might be localised to the temporal lobe or more widespread.

Only two studies have been published including seizures originating in sites other than the temporal lobe (Stefan et al., 1990; Marks et al., 1992). Ictal scans in these studies showed hyperperfusion at the sites of extratemporal foci in a total of 15 patients.

Ictal studies of ICMR and rCBF in animal models of focal epilepsy

Ictal studies in animal models of focal epilepsy have largely been of metabolism using the deoxyglucose method, with the aim of delineating the structures through which seizure activity spreads. In the main, seizures originating in the motor cortex (induced in most cases by local penicillin injection) or in the amygdala or hippocampus (induced by kindling, electroshock, penicillin injection or kainic acid injection).

In the area of the penicillin focus in the motor cortex, there is a circumscribed area whose metabolic rate is increased 2-3 fold. The surrounding cortex, has normal or depressed metabolism. Depressed metabolism is also seen in cortical areas distant from the focus. Lesser degrees of increased metabolism are seen in columnar patches of the homotopic cortex (Collins, 1976). Increases in metabolism are also seen in homolateral and contralateral cingulate gyri, caudate and globus pallidus (Collins, 1978).

Where seizures are induced in the limbic area (medial entorrhinal cortex) increases in metabolism are seen in the dentate gyrus, Ammon's horn (with small increases contralaterally), ipsilateral amygdala and nucleus accumbens. During severe seizures the hippocamapal formations are activated bilaterally, as are amygdala, accumbens, substantia nigra (pars reticulata), anterior and periventricular thalamic nuclei, septal nuclei (Blackwood et al., 1981; Collins et al, 1983; Lothman et al., 1985), increases being from 30-180%, highest in limbic structures.

Coupling of blood flow and metabolism in epilepsy

The few studies of both blood flow and metabolism in patients with interictal hypometabolism suggest that the tissue is not ischaemic (Kuhl et al., 1980), and that reduced perfusion is probably due to reduced function. Early studies attempting to determine whether the brain became hypoxic during seizures (i.e. was the rise in blood flow adequate for metabolic demand) yielded conflicting results (Jasper & Erickson, 1941; Davis et al., 1944; Stone et al., 1945; Davies & Redmond, 1947; Gurdijan et al., 1947; Meyer et al., 1965), partly because of difficulty in eliminating the effects of systemic metabolism. Detailed work by Plum et al (1968) and Posner et al. (1969) showed that the increase in CBF during seizures was in excess of that required for adequate oxygenation of the brain as a whole. They also showed that the venous oxygen tension rose after generalised seizures, giving a counterpart in generalised seizures to Penfield's observations of saturated venous blood draining from

areas of brain involved in focal seizures, and showing that blood flow remained high after cessation of seizure activity. Neurological damage is known to occur during prolonged seizure activity, both in animal models and in humans (Norman, 1964; Corsellis & Meldrum, 1976). In animal studies the brain areas affected tend to be those which become hypermetabolic and hyperperfused. In animal studies, both neuronal hyperactivity, with concomitant increase in ICMRGlc and rCBF, and its persistence for 25-30 minutes appear to be necessary for the development of neuronal necrosis (Ingvar, 1986). (This may parallel the increased incidence of chronic temporal lobe epilepsy and its associated medial temporal sclerosis when childhood febrile convulsions are prolonged (Nelson & Ellenberg, 1976)). Although some studies in rats have shown local mismatches between perfusion and metabolism during seizures (Ingvar & Siesjo, 1983; Ingvar et al., 1984; Tanaka et al., 1990), differences in timing of the measurements of measure blood flow and metabolism, and the known tendency of the IAP method to underestimate high flows (see chapter 4 of this work), make the significance of this finding uncertain. PET studies using the ^{15}O steady state and bolus inhalation techniques in human status epilepticus suggest that blood flow is adequate for metabolic demand (Franck et al., 1986), although the resolution of in vivo imaging techniques may not be sufficient to show very localised changes.

Rationale for the present work

1. Interictal rCBF in focal epilepsy

The results of studies of rCBF in patients with complex partial seizures have varied considerably, in terms of the proportion of patients showing abnormalities, the types of abnormality shown, the correlation of these abnormalities with clinical factors and EEG localisation. Possible reasons for these variations include;

1. Relatively small (<40 patients) populations have been studied.
2. The populations studied have in general included only patients who are having frequent seizures, making correlation with other factors difficult.
3. Most studies have utilised imaging equipment of insufficient spatial resolution to distinguish important anatomical structures.
4. Reporting practices have varied, some groups using visual analysis only, some also using numerical analysis. Thresholds for reporting abnormalities are often not defined.

To try to resolve the differences between previous studies, a study with the following characteristics has been carried out;

1. The patient population (92) is larger than in previous studies
2. The patient population includes a wide range of clinical characterictics
3. High resolution imaging equipment is used
4. Both visual and numerical analysis of images are performed

2. Ictal and postictal rCBF in focal epilepsy

Seizures cannot be predicted, and measurement of rCBF during them is made very difficult by the acompanying behavioural alterations. The first practicable method for studying rCBF during or soon after seizures was therefore SPECT using iodine labelled amphetamine compounds. The compound could be injected at the time of the seizure. Its pattern of distribution remained after the initial uptake and scanning could therefore take place after the patient had recovered from the seizure. Several studies were carried out, but amphetamine compounds suffered from the problem that contamination of I^{131} with I^{133} increased the effective radiation dose and degraded images. In addition, uptake into brain tissue was over a period of minutes, blurring temporal resolution at a time when rapid changes are taking place. ^{99m}Tc labelled

HMPAO overcame all these problems, and the results of 3 studies have been published, suggesting a series of changes following complex partial seizures of temporal lobe origin. These changes have yet to be confirmed, and no helpful data have been presented regarding complex partial seizures of extratemporal origin.

A study of ictal and postictal rCBF has therefore been carried out of 42 patients with complex partial seizures, originating in the temporal lobe in 33 and in extratemporal sites in 9, to define patterns of change during and after complex partial seizures, and to determine whether CPS of extratemporal origin show different changes.

3. Validation of ^{99m}Tc labelled HMPAO as an indicator of rCBF in epilepsy.

It has been shown that the relationship between HMPAO uptake and rCBF is not linear. As flow becomes higher, the rate of increase in HMPAO uptake becomes less. This is because the changes from a lipophilic to a hydrophilic compound takes enough time for a degree of washout to occur after the first pass bolus has passed through brain tissue. This effect is clearly more marked at higher flow rates and theoretically, once flow has reached a certain level, the amount of HMPAO retained will start to decrease as flow rises further, rather than increase. The effect has been modelled mathematically and has been detected experimentally in normal rats, and in models of ischemia as a fall-off in the rate of increase of HMPAO uptake as flow rises. A correction factor has been derived by Lassen (Lassen et al., 1988) which linearises the relationship. During seizures, however, very high flows indeed may occur, in human and animal studies up to 5 times normal rates, and no validation of HMPAO has been carried out in this situation.

A study of rCBF in penicillin induced focal seizures in the rat has been carried out using ^{14}C labelled iodoantipyrine and ^{99m}Tc labelled HMPAO in a double-label technique, to see whether the relationship between rCBF and HMPAO uptake remains linear at the flow rates seen during seizures

Aims of the present work

This work includes studies of interictal, ictal and postictal changes in rCBF in a series of patients with complex partial seizures of both temporal and extratemporal origin. The aims of these studies are;

1. To define the changes in rCBF seen interictally, ictally and postictally in patients

with complex partial seizures of temporal lobe origin, and to determine how such patterns of change differ from those seen in patients with complex partial seizures of extratemporal origin.

2. To determine the clinical, EEG, imaging and pathological associations of rCBF changes.

3. To validate the radiotracer used in these studies using an animal model of epilepsy.

Illustrations

Figure 1.1.

Surface EEG recording of a temporal lobe seizure with bilateral surface manifestations. On channels 6 and 15 the initial flattening of the trace followed by the gradual appearance of a high frequency discharge can be most clearly seen.

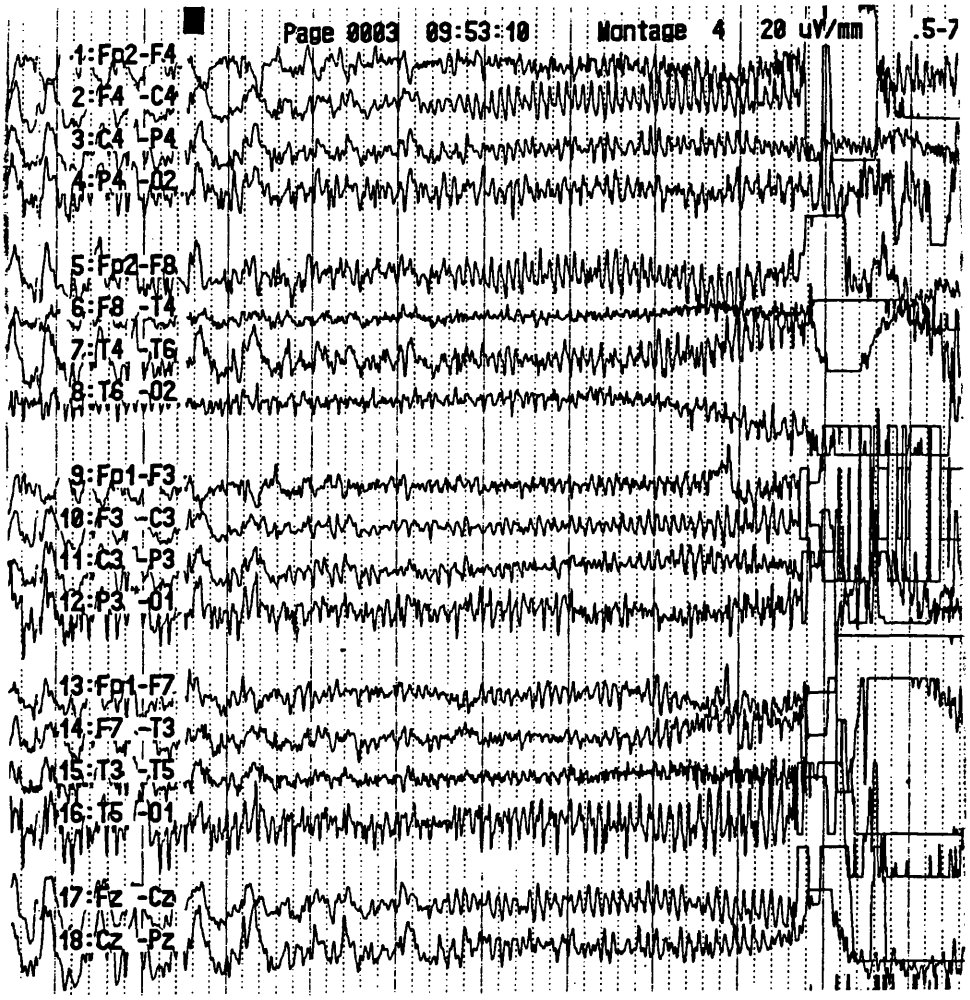

Figure 1.2

Intracranial EEG recording of a temporal lobe seizure. On the channel indicated (recording from the hippocampus) a flattening of the trace can be seen, followed by the progressive appearance of a high frequency discharge. The discharge is initially sinusiodal, but becomes progressively sharper in appearance as the frequency diminishes and the amplitude increases.

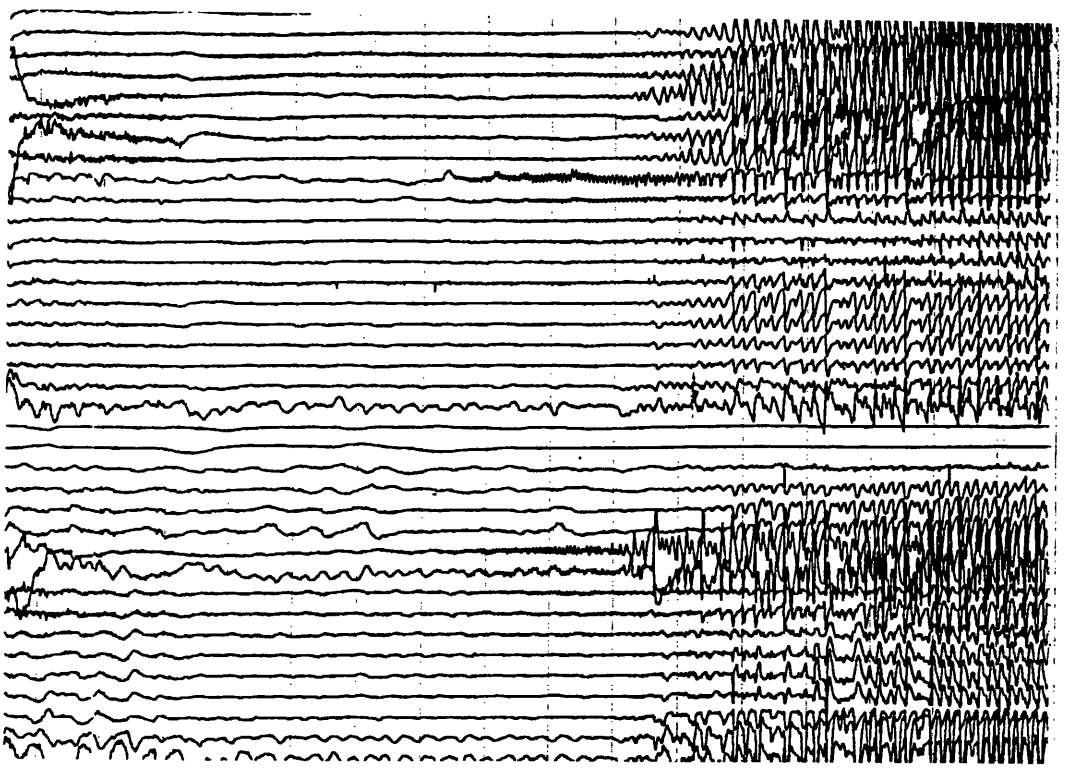

Figure 1.3

The relationship between potentials recorded on the cellular and macroscopic levels during interictal and ictal discharges (From Ayala et al., 1970).

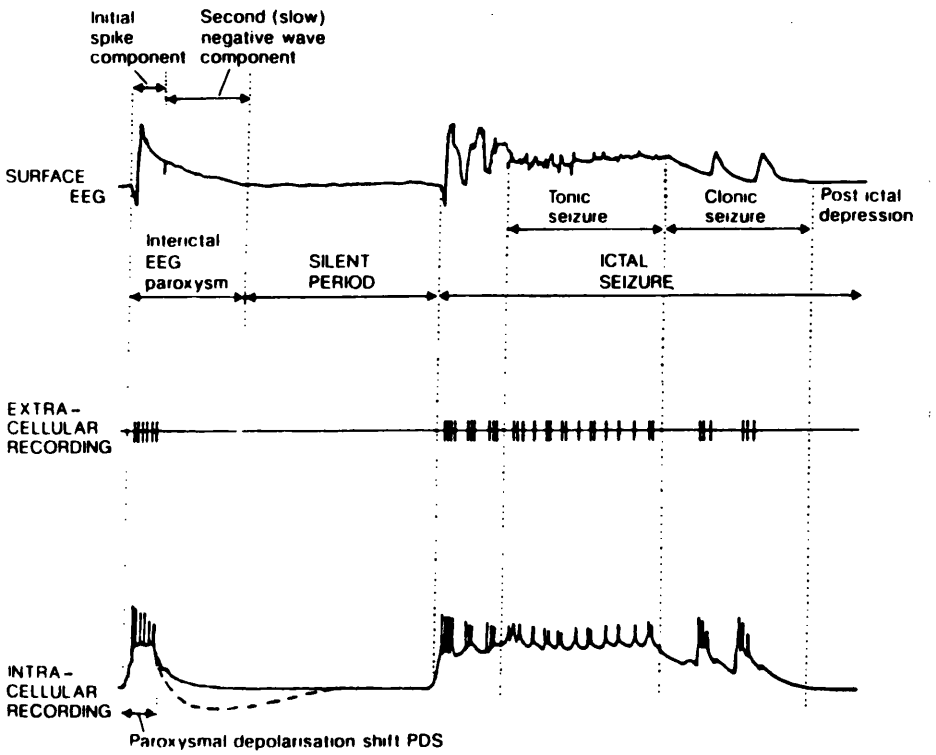

Figure 1.4

Schematic representation of the pathophysiology of focal epilepsy.

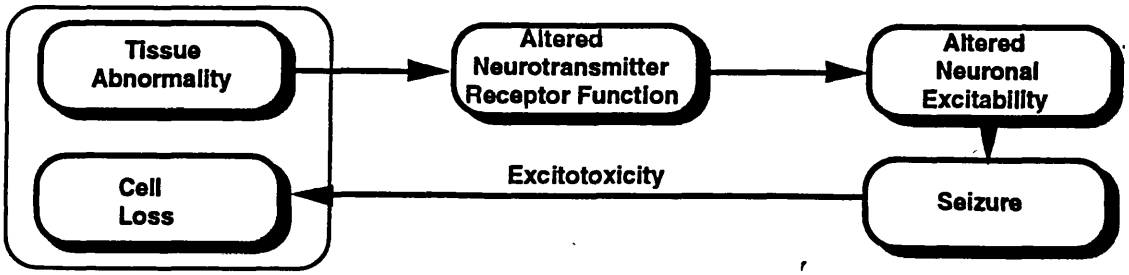

Chapter 2

Interictal regional cerebral blood flow in patients with complex partial seizures

Introduction

Previous studies of interictal rCBF in patients with focal epilepsy are described in the general introduction to this work. The majority of patients in these studies have had epilepsy of temporal lobe origin. With one exception these studies have individually been of relatively small numbers of patients, have been carried out using a variety of tracers and scanning methods, or have been carried out using equipment of relatively low spatial resolution. Most studies have included patients with intractable seizures, few including patients whose seizure control is good. Some have included patients with anatomic lesions.

The results of these studies have varied, in terms of the proportion of patients in whom abnormal rCBF is found, what abnormalities are seen, and how they correlate with clinical factors and the results of such investigations as EEG and structural imaging (CT and MRI). One can hypothesise that this is because the of heterogeneity of previous studies.

This study sets out to determine, in a population of 92 patients with complex partial seizures, without gross anatomical lesions, and with a full range of seizure control;

1. What proportion of patients have abnormal interictal rCBF.
2. What types of abnormality are found.
3. What clinical factors correlate with rCBF abnormalities

Subjects

The subjects were 92 (48 male, 44 female) patients with complex partial seizures ± secondary generalised seizures. They were divided into temporal and extratemporal groups according to their clinical features, and the results of MRI and interictal and ictal EEG recordings. All patients had CT, and 0.15T MRI with coronal T1 and T2 temporal lobe views. Patients with gross anatomic lesions were excluded from the study.

The clincal characteristics of individual patients are given in Table 2.1, with descriptive statistics of temporal and extratemporal groups in Table 2.2. The patients were gathered from 2 sources;

1. General neurology clinics.
2. A clinic for intractable epilepsy, including patients being worked up for surgical treatment.

Patients from the first source included a majority whose seizures were well controlled, while the patients from the second source all had unacceptably high seizure frequencies despite the best available medical therapy. Only patients in whom clinical localisation of the focus was supported at least by the results of multiple surface EEG recordings were included. In 48 patients surface ictal EEG recordings also supported the localisation (24 also had sphenoidal recordings, and 20 had foramen ovale recordings). In 23 patients localisation was supported by focal areas of signal change on MRI, including 9 patients who otherwise had only interictal EEG localisation.

1. Temporal group

All 81 patients in this group had clinical features in the aura, the seizures itself or in the postictal manifestations to suggest temporal lobe involvement (e.g. abdominal aura, duration of stare of >1minute, prominent postictal features such as automatisms, confusion, drowsiness), and epileptiform abnormalities on interictal EEG localised to one or both temporal areas. Ictal EEG recordings supported temporal lobe origin for for seizures in 39 patients, with sphenoidal recordings in 28 and foramen ovale recordings in 22. MRI supported interictal localisation in 21 patients. The clinical characteristics of the temporal group are given in Table 2.2

2. Extratemporal group

All 11 patients in this group had clinical features suggesting extratemporal origin for seizures; ten patients had short (<20s) absences with no prodrome and rapid recovery, suggestive of frontal origin. One of these patients also had atonic seizures. The remaining patient had complex partial seizures with a visual prodrome suggesting occipital origin. In 9 patients interictal localisation to one or other frontal lobe was supported by ictal EEG surface recordings. Frontal signal abnormalities were seen on MRI images in two patients. The patient with clinical ictal features suggestive of an occipital seizure source had ictal EEG recordings suggesting left occipital origin for her seizures. The clinical characteristics of the extratemporal group are given in Table 2.1, with descriptive statistics in Table 2.2.

Methods

SPECT method: HMPAO

HMPAO (hexamethylpropyleneamin oxime - Ceretec, Amersham International) is a lipophilic oxime (Neirinckx et al., 1987). It is injected intravenously. It is distributed throughout the pulmonary and systemic circulation, 4% of the intravenous dose of 500MBq eventually reaching the brain. Brain uptake is in the pattern of rCBF. After intravenous injection, 85% of brain uptake occurs in 30 seconds, the other 15% occurring substantially in the subsequent 30 seconds (Lassen et al., 1988; see Appendix, Fig. 4). Inside brain tissue, by a mechanism unknown, the molecule becomes hydrophilic, and cannot recross the blood brain barrier. It is therefore trapped in brain tissue in the distribution of rCBF at the time of the first pass through brain tissue after the injection. Because of the small fraction of HMPAO taken up into brain in the subsequent 30 seconds, a large change in rCBF during this time may be reflected in the final distribution of HMPAO. This final distribution remains relatively constant for 8h, and scanning can therefore be carried out during that time, although the 6h half life of Tc^{99m} means that the sooner the scan is carried out, the better the image.

The characteristics of this compound and previous work relating to it are further discussed in Chapter 4, methods section, and in the Appendix.

SPECT method - HMPAO injection

Visual and other stimuli may cause neuroactivation and significant focal increases in cerebral perfusion (Woods et al., 1991), so the patients were injected lying awake in a quiet room with eyes closed.

SPECT method - image acquisition

The scanner used in this work is a Strichmann 810 dedicated head imager. The software supplied with the system runs on an Apple computer, which controls the gantry, and produces and analyses the images. Scanning was carried out within 2h of injection producing 12mm axial slices through the brain. The software used with the imager allows reconstruction of these images in any chosen plane including coronal, saggittal and axial, with any degree of tilt. Slice acquisition time was 3 minutes, total

acquisition time 30-60 minutes depending on the number of slices required to image the whole head, and depending on whether the slices overlapped (in some patients, overlapping slices were acquired -this had the effect of slightly improving image quality in the coronal plane, but did not affect data as displayed or analysed in other pianes).

SPECT method - visual analysis of images

The images were reported independently by visual interpretation by 2 investigators (including the author), using orbitomeatal, transaxial and coronal views of the whole brain. In eqivocal cases, the final report was determined by consensus conference. The images were analysed blind to data other than the diagnosis of epilepsy.

With a non-quantitative technique such as HMPAO SPECT it is not possible to say absolutely whether, for example, a volume of uptake higher than that in the rest of the brain represents high perfusion in that area or low perfusion in the rest of the brain. Reports were therefore based on the assumption that where one volume of the brain is different from the rest, then it is the smaller volume which was more likely to be the abnormal one. In assessing cortical areas, comparisons were made with both contralateral homotopic structures, and with ipsilateral structures, as well as with subcortical and subtentorial structures.

Only those abnormalities which were seen on more than one 12mm slice were considered significant. This practice is adopted to prevent over-interpretation of abnormalities due to small variations in grey matter density, or the effect of small degrees of tilt or anatomic asymmetry, where the boundary between two areas of different flow were near-parallel to the plane of the slice.

SPECT method - numerical analysis of images

Numerical analysis of images was carried out using the software supplied with the Strichmann system. The regions of interest analysed used were;

1. Frontal - anterior frontal cortex
2. Mesial temporal - hippocampus from anterior midbrain to amygdaloid nucleus
3. Lateral temporal - from 2 cm behind temporal pole to the level of the posterior midbrain 4. Basal ganglia - head of the caudate nucleus and surrounding area
5. Thalamus

6. Parietal - the area posterior to the central sulcus 2cm superior to the level of the sylvian fissure
7. Occipital - calcarine cortex, sufficiently superior to include no cerebellum

Typical regions of interest are illustrated in Figure 2.1-2.3. They were determined by reference to an MRI brain atlas in consultation with an experienced neuroradiologist.

Each region was analysed on the slice orientation displaying the anatomy best. In practice, these were transaxial slices in the case of temporal lobe regions, and orbitomeatal slices for other regions. Analysis was carried out on 24mm (i.e. double thickness) slices.

The system software calculated the number of counts per area of the region of interest defined. An asymmetry index was calculated for each ROI as follows;

$$100 * (R - L) / ((R + L) / 2)$$

where R and L were the count density in right and left homotopic regions of interest. This index gives a positive value where the count density is greater on the right. This obviously may be the case whether this is due to right sided hyperperfusion or left sided hypoperfusion.

The upper limit of normal for the asymmetry index was fixed at 9%, based on data from a series of 10 normal subjects (Duncan et al., 1990a), and normal data from the literature (Rowe et al., 1989b; 1991a; b - see discussion).

Numerical analysis was carried out blind to the results of visual analysis.

SPECT method - numerical assessment of visual analysis

In a separate experiment, mesial and lateral temporal regions were identified and assessed visually for symmetry on 54 images by the same investigators who analysed the images from the main study. Mesial and lateral temporal regions of interest were defined on the same slices by an investigator who was blind to the results of the visual assessment of the regions, and asymmetry indices were calculated as above.

Acquisition of clinical data

Clinical data were acquired by means of a combination of review of case notes and patient interview. The data acquired were;

1. Patient age
2. Age at onset of epilepsy
3. Length of history of epilepsy
4. History of febrile convulsions or other antecedent for seizures
5. History of secondary generalised convulsions
6. Seizure frequncy in the 3 months before scanning
6. Estimated seizure frequency throughout life
7. Estimated total number of seizures
8. Time between last reported seizure and scan

Defining the 'interictal' period

The term 'interictal' may be defined clinically, or in terms of the results of an investigation, such as psychometric evaluation or EEG. The length of time it takes each of these parameters to return to whatever is normal for the patient may be very different. Following a seizure the EEG, for example, may remain abnormal even some days after the event, and after the patient has returned to feeling and behaving normally (Gotman, 1991). How long after a seizure the patients can be said to be 'interictal' depends on the parameter used, each parameter having its own postictal and interictal periods. Ideally, one would define 'interictal' in terms of when the rCBF abnormalities seen during and soon after a seizure return to the resting state. This would require multiple rCBF studies and could not, of course be done for each patient, or even in any one patient, for reasons of radiation exposure. Nor was it practicable to administer multiple EEG recordings or psychometric assessments on each patient; the relevance of an interictal period determined in this way would have uncertain applicability to rCBF changes in any case.

Since the great majority of patients are back to normal in terms of how they feel, in terms of their behaviour and of their EEG (Gotman, 1991) within 24h of a seizure, the term 'interictal' has been defined in this study as 24h from the last reported seizure. There were in fact no patients in this study who did not feel 'back to normal' by the time the interictal scan was done, but there were 11 patients, with seizure frequencies of between 50 and 1100 per year, where the interictal scan was done between 2.5 and 24h after a seizure because of practical difficulty (e.g.seizure

frequency too great, or patient living too far away to justify repeat examination) in scanning after a greater interval.

Chapter 2

Results

Temporal group

The results of visual and numerical analysis of interictal scans in the temporal and extratemporal groups are given in Table 2.3, and are summarised in Table 2.4. Descriptive statistics relating to asymmetry indices in Table 2.5

rCBF: visual analysis of images

Of the 81 patients, the images were reported as normal in 38 (47%) and abnormal in 43 (53%). Left temporal hypoperfusion was seen in 24 patients, right temporal hypoperfusion in 12 patients (Figs 24 and 2.5), and bilateral temporal hypoperfusion (more profound on the left) in 1 patient (Fig 2.6). There was hypoperfusion extending into the ipsilateral frontal lobe in 2 patients, and involving the whole hemisphere in a further 2 patients. In all these cases, the degree of hypoperfusion was judged visually to be greatest in the temporal lobe. Two patients showed hyperperfusion, one in the mesial temporal cortex, one in the lateral cortex (Fig 2.7).

Asyymetry indices associated with the above abnormalities (excluding the patients with hyperperfusion - see below) are shown in Table 2.6. The degree of asymmetry was greater in the lateral temporal structures in the majority (24/41) of these patients, in medial structures in a smaller proportion (15/41), and the same in 2/41, but the difference between the means was not statistically significant. The proportion of patients with laterally predominant hypoperfusion on the left was 17/24, and on the right 11/17. The difference between these proportions was not significant (Chi^2). Comparison of clinical characteristics in patients with asymmetry greater in the lateral ROI with those with asymmetry greater in the mesial ROI showed no significant differences. In the 4 patients with hypoperfusion extending outside the temporal lobe the degree was less than the maximal degree of hypoperfusion in the temporal lobe.

Correlation of rCBF with clinical factors: visual analysis of images

The descriptive statistics of clinical characteristics and ROI asymmetry indices for the whole temporal group, and the groups of patients in whom cerebral perfusion was judged visually to be normal and abnormal are given in Table 2.2. The clinical characteristics listed are patient age, age at onset of epilepsy, length of history, overall seizure frequency, recent (in the three months before scanning) seizure frequency, cumulated number of seizures, and time between the scan and the last reported seizure.

They are given with means, medians and ranges (the latter two are given because of the skewed nature of some of the data - see below). The frequency distributions of these parameters are shown in Figure 2.8-2.14. The top histograms shows the frequency distribution for the whole group, the middle ones show those for patients with normal rCBF, and the bottom ones those for patients with abnormal rCBF. Non-parametric statistics (Mann-Whitney U test) are used to compare groups, and the Chi^2 goodness of fit test to test the frequency distribution of data. Where the frequency distribution differed obviously from normal, the curve fit was not tested statistically.

Patient age (Fig 2.8)

The frequency distribution of patient age was normal, as was the frequency distributions of age for the normal rCBF group (p=0.28, 0.37, respectively). The frequency disrtibution of the abnormal group appeared approximately normal, but the difference from a normal distribution was significant (p=0.009). Mean age for the whole group was 26 years, with a standard deviation of 9.73 and a range of 4-54 years. The equivalent figures for the normal and abnormal rCBF groups were 28.7, 9.1, 15-53 and 23.8, 9.9, 4-54, respectively. The difference between these means was marginally significant (p=0.044), until the Bonferoni correction was applied.

Age at onset of epilepsy (Fig 2.9)

The frequency distribution of age at onset of epilepsy was reverse exponential (p=0.81) with most patients at the lower end of the range with age at onset of less than 10 years. The frequency distribution of age at onset in the group with normal rCBF did show a decrease with age, but there was a higher proportion of patients with a later age at onset. By contrast, the frequency distribution in patients with abnormal

rCBF was again clearly exponential (p=0.28), with almost half (21/44) the patients having an age of onset of epilepsy before five years. The median age at onset for the whole group was 8 years, with an interquartile range of 15 and a total range of less than one year to 45 years. The equivalent figures for the normal and abnormal rCBF groups were 13.5, 13.5, 0-41 and 5, 9, 1-45, respectively; age at onset in the abnormal group was significantly less than that in the normal group (p=0.003; p=0.018 after Bonferoni correction).

Length of seizure history (Fig 2.10)

The frequency distribution of length of history was normal (p=0.19), but weighted slightly toward the lower end of the range. The frequency distributions of length of history for the normal and abnormal rCBF groups were similar (p=0.86, 0.30). The mean length of history for the whole group was 16 years with a standard deviation of 9.7 and a range of 1-38 years. The equivalent figures for the normal and abnormal rCBF groups were 15.3, 7.6, 2-28 and 16.2, 9.5, 1-38, respectively. The difference between those means was not significant.

Seizure frequency (Fig 2.11, 2.12)

The frequency distribution of seizure frequency, both overall and recent, showed a decrease as seizure frequency increased, with most of the patients at the lower end of the range, and more than half having a seizure frequency of less than 200/year. The median seizure frequency was 150/year, with an interquartile range of 350 and an overall range of 2-5000/year. The medians, interquartile and total ranges for the normal and abnormal rCBF groups were 295, 325, 2-4000/year and 150,650, 2-5000/year, respectively. The median recent seizure frequency was 150, with an interquartile range of 450 and a total range of 0-3500/year. The equivalent figures for the normal and abnormal rCBF groups were 150, 345, 2-2000/year and 150, 602, 0-3500/year, respectively. The differences between normal and abnormal groups was not significant.

Cumulated number of seizures (Fig 2.13)

The frequency distribution of cumulated number of seizures in all three rCBF groups showed a decrease as the cumulated number of seizures increased, with almost half the whole group having had less than 3000 seizures in their lifetime. The range

was great, however, with 17 patients having had 9000 seizures or more. The median cumulated seizure number for the whole group was 2000, with an interquartile range of 6100 and a total range of 20-64000. The equivalent figures for the normal and abnormal groups were 3850, 5700, 50-64,000 and 7454, 5400, 20-5500, repectively. The differences between the groups was not significant.

Time since last seizure (Fig 2.14)

Most patients (55/81) were scanned within 4 days of the last reported seizure, although the range was wide, and there were 14 patients at the upper end of the range who were scanned at 14 days or more. The median time since last seizure was 2 days, with an interquartile range of 5 and a total range of 0.1-180. The frequency distribution in the normal and abnormal groups were similar, and the median, interquartile and total ranges were 2, 3, 0.6-60 and 2, 5, 0.1-80, respectively. The difference between the normal and abnormal groups was not significant.

The occurrence of secondary generalised seizures

There were no significant differences in any of the clinical factors or in asymmetry indices between patients with (52/81) and without (29/81) secondary generalised seizures.

rCBF: numeric analysis

Correlations between asymmetry indices and clinical factors

Individual asymmetry indices are given in Table 2.3, and mean and other descriptive statistics of asymmetry indices for frontal, mesial and lateral temporal, basal ganglia, thalamus, parietal and occipital ROIs in Table 2.5. Their frequency distributions are shown in Figure 2.15

All the ROI frequency distributions were approximately normal (note the differing scales on the Y axes of the histograms). With the exception of the frontal, basal ganglia and occipital ROIs, there appeared to be a bias toward negative values (i.e. left sided hypoperfusion). This was tested by splitting the data for each ROI into positive and negative values, removing the signs and comparing the means using the Mann-Whitney U test. The descriptive statistics of the asymmetries for left and right ROIs are given in Table 2.7. The biggest difference was in the lateral temporal ROI, with a mean asymmetry index of 4.12 for right sided hypoperfusion and 9.6 for left sided hypoperfusion ($p<0.001$). None of the other differences was significant. The lateral temporal ROI also differed in exhibiting a much wider range of asymmetry than the other ROIs, with longer 'tails' at the extremes, more obviously on the left. The shape of the histogram also suggested a bimodal distribution, with separate peaks around -10 and +5. The mesial temporal ROI showed a more even distribution, and a generally flatter curve. The largest absolute asymmetry indices were in the lateral temporal ROI (mean 7.9%) and the mesial temporal ROI (mean 5.5%). The other 5 ROIs had mean asymmetries of 4.3% or less. Analysis of the variance showed that the differences between mean ROI asymmetries were significant ($p<0.001$).

Spearman rank correlation tests were used to test correlations between asymmetry indices and clinical parameters. For this purpose the sign of asymmetry indices were ignored. There was no significant correlation between asymmetry indices for any ROI and any of the clinical data. In particular, there was no correlation between the degree of asymmetry and age at onset of epilepsy i.e. age at onset of epilepsy, while being an important determinant of the presence of hypoperfusion as asessed visually, did not appear to be related to its degree. There were no significant differences in asymmetry index between patients with and without secondary generalised seizures.

Relationship with the results of visual analysis

The results of the experiment undertaken to define the relationship between the reporting of the investigators in this study are illustrated in Fig 2.16. The open symbols represent regions judged visually as normal, and the closed ones regions judged visually as abnormal.

The asymmetry in regions reported as normal ranged from 0-8% for both lateral and mesial ROIs. For abnormal regions the asymmetry ranged from 7-51% for mesial regions and 7-58% for lateral regions.

On examining visual reports it was apparent that separate judgements as to whether hypoperfusion was predominantly mesial or lateral were not made, and that asymmetries of the thalamus and basal ganglia were not reported. When comparing verbal and visual 'reports', therefore, asymmetries of the thalamus and basal ganglia were ignored, and a visual report of temporal hypoperfusion was taken to agree with a numerically determined hypoperfusion of either the mesial or the lateral temporal ROI, or both.

The results of both types of analysis are summarised for comparison in Table 2.4.

Visual analysis identified abnormalities in 43/81 scans (53%), while numerical analysis identified abnormalities in 39/81 scans (47%). Visual analysis identified abnormalities not picked up by numerical analysis in 15 scans, and numerical analysis identified abnormalities not picked up by visual analysis in 12 scans. The reports agreed in 55 (the numbers add up to 82 because in one scan both visual and numeric abnormalities were identified, neither of which was detected by the other method).

The values for each ROI were divided into groups according to whether the scan had been reported visually as normal or abnormal, and the sign of the asymmetry index removed. Differences between groups were tested using the Mann-Whitney U test. The difference was significant only in the mesial and lateral temporal ROIs, where the asymmetry indices associated with scans reported visually as abnormal were significantly greater than those associated with scans reported as normal ($p<0.001$; $p<0.02$, respectively, corrected for the number of tests done).

Asymmetry of basal ganglia and thalamus

Significant asymmetry of the basal ganglia or thalamic ROIs was seen in 8 patients. All 8 patients also had temporal hypoperfusion; in 2 cases the low side was ipsilateral to the hypoperfused temporal lobe, in 3 cases contralateral. Asymmetry of

the thalamic ROI was seen in 2 patients, both of whom had temporal hypoperfusion ipsilateral to the lower thalamic ROI value. One patient had asymmetry of both ROIs, the low side ipsilateral to temporal hypoperfusion.

Extratemporal group

The clinical data for the 11 patients with complex partial seizures originating outside the temporal lobe are shown in Table 2.1, with descriptive statistics in Table 2.2. None of the means differed significantly from those in the temporal group (Mann-Whitney U test).

The results of visual and numeric analysis of the interictal images in the extratemporal group are given in Table 2.3., with descriptive statistics in Table 2.5. All the images were visually reported as normal. The largest asymmetry index seen in this group was 7.5%; numerical analysis was therefore also normal. Frequency distributions of the ROI data are shown in Figs 2.17. Small numbers notwithstanding, there was no clear evidence of any difference in frequency distribution from the temporal group.

Based on absolute values for asymmetry indices, the difference of 1.4 vs 5.37% between lateral temporal ROIs for extratemporal and temporal groups respectively was statistically significant ($p=0.01$, Mann-Whitney U test). None of the other differences between the extratemporal and temporal groups was significant.

In view of the small numbers involved and the fact that all the scans were normal, no correlations were made between asymmetry indices and clinical factors.

Chapter 2

Illustrations and Tables

Figure 2.1

HMPAO SPECT: Orbitomeatal slice illustrating frontal (a,b), basal ganglia (c,d), occipital (e,f), and thalamic (g,h) regions of interest used in numerical analysis of images (patient 2, extratemporal group).

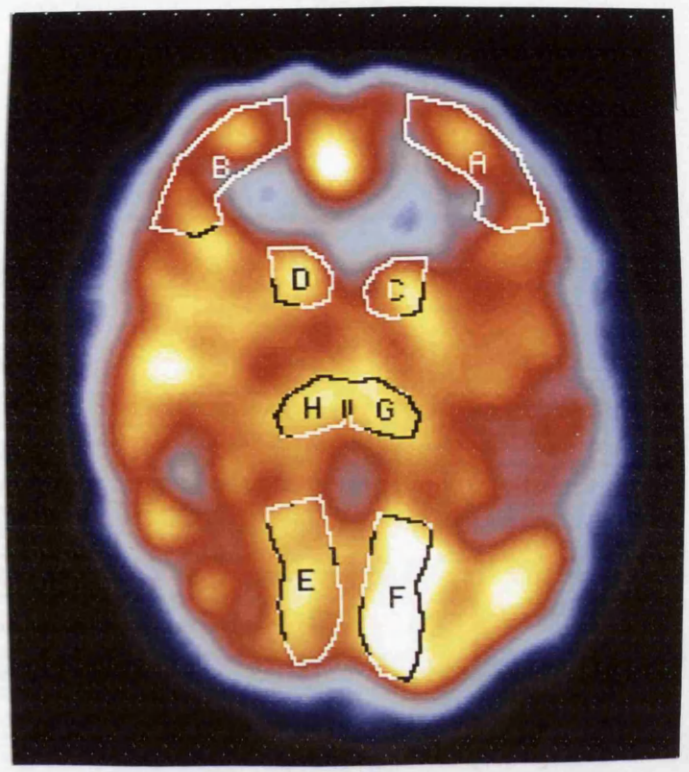

Figure 2.2

HMPAO SPECT: Orbitomeatal slice illustrating parietal region of interest used in numerical analysis of images (patient 2, extratemporal group).

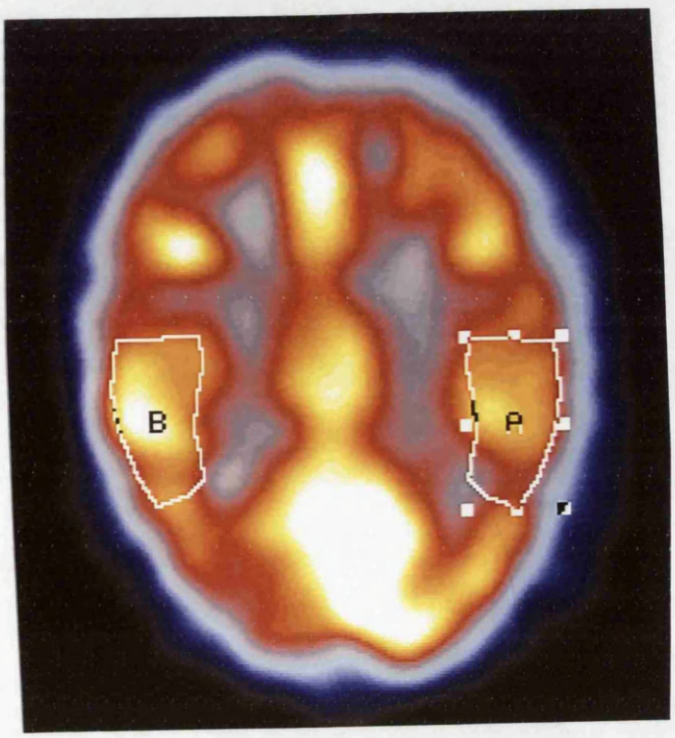

Figure 2.3

HMPAO SPECT: Transaxial slice illustrating the mesial (a,b) and lateral (c,d) temporal regions of interest used in numerical analysis of images (patient 2, extratemporal group).

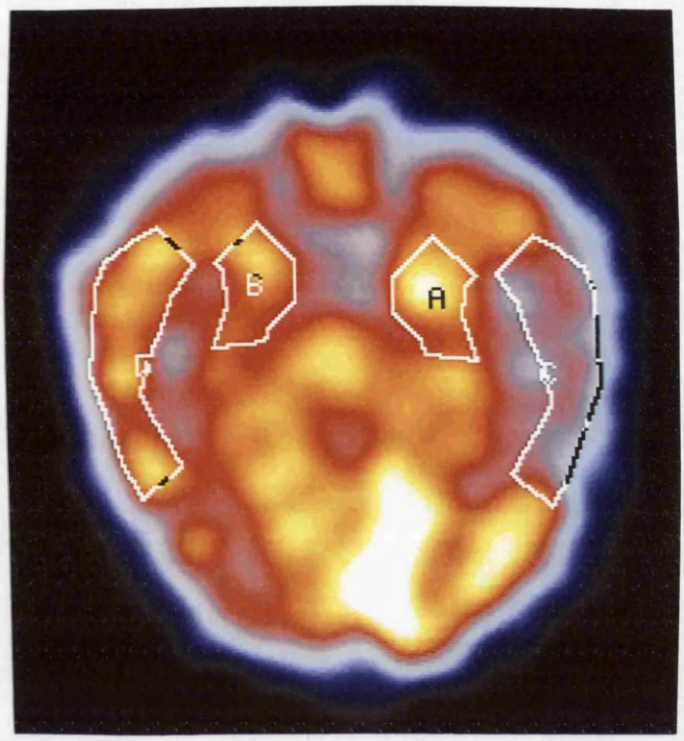

Figure 2.4

Interictal HMPAO SPECT: Transaxial slice showing hypoperfusion of the whole of the left temporal lobe, more marked in the lateral cortex (patient 62).

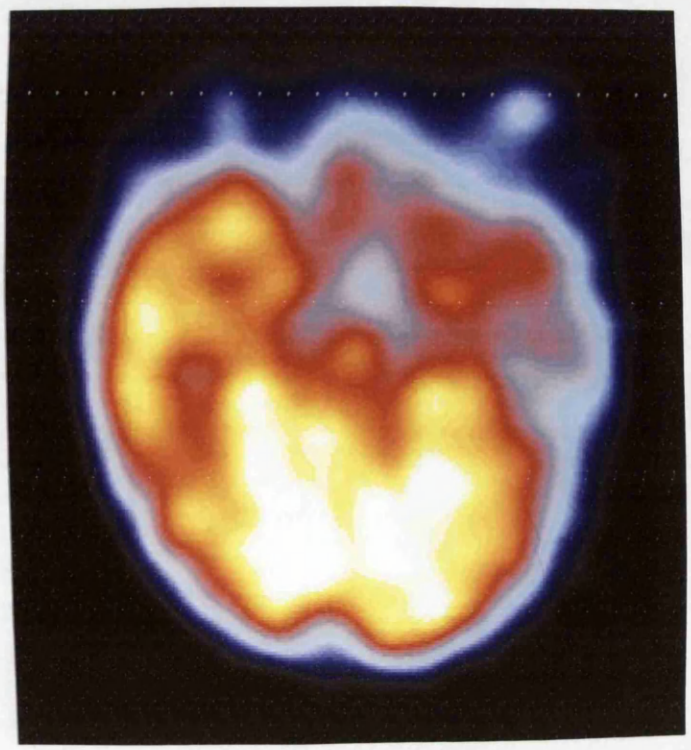

Figure 2.5

Interictal HMPAO SPECT: Orbitomeatal slice showing left temporal hypoperfusion more marked in the mesial cortex (patient 63)

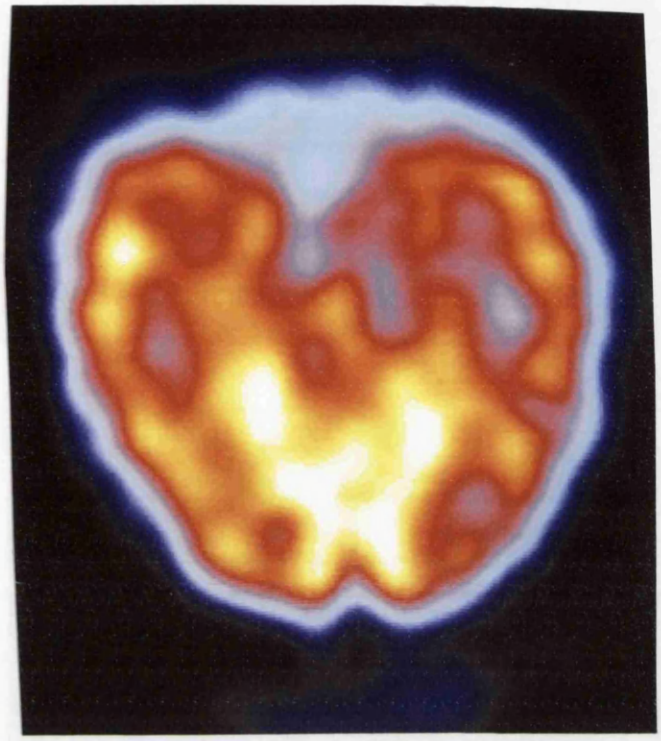

Figure 2.6

HMPAO SPECT: Orbitomeatal slice showing bilateral temporal hypoperfusion, more profound on the left (patient 59).

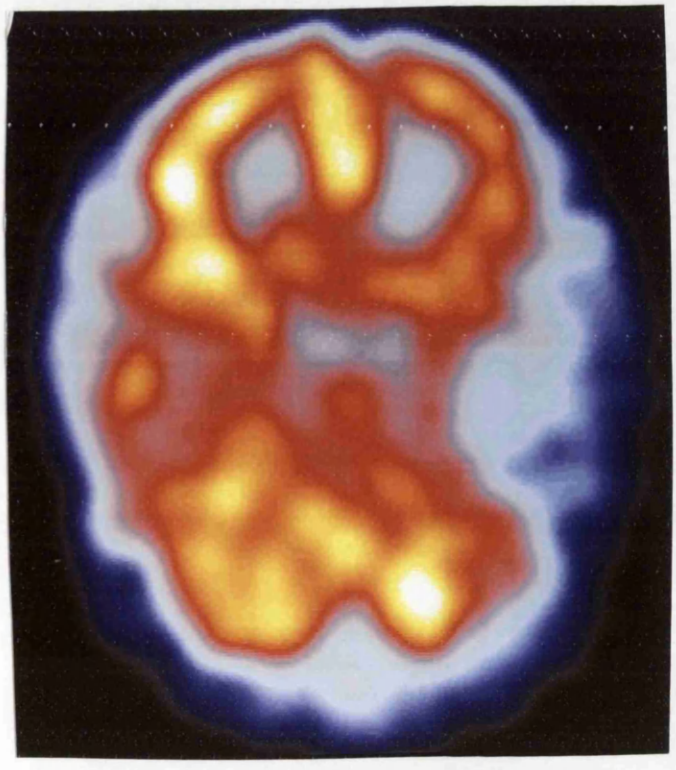

Figure 2.7

Interictal HMPAO SPECT: Transaxial slice through the temporal lobe showing hyperperfusion of the right lateral temporal cortex (patient 72).

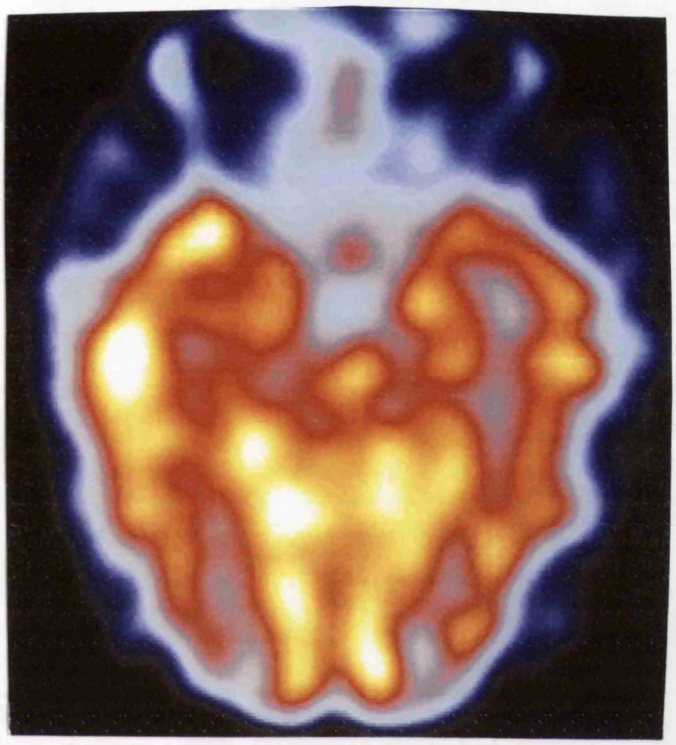

Figure 2.8

Temporal group: frequency distribution of patient age

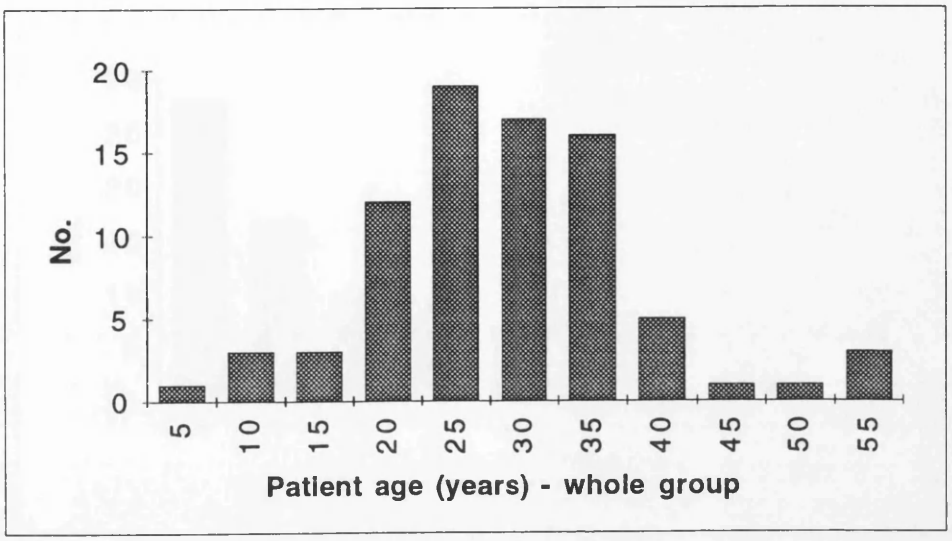

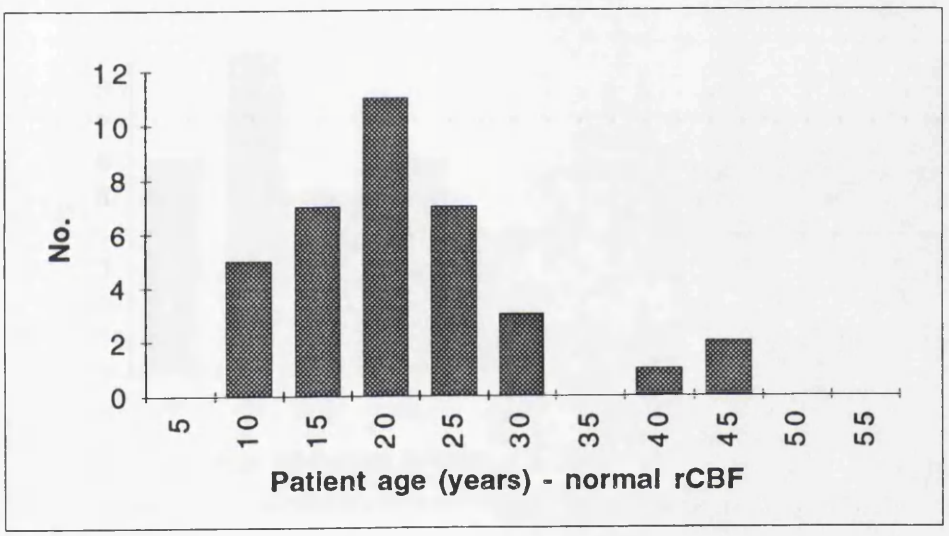

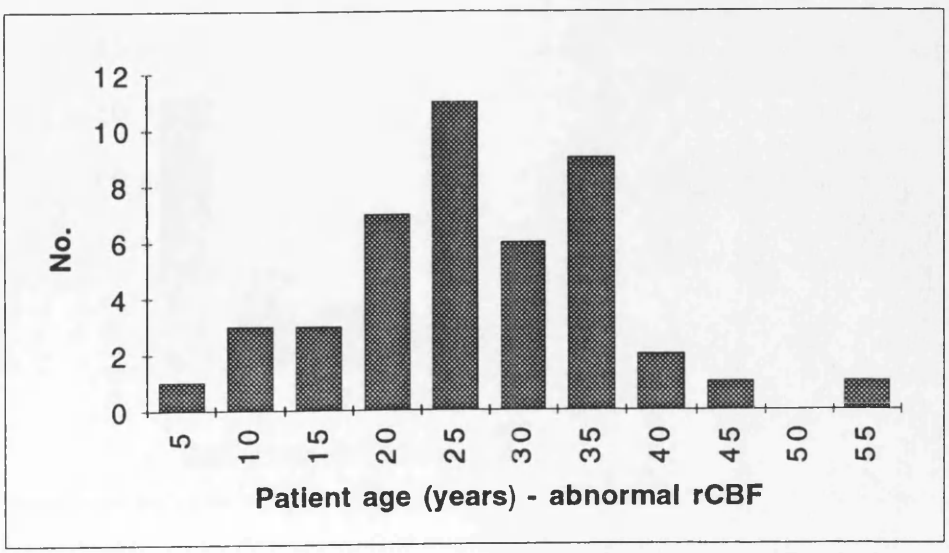

Figure 2.9

Temporal group: frequency distribution of age at onset of epilepsy

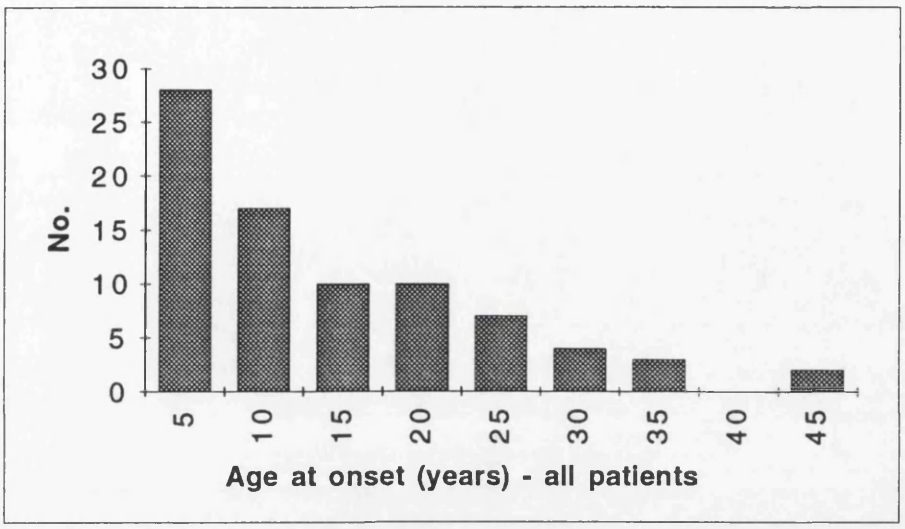

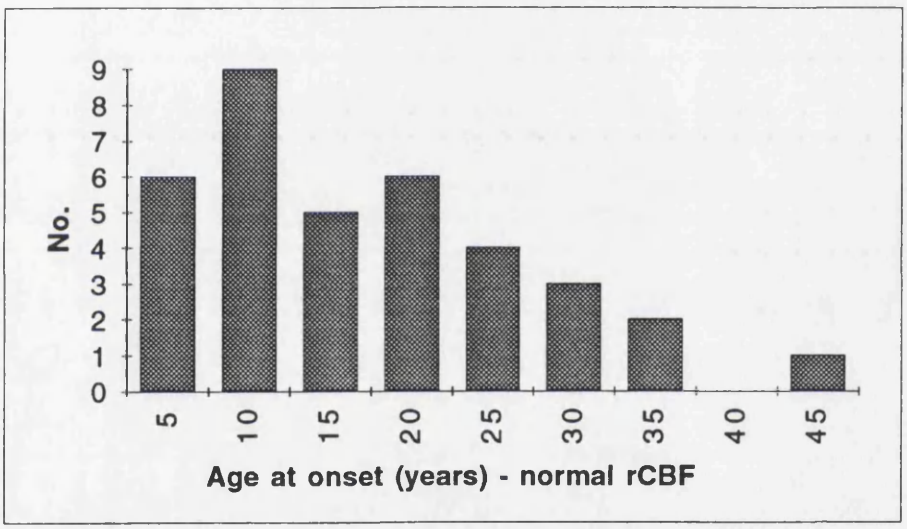

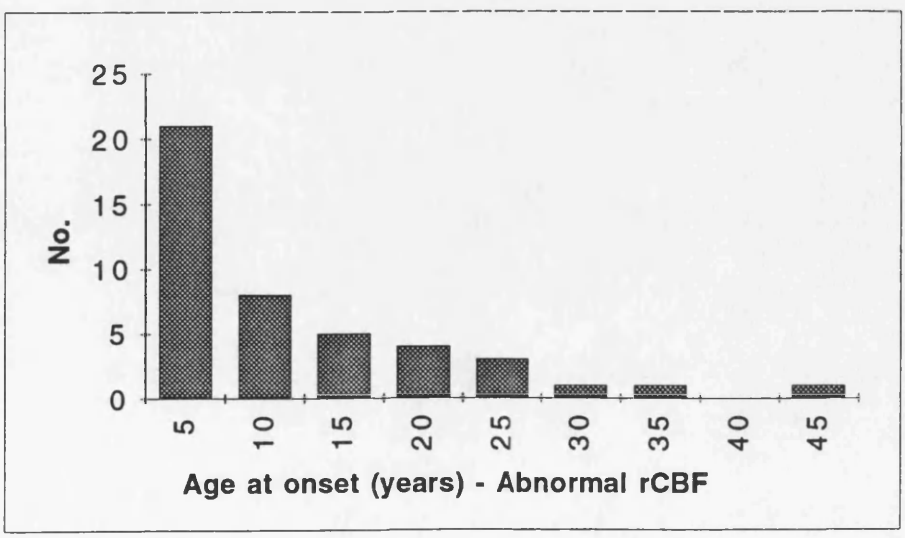

Figure 2.10

Temporal group: frequency distribution of length of history of epilepsy

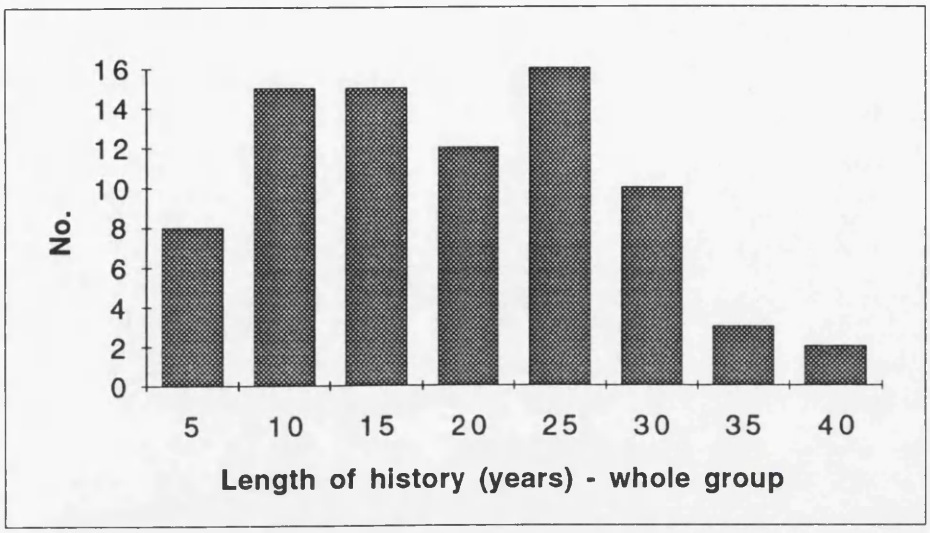

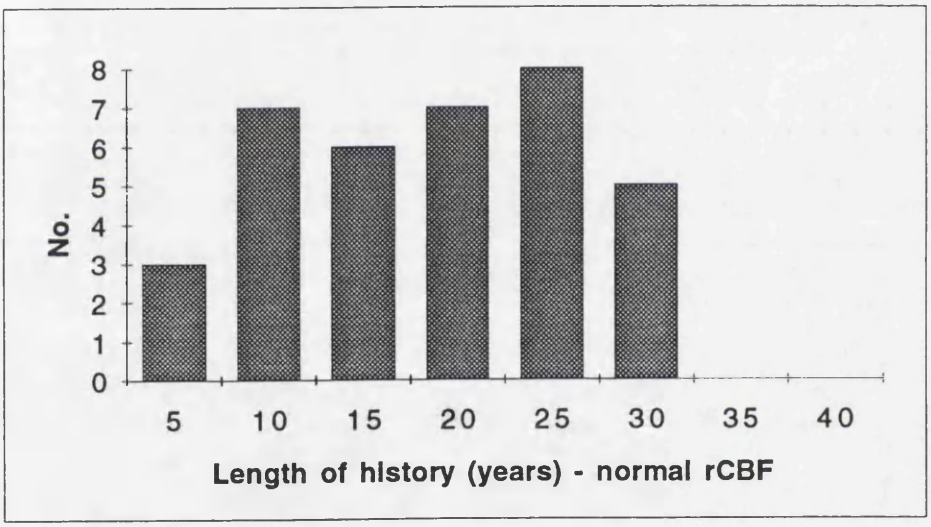

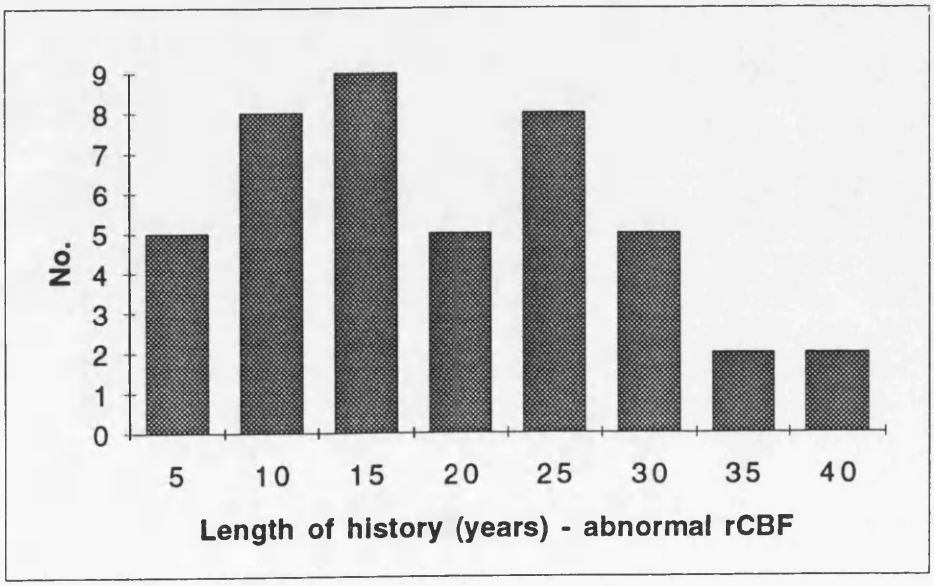

Figure 2.11

Temporal group: frequency distribution of seizure frequency

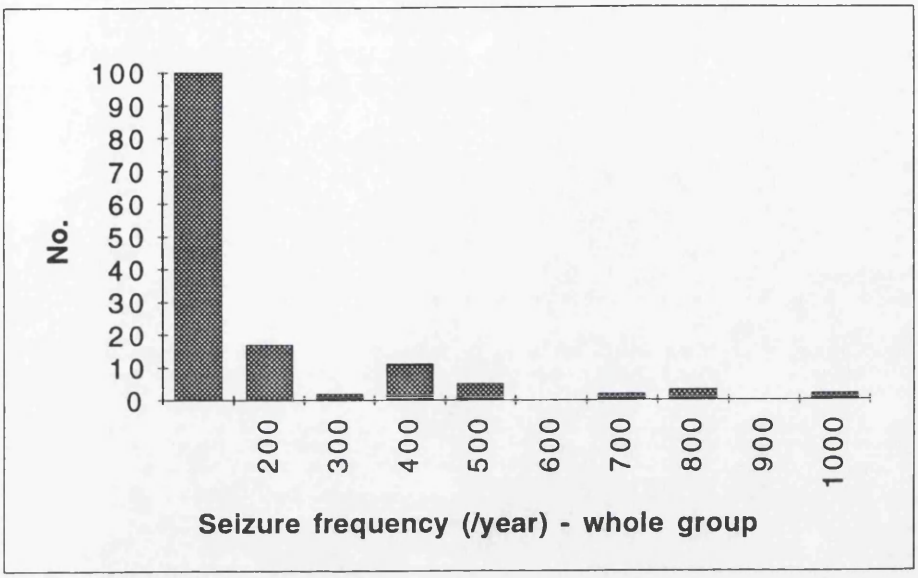

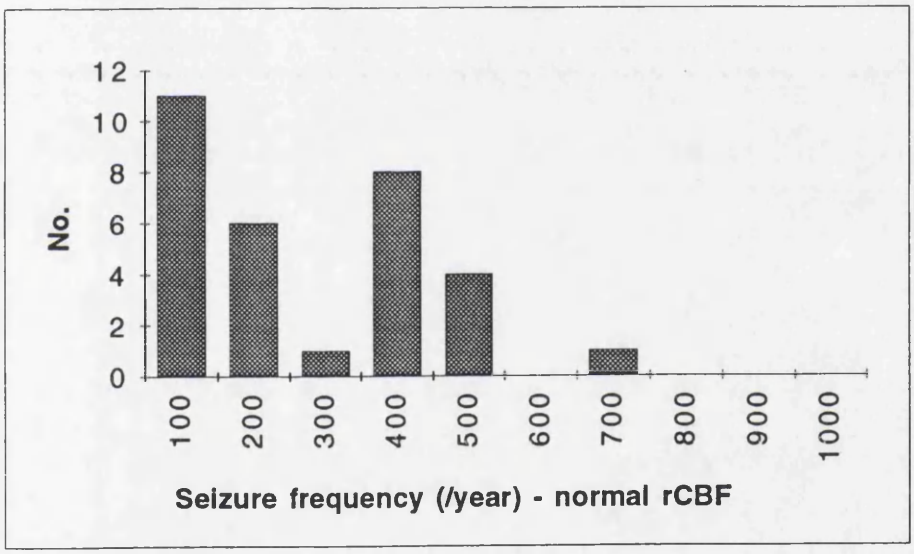

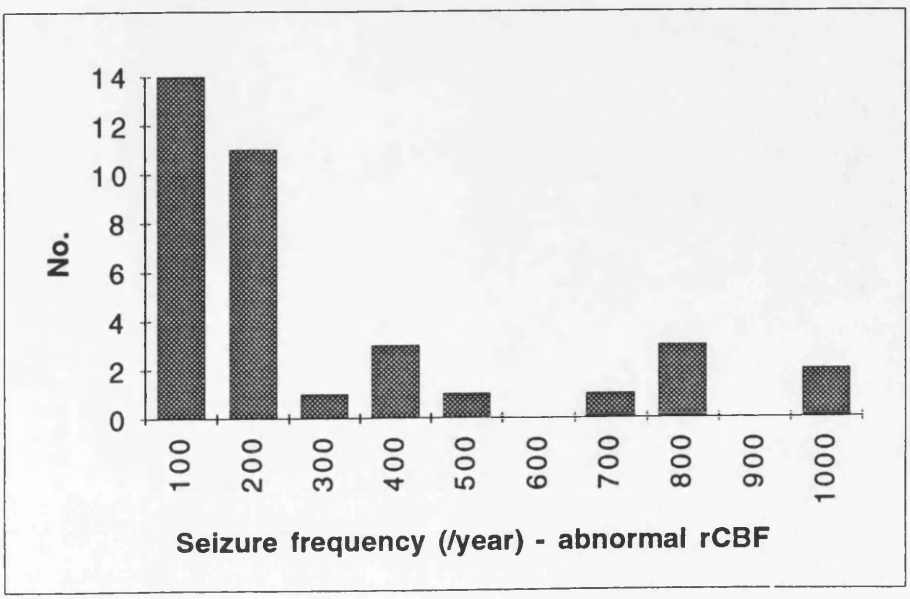

Figure 2.12

Temporal group: frequency distribution of recent seizure frequency

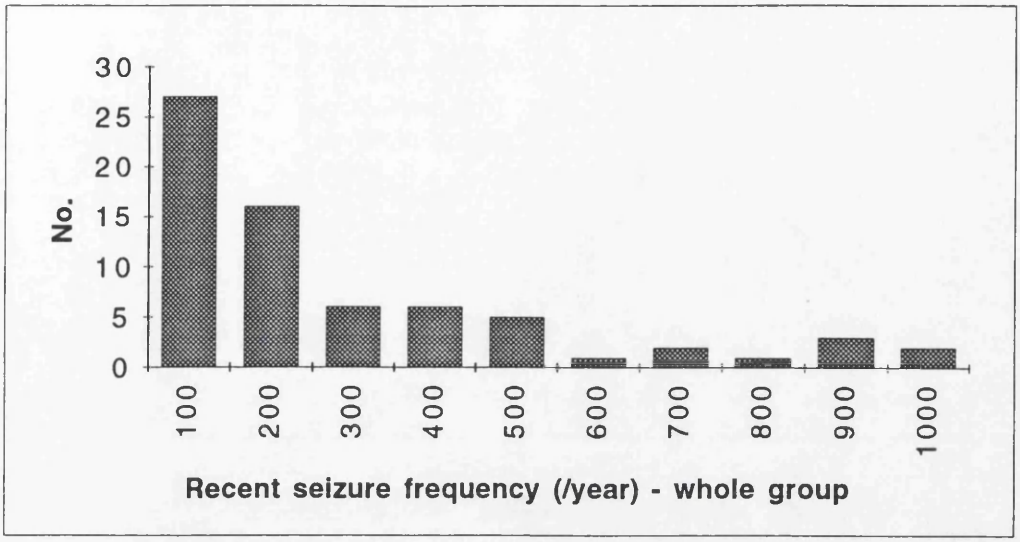

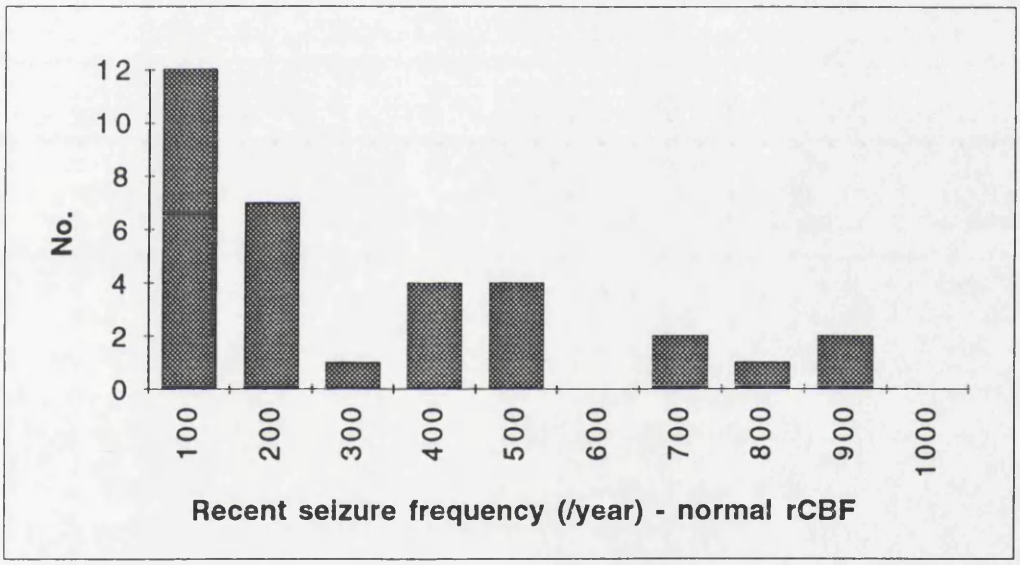

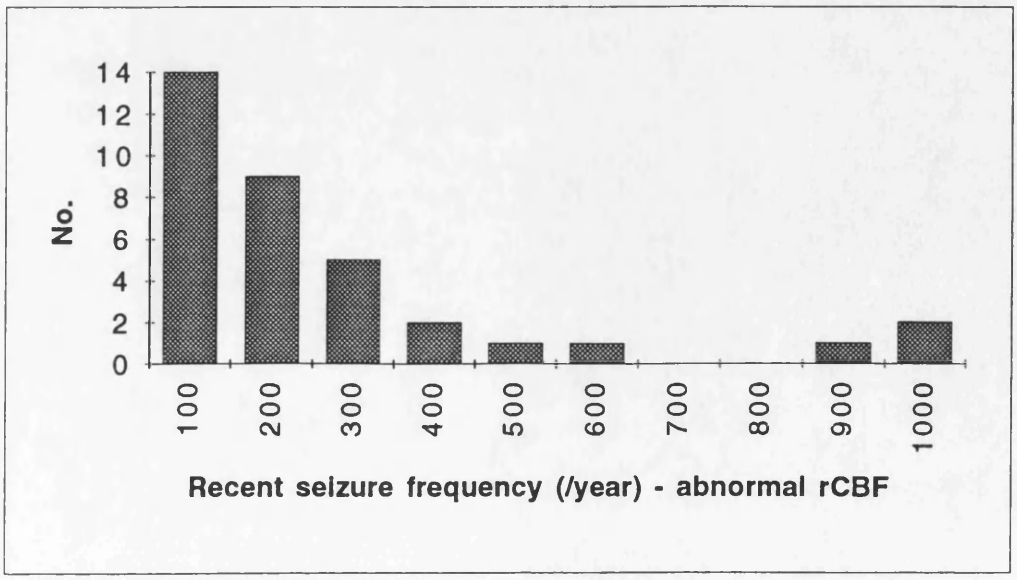

Table 2.13

Temporal group: frequency distribution of cumulated seizure number

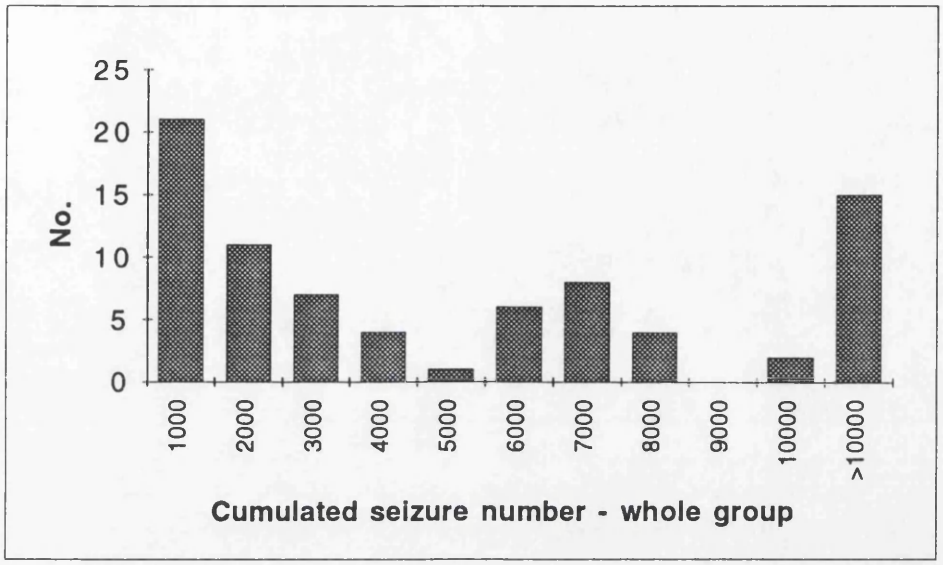

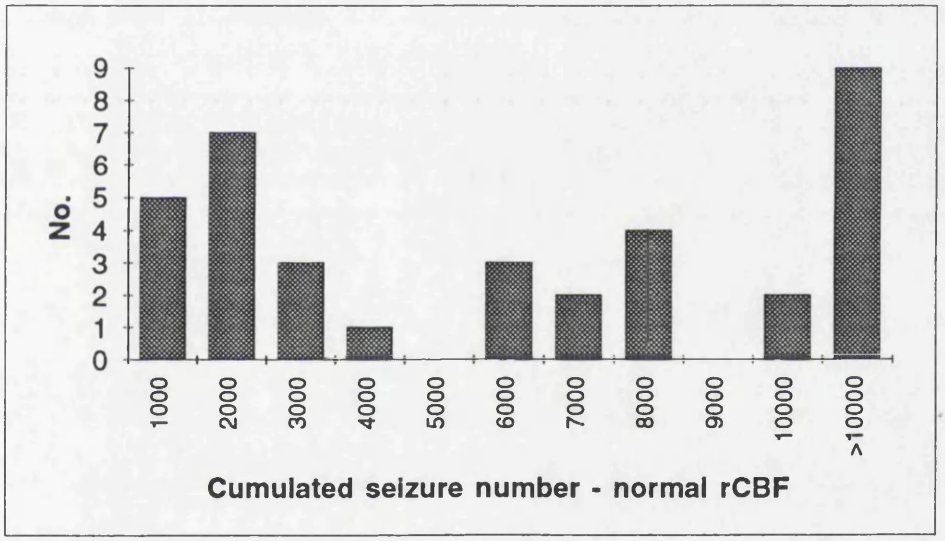

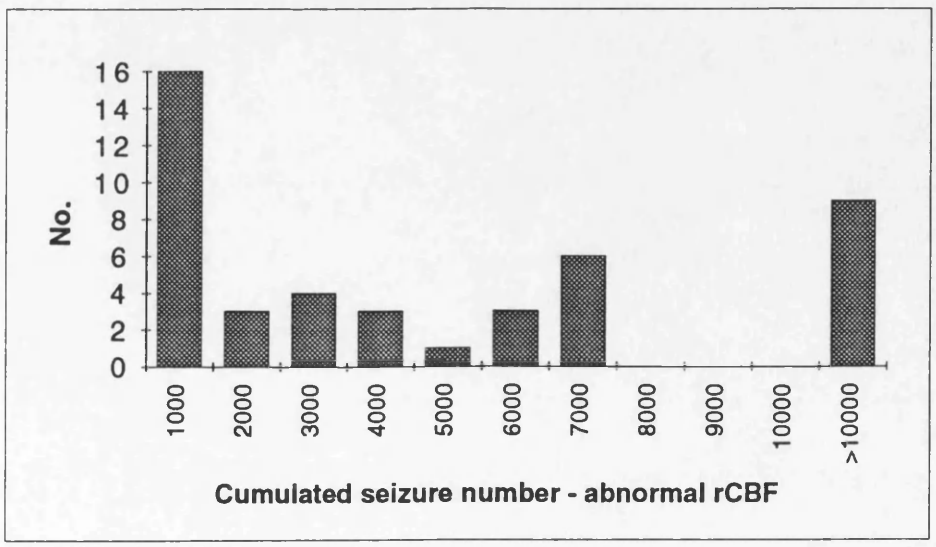

Figure 2.14

Temporal group: frequency distribution of time since last seizure

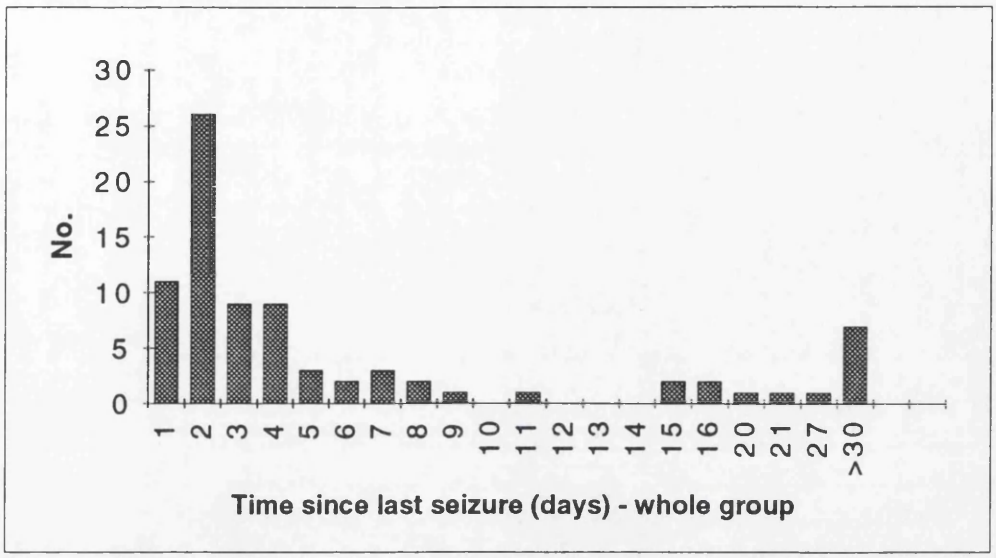

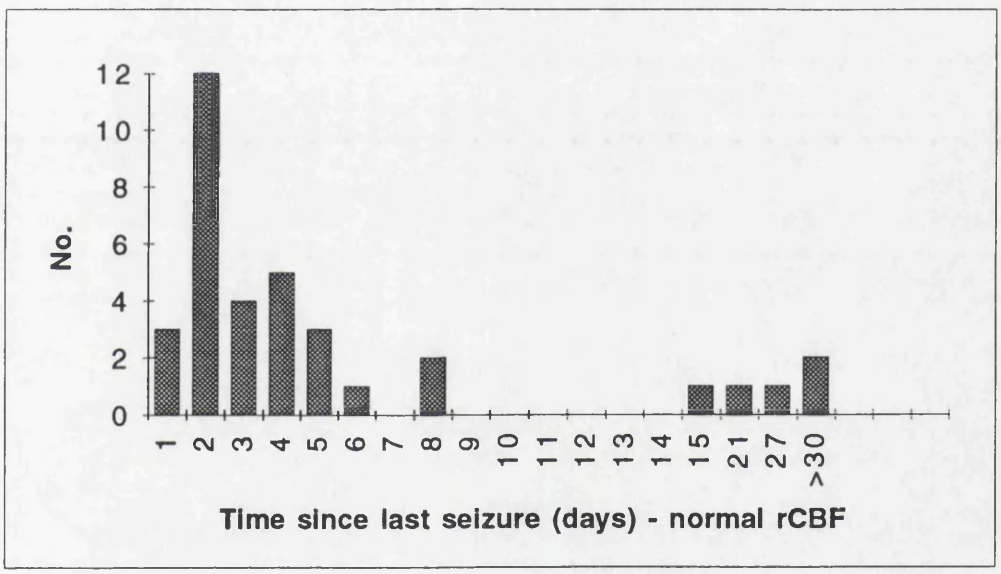

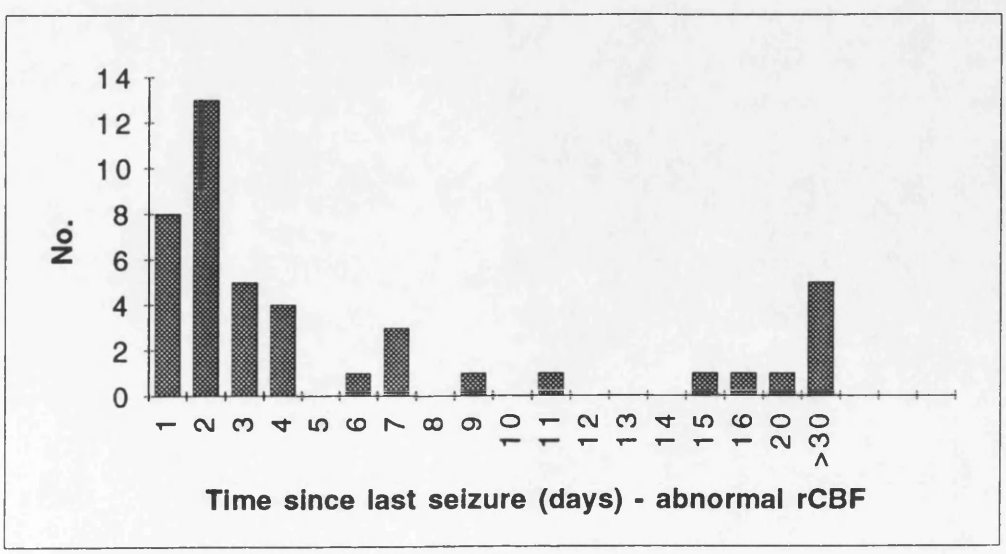

Figure 2.15

Temporal group: frequency distribution of asymmetry indices

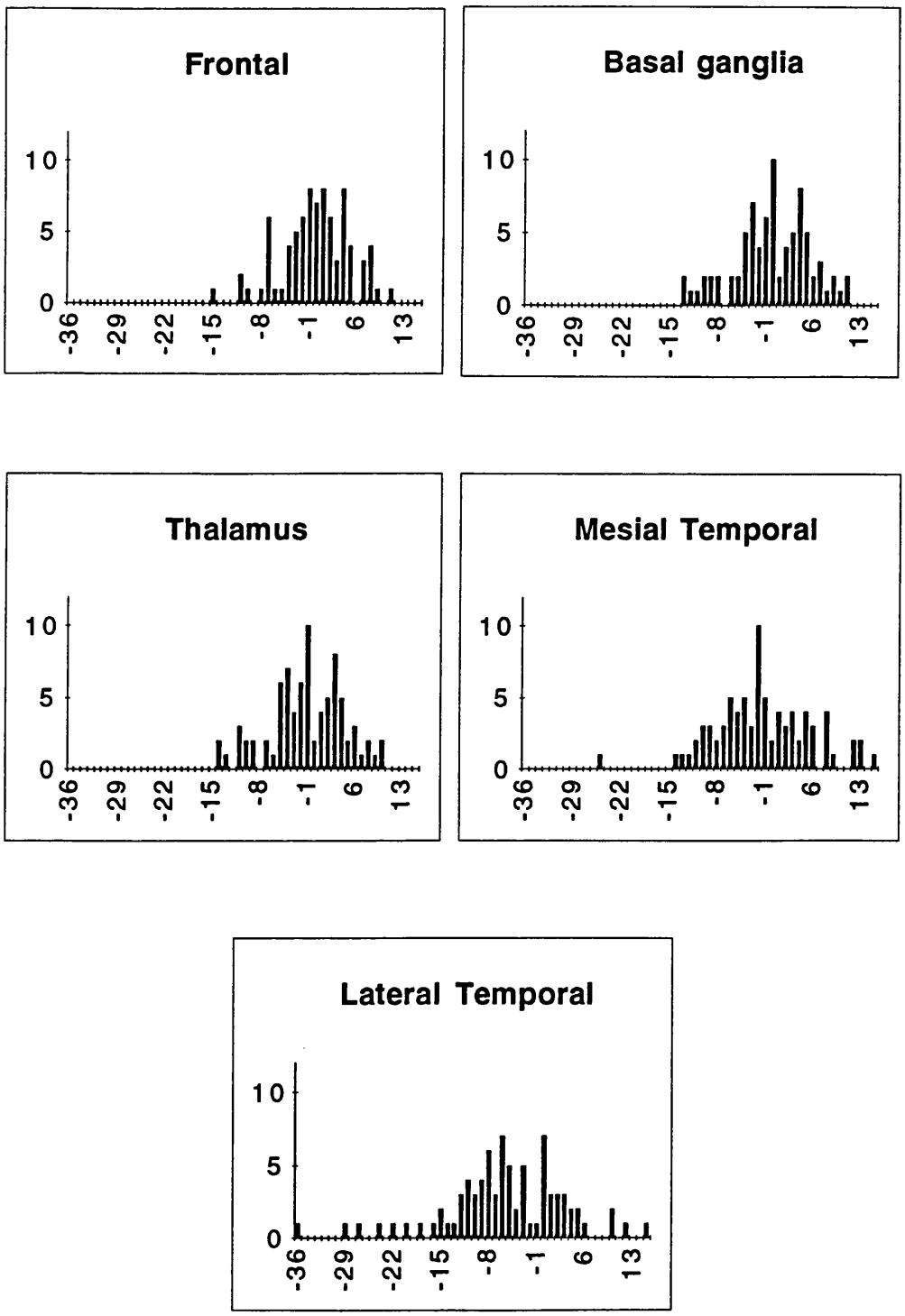

Figure 2.15

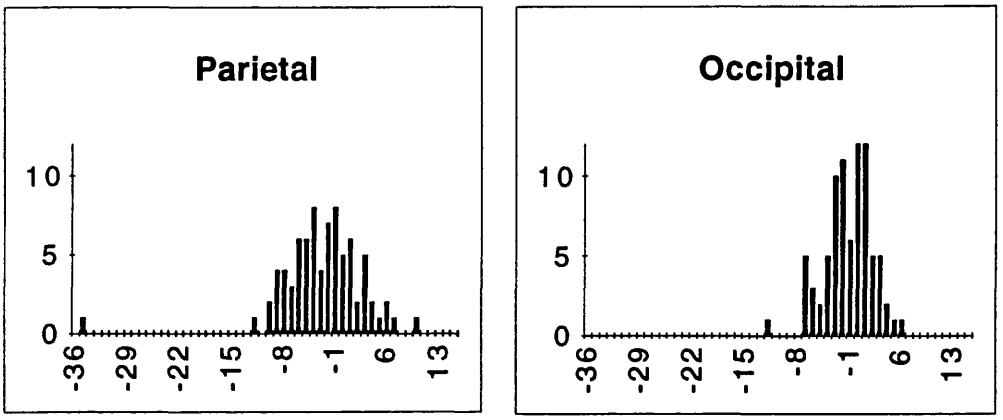
Parietal
10
5
0
-36
-29
-22
-15
-8
-1
6
13
Occipital
10
5
0
-36
-29
-22
-15
-8
-1
6
13

Figure 2.16

Asymmetry indices of regions of interest visually judged symmetric or asymmetric

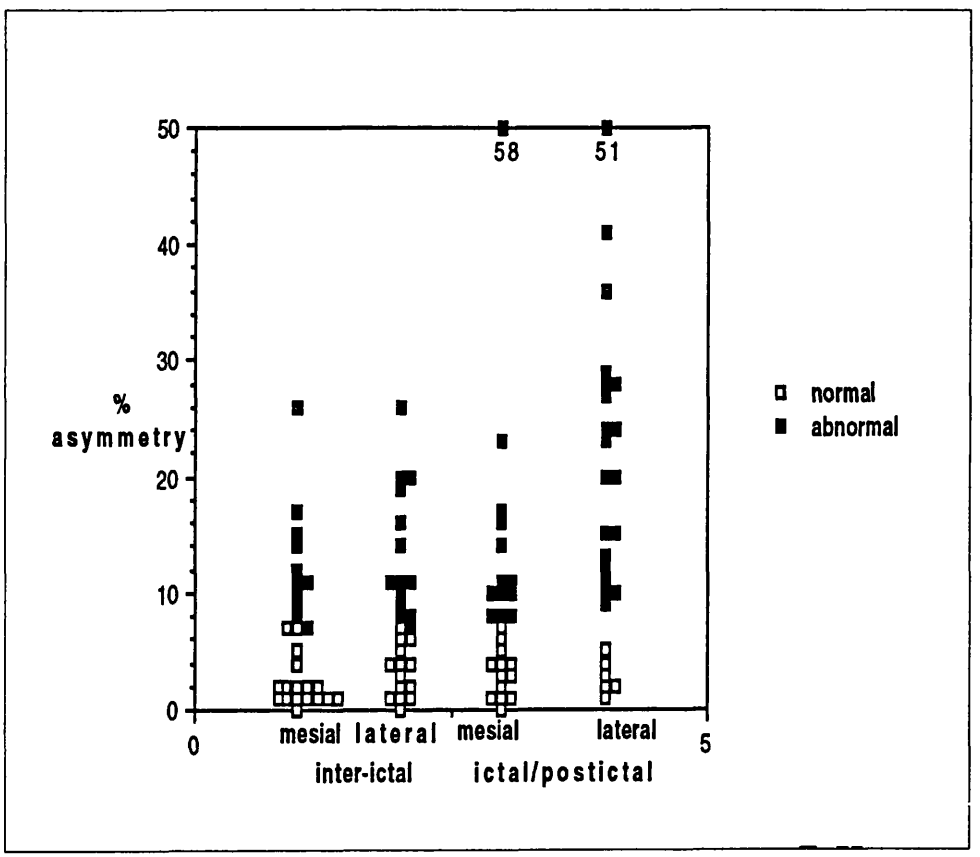

Figure 2.17

Extratemporal group: frequency distribution of asymmetry indices

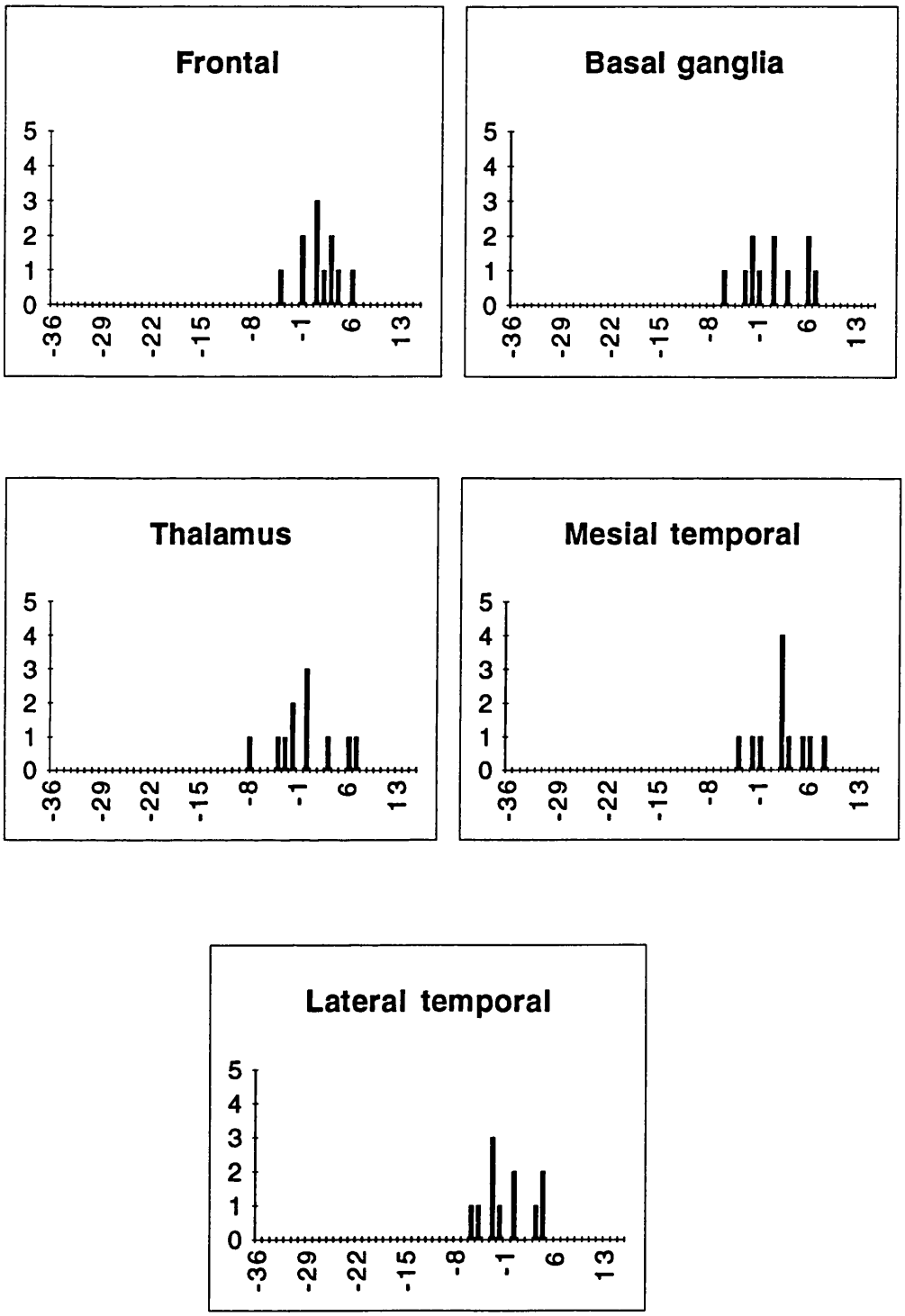

Figure 2.17

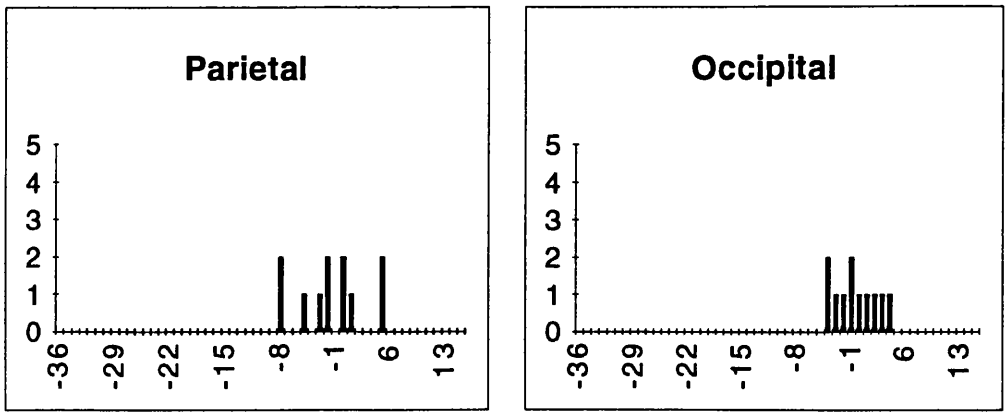
Parietal
5
4
3
2
1
0
-36
-29
-22
-15
-8
-1
6
13
Occipital
5
4
3
2
1
0
-36
-29
-22
-15
-8
-1
6
13

Table 2.1

PATIENT CLINCAL DATA

Temporal group

Patient	Patient age (years)	Length of history (years)	Age at onset of epilepsy (years)	Seizure frequency (/year)	Recent seizure frequency (/year)	Cumulated seizure number	Time since last seizure (days)	Sec. Gen. seizures
1	32	17	15	80	250	4500	0,3	+
2	17	16	1	25	20	500	15	+
3	33	31	2	100	20	3000	2	-
4	29	21	8	60	60	1300	4	-
5	17	16	1	30	20	320	3	+
6	9	12	3	25	15	400	20	-
7	39	6	33	300	25	2000	4	+
8	31	14	17	360	360	6000	0,3	+
9	42	12	30	20	5	250	70	+
10	24	21	3	144	144	2900	6	+
11	28	22	6	1500	1500	33000	5	+
12	39	26	13	300	400	9000	1	+
13	29	23	6	2	2	50	60	-
14	22	7	15	1000	700	7000	1	-
15	4	1	3	900	900	900	0,1	+
16	52	11	41	400	400	5000	1	+
17	20	18	2	150	250	2700	3	-
18	29	2	27	120	25	250	15	-
19	28	28	0	1600	1600	48000	7	+
20	30	15	15	100	120	2000	21	+
21	23	13	10	1100	1100	15000	0,7	+
22	19	15	4	300	150	5000	1	+
23	29	9	20	12	150	500	1	+
24	28	20	8	25	25	500	3	+
25	15	14	1	150	150	1000	5	+
26	47	23	24	50	6	1500	30	+
27	53	22	31	25	25	800	3	-
28	29	13	16	35	25	600	3	+
29	29	26	3	300	600	7800	1	-
30	33	16	17	400	400	7000	1	-
31	15	14	1	360	360	5400	0,6	+
32	31	13	18	100	100	1300	1	+
33	17	11	6	40	40	500	14	+
34	31	26	5	1200	800	30000	1	+
35	22	16	6	2000	2000	32000	1	+
36	19	4	15	4	2	20	180	-
37	23	21	2	150	150	3500	1	+
38	27	26	1	400	300	6500	1,2	+
39	26	16	10	4000	800	64000	7	+
40	29	8	8	50	1700	500	0,25	-
41	22	17	5	360	300	6000	3	+
42	30	29	1	1000	1000	29000	30	+
43	24	16	8	80	80	1500	4	+
44	26	23	3	4	4	100	90	+
45	31	13	18	180	100	1800	2	-
46	23	14	19	300	400	5000	0,6	+
47	36	23	13	290	290	7000	1	+
48	54	9	45	50	50	500	6	-
49	15	11	4	600	600	7000	1,5	+
50	29	27	2	720	500	19000	1	+
51	24	24	1	10	0	500	2	-
52	16	27	25	2	250	100	30	-
53	32	26	20	50	50	1400	2	-

Table 2.1

Patient	Patient age (years)	Length of history (years)	Age at onset of epilepsy (years)	Seizure frequency (/year)	Recent seizure frequency (/year)	Cumulated seizure number	Time since last seizure (days)	Sec. Gen. seizures
54	23	3	20	300	300	900	1	+
55	32	6	26	25	25	500	14	-
56	31	31	1	150	1600	5000	1,5	+
57	13	7	6	1000	2000	7000	1	-
58	22	2	20	300	380	600	3	-
59	18	7	11	700	100	5000	2	-
60	25	20	5	100	100	2000	8	+
61	13	2	11	250	250	500	2	+
62	5	4	1	1000	1000	4000	1	-
63	12	6	6	960	960	6000	1	-
64	21	20	1	120	100	2000	0,9	+
65	25	24	1	180	6	5000	1	-
66	29	3	26	100	800	1000	1	+
67	15	7	8	2000	2000	14000	2	+
68	39	37	2	80	10	1000	2	+
69	31	26	5	700	3500	52000	0,7	+
70	19	5	14	360	150	1800	27	-
71	31	8	23	650	1200	6000	1	+
72	24	32	1	60	25	1500	1,5	-
73	21	11	10	5000	150	55000	1,2	+
74	8	7	1	120	120	900	0,7	+
75	21	15	6	400	150	2500	2	+
76	22	8	14	150	150	1200	3	+
77	23	22	1	400	400	10000	1	+
78	22	12	10	2000	250	24000	10	-
79	38	38	1	50	50	1700	6	+
80	32	8	24	100	50	800	3	-
81	30	23	7	40	80	1000	0,8	+
Extratemporal group								
1	6	1	5	7200	7200	1200	0,5	-
2	26	8	18	300	300	2500	1	-
3	38	19	19	500	500	1000	11	+
4	21	20	1	1000	1000	21000	2	+
5	18	8	10	1750	1750	15000	0,1	+
6	34	25	9	400	400	12000	0,5	+
7	28	20	8	500	1000	16000	0,5	+
8	20	6	14	300	0	1800	90	-
9	35	21	14	1800	1800	40000	1	+
10	24	12	12	50	50	600	49	+
11	24	22	2	150	150	3500	1,5	+

Table 2.2

CLINICAL DATA: DESCRIPTIVE STATISTICS

TEMPORAL GROUP (n=81)

variable	mean	median	minimum	maximum	std.dev.
Patient age	26,0	26,0	4,0	54,0	9,7
Length of history	16,0	15,0	1,0	38,0	8,8
Age at onset	10,8	8,0	0,0	45,0	10,1
Seizure frequency	479,7	150,0	2,0	5000,0	808,4
Recent seizure frequency	434,9	150,0	0,0	3500,0	623,8
Cumulated seizure number	7460,0	2000,0	20,0	64000,0	13140,4
Time since last seizure	9,5	2,0	0,1	180,0	24,4

Temporal group-normal rCBF (n=36)

variable	mean	median	minimum	maximum	std.dev.
Patient age	28,7	29,0	15,0	53,0	9,1
Length of history	15,3	15,5	2,0	28,0	7,7
Age at onset	14,1	13,5	0,0	41,0	10,0
Seizure frequency	453,3	295,0	2,0	4000,0	764,5
Recent seizure frequency	363,7	150,0	2,0	2000,0	472,3
Cumulated seizure number	7763,5	3850,1	50,0	64000,0	13054,0
Time since last seizure	6,6	2,0	0,6	60,0	11,7

Temporal group-abnormal rCBF (n=45)

variable	mean	median	minimum	maximum	std.dev.
Patient age	23,8	23,0	4,0	54,0	9,9
Length of history	16,2	14,5	1,0	38,0	9,5
Age at onset	8,3	5,0	1,0	45,0	9,5
Seizure frequency	510,9	150,0	2,0	5000,0	856,9
Recent seizure frequency	502,5	150,0	0,0	3500,0	727,7
Cumulated seizure number	7454,4	2950,0	20,0	55000,0	12692,3
Time since last seizure	12,0	2,0	0,1	180,0	31,3

EXRATEMPORAL GROUP (n=11)

variable	mean	median	minimum	maximum	std.dev.
Patient age	24,9	24,0	6,0	38,0	9,0
Length of history	14,7	19,0	1,0	25,0	8,0
Age at onset	10,2	10,0	1,0	19,0	6,0
Seizure frequency	1268,2	500,0	50,0	7200,0	2057,1
Recent seizure frequency	1286,4	500,0	0,0	7200,0	2060,7
Cumulated seizure number	10418,0	3500,0	600,0	40000,0	12234,0
Time since last seizure	14,3	1,0	0,1	90,0	29,0

Table 2.3

VISUAL AND NUMERIC ANALYSIS OF IMAGES

Temporal group

Patient	Visual report of scan			Asymmetry index ROI (%) Frontal	Bas Gang Thalamic	Mesial Temp	Lateral Temp	Parietal	Occipital
1	0	0	0	-0,8	-1,1	-1,1	-1,2	-3,4	-1,9	-2,7
2	2	0	4	-2	3,5	3,5	-6,3	-10,8	-5	3,1
3	2	0	4	12	6,5	6,5	-11,3	-19,5	1,1	-6,1
4	0	0	0	3,3	2,5	2,5	-0,4	-4,4	2,5	3,4
5	0	0	0	-2,5	-2,2	-2,2	3,1	0,8	-4,7	3,8
6	2	0	4	-7,9	-0,5	-0,5	-13,4	-11,2	-9,1	-1,5
7	0	0	0	1,9	0,0	0	-0,1	0,1	-2,6	-6,8
8	2	0	4	-1,6	2,7	-2,7	-12,1	-8,1	-2	-6,8
9	2	5	4	9,9	-12,3	-12,3	8,8	6,8	-5,3	-3,1
10	2	0	4	-2,1	-12,6	-12,6	5	-13,9		0,6
11	0	0	0	-6,5	4,3	4,3	-5,7	-8,7	6,1	0,4
12	0	0	0	8,6	-2,9	-2,9	3,5	-7,2	-5,1	-2,8
13	0	0	0	4,2	-0,4	-0,4	0,6	-8,5	-3,1	-1,5
14	0	0	0	2,4	9,7	9,7	1	-5,8	-8,7	-6,4
15	2	5	4	-1,8	2,4	2,4	12,8	3	0	-1,6
16	0	0	0	-3,9	4,5	4,5	2,7	0,7	1,3	1,5
17	2	5	9	-1,9	3,0	3	6	10,8	-2,5	0,1
18	0	0	0	1,2	0,8	0,8	0,2	-6,5	-7,6	-1,6
19	0	0	0	-4	-5,9	-5,9	6,1	0,6	3,5	-3,6
20	0	0	0	-6,5	5,2	5,2	1,6	2	0,7	-0,1
21	2	0	4	2,8	-11,3	-5,4	-4,4	11,2	-9,8	-2,6
22	2	5	4	2,5	9,3	9,3	2,8	10,8	1,5	-5,3
23	0	0	0	-0,8	0,0	0	-10,9	-6,8	0	1
24	0	0	0	-10,1	-1,1	-1,1	-5,4	-7,3	-0,5	-1,3
25	2	5	4	4,4	-1,5	-1,5	9,2	0,9	3,4	1,4
26	0	0	0	1,6	4,2	4,2	-2,1	1,8	4,1	1,8
27	0	0	0	2,7	3,3	3,3	-7,5	-7,2	6	-0,3
28	2	0	4	-6,8	-4,0	-4	-4,3	-7,6	-2	-2,3
29	0	0	0	-6,2	-0,6	-0,6	-1,9	-1,9	-9	-0,3
30	0	0	0	2,2	6,9	6,9	1,9	-5,9	1	-5,5
31	0	0	0	4,9	-3,3	-3,3	-1,6	0,8	-3,5	-1,8
32	0	0	0	-6,9	-3,4	-3,4	-4,2	-3,2	-2,1	1,5
33	2	0	4	4,7	-0,2	-0,2	-3,7	-12,3	0,2	-3,8
34	2	5	4	-0,5	12,0	12	13	5,1	-0,3	-0,2
35	0	0	0	0,9	4,2	4,2	-5,3	-5,7	-1	0,7
36	2	5	4	4,7	5,2	5,2	5,1	2,4	-6,1	0
37	2	5	9	5,8	11,1	11,1	6,4	3,4	10,1	0,6
38	0	0	0	-3,4	0,8	0,8	-1,4	-5,2	-3,8	3,5
39	0	0	0	1,3	-2,6	-2,6	-0,4	-17,9	-7,8	1,4
40	2	5	4	3	-5,5	-5,5	15,3	1,1	-0,2	2,6
41	0	0	0	0,9	-7,5	7,5	-3,1	-10,8	0,2	1,3
42	2	0	4	-0,6	-2,1	-2,1	-1,4	-5,1	-2,2	-1,9
43	0	0	0	8,5	-8,2	-8,2	-0,5	-4,8	-5,6	0,3
44	2	0	4	4,9	-2,9	-2,9	-1,7	-9,1	-4,4	-3
45	0	0	0	1,4	-9,4	-9,4	4,6	-2,3	-2,3	1,2
46	0	0	0	-2,8	4,8	4,8	-2,7	-10,1	-3,9	1,1
47	0	0	0	-3	1,1	1,1	-4,2	-2,6	-11,8	0,4
48	2	0	4	1,9	2,0	2	-9,4	-23,6	-5,4	-3
49	0	0	0	-0,2	-3,7	-3,7	-1,2	0,9	-1	0,3
50	2	5	4	8,1	-9,8	-9,8	8,3	4	-3,9	-4,8
51	2	0	4	1,1	-3,1	-3,1	-1	-2,4	-2	-1,1
52	2	0	4	-0,5	-1,2	-1,2	-8,8	-15,1	7,9	0,1
53	0	0	0	7	4,7	4,7	5,1	-2,7	-5,1	-2,3
54	0	0	0	5,3	2,5	2,5	-3	4,7	-8,9	0
55	0	0	0	7,4	7,9	7,9	8,5	-10	-3,7	1,3

Table 2.3

Patient	Visual report of scan			Asymmetry index ROI (%) Frontal	Bas Gang Thalamic		Mesial Temp	Lateral Temp	Parietal	Occipital
56	2	5	4	-0,7	-3,5	-3,5	12,1	3,7	-0,9	4,7
57	2	5	4	0,8	5,6	5,6	-1,7	5,7	-3,3	-2,3
58	2	0	4	-1,9	1,7	1,7	-3,2	-7,2	-4,6	5,2
59	2	6	4	-3,8	4,5	4,5	-6	-10,5		2,7
60	2	0	4	3,9	0,3	0,3	-9,5	-11,3	-4,8	2,8
61	2	5	4	0,5	0,4	0,4	13,9	2,7	-1,1	4,6
62	2	0	4	-10,2	-0,3	-7,3	-9	-28,6	-7	-11,9
63	2	0	4	7,2	0,3	0,3	-8,3	-5	-3,8	3,1
64	2	0	4	-5,6	-0,6	-0,6	3,1	-21,7	-8,2	2,1
65	2	7	4	4,4	0,4	0,4	-2	-5,7	2,3	2,1
66	0	0	0	5,3	7,2	7,2	-6,1	-7	-1,8	-0,6
67	0	0	0	-1,3	5,1	5,1	-2	12,8	-7,6	-5,5
68	2	0	4	0,7	-2,8	-2,8	1,2	-1	-0,5	6,4
69	2	0	1	-14,3	-10,0	-0,4	-24,3	-41,6	-34,7	-3,9
70	0	0	0	4,1	5,4	5,4	3,1	-5,8	-5,4	-3,1
71	2	0	4	0,6	0,1	3,1	-3,8	-7,5	4,1	-6,6
72	1	5	9	-6,5	3,8	3,8	2,9	-14,6	-0,3	-0,7
73	2	5	4	8,2	0,8	0,8	-6,1	-4,6	3,1	-1,1
74	2	0	4	5,5	7,2	7,2	-5,9	-14,8	-6,7	-4,7
75	0	0	0	0,3	4,7	4,7	5,9	15,4	1,6	1,9
76	0	0	0	1,6	-8,1	-8,1	8,5	-4,3	-7,3	-2,8
77	2	0	1	-10,9	-7,3	-4,4	0,9	-7,1	1,9	3,3
78	2	0	4	-9,7	8,5	8,5	4,7	-9,8	5,9	-1,3
79	2	0	4	-8,7	10,9	-4,4	1,2	-9,7	-8,8	3,4
80	2	0	4	-0,3	3,1	3,1	-10,9	-26,9	-1,6	-2
81	0	0	0	2,6	-5,0	-5	-3,8	-2,3	-4,9	-2,3
Extratemporal group										
1	0	0	0	3,4	6,0	0,0	-2,4	-5,9	0,1	3,6
2	0	0	0	0,8	5,9	0,0	5,6	-0,4	-5,0	-0,9
3	0	0	0	2,1	0,3	-3,8	1,4	-3,6	-1,5	-1,5
4	0	0	0	1,1	-1,3	-7,1	1,7	-6,0	5,4	-4,3
5	0	0	0	0,6	0,7	6,6	-4,6	-3,9	-7,1	-3,7
6	0	0	0	0,1	-2,7	-2,7	-1,5	3,7	-2,5	1,4
7	0	0	0	2,8	5,9	3,8	1,7	-3,5	0,5	-2,7
8	0	0	0	-1,4	-2,0	-1,7	1,2	3,9	1,3	-1,1
9	0	0	0	-4,1	-6,0	0,1	7,7	-0,1	-1,0	2,3
10	0	0	0	-1,6	2,1	-1,5	4,4	-2,3	-7,6	-4,3
11	0	0	0	5,3	-3,8	7,5	2,3	2,3	5,4	0,3

Codes for visual reports

204 Left temporal hypoperfusion
254 Right temporal hypoperfusion
264 Bilateral temporal hypoperfusion
209 Left frontal and temporal hypoperfusion
259 Right frontal and temporal hypoperfusion
201 Left hemisphere hypoperfusion
159 Right temporal and frontal hyperperfusion
274 Right hippocampal hyperperfusion with lateral temporal hypoperfusion

Table 2.4

VISUAL AND NUMERICAL ANALYSIS OF IMAGES

Summary of results of interictal HMPAO SPECT

Temporal group (n=81)

Visual analysis	normal - 38/81=47% abnormal - 43/81=53%
	temporal hypoperfusion - 38 (24 left, 12 right, 1 bilateral) frontotemporal hypoperfusion - 2 (both right) hemispheric hypoperfusion - 2 (left)
	temporal hyperperfusion - 1 (right)
	Hippocampal hyperperfusion with lateral temporal hypoperfusion - 1(right)
Numerical analysis	normal - 42=53% abnormal - 39=47%
	temporal hypoperfusion - 33 (20 left, 13 right) frontal hypoperfusion - 1 (left) parietal hypoperfusion - 3 (2left, 1 right) hemispheric hypoperfusion - 1 (left)
	temporal hyperperfusion - 1 (right)

Extratemporal group (n=11)

Visual analysis	normal - 11 (all)
Numerical analysis	normal - 11 (all)

Table 2.5

NUMERICAL ANALYSIS: DESCRIPTIVE STATISTICS OF ABSOLUTE ASYMMETRY INDICES

Whole temporal group (n=81)

ROI	mean	median	minimum	maximum	std.dev.
Frontal	4,0	3,0	0,2	14,3	3,1
Basal ganglia	4,3	3,5	0,0	12,6	3,4
Thalamus	4,3	3,5	0,0	12,6	3,4
mes Temporal	5,5	4,6	0,1	24,3	4,3
lat Temporal	7,9	5,9	0,1	41,6	7,1
Parietal	4,2	3,5	0,0	34,7	4,5
Occipital	2,5	2,0	0,0	11,9	2,1

Temporal group - normal rCBF (n=38)

ROI	mean	median	minimum	maximum	std.dev.
Frontal	3,8	3,2	0,2	10,1	2,6
Basal ganglia	4,2	4,3	0,0	9,7	2,7
Thalamus	4,2	4,3	0,0	9,7	2,7
mes Temporal	3,5	3,1	0,1	10,9	2,7
lat Temporal	5,6	5,0	0,1	17,9	4,3
Parietal	4,3	3,9	0,0	11,8	2,9
Occipital	2,1	1,5	0,0	6,8	1,8

Temporal goup - abnormal rCBF (n=43)

ROI	mean	median	minimum	maximum	std.dev.
Frontal	4,1	3,0	0,3	14,3	3,5
Thalamus	4,5	3,1	0,1	12,6	3,9
Basal ganglia	4,5	3,1	0,1	12,6	3,9
mes Temporal	7,2	6,1	1,0	24,3	4,7
lat Temporal	9,8	7,6	0,9	41,6	8,3
Parietal	4,2	3,3	0,0	34,7	5,4
Occipital	2,9	2,6	0,0	11,9	2,3

Extratemporal group (n=11)

ROI	mean	median	minimum	maximum	std.dev.
Frontal	2,1	1,6	0,1	5,3	1,6
Basal ganglia	3,3	2,7	0,3	6,0	2,3
Thalamus	3,2	2,7	0,0	7,5	2,9
mes Temporal	3,1	2,3	1,2	7,7	2,1
lat Temporal	3,2	3,6	0,1	6,0	1,9
Parietal	3,4	2,5	0,1	7,6	2,7
Occipital	2,4	2,3	0,3	4,3	1,4

Table 2.6

NUMERICAL ANALYSIS OF IMAGES

Comparison of asymmetries in images visually reported as abnormal

	Region of interest; asymmetry index (%)			
Patient	mes. Temp	lat. Temp	Frontal	Parietal
2	6,3	10,8		
3	11,3	19,5		
6	13,4	11,2		
8	12,1	8,1		
9	8,8	6,8		
10	5	13,9		
15	12,8	3		
17	6	10,8	1,9	2,5
21	4,4	11,2		
22	2,8	10,8		
25	9,2	0,9		
28	4,3	7,6		
33	3,7	12,3		
34	13	5,1		
36	5,1	2,4		
37	6,4	3,4	5,8	5,4
40	15,3	1,1		
42	1,4	5,1		
44	1,7	9,1		
48	9,4	23,6		
50	8,3	4		
51	1	2,4		
52	8,8	15,1		
56	12,1	3,7		
57	1,7	5,7		
58	3,2	7,2		
59	6	10,5		
60	9,5	11,3		
61	13,9	2,7		
62	9	28,6		
63	8,3	5		
64	3,1	21,7		
68	1,2	1		
69	24,3	41,6	14,3	34,7
71	3,8	7,5		
73	6,1	4,6		
74	5,9	14,8		
77	7,1	1,9	8	3
78	4,7	9,8		
79	9,7	8,8		
80	10,9	26,9		

Chapter 2

Discussion

Accuracy and limitations of data

The data acquired in this study may be divided into clinical data, data from visual analysis of images and data from numeric analysis of images. The methods of acquisition of the data entail some potential inaccuracies and uncertainties.

1. Clinical data

Patient age can be regarded as accurate. Age at presentation of epilepsy, and therefore the length of seizure history, was a matter of record in all but 6 patients whose epilepsies began before their available records (these patients were, however, good witnesses). A few patients had suffered clinical events of uncertain nature for some time before medical attention was sought, or before a diagnosis was made. In all of these cases in this study, a retrospective diagnosis of seizures could be made with confidence, but the patient and/or parents were uncertain of the age of onset in several cases, the uncertainty amounting to no more than 1 year in any patient.

Seizure frequency is the most problematic of the clinical data. Although each patient's case notes were gone through carefully, many of the records of admissions or outpatient visits did not give a figure for seizure frequency, and the patient's memory or that of relatives had to be relied on. Recent seizure frequency figures are certainly more likely to have reflected accurately the patient's experience. Where diurnal seizures were known to occur without the patient being aware of it, every effort was made to obtain good accounts of seizure frequency from relatives. Inevitably, some of these will have been missed, as will some nocturnal seizures. These factors will lead to a general underestimation of seizure frequency, affecting some patients (e.g. those living alone) more than others.

Seizure frequency and cumulated seizure number are therefore regarded as representing a general indication of seizure control over the years, and the lack of correlations with other data are interpreted in the light of this.

2. Visual interpretation of images

The two observers who interpreted the images in this study were experienced in interpreting SPECT images, and interpreted those images according to the same criteria (see methods section). Few disagreements between observers occurred, and those were all resolved by consensus conference. Independent analysis followed by consensus conference for disagreements is an accepted method for producing consistent visual interpretation of images (Rowe et al., 1989a; b; 1991a; b; Lee et al., 1986;1987a; b; 1988; Shen et al., 1990). In visually assessing scans, observers made the assumption that, where two areas of the brain had different signal (e.g. one temporal lobe appeared to have lower activity than the rest of the cortex) that it was the smaller area which was abnormal. Assessment depended not only on side-to-side differences, but on the normal relationship between ipsilateral structures. For example, in the normal SPECT image, perfusion in the mesial and lateral temporal cortex are roughly the same, and the same as perfusion in the frontal cortex. Perfusion in the mesial occipital cortex and cerebellum is higher, but lower in the lateral occipital cortex (Fig 4.1). In assessing the significance of a possible abnormality in perfusion, account was taken of whether it had well defined boundaries and whether those boundaries respected those of anatomic structures. The images produced were of sufficient spatial resolution to allow confident and precise anatomical location of abnormalities in the great majority of cases. Doubtful cases were resolved by direct comparison with the patient's anatomical imaging (CT or MRI). This type of procedure gave an interictal abnormality rate similar to that found in the studies of Rowe et al. (1989b; 1991a), whose numeric asymmetry threshold was also similar to that in this study (8.1-10.0% cf 8% in this study).

The experiment carried out to define numerically the method of visual analysis, was designed to do so only to a limited extent, that of quantifying (in terms of the asymmetry index used) what asymmetry of the color scale was regarded by the observers as being outside normal limits. This took no account of other factors such as the morphology of an abnormality (see above) which were normally considered as part of visual analysis. The upper limit of normal of 8% given by this method was remarkably consistent, a consistency which probably reflected the experience of the observers. This internal consistency of the results of visual analysis, and their consistency with other work producing similar abnormality rates, support the accuracy of the observers and the methods used.

c. Numeric interpretation of images

HMPAO SPECT can produce quantified images of cerebral perfusion in three ways;

1. Absolute quantition of cerebral perfusion. There are no methods available which are practicable in the clinical setting.
2. Semiquantitation (Rowe et al., 1989b; Rowe et al., 1991a; b). Regions of interest are defined on slices from the scan, and the number of counts per voxel computed. The ROIs are expressed as a percentage of a reference area which is assumed to have a constant perfusion. The choice of reference area is problematic, particularly in epilepsy where even subcortical structures and the cerebellum (Sperling et al., 1990; Sackellares et al., 1990; Henry et al., 1990; Bernardi et al., 1983; Duncan et al., 1990b; Theodore et al., 1986b; Rowe et al., 1991a) may be asymmetric. The best approach is probably to use the average value for the whole brain, accepting that it will contain and be affected by the abnormal area; the larger the abnormality, the bigger the error. This approach makes the same assumption as visual analysis of images i.e. that if the brain consists of two areas of different signal, it is the smaller area that is likely to represent the abnormality.
3. Quantitation of asymmetry. ROIs are defined and the number of counts per pixel computed. An asymmetry index is calculated. This gives no indication as to whether a structure on one side is hypoperfusion or the homotopic structure is hyperperfused.

While the second approach does give an indication of which is the abnormal side where there is an asymmetry, the abnormality will be underestimated to a greater extent as its size increases, therefore making correlation of numerical analysis with clinical and other factors difficult. Because of this problem, and because visual analysis was also carried out, the third type of numerical analysis was chosen for the present study as being the simplest that would permit assessment of the degree of an abnormality, and correlation of perfusion abnormalities with other factors. A comparison of localisation using simple asymmetry indices and normalised data has shown the former to be a better predictor of the side of the focus (Rowe et al., 1991a).

Temporal group

Comparison with previous SPECT work and with PET studies of regional cerebral blood flow and local cerebral metabolic rate

1. Proportion of patients showing abnormalities of rCBF

In this series 53% of patients had abnormal rCBF. This compares with the range for previous studies of temporal lobe epilepsy of 46-80% (Bonte et al., 1983a; Grasso et al 1989; Rowe et al, 1991a; Ryding et al., 1988; Shen et al., 1990; Uren et al., 1983). Only the study at the lower end of this range showed a lower proportion than the present study (Rowe et al., 1991a). There may be several reasons for these differences.

The present study was of patients with a wide range of seizure frequencies, while those previous studies which were of reasonably large size and used comparable imaging methods (i.e. those using tomographic imaging of the distribution of IMP, HIPDM or HMPAO: (Bonte et al., 1983; Uren et al., 1983; Ryding et al., 1988; Grasso et al 1989; Rowe et al, 1991a; Shen et al., 1990)) have been of patients with intractable disease, and presumably higher seizure frequencies. Mean seizure frequency in the present study was higher in patients with abnormal rCBF (511/year c.f. 453/year), albeit the difference did not reach statistical significance. Rowe et al. (1991) suggested that one reason for these differences in abnormality rate could be the fact that their study consisted of only presurgical patients with 'hard' EEG localisation data. This was the case in 40/81 of the temporal group of patients in the present study. Of these patients 23/40 (57.5%) had abnormal rCBF, compared with 20/41 (49%) of the non presurgical patients. This provides no support for differences in seizure frequency as an explanation for the differences in abnormality rate found in different studies.

Differences in analysis of images could also account for differences in the proportion of patients with abnormal rCBF. Comparisons in this respect are difficult. The group of Rowe et al., (1989b; 1991a; b) and that of Lee et al. (Lee et al., 1986; 1987a; b; 1988; Shen et al., 1990) use the same procedure as this study, that of reporting by independent observers. Their rates of abnormality differ substantially, at 46% for Rowe's (1991) study and 73% for Lee's (Shen et al, 1990). Both had similar patient populations. Some of the results of Shen et al. were based on multiple interictal studies, which might explain a higher abnormality rate if interictal hypoperfusion were a variable (in time) phenomenon. Rowe et al., (1990a) documented two patients in whom this appeared to be the case, although other evidence

suggests that both interictal hypometabolism and hypoperfusion are stable findings in some patients at least (Kuhl et al., 1980; Jibiki et al., 1990).

The use of different perfusion tracers might result in different sensitivity to abnormalities. The studies of Lee et al., and Shen et al., use HIPDM as a tracer. They report a high abnormality rate (e.g. 73% for Shen et al.), while the present study and those of Rowe et al. used HMPAO, both groups finding a lower abnormality rate. However, Shen et al. performed multiple studies in some patients. Other series finding such a high abnormality rate (Biersack et al., 1986; Podreka et al., 1988; Grasso et al., 1989) have also found a relatively high proportion of false localising (with respect to EEG data) abnormalities. The threshold for reporting abnormalities was not numerically defined in any of these studies, and so could not be excluded as an explanation for this difference.

Differences in the spatial resolution of the imaging equipment used do not in themselves explain differences in abnormality rate. The study with the highest resolution equipment is the present one (53%), then Rowe et al. (46%), then Shen et al. (73%), then Grasso et al. (74%).

No single factor can explain these differences in abnormality rate. However, the present study and that of Rowe et al., (1991a) used similar methods (tracer, spatial resolution of imager, reporting practice) and have similar results despite differing patient populations (a full spectrum of disease severity vs. presurgical patients with severe disease only). Shen et al., (1990) used a different tracer, repeated SPECT in some patients, used an imager with slightly poorer spatial resolution, a similar reporting practice, in a patient population with severe disease, and obtained a high abnormality rate.

Considering the three groups with most experience of SPECT cerebral perfusion studies in epilepsy, then, it appears that the use of different tracers and the practice of repeating interictal studies remain likely explanations for the differences seen. Relative over-reporting may be responsible for high abnormality rates in studies which also have high false-localisation rates.

Type of abnormality of rCBF

Rowe's (1991a) study included only 2/51 patients with abnormalities other than unilateral temporal hypoperfusion (bilateral temporal hypoperperfusion). Lee et al., (1988) had 9/13 patient with extensive hemispheric hypoperfusion, but Shen et al. (1990) only had 2/34 with extensive hypoperfusion. Adding these series together, this makes 11% of patients with hypoperfusion extending outside the

temporal lobe, compared with 4.5% in the present study. This difference may be due to the imaging methods used. The highest proportions of patients with extensive hypoperfusion were seen in studies using low resolution equipment and slice orientations where (in particular) the distiction between temporal lobe and adjacent frontal lobe might be difficult to make. Rowe's group used equipment with resolution close to that in this study (12mm c.f. 10mm), and found 4% of patients with extensive hypoperfusion, similar to the proportion in this study.

This study found interictal hyperperfusion in only two patients. In one, who had hyperperfusion of the hippocamus with lateral hypoperfusion, the scan was repeated with the same result. No EEG recording was carried out at the time of the injection, so subclinical seizure activity could not be ruled out as a cause, although there was no clinical indication of it. In the other case hyperperfusion involved the lateral temporal and posterior frontal cortex. EEG was recorded at the time of the injection, no seizure activity was recorded, and none had been reported in the previous 3 weeks. This phenomenon has been reported previously (Duncan et al., 1990a; Grasso et al., 1989; Stefan et al., 1990; Uren et al., 1983), and is of uncertain significance. It is difficult to believe that the hyperperfusion is secondary to the metabolic demand of electrical activity, when the patient is clinically normal with no discharges on EEG. Postictal metabolic debt would also seem an unlikely explanation, given that the phenomenon is seen hours or days after the last seizure.

A previous study using HMPAO SPECT where the images were reported by the same observers as in the present study (Duncan et al., 1990a) found interictal hyperperfusion in 30% of a series of 40 patients with complex partial seizures. The software used to construct the images from raw data in the present study was more sophisticated, and it may be that the difference is due to the change. Since this early study the images have been reconstructed using the new software. Only in 3/12 cases did the same observers think there was unequivocal hyperperfusion. A change in reporting practice (e.g. an increase in threshold for reporting an asymmetry as significant) might also explain this difference, and could not be ruled out.

Comparison with PET studies of ICMR

In general SPECT studies of cerebral perfusion, have given similar results to PET studies of metabolic rate, but with a lower proportion of patients showing abnormalities, and some SPECT studies showing patients with interictal hyperperfusion (for review of PET and SPECT studies, see Chapter 1). The same applies to the present study, the only minor exception being that 2 patients showed hypoperfusion of only part of the temporal lobe, a feature not reported in PET studies.

Such abnormalities might not be detectable using PET or SPECT systems of lower spatial resolution than in the present study.

Numeric analysis of images

Comparison with the results of visual analysis

The method of numeric analysis employed in this study could not in itself provide a 'report' in the way that visual analysis could, in that it could identify structures in which the asymmetry in perfusion was outside the chosen normal limits, but could not in itself identify the abnormal side, or detect bilateral and symmetric abnormalities. Comparison between visual and numerical analysis was therefore made on the basis of whether the results of the numeric analysis of an image was *compatible* with the results of visual analysis, rather than whether the two methods provided exactly the same information.

Numeric analysis identified fewer abnormalities overall than did visual analysis, 39/81 (47%) as opposed to 43/81 (53%). The visual/numerical analysis experiment showed that, disregarding the morphology or extent of an abnormality, the two observers regarded asymmetries of 8% and more as abnormal. The upper limit of normal that had been chosen for numerical analysis was 9%. Lowering the limit of normal to 8% would have made abnormal 6 scans which had been visually and numerically interpreted as normal. It would have identified abnormalities in 3 scans interpreted numerically as normal and visually as abnormal, the site in 2 cases agreeing with numerical analysis, and in 1 case disagreeing. It would appear, therefore, lowering the upper limit of normal would have made agreement between the methods worse, that the discrepancy in limit of normal was therefore not in itself the cause of the difference in the number of scans identified as abnormal.

There are two other possible sources for discrepancies. Firstly, the regions of interest used were made up of double thickness slices, and therefore included a reasonably large volume of brain. This volume (as indicated by the area of the region of interest) was relatively constant from patient to patient, and was usually smaller than the total volume of the structure being measured. In contrast, the volume of brain which was considered visually to be abnormal varied. At minimum, it had to involve more than one slice, but the area considered as significantly abnormal varied according to amount by which the signal differed from surrounding tissue. Secondly, an abnormality was more likely to be considered significant on visual analysis if its boundaries respected those of an anatomical structure and if they were well defined, even if the difference in signal looked quite small. In the study of Rowe et al. (1991a)

21/46 (46%) were reported visually to have abnormal rCBF compared to 27/46 (58%) of patients who had asymmetry indices outside their normal range of -10 to +8.1% (based on 10 normals). These results were based on temporal ROIs only, and are similar to those in the present study. There are currently no other studies with results comparable to the present one.

Mesial vs lateral temporal hypoperfusion

Until the present study, the difference in degree of mesial and lateral hypoperfusion has not been addressed. One small PET (Sackellares et al, 1990) study showed the degree of hypometabolism tends to be greater in the lateral temporal cortex in most (13/17) of their patients, but with 2 patients showing the reverse, a higher proportion than in the present study (25/41). Their 17 patients all had confirmation of a mesial rather than lateral temporal focus, a confirmation available in 38 of the patients in this study, 23 of whom had temporal hypoperfusion. Hypoperfusion was greater in the lateral cortex in 14/23, a proportion not statistically diferent from the results of the group as a whole or that obtained by Sackelleres et al (Chi^2).

Differences in left-right asymmetry

Absolute asymmetry was greater for the left lateral temporal ROI as compared to the right, seen both as a statistically significant difference in means, and in the shape of the frequency distribution (Fig 2.15) (and was probably reflected in the higher number of patients in whom left temporal hypoperfusion was visually reported). This asymmetry in abnormality of rCBF was also found by Valmier et al (1987) Rowe et al. (1991a), and has been found to be true for local metabolic rate (Theodore et al., 1988).

The reason for the difference is unclear. It has been suggested that lateral temporal hypoperfusion in patients with mesial temporal foci is due to deafferentation effects (Rowe et al., 1991b). The functional importance of the hippocampus is greater on the dominant side (Goldstein & Polkey, 1993), and it may be that dysfunction causes greater distant effects. In this study there was no difference in the proportion of patients with hypoperfusion predominant in mesial and lateral ROIs between groups with right and left sided abnormalities which might support this explanation. Patients with temporal lobe epilepsy do have a high incidence of anomalous dominance (see below), which might account for individual variations.

Asymmetry of the basal ganglia and thalamus.

Previous studies of cerebral perfusion have not addressed the matter of abnormalities of subcortical structures such as the basal ganglia and the thalamus, in most cases because the imaging methods have lacked the spatial resolution to distinguish these structures. Studies of metabolic rate have shown that changes in the basal ganglia and thalamus tend to mirror those in cortical structures i.e to show hypometabolism when the temporal cortex is hypometabolic (Bernardi et al., 1983; Henry et al., 1990; Sackellares et al., 1990; Sperling et al., 1990). There were two patients in this study where the changes were opposite in direction, but most agreed.

Correlation of regional cerebral blood flow with clinical data

Correlations can be made on the basis of visual interpretation of images by dividng patients into normal and abnormal groups and comparing clinical parameters in the groups, or by simply correlating data from numerical analysis of images (e.g. absolute values for lCMR or symmetry indices) with clinical parameters.

Two studies, one of 89 patients (Duncan et al., 1990c) and one of 63 patients (Duncan et al., 1992) have used the first method. The former study found that patients with abnormal cerebral perfusion had longer histories of epilepsy, and earlier age at onset, and a higher seizure frequency, i.e the same as in the present study, although the only statistically significant difference was in age at onset. The latter study found the same types of difference, but only the difference in length of history was significant in this instance.

The striking and statistically significant difference in this study was in age at onset of epilepsy. Not only were the means of age at onset different for the two groups, but the frequency distributions looked different: although both tended to decrease with time, the normal group could be viewed as a normal distribution biased toward early onset. It differed significantly from an inverse exponential distribution ($p=0.980$), while the abnormal group did not ($p=0.280$). Rowe et al. (1991a; b), Theodore et al. (1988) and Valmier et al. (1987) used numerical data to correlate clinical data with the degree rather than incidence of abnormality, and found correlations with age at onset of epilepsy (Rowe et al., 1991), length of history (Theodore et al., 1988) and seizure frequency (Valmier et al., 1987). In the present study there was no correlation between degree of abnormality and any of the clinical parameters. Numerical data did however support the association between the occurrence (rather

than degree) of hypoperfusion to the extent that there was a good correlation (R^2=0.670, p=0.001) between age at onset and the sum of asymmetry indices for all the patients of a given age at onset.

The present study and that of Duncan et al. (1990c) are the largest to make correlations between clinical factors and focal abnormalities of cerebral perfusion, and the present study is the only one to correlate clinical factors with both the incidence and the degree of abnormality, using both visual and numerical data. Both studies include patients with a wider range in these parameters than previous studies. In the present study, visual and numerical methods agreed in identifying age at onset as the most important factor in determining the occurrence of abnormal cerebral perfusion. While most evidence therefore points to age at onset as being the most important association, there is some evidence of associations with length of history and seizure frequency. The latter in particular cannot be ruled out, given the inaccurate nature of seizure frequency data (see above).

Correlation between the site of abnormality in cerebral perfusion and the site of the epileptic focus

The majority of temporal lobe seizures originate in the hippocampus (Quesney, 1986; Wieser, 1983). Most patients with complex partial seizures have a mesial temporal lobe focus, and most of the remainder have frontal lobe foci (Williamson et al., 1987). All patients with complex partial seizures presenting to an epilepsy clinic will have some estimation of the site of the focus made, usually based on clinical factors and surface interictal EEG data. Figures for the former are not available, but false lateralisations based on surface interictal EEG vary from 34% to 5% depending on the methods used and patient selection (Lieb et al, 1981)). However, in patients responding well to drug treatment, the localisation of the focus has no therapeutic implications, and further investigations to establish localisation are not justified (in terms either of cost or of invasiveness). For these reasons approximately half (41/81) of the patients in this study had localisation based only on clinical factors and interictal EEG. The errors most likely to result from this are that some patients with frontal foci might be are misplaced in the temporal group, and that patients in either group might be falsely lateralised. In the event, the only clear inconsistency between interictal HMAPO SPECT localisation and other localising data was in patient 59, who had bilateral temporal hypoperfusion but a unilateral focus, and patient 28 who had unilateral temporal hypoperfusion and bilateral temporal foci. Both patients

had localisation based on videotelemetry with foramen ovale recordings, although obviously in only one case was localisation confirmed by an operative result. This low false localisation rate is consistent with previous studies, in that those studies (Rowe et al., 1989b;1991a; b) with low proportions of patients showing abnormal cerebral perfusion tend to have low proportions of patients with false localising SPECT abnormalities. This study included no patients with evidence of a lateral temporal focus, and therefore did not provide any evidence that abnormalities of cerebral perfusion are different in mesial and lateral foci.

The data for the lateral temporal ROI were different from the others in having an obviously different frequency distribution, being the only ROI to show a significantly asymmetric distribution, and having a larger mean asymmetry than the others. The mesial temporal ROI showed the second largest mean asymmetry. The results of numeric analysis for the temporal group as a whole were therefore consistent with the focus localisation.

Possible reasons for interictal hypoperfusion

1. Anomalous location of function

Right hemisphere dominance, mixed dominance, and anomalous localisation of memory and speech function (e.g. where both verbal and visual memory are located in the same temporal lobe, or where there is representation of speech in both hemispheres) are relatively common in patients with temporal lobe epilepsy (Rausch & Walsh, 1984), particularly in temporal lobe epilepsy of early onset. The reason is thought to be that where seizures originate in one temporal lobe function which would normally develop in that temporal lobe develops in the contralateral temporal lobe. Motor dominance may also be affected, resulting in an excess incidence of left handedness in patients with temporal lobe epilepsy of early onset (Rausch & Walsh, 1984). This means that the temporal lobe that is the site of the focus does not function, and would therefore be expected to have lower metabolic rate and blood flow. This explanation is consistent with the correlation found in this study between hypoperfusion and epilepsy of early onset.

Where the anatomic location of neuropsychological function is uncertain, one would not expect to find a good correlation between the anatomic location of focal neuropsychological deficits and areas of reduced cerebral perfusion (e.g. in a patient with a left temporal focus and left temporal hypoperfusion both visual and verbal memory might be located in the right temporal lobe, with no neuropsychological deficit). This does appear to be the case; Homan et al. (1989) found a good correlation

between neuropsychological and perfusion deficits in a large group of patients, but not on the individual level. Such a finding might also indicate that more than one factor was responsible for hypoperfusion.

2. Interictal and subclinical ictal epileptiform activity

Interictal spiking activity has been shown to be associated with neuronal inhibition in surrounding tissues; ictal discharges are also associated with surround inhibition (Prince et al., 1967; Gumnit & Takahashi, 1975), and with hypometabolism and hypoperfusion in surrounding tissues, in man (see Chapter 3) and in animals (see Chapter 4). However, in 2 studies (Engel et al., 1982b; Theodore et al., 1983) no correlation was found between interictal hypometabolism and spiking on EEG. Since seizures are often followed by increases in spike activity which may last from a few hours up to 2 days (Gotman, 1991), a correlation between either seizure frequency or the time of scanning in relation to the most recent seizure, and hypoperfusion might be regarded as supporting a causal relationship between hypoperfusion and spiking, but there were no such relationships in the present study.

3. Neuronal loss

Neuronal loss occurs in the hippocampus of patients whose seizures originate in the mesial temporal lobe (Sommer, 1880, Meldrum & Corsellis, 1984; Babb & Brown 1986). It may also occur at sites distantly activated by seizure discharges (Duncan et al., 1990b; Leifer et al., 1991). This is thought to relate to the production of excess excitotoxic neurotransmitters such as glutamic acid (Cotman & Monaghan,1986; Greenamyre, 1986) during seizures. An association between hypoperfusion and length of seizure history, and possibly seizure frequency would be compatable with this mechanism. Such correlations were not found in this study but have been in other studies (Theodore et al., 1988; Valmier et al., 1987). Hippocampal neuronal loss might therefore contribute not only to low metabolism and blood flow locally, but more distantly in the lateral temporal lobe and its connections. Such neuronal loss is particularly conmmonly found in patients with temporal hypometabolism (Engel et al., 1982a). Of the 14 patients in the present series who had pathologically confirmed mesial temporal sclerosis, 11 had temporal hypoperfusion on interictal SPECT. This may simply be a selection effect; a history of febrile convulsions and the finding of unilateral temporal hypoperfusion were both factors which positively biased selection for surgical treatment. Rowe et al., (1991)

found mesial temporal sclerosis in only 54% of their cases with ipsilateral temporal hypoperfusion. Nonetheless, the distribution of temporal hypoperfusion weighted toward early age at onset of epilepsy found in the present study shows an interesting parallel with that of hippocampal sclerosis found by Sagar & Oxbury (1987).

Possible reasons for interictal hyperperfusion

In a previous study (Duncan et al., 1990a) where HMPAO injection was carried out with concurrent EEG recording, no evidence of subclinical seizure activity was found. There was no history of recent seizures, and no evidence of postictal change on EEG. In the present study EEG was not recorded, but there was no clinical evidence of recent or ongoing seizure activity.

Recent data suggest the possibility that HMPAO uptake overestimates blood flow in areas of reperfusion after cerebral infarction (Sperling & Lassen, 1993). It is possible that this happens in other circumstances, such as following repeated or lengthy seizures, and that these areas of high HMPAO uptake do not represent high flow at all. Duncan et al. (1990a) found that interictal hyperperfusion did not persist on rescanning in 50% of cases. In view of the point made earlier in this discussion regarding the effect on such findings of changes in image reconstruction software (and possibly of changes in reporting practice), the significance of this finding must be regarded as questionable. There are no other data available regarding interictal hyperperfusion, allowing little discussion of other possible causes, beyond pointing out the evidence against the involvement of ongoing seizure activity.

Extratemporal group

The small size of the extratemporal group, and the fact that all the scans were normal made comparisons between temporal and extratemporal patients difficult, in particular with respect to frequency distribution of asymmetry indices. While a larger series may well have found some patients with localised areas of hypoperfusion, the fact that none out of the 11 in this study showed abnormalities made the group significantly different from the temporal group in this respect ($p=0.005$), and does constitute evidence that interictal cerebral perfusion is different in patients with temporal and extratemporal foci.

Conclusions

1. Approximately half of patients with complex partial seizures of temporal lobe origin have significantly abnormal regional cerebral perfusion.
2. Most abnormalities consist of hypoperfusion in, or of greatest degree in, in the temporal lobe.
3. Hypoperfusion is greater in degree in the lateral rather than the mesial temporal lobe in most patients.
3. Patients whose epilepsy started at an early age are much more likely to have abnormal cerebral perfusion, but there is no correlation between age at onset of epilepsy and the degree of hypoperfusion. There may be weaker relationships with length of seizure history and seizure frequency.
4. The method of numerical analysis used has limitations but was useful in allowing correlation with other data. In this study it was in good agreement with the results of visual analysis.
5. The fact that no abnormalities were seen in the small extratemporal group of patients was statistically significant, and suggests that abnormal cerebral perfusion may be less common in such patients.

Chapter 3

Ictal and postictal regional cerebral blood flow in complex partial seizures

Introduction

Penfield (1933; 1937) made the first observations of changes in rCBF during and after focal seizures. These observations had the advantage of being continuous in time, but the disadvantages of involving patients with focal motor epilepsy only, and of including only a relatively small area of the surface of the brain. With the advent of EEG in the thirties, intraoperative induction of seizures ceased. Further study of rCBF changes during and soon after seizures then awaited the advent of in vivo imaging techniques, such as PET and SPECT. The utility of these was, however, limited by the need to have the patient in the scanner while the seizure was taking place, and by the relatively long time resolution of PET techniques. Amine tracers of rCBF such as IMP and HIPDM (Holman et al., 1984) overcame this problem to some extent. These compounds are taken up into brain tissue in the distribution of rCBF. The distribution is then fixed for several hours, allowing acquisition of images of rCBF at the time of injection to take place during that time.

The more recent development of HMPAO (Neirinckx et al., 1987: hexamethyl propyleneamine oxime - see introduction section, Chapter 4) improved on the temporal resolution of these compounds. The image given by ^{123}I-HIPDM, for example, reflects 75% of uptake over the first 2 minutes after injection and 25% over a further 30 minutes (Holman et al., 1984), while the image given by HMPAO reflects 90% of uptake over the first minute (Neirinckx et al., 1987). The distribution of HMPAO remains stable for longer than the amine compounds, allowing a longer time between injection and scanning. Labelling with ^{99m}Tc also makes HMPAO technically easier to use.

During the period of the present study series of patients have been studied using HIPDM (Lee et al., 1987a;1988; Shen et al., 1990). These have shown focal increases in rCBF, but have produced images lacking in spatial resolution, partly because of the use of low resolution scanning equipment, but also partly because a protracted period of tracer uptake will blur the morphology of any change in rCBF which has changed in extent during that time (much in the way that a long exposure will cause blurring of a photograph of a rapidly moving subject). Three studies using HMPAO have been carried out (Rowe et al., 1989b; 1991b; Newton et al., 1992) which have shown changes in rCBF in complex partial seizures of mesial temporal lobe

origin and have suggested a time course for these changes, i.e. that during the seizure the whole temporal lobe is hyperperfused, that in the early postictal period the lateral temporal cortex becomes hypoperfused, and that only in the late postictal period does the mesial temporal cortex become hypoperfused. Most complex partial seizures originate in the temporal lobe (Williamson et al., 1987). Of the rest, most originate in the frontal lobe. Complex partial seizures of extratemporal origin have not been studied, and the disturbances in perfusion associated with them are unknown.

The aims of the present study are:

1. To define the morphology of changes in cerebral perfusion during and soon after complex partial seizures of temporal origin, and to determine whether different changes are seen during and after seizures originating elsewhere in the brain.
2. To define the time course of any changes seen
3. To determine the relationship of ictal/postictal changes in cerebral perfusion with the location of the epileptic focus as defined by EEG and MRI.

Subjects

The subjects for this study were 42 (17 male, 25 female) patients with medically intractable complex partial seizures being assessed for suitability for surgical treatment. They were between 5 and 53 years of age, length of history 1-31 years, age at onset of epilepsy 1-37 years and seizure frequency 150-3500 per year. 26/42 patients had secondary generalised as well as complex partial seizures. All the patients were from the series described in the previous chapter (33 from the temporal group and 9 from the extratemporal group), and the patient identification numbers are the same.

All the patients had MRI with axial and coronal T1 and T2 weighted images. All had interictal EEG surface recordings. All but 2 patients had localising ictal surface EEG recordings, and those 2 had localised signal changes on MRI compatible with interictal EEG localisation and the clinical appearances of the seizure, as well as operative confirmation of localisation (i.e. a good result from anterior temporal lobectomy). Nineteen patients had sphenoidal recordings, and 20 had foramen ovale recordings (14 with multiple contact electrodes). In 26 patients localisation was confirmed by the results of temporal lobectomy. Abnormal pathology was found in the resected specimen in 22 patients. The patients were being assessed for temporal lobectomy only (operative treatment for extratemporal seizures was not offered) so, if ictal surface EEG suggested an extratemporal source for seizures, no invasive recording was done, and no operation carried out. The data supporting localisation of the focus in each patient is given in Table 3.1.

Methods

SPECT methods - HMPAO

HMPAO is discussed in Chapter 2, methods section, and chapter 4.

SPECT methods - HMPAO injection and image acquisition

The subjects were admitted to a neurological ward. They were observed for 3 days, during which time their medication was reduced. The extent to which this was done depended on the pre-admission seizure frequency, and on the history of change in seizure frequency during previous admissions (it is usual but not universal for seizure frequency to diminish during admission to hospital).

On the third day, a cannula was inserted into a vein in one arm and heparinised. The patient stayed in the day room of the ward, so that the alarm could be given quickly should a seizure occur. On feeling a seizure was about to occur the patient would press the alarm button and notify a nurse, who would note the time and summon a member of the medical staff. If the patient had no warning of an impending seizure, then other patients or staff in the day room would raise the alarm.

The ^{99m}Tc and HMPAO were stored in separate containers in a shielded box in the ward sideroom. The doctor quickly mixed the two, injecting the appropriate amount intravenously. The time between the end of the 'motionless stare' phase of the seizure and the injection, as well as the seizure manifestations themselves, were noted. The patient was taken to the scanner and the image acquired within 2 hours of the injection.

Acquisition of the image was carried out in the manner described in Chapter 2, methods section, as was visual and numerical analysis. Postictal images were analysed visually with the interictal image (which had been analysed previously, blind to all data but the diagnosis of epilepsy and the time of the last reported seizure) so that changes could be assessed. The investigators were blind to all data except the diagnosis of epilepsy, which scan was interictal and which was postictal, and the time of the injection.

Chapter 3

Results

The results of visual analysis of interictal and ictal/postictal scans is given in Table 3.2. The results of numerical analysis of ictal/postictal scans in Table 3.3, and the ictal/postictal change in asymmetry index in Table 3.4. The results of visual and numerical analysis of images are summarised in Table 3.5 Tables 3.1 and 3.3 also include the timing of ictal/postictal injections. Patient identification numbers correspond with those in Chapter 2.

Temporal group - visual analysis

Interictal results

Of the 33 patients 13/33 had normal interictal cerebral perfusion. The remainder had hypoperfusion of part or all of one temporal lobe (15), bilateral temporal hypoperfusion (1), temporal hypoperfusion extending into the ipsilateral frontal lobe (1) or into the ipsilateral hemisphere (2), or frontotemporal hyperperfusion (1).

Ictal/postictal results

Timing of injections

The timing of injections ranged from during the seizure (n=8), up to 1 minute postictally (n=15), up to 2 minutes postictally (n=6), up to 3 minutes postictally (n=3) and more than 3-15 minutes postictally (n=5).

Most of the changes seen fell into 3 groups;

1. Hyperperfusion of the whole temporal lobe (Figure 3.1).
2. Hyperperfusion of the hippocampus, with hypoperfusion of the ipsilateral lateral temporal cortex. Patients were included in this group if perfusion in the hippocampus was equal to that of the contralateral hippocampus (and therefore hyperperfused relative to lateral structures). Patients were also included in this group if lateral temporal hypoperfusion extended into the ipsilateral frontal lobe or hemisphere, but where hypoperfusion was most marked in the lateral temporal lobe (Figure 3.2).
3. Hypoperfusion of the whole temporal lobe. Patients in whom there was hypoperfusion of the hippocampus only, and patients in whom hypoperfusion of a lesser degree extended into the ipsilateral frontal lobe or hemisphere were included in this group (Figure 3.3).

These changes are referred to as Types 1, 2 and 3 change.

Type 1 change was seen in 4 scans, all following injection during the seizure.

Type 2 change was seen in 21 scans, following injection during the seizure or up to 6 minutes after. The hippocampal area was thought to hyperperfused relative to the contralateral hippocampus in 7 of these scans, and isoperfused compared to the contralateral hippocampus but hyperperfused compared to the ipsilateral temporal cortex in the remainder. Type 2 change occurred bilaterally in 2 patients (Figure 3.4). Hypoperfusion of the lateral temporal cortex was judged to extend into the frontal lobe in 9 scans (Fig. 3.5), and to involve the whole hemisphere in 3 (Figure 3.6). Type 3 change was seen in 4 scans, following injection between 1.5 and 15 minutes after the seizure. Hypoperfusion involved only the mesial temporal cortex in 1 patient, the temporal lobe only in one patient and extended into the ipsilateral frontal lobe in the remaining two.

In three cases the interictal scan showed temporal hypoperfusion (in two cases of the whole temporal lobe, in one of the mesial temporal lobe only), and the postictal scan showed resolution of the hypoperfusion. The timing of the injections ranged from 0.5 to 5 minutes postictally.

Five postictal scans (2 in the same patient) showed no change ictally or postictally. Two of the interictal scans in these patients were normal, three abnormal. The timing of the injections ranges from during the seizure to 3 minutes postictally.

Extratemporal group - visual analysis

Interictal results

All 9 interictal scans in this group were normal.

Timing of injections

Injections were carried out during the seizure (n=2) or up to 5 minutes postictally (n=8).

Ictal/postictal results

Three patients, injected during the seizure and 0.5 and 2 minutes postictally, had unilateral frontal hypoperfusion (Figure 3.7). Two patients, injected during the seizure and 2 minutes postictally, had hyperperfusion of the anterior frontal lobe with diffuse hypoperfusion of the contralateral hemisphere (Figures 3.8 and 3.9). One patient, injected 0.5 minutes postictally, had hyperperfusion most intense in the calcarine cortex, extending into the neighbouring lateral occipital cortex, accompanied by diffuse hypoperfusion of the ipsilateral hemisphere (This patient's postictal image is shown with regions of interest in Figures 2.1-2.3).

Correlation of interictal and postictal SPECT with other data localising the epileptogenic zone

Temporal group

1. Type 1 change: in all 4 cases this occurred in the temporal lobe that was the site of the focus.
2. Type 2 change: Hippocampal hyperperfusion (relative either to the contralateral hippocampus or to the ipsilateral lateral cortex) occurred at the site of the focus. Where the accompanying lateral hypoperfusion extended outside the temporal lobe, it did so in all cases to a lesser degree. Two patients showed Type 2 change bilaterally. In one ca

se there were bilateral independent mesial temporal foci. In the other, seizure activity spread rapidly (within 1 second) from one temporal lobe to the other.
3. Type 3 change: This occurred only or maximally in the temporal lobe that was the site of the focus.
4. Resolution of interictal abnormality: The interictal abnormalities seen in all 3 cases were at the site of the focus.

Extratemporal group

1. Unilateral frontal hypoperfusion. In all 3 cases this occurred in the frontal lobe that was the site of the focus.
2. Frontal hyperperfusion with contralateral (frontal or hemispheric) hypoperfusion. In both cases the hyperperfusion occurred in the frontal lobe that was the site of the focus.
3. Left occipital hyperperfusion with hypoperfusion of the rest of the ipsilateral hemisphere. Surface EEG onsets confirmed occipital origin, but suggested a right sided focus. The MRI abnormality was in the left lateral occipital cortex, although hyperperfusion was maximal in the calcarine cortex.

Comparison of results of visual and numerical analysis of ictal/postictal scans

The results of visual and numerical analysis are summarised in Table 3.5. Patients 28, 46 and 80 are excluded from numerical analysis, as the method is insensitive to bilateral symmetric changes.

Using the same criteria as in Chapter 2, Asymmetry indices were compatible with visual analysis in 20 of the 34 scans (59%).

In the temporal group, asymmetry indices were compatible with Types 1, 2 and 3 change in 1, 13 and 4 patients respectively, compared with 4, 21 (including 3 with bilateral change excluded from numeric analysis) and 4 for visual analysis. Asymmetry indices were compatible with resolution of hypoperfusion in 1 patient (3 patients on visual analysis), and with no change in 1 (5 patients on visual analysis).

There were therefore 9 abnormalities identified visually which were not detected by numeric analysis, in all 9 cases lateral temporal hypoperfusion. Asymmetry indices identified abnormalities not seen on visual analysis in 4 scans. The asymmetry index was lower on the side of the focus in all 4 cases, involving the

frontal lobe in 1, the parietal lobe in 2 and the mesial temporal lobe in 1 case.

Numerical and visual analysis were compatible in all the ictal/postictal scans in the extratemporal group.

Ictal/postictal changes in asymmetry indices

Ictal/postictal changes in asymmetry indices are given in Table 3.3. In deciding the polarity of the change, it was assumed that the change took place on the side of the focus as determined by EEG and structural imaging data. In the two extratemporal cases where visual analysis suggested hyperperfusion in one frontal lobe and hypoperfusion in the other, the change in asymmetry index is given as positive i.e. reflecting the whole change in asymmetry as being due to hyperperfusion. The data had a normal frequency distribution.

The relationship between ictal/postictal changes and the timing of injections is illustrated in the form of scatter diagrams in Figs 3.10-3.16. The scans in the temporal group were sorted into subgroups (ictal (=0), up to 1 minute, up to 2 minutes, up to 3 minutes and more than 3 minutes) according to the timing of injections. The mean asymmetry indices for each epoch are shown in Fig 3.17. No error bars have been included, but the means and standard errors are given in the table included in the figure.

Temporal group

In the following, the terms 'increase' and 'decrease' refer to the side ispilateral to the focus.

1. Frontal ROI (Fig 3.10). Changes ranged from 21.9 to -20.2%, though most were between 10 and -10%. There was a tendency toward a gradual decrease in perfusion as time postictally increased (R^2=0.-366, p=0.033), though the mean % change remained near zero until 3 minutes postictally (Fig 3.17).
2. Basal ganglia ROI (Fig 3.11). Changes ranged from 17.9 to -8.8%, the majority lying between 10 and -10%. There was no apparent difference with time. Mean % changes were small (Fig 3.17). They appeared to become less positive immediately postictally, and become gradually and slightly more positive thereafter.
3. Thalamic ROI (Fig 3.12). Changes ranged from 12.6% to -16.1%. There was no apparent difference with time, and mean % changes were small (Fig 3.17), again showing no apparent trend.

4. Mesial temporal ROI (Fig 3.13). Changes ranged from 57.5 to -19.2%. All but one of the changes up to 30 seconds postictally were positive, indicating hyperperfusion on the side of the focus. After this time the scatter was wide, but there was a tendency for changes to become more negative as time postictally increased (R^2=0.-344, p=0.046). However, the mean % change remained positive until after 3 minutes postictally (Fig 3.17), only then becoming negative.

4. Lateral temporal ROI (Fig 3.14). Changes ranged from 60.2 to -37.7%. During the seizure most indices were positive (4 vs. 3), and there was a distinct tendency for indices to decrease as time postictaly increased (R^2=0.-363, p=0.035), the mean % change becoming negative after 1 minute postictally, (Fig 3.17).

5. Parietal ROI (Fig 3.15). Changes ranged from 48 to -25.3%. During the seizure all changes were positive, although a single change of 48% was to a great extent responsible for the mean ictal change being as high as 13.4%; the rest of the ictal increases were between 0.8 and 16.9%. There was a tendency for changes to become more negative with time, 6/7 changes after 180 seconds being negative. The mean % change also became more negative as time postictally increased (R^2=-0.468, p=0.007)(Fig 3.17).

6. Occipital ROI (Fig 3.16). Changes ranged from 16.3 to -11.7%. Individual and mean (Fig 3.17) changes were small, and there was no apparent difference in change with time.

Summary of postictal ictal/postictal changes in asymmetry index, and of differences between ROIs in the temporal group

The biggest changes were seen in the mesial temporal, lateral temporal and parietal ROIs. Differences are assessed using the paired t-test.

In all three, most perfusion changes were positive during the siezure (all in the mesial temporal and parietal ROIs), the mean change being highest in the mesial temporal ROI. None of the differences beteween means was statistically significant.

In frontal, lateral temporal and parietal ROIs changes became negative more quickly than in the mesial temporal ROI; the mean change up to 1 minute postictally was more positive in the mesial temporal ROI than in the frontal (p=0.005), lateral temporal (p=ns) and parietal (p=0.006) ROIs. The change after 3 minutes postictally was less negative in the mesial temporal ROI than in the frontal (p=ns), lateral temporal p=0.040) and parietal (p=0.04) ROIs.

Changes in the basal ganglia and thalamic ROIs were relatively small; the biggest was in the thalamus at 7.27%.

Extratemporal group

Scatter diagrams illustrating ictal/postictal changes in asymmetry index are shown in Figs 3.18-3.24. The small numbers in this group did not give a sufficient spread of data to assess any possible changes with time. The changes seen were small, only 4 changes being outside the +15 to -15% range, the great majority between +10 and -10%. These were seen in the frontal lobe (1 patient), the thalamus (2 patients) and the occipital lobe (the 1 patient in whom localising evidence suggested an occipital focus).

Differences between temporal and extratemporal groups

Differences in change of asymmetry index between temporal and extratemporal groups were significant only for the mesial temporal ROI ($p=0.010$, unpaired t-test).

Chapter 3

Illustrations and Tables

Figure 3.1

Ictal HMPAO SPECT, left mesial temporal seizure: transaxial slice showing hyperperfusion of the whole temporal lobe (patient 69, scan 3)

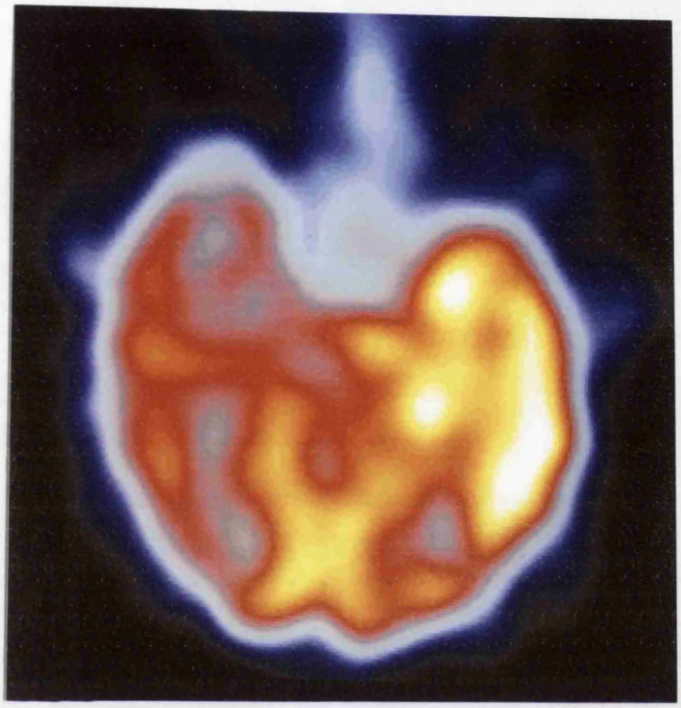

Figure 3.2

Postictal HMPAO SPECT, 2 minutes following right mesial temporal seizure: transaxial slice showing hyperperfusion of the right hippocampus with hypoperfusion of the rest of the ipsilateral temporal lobe (patient 56)

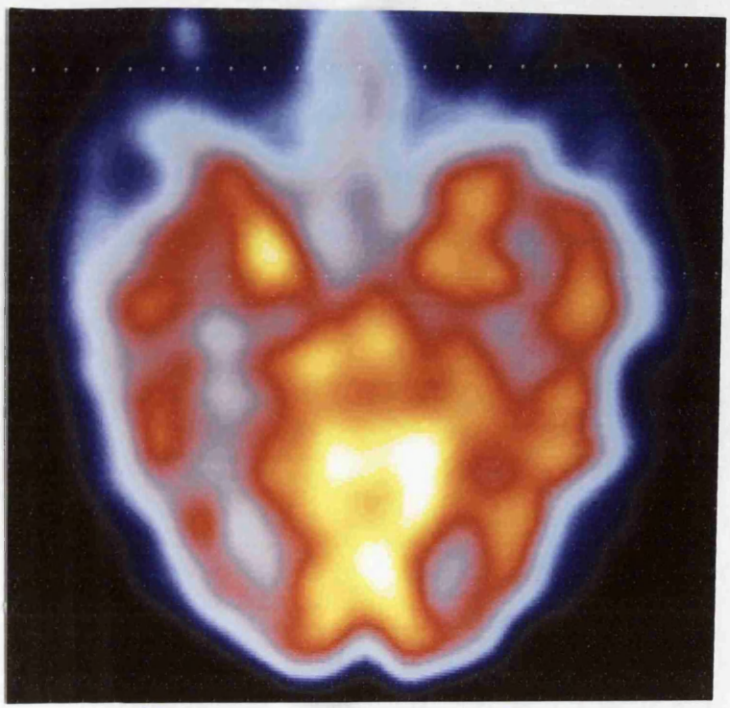

Figure 3.3

Postictal HMPAO SPECT, 3 minutes following left mesial temporal seizure: transaxial slice showing left temporal hypoperfusion, with some sparing of the mesial temporal cortex (patient 11)

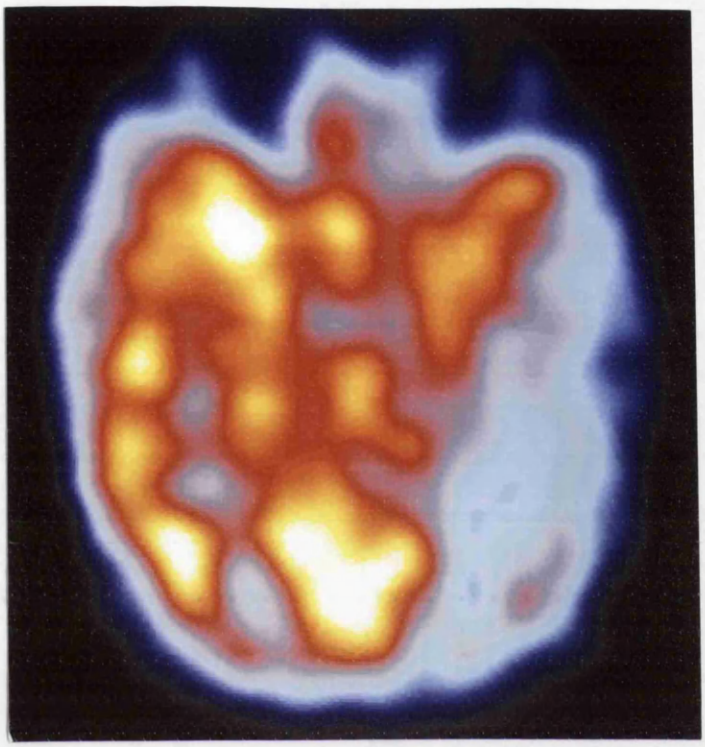

Figure 3.4

Postictal HMPAO SPECT, 2 minutes after right mesial temporal seizure: transaxial slice showing bilateral mesial temporal hyperperfusion with bilateral hypoperfusion of the lateral temporal cortex (patient 46)

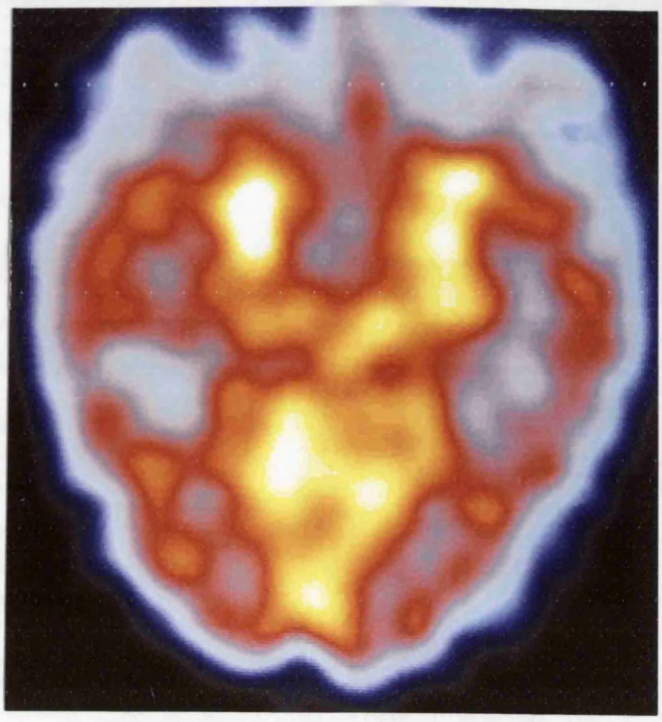

Figure 3.5

Postictal HMPAO SPECT, 15 minutes following left mesial temporal seizure: orbitomeatal slice showing left temporal and frontal hypoperfusion (patient 62, first postictal scan).

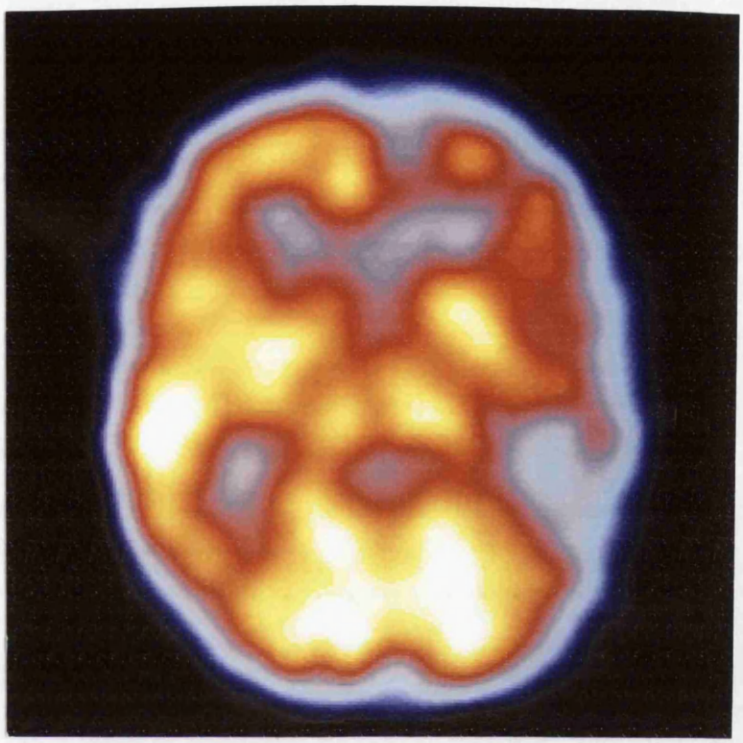

Figure 3.6

Postictal HMPAO SPECT, 2 minutes following right mesial temporal seizure: transaxial slice showing hypoperfusion of the right hemisphere and hyperperfusion of the right mesial temporal lobe (patient 27)

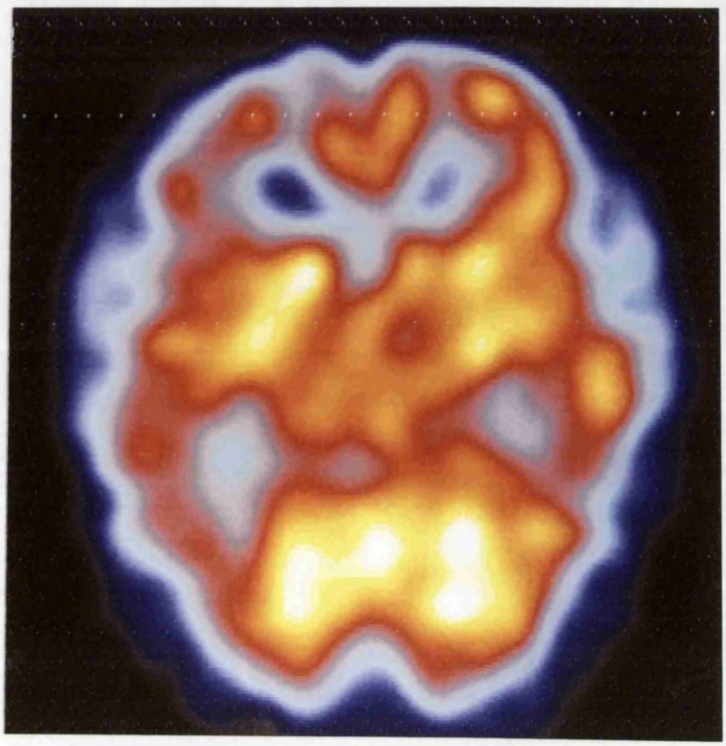

Figure 3.7

Ictal HMPAO SPECT, right frontal seizure: orbitomeatal slice showing right frontal hypoperfusion (patient 1, extratemporal group)

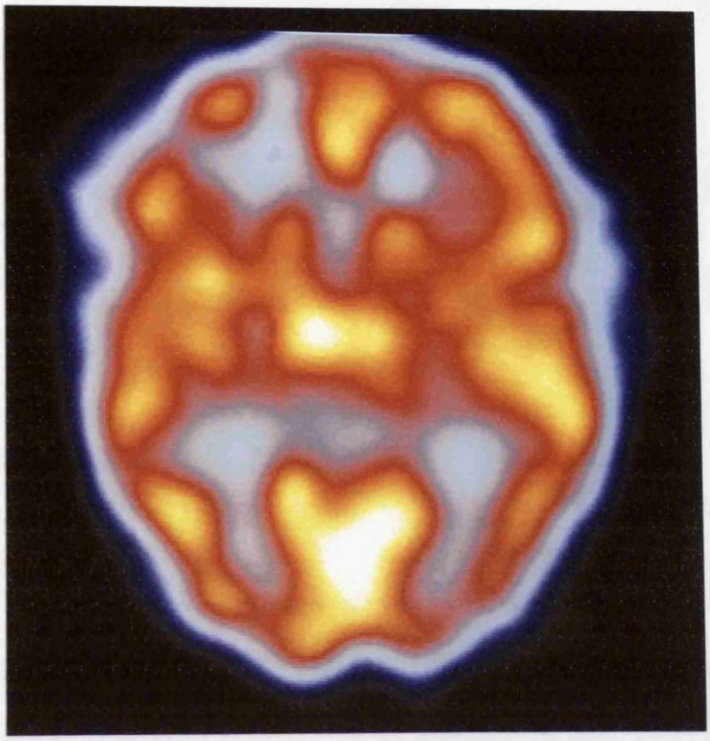

Figure 3.8

Interictal HMPAO SPECT: orbitomeatal slice showing normal perfusion (patient 7, extratemporal group)

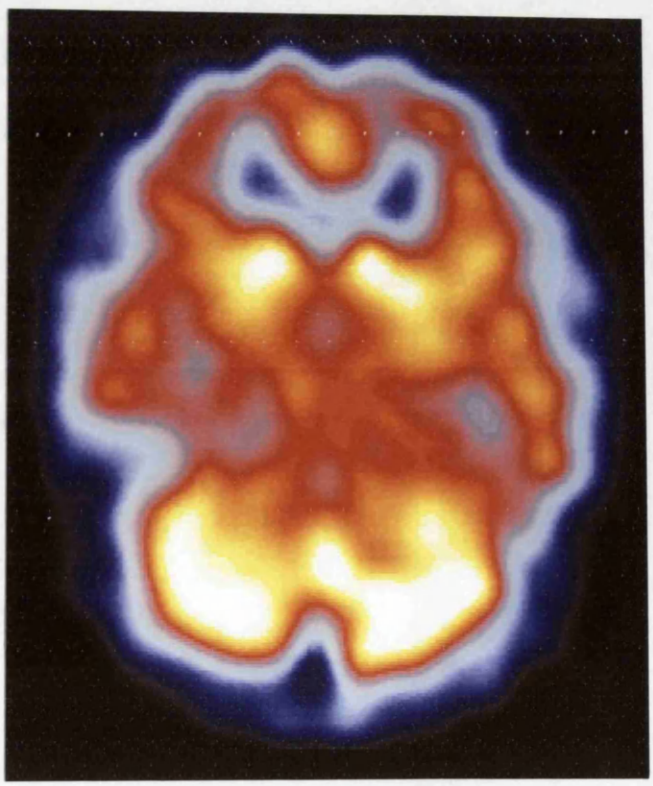

Figure 3.9

Postictal HMPAO SPECT, 2 minutes following right frontal seizure in the same patient as illustrated in Figure 3.8: orbitomeatal slice showing right frontal hyperperfusion and left frontal hypoperfusion

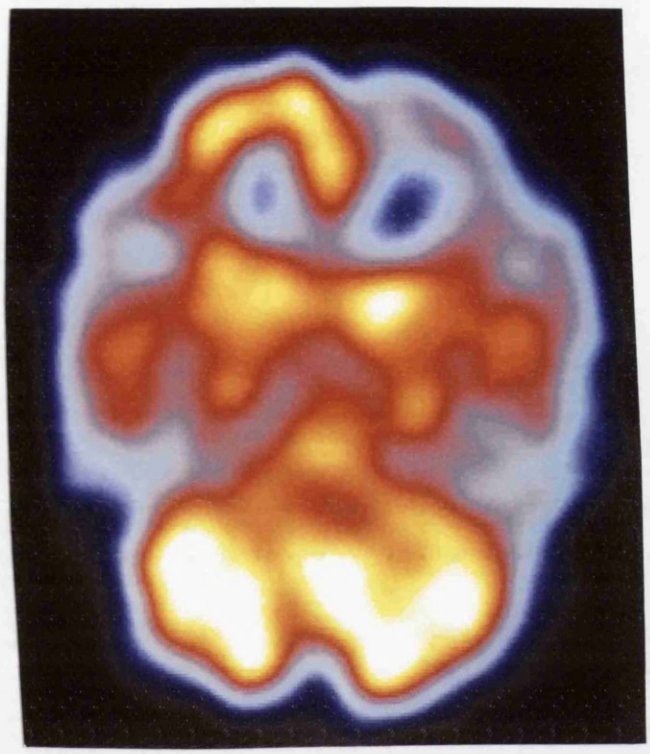

Figure 3.10: Temporal group Frontal ROI

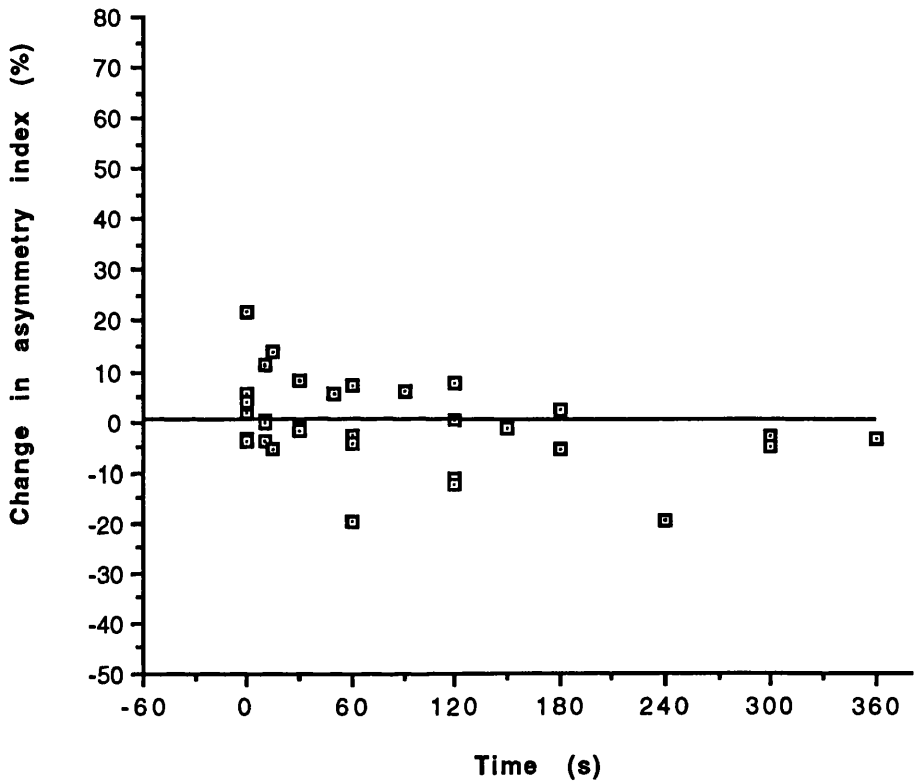

Figure 3.11: Temporal group Basal ganglia ROI

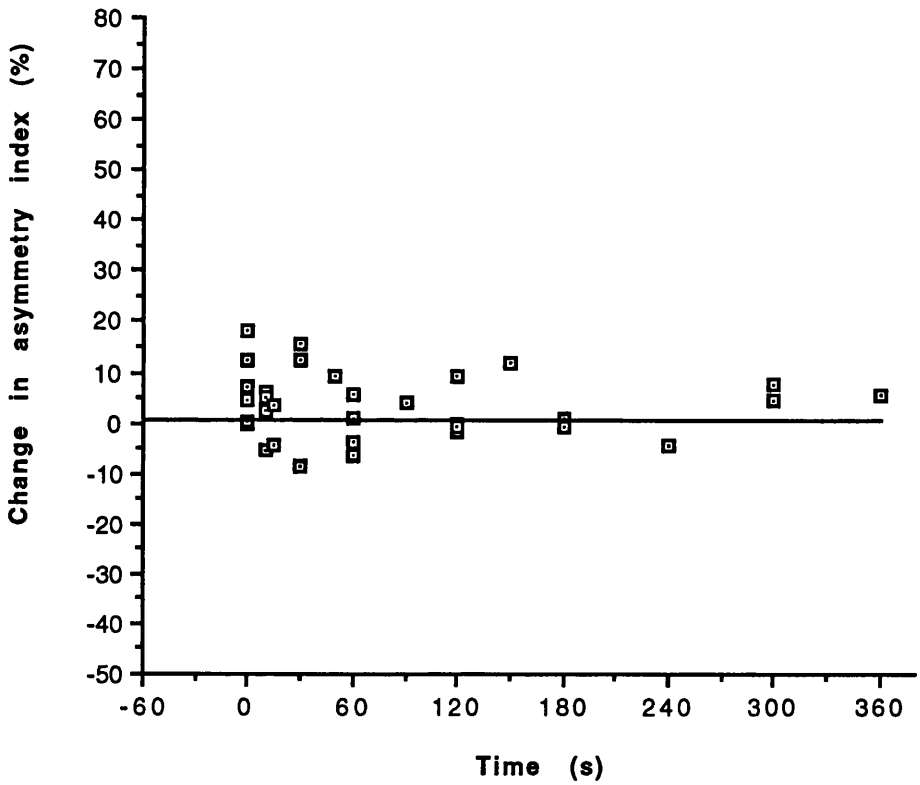

Figure 3.12: Temporal group Thalamic ROI

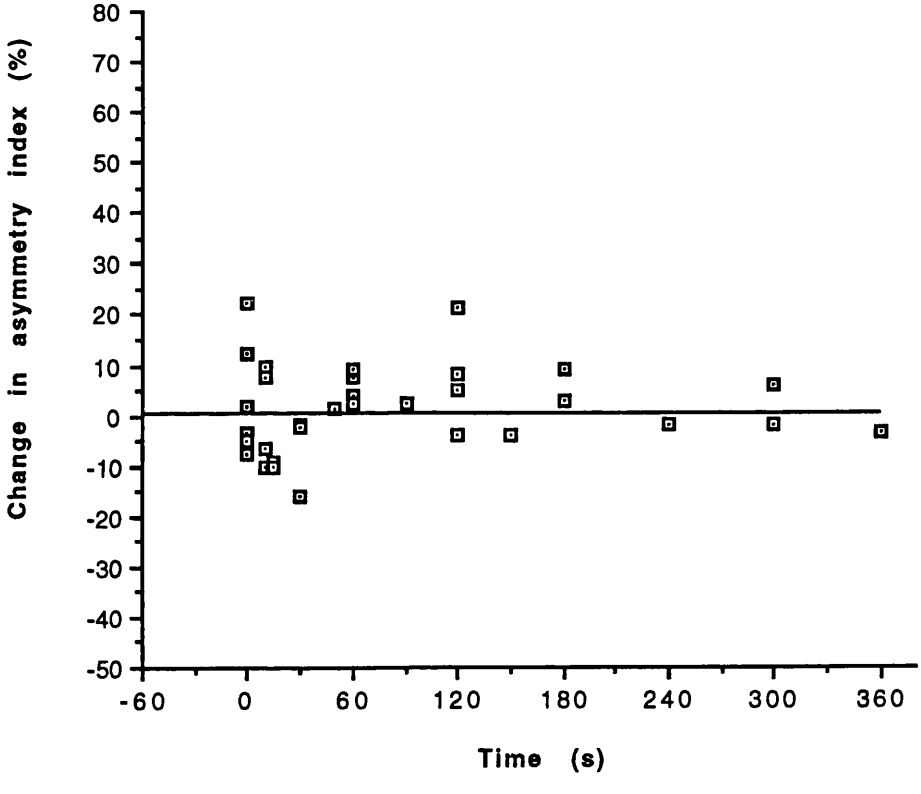

Figure 3.13: Temporal group Mesial temporal ROI

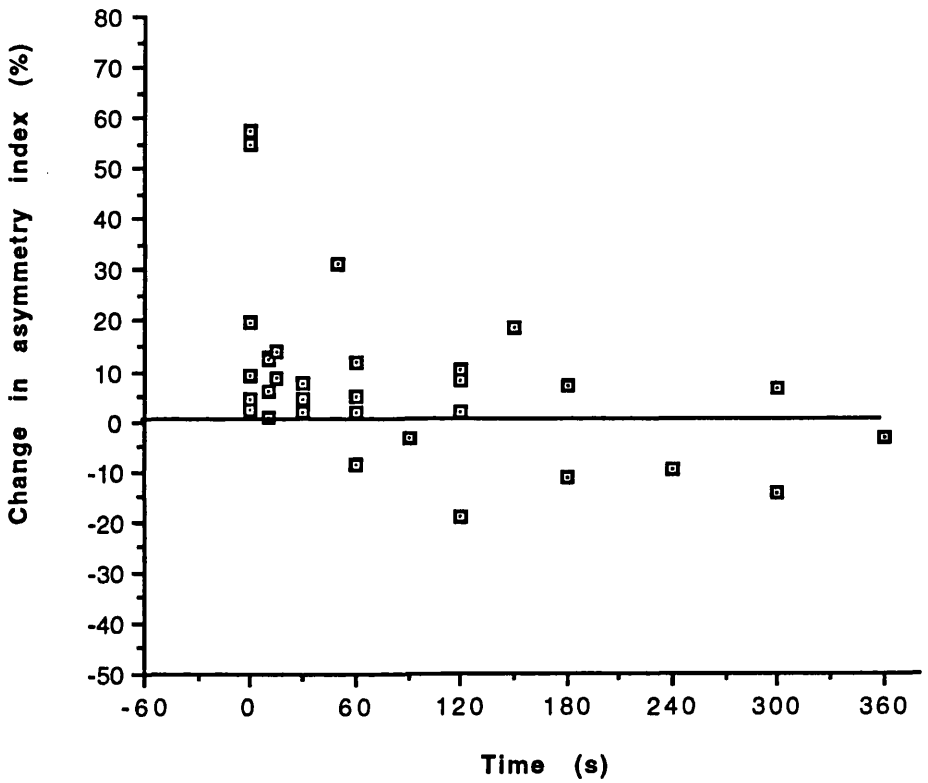

Figure 3.14: Temporal group
Lateral temporal ROI

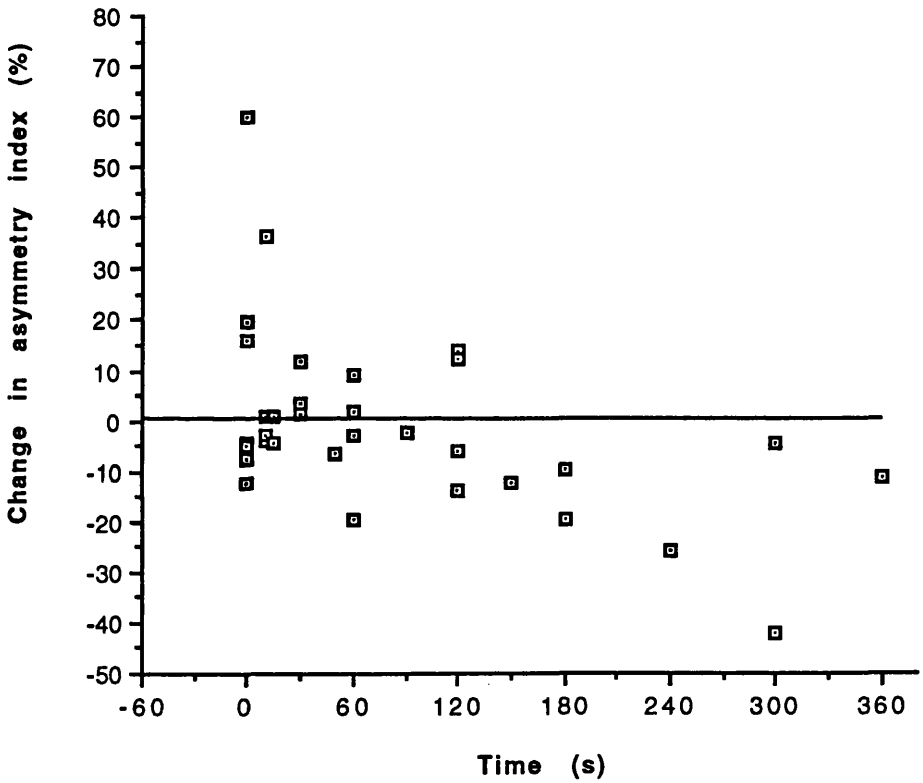

Figure 3.15: Temporal group Parietal ROI

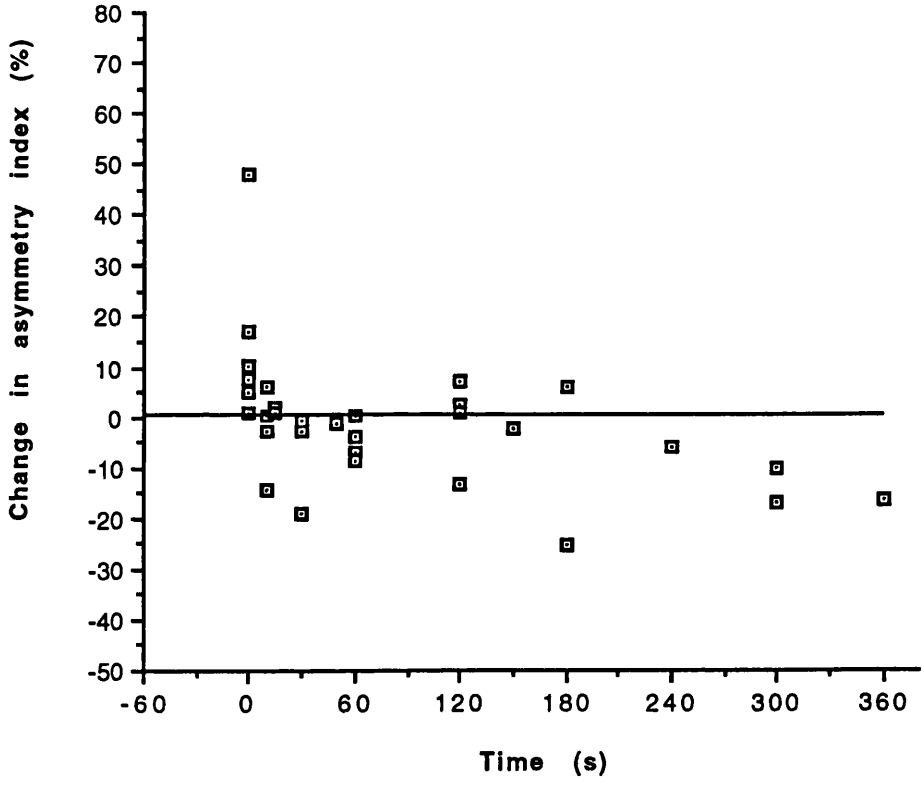

Figure 3.16: Temporal group Occipital ROI

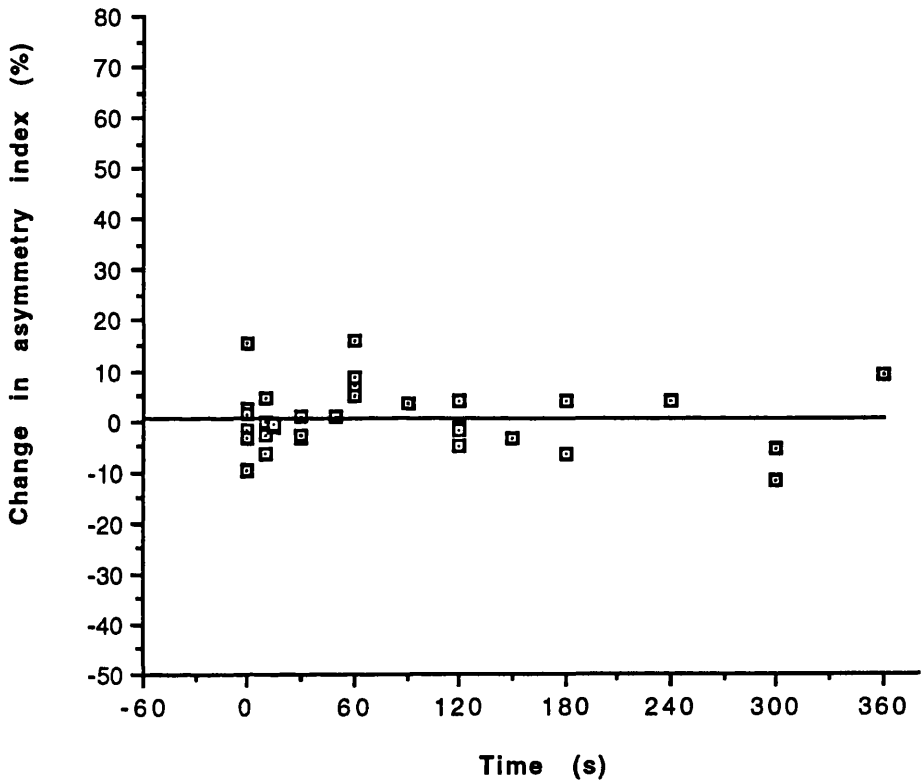

Figure 3.17

NUMERIC ANALYSIS OF IMAGES
Mean ictal/postictal changes in asymmetry index (% - Y axis) during siezure (n=7) and up to 1 (n=14), 2(n=5), 3 (n=3) and more than 3 (n=5) minutes postictally (X axis)

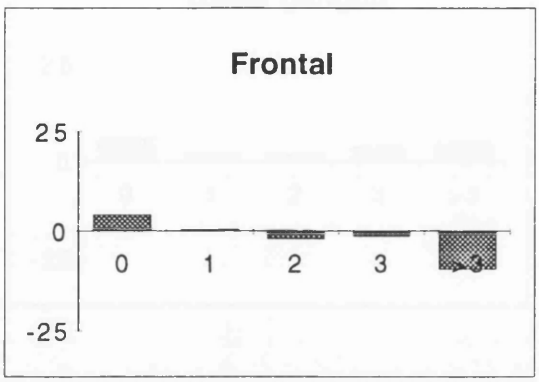

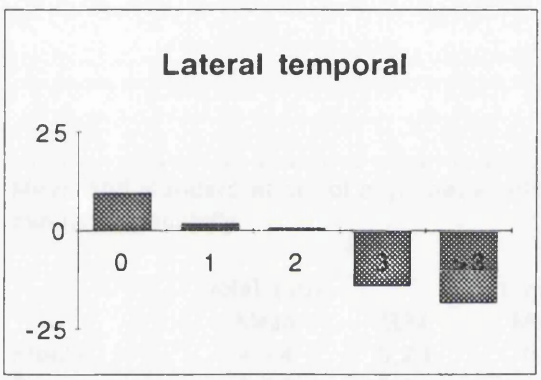

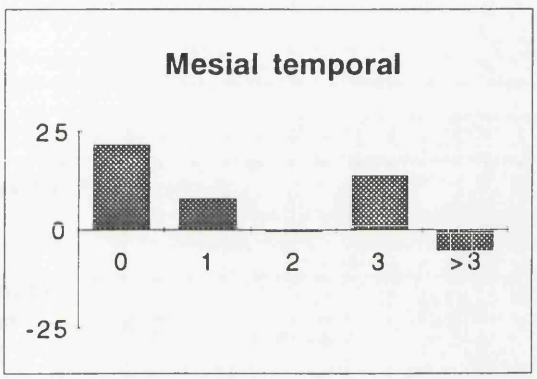

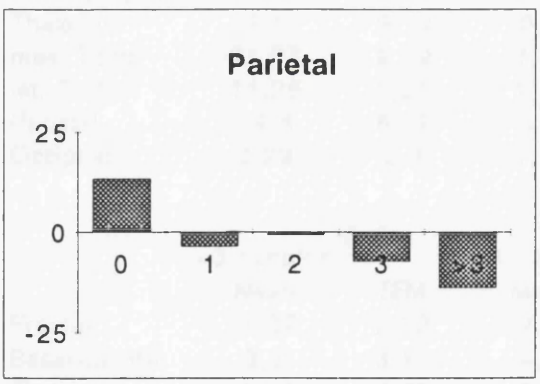

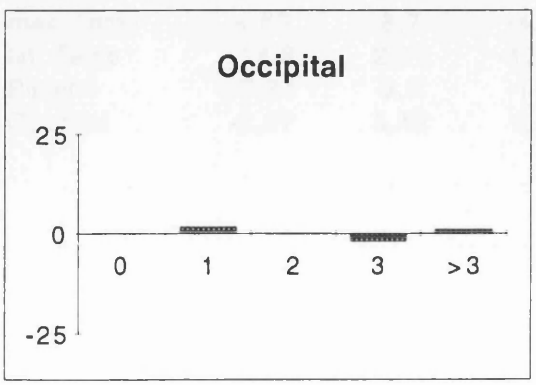

Figure 3.17

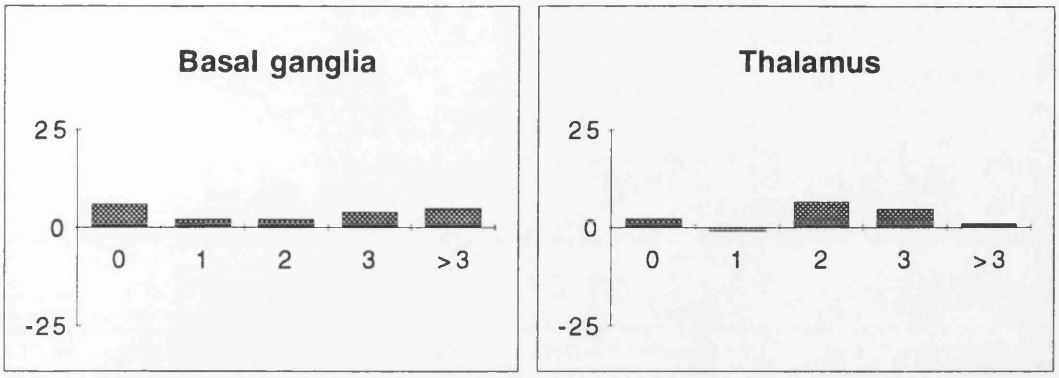

Mean and standard errors of asymmetry indices for 0, <1, <2, <3 and >3 minutes postictally

	Ictal (=0)		<1 minute		<2 minutes	
	Mean	SEM	Mean	SEM	Mean	SEM
Frontal	4,24	3,24	0,5	1,83	-1,98	4,17
Basal ganglia	5,99	2,64	2,31	1,6	2,2	2
Thalamus	2,4	3,19	-0,79	1,84	4,92	2,46
mes. Temp	21,77	9,19	7,78	2,42	-0,46	5,27
lat. Temp	11,26	9,25	1,74	3,32	0,86	5,42
Parietal	14,8	6,99	-3,59	1,8	-0,68	4,34
Occipital	0,99	2,9	1,95	1,61	-0,02	1,67

	<3 minutes		>3 minutes	
	Mean	SEM	Mean	SEM
Frontal	-1,37	2,22	-9,54	3,56
Basal ganglia	3,2	3,13	4,4	2,73
Thalamus	2,67	3,73	0,3	2,58
mes. Temp	4,83	8,7	-4,32	2,98
lat. Temp	-13,9	2,91	-17,56	6,2
Parietal	-7,37	9,9	-14,6	2,86
Occipital	-2,27	3,43	1,02	4,17

Figure 3.18: Extratemporal group Frontal ROI

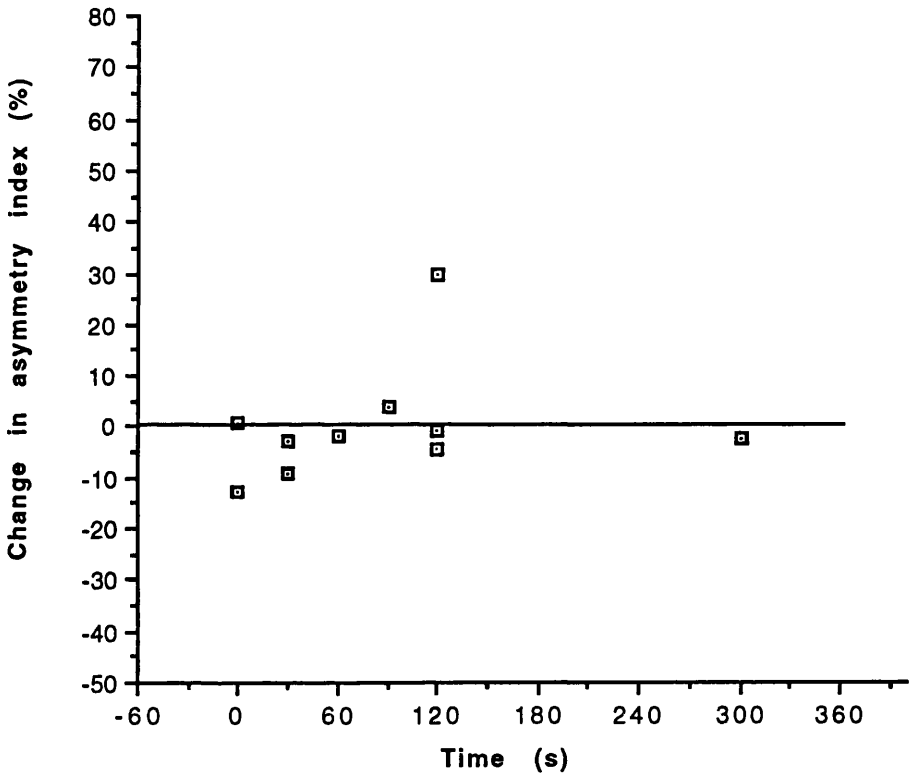

Figure 3.19: Extratemporal group Basal ganglia ROI

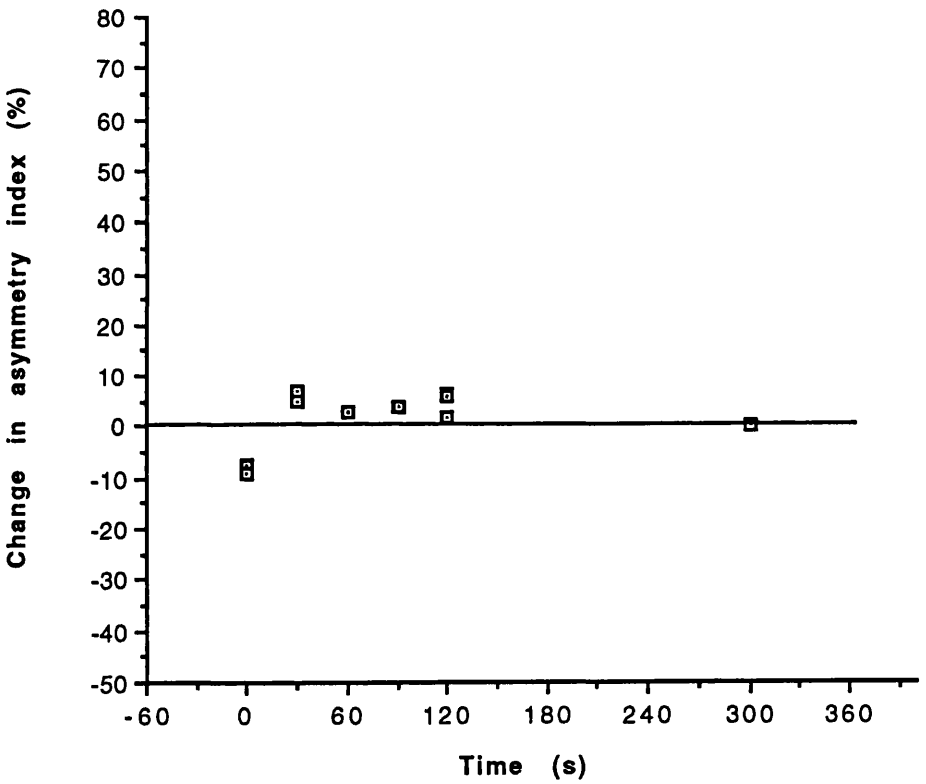

Figure 3.20: Extratemporal group Thalamic ROI

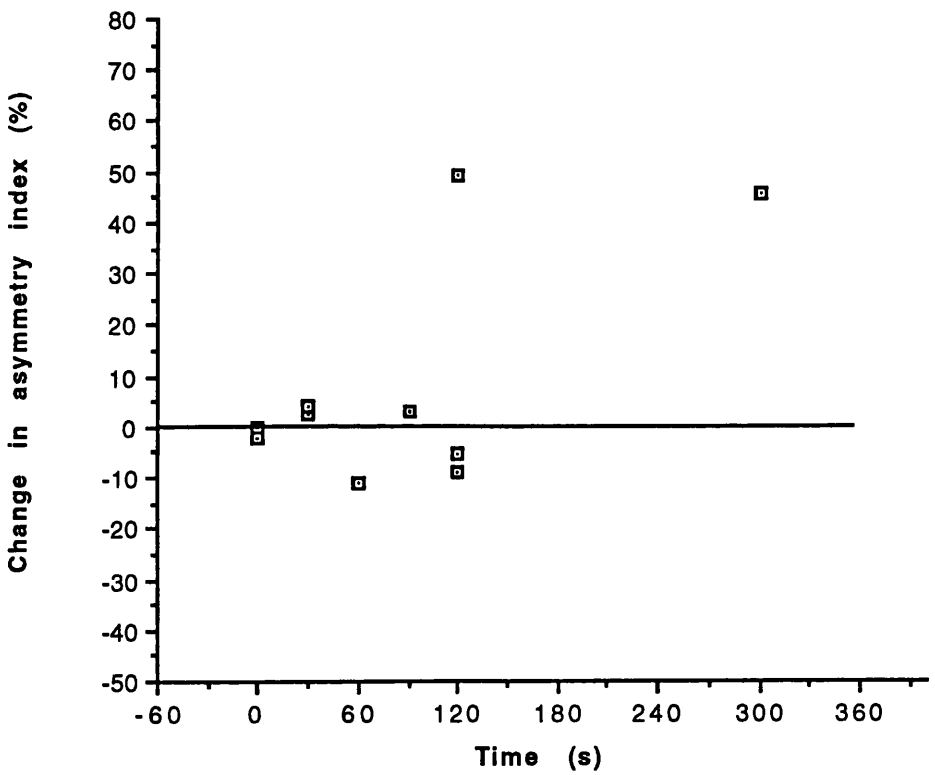

Figure 3.21: Extratemporal group Mesial temporal ROI

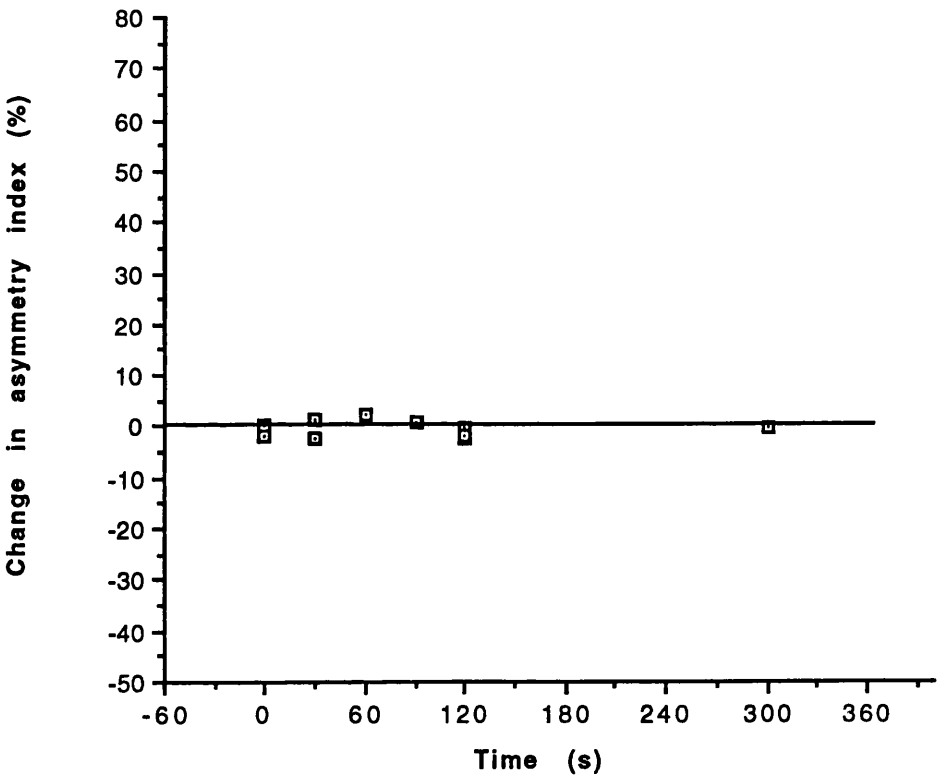

Figure 3.22: Extratemporal group Lateral temporal ROI

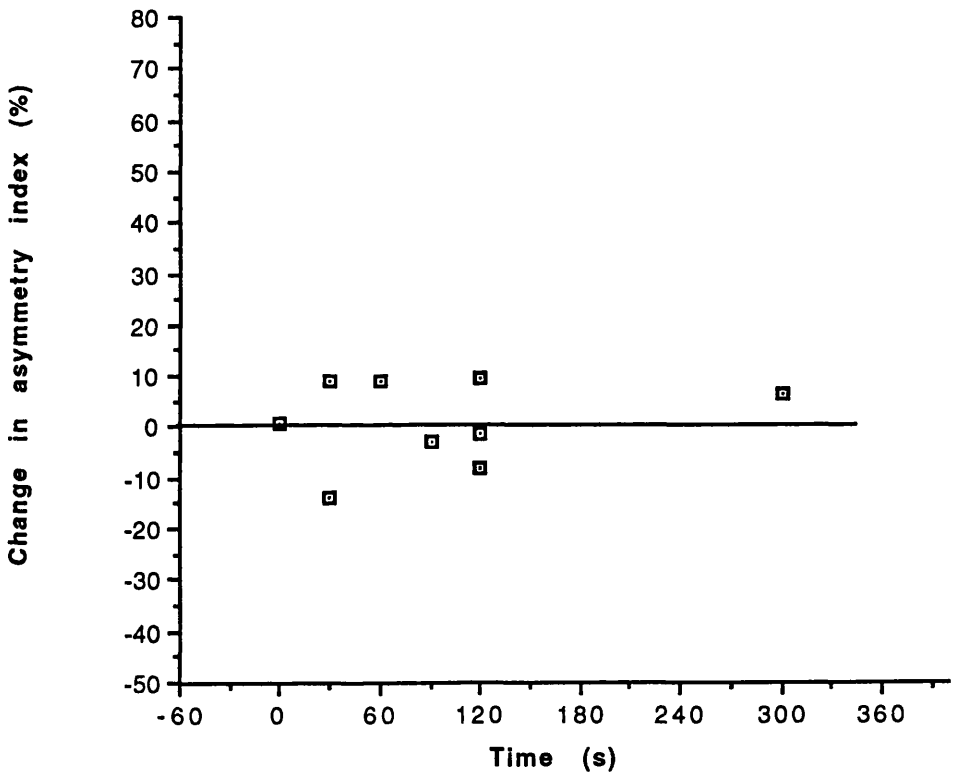

Figure 3.23: Extratemporal group Parietal ROI

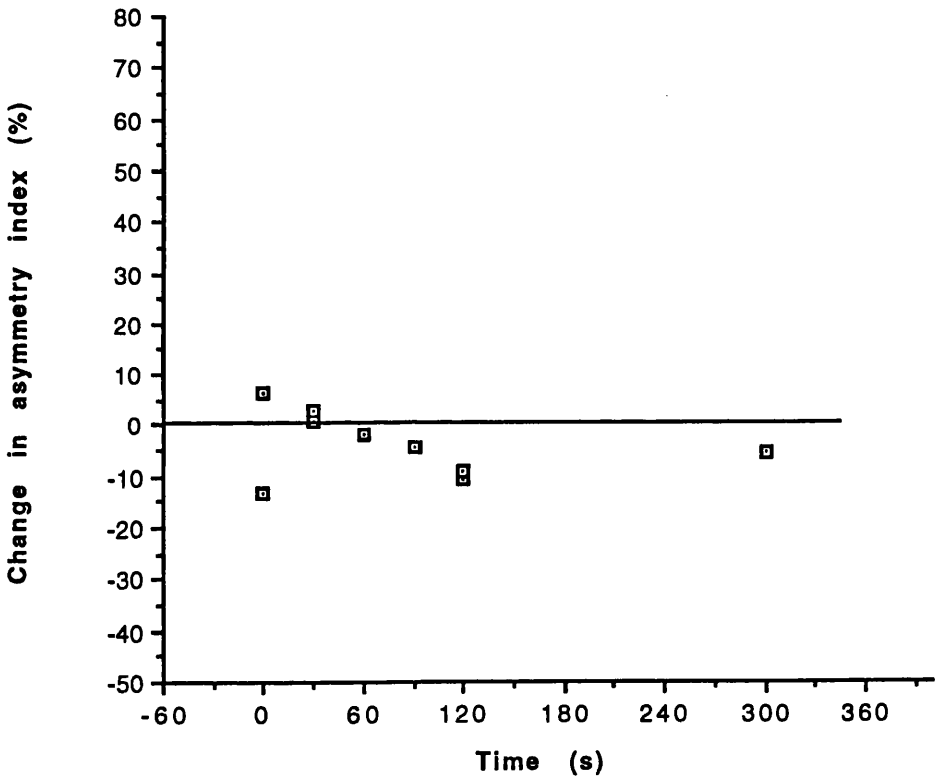

Figure 3.24: Extratemporal group Occipital ROI

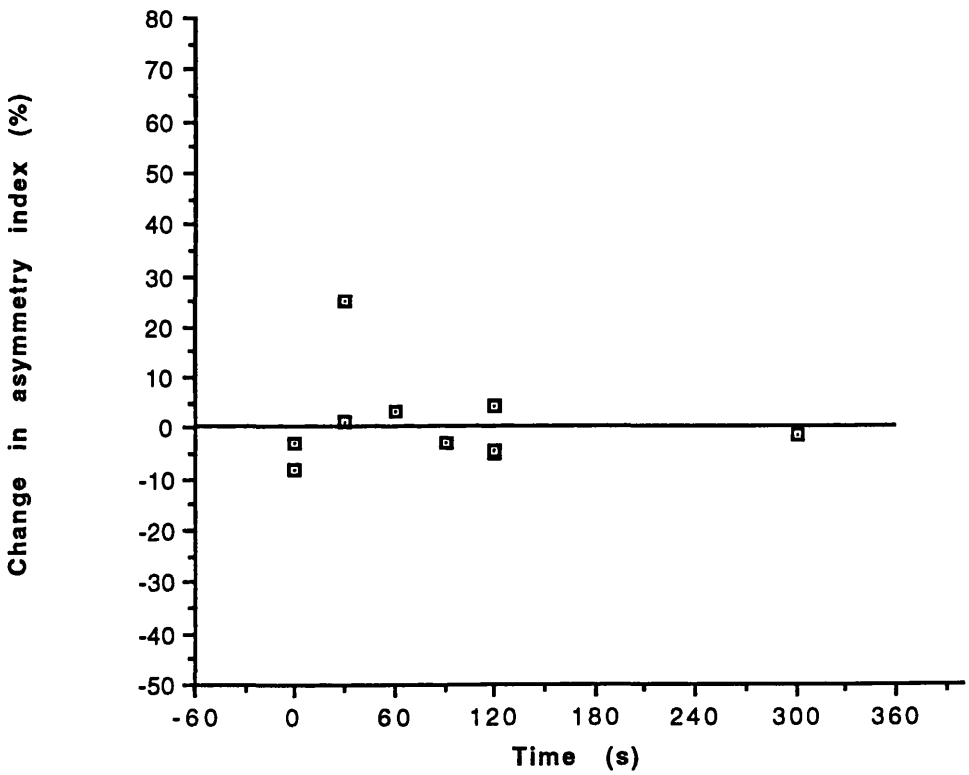

Table 3.1

DATA SUPPORTING FOCUS LOCALISATION

Temporal group

Patient	Ictal surface EEG	Sphenoidal recording	Foramen ovale recording	MRI	Operative result	Pathology
1	+	+	+		+	AHS
8	+	+	+		+	AHS
11	+	+	+			
17	+	+	+	+	+	AHS
21	+			+		
25	+	+	+		+	AHS
27	+					
28	+		+			
31	+	+	+		+	AHS
32	+		+		+	Normal
41				+		
45	+	+	+		+	MTS
46	+	+		+	+	Hamartoma
47	+	+	+	+	+	Normal
49				+		
56	+	+	+		+	MTS
58	+	+	+		+	Normal
59	+	+			+	AHS
60	+	+	+		+	Normal
61	+				+	Inflammatory infiltrate
62	+				+	Vascular malformation
63	+				+	AHS
64	+	+	+		+	AHS
67	+				+	Inflammatory infiltrate
68	+		+		+	AHS
69	+	+	+	+	+	Extensive gliosis
70	+				+	Benign cyst
71	+				+	AHS
72	+	+	+		+	AHS
75	+			+	+	Small glioma
77	+	+	+		+	Normal
78	+	+	+		Failed	AHS
80	+	+	+		+	Normal

MTS=Mesial temporal sclerosis AHS=Ammon's horn sclerosis

Extratemporal group

1	+		+	
2	+		+	
3	+			
4	+			
5	+			
6	+		+	
7	+		+	
8	+			
11	+			

Table 3.2

VISUAL ANALYSIS
Results of ictal/postictal SPECT: change from interictal image

Temporal group

Patient	Interictal image	Postictal image	Time (s)
1	Normal	2L	30
8	Left temporal hypoperfusion	2L	60
11	Normal	2L	300
17 (1)	Right frontotemporal hypoperfusion	No change	0
17 (2)	Right frontotemporal hypoperfusion	No change	0
21	Left temporal hypoperfusion	2L	150
25	Right temporal hypoperfusion	1R	0
27	Normal	2R	120
28	Left temporal hypoperfusion	2B	0
31	Normal	2R	360
32	Normal	No change	30
41	Normal	2L	120
45	Normal	2R	10
46	Normal	2B	120
47	Normal	2L	10
49	Normal	No change	180
56	Right temporal hypoperfusion	2R	120
58	Left temporal hypoperfusion	2L	15
59	Bilateral temporal hypoperfusion	3L	90
60	Left temporal hypoperfusion	1L	0
61	Right temporal hypoperfusion	3R (mesial)	120
62 (1)	Left temporal hypoperfusion	3L	900
62 (2)	Left temporal hypoperfusion	No change	60
63	Left mesial temporal hypoperfusion	Normal	300
64	Left temporal hypoperfusion	2L	10
67	Normal	2R	10
68	Left temporal hypoperfusion	1L	0
69 (1)	Left hemispheric hypoperfusion	2L	50
69 (2)	Left hemispheric hypoperfusion	2L	0
69 (3)	Left hemispheric hypoperfusion	1L	0
70	Normal	3L	240
71	Left temporal hypoperfusion	Normal	60
72	Right frontotemporal hyperperfusion	2R	60
75	Normal	2R	15
77	Left hemispheric hypoperfusion	2L	180
78	Left temporal hypoperfusion	Normal	30
80	Left temporal hypoperfusion	2B	90

Key to changes in temporal group:

1 Hyperperfusion of whole temporal lobe
2 Hippocampal hyperperfusion with hypoperfusion of lateral structures
3 Hypoperfusion of whole or part of temporal lobe

L=left R=right B=bilateral

Table 3.2

Extratemporal group

Patient	Interictal image	Postictal image	Time (s)
1	Normal	Right frontal hypoperfusion	0
2	Normal	Left occipital hyperperfusion & left hemispheric hypoperfusion	30
3	Normal	Right frontal hypoperfusion	30
4 (1)	Normal	No change	300
4 (2)	Normal	No change	120
5	Normal	No change	60
6	Normal	Right frontal hyperperfusion & left hemispheric hypoperfusion	120
7	Normal	Right frontal hyperperfusion & left frontal hypoprfusion	0
8	Normal	No change	90
11	Normal	Left frontal hypoperfusion	120

Table 3.3

NUMERICAL ANALYSIS OF IMAGES
Ictal/postictal scans: asymmetry indices (%)

Temporal group

Patient	Frontal	Basal ganglia	Thalamus	mes. Temp	lat. Temp	Parietal	Occipital
1	-2,2	11,2	-0,6	3,3	-8,3	-17,0	-6,1
8	-4,4	3,1	-5,1	-6,8	-6,1	-1,9	9,5
11	-1,5	7,3	8,6	-14,6	-46,4	-14,4	-11,3
17 (1)	-5,6	2,9	-4,4	10,2	3,0	7,9	-3,3
17 (2)	3,3	2,8	4,9	10,3	6,6	2,3	2,5
21	1,4	-1,9	5,8	19,6	-1,3	-11,2	-9,6
25	6,3	-6,1	3,1	-10,7	-11,1	11,3	2,7
27	13,8	1,7	-0,4	2,7	6,9	13,1	-1,4
31	8,5	2,5	0,2	-4,7	11,9	12,8	7,4
32	-8,5	12,3	-1,1	-2,3	-1,8	-1,7	4,3
41	-11,5	1,8	13,9	5,2	-24,7	-12,9	-0,3
45	-2,4	-3,4	0,1	-8,4	-6,3	4,0	-1,7
47	-2,9	3,6	8,5	8,1	-5,5	-11,5	-6,3
49	2,3	-2,9	5,3	-12,4	-8,8	5,0	4,1
56	6,7	-3,6	4,5	-7,1	16,2	1,3	0,8
58	-7,2	-2,0	-7,4	5,4	-11,8	-2,5	4,1
59	2,1	8,3	2,1	-9,5	-12,8	-6,9	6,4
60	0,2	12,6	3,5	-0,4	4,9		-6,6
61	0,8	-0,2	5,2	15,8	-3,4	0,0	-0,2
62 (1)	-26,9	10,4	0,0	-15,7	-36,7	-27,2	-2,6
62 (2)	-3,3	-6,7	1,9	2,7	-19,3	-13,8	-4,9
63	10,0	8,1	-1,3	-1,6	-0,7	6,1	-2,4
64	5,5	4,3	-10,6	-3,0	-14,7	6,4	1,9
67	-1,4	-0,2	-1,5	-1,2	13,6	-10,4	-0,9
68	4,3	-2,5	2,2	-1,1	-5,8	0,3	4,5
69 (1)	-8,6	-0,7	0,4	7,1	-48,3	-35,9	-3,0
69 (2)	-10,2	-2,9	2,6	33,2	-21,8	-17,8	-0,8
69 (3)	7,6	7,9	12,5	30,8	18,6	13,3	11,7
70	-15,5	1,0	3,8	-6,5	-31,7	-11,5	0,7
71	-3,9	1,1	0,8	-2,1	-10,5	-4,5	2,1
72	-13,7	0,1	1,3	-5,6	5,0	-4,4	4,4
75	14,2	0,2	-5,5	7,8	16,4	2,7	1,2
77	-16,1	-7,9	-1,5	8,0	-17,6	-23,4	-3,3
78	-1,3	-0,3	-7,6	3,0	-6,2	3,0	-2,1

Extratemporal group

1	16,2	13,4	-0,2	-4,4	-4,9	6,8	-4,7
2	-2,1	0,9	2,3	3,4	-25,5	-4,5	12,9
3	11,3	7,1	0,1	2,6	5,5	1,2	-0,1
4 (1)	-1,3	-1,2	-1,4	1,2	0,6	-1,0	-5,7
4 (2)	-5,4	0,6	2,1	-0,4	5,5	-5,4	-9,2
5	-1,1	3,5	-4,8	-2,1	5,2	-8,7	-0,1
6	-20,9	5,8	6,2	3,5	-4,2		-2,9
7	2,0	-3,0	1,7	2,0	-2,7	-13,9	-5,5
8	2,4	1,7	1,4	1,4	1,0	-3,2	-3,9
11	5,9	0,2	2,0	0,4	0,9	-3,7	-4,0

Table 3.4

NUMERICAL ANALYSIS: ICTAL/POSTICTAL SCANS

Change in asymmetry index from interictal image (%)

Temporal group: ROI

Patient	Frontal	Bas.Gang	Thalamus	mes. Temp	lat. Temp	Parietal	Occipital	time
1	-1,4	12,3	-1,8	4,5	11,7	-18,9	-3,4	30
8	-2,8	5,8	-2,4	5,3	2,0	0,1	16,3	60
11	5,0	3,0	4,3	-8,9	-37,7	-20,5	-11,7	300
17 (1)	-3,7	-0,1	-7,4	4,2	-7,8	10,4	-3,4	0
17 (2)	5,4	-0,2	1,9	4,3	-4,2	4,8	2,4	0
21	-1,4	9,4	11,2	24,0	-12,5	-1,4	-7,0	150
25	1,9	4,6	-4,6	19,9	-11,1	7,9	1,3	0
27	11,1	-1,6	-3,7	10,2	14,1	7,1	-1,1	120
31	3,6	5,8	4,5	-3,1	11,1	16,3	9,2	360
32	-1,6	15,7	-2,3	1,9	1,4	-2,8	2,8	30
41	-12,4	9,3	6,4	8,3	-13,9	-13,1	-1,6	120
45	-3,8	6,0	9,5	13,0	-4,0	6,3	-2,9	10
47	0,1	2,5	7,4	12,3	-2,9	0,3	-6,7	10
49	2,5	0,8	9,0	-11,2	-9,7	6,0	3,8	180
56	7,4	-0,1	8,0	-19,2	12,5	2,2	-3,9	120
58	-5,3	-3,7	-9,1	8,6	-4,6	2,1	-1,1	15
59	5,9	3,8	-2,4	-3,5	-2,3	-6,9	3,7	90
60	-3,7	12,3	-3,2	9,1	16,2	4,8	-9,4	0
61	0,3	-0,5	4,8	1,9	-6,1	1,1	-4,8	120
62 (1)	-16,7	10,7	0,3	-6,7	-8,1	-20,2	9,3	900
62 (2)	6,9	-6,4	2,2	11,7	9,3	-6,8	7,0	60
63	-2,8	7,8	-1,6	6,7	4,3	9,9	-5,5	300
64	11,1	4,9	-10,0	6,1	7,0	7,0	-0,2	10
67	-0,1	-5,3	-6,6	0,8	0,8	-2,8	4,6	10
68	3,6	0,4	-5,0	-2,3	-4,8	0,8	-1,9	0
69 (1)	5,7	9,3	10,4	31,4	-6,7	-1,2	0,9	50
69 (2)	4,1	7,1	12,6	57,5	19,8	16,9	3,1	0
69 (3)	21,9	17,9	12,5	55,1	60,2	48,0	15,6	0
70	-19,6	-4,5	-1,6	-9,6	-25,9	-6,1	3,8	240
71	-4,5	1,0	0,7	1,7	-3,0	-8,6	8,7	60
72	-20,2	-3,8	-2,5	-8,5	19,6	-4,1	5,1	60
75	13,9	-4,5	-10,2	13,7	1,0	1,1	-0,7	15
77	-5,2	-0,5	2,9	7,1	-10,5	-25,3	-6,6	180
78	8,4	-8,8	-16,1	-7,7	3,6	-2,9	-0,8	30

Extratemporal group

1	-12,8	-7,4	-0,2	-2,0	1,0	6,7	-8,3	0
2	-2,9	5,0	2,3	-2,2	-13,8	0,5	25,1	30
3	-9,2	6,8	3,9	1,2	9,1	2,7	1,4	30
4 (1)	-2,4	0,1	45,7	-0,5	6,6	-5,5	-1,4	300
4 (2)	-4,3	1,9	49,2	-2,1	9,5	-10,8	-4,9	120
5	-1,7	2,8	-11,2	2,5	9,1	-1,6	3,6	60
6	30,0	6,5	-8,9	-0,2	-7,9		4,3	120
7	0,8	-8,9	-2,1	0,3	0,8	-13,4	-2,8	0
8	3,8	3,7	3,1	0,6	-2,9	-4,5	-2,8	90
11	-0,6	5,8	-5,5	-1,9	-1,4	-9,1	-4,3	120

Table 3.5

VISUAL AND NUMERICAL ANALYSIS OF IMAGES
Summary of ictal/postictal changes in cerebral perfusion

Temporal group (33 patients, 37 scans)

1. Visual analysis

Change	Number	Timing of injections (seconds postictal)
1	4 (3L, 1R)	0
2	21 (11L, 7R, 3B)	0-360
3	4 (3L, 1R)	90-900
Abnormal > normal	3	30-300
No change (normal)	2	30, 180
No change (abnormal)	3	0-60

2. Numerical analysis

Change		
1	1	Sides agreed with
2	13	visual analysis
3	4	
Abnormal > normal	1	
No change (normal)	1	
No change (abnormal)	0	

3. Disagreements between visual and numerical analysis

Hypoperfusion identified numerically but not visually:	5 (1 frontal, 1 mesial temporal, 1 lateral temporal, 2 parietal)
Hypoperfusion identified visually but not numerically:	8 (all lateral temporal)

Key to changes in temporal group:

1 Hyperperfusion of whole temporal lobe
2 Hippocampal hyperperfusion with hypoperfusion of lateral structures
3 Hypoperfusion of whole or part of temporal lobe
L=left R=right B=bilateral

Table 3.5

Extratemporal group (9 patients, 10 scans)

1. Visual analysis

Frontal hypoperfusion	3 (2R,1L)	0-120
Frontal hyperperfusionwith contralateral hypoperfusion	2 (hyperperfusion on R)	0-120
Occipital hyperperfusion with ipsilateral hemispheric hypoperfusion	1 (L)	30
No change	4	60-300

L=left R=right B=bilateral

2. Numerical analysis

Results as for visual analysis - no disagreements

Chapter 3

Discussion

Control studies

In this study, the interictal images (visual analysis and asymmetry indices) acted as control values for ictal and postictal studies. This practice entailed the assumption that any change seen on ictal or postictal images was due to the seizure. As has been discussed in Chapter 2, there is evidence that HMPAO SPECT findings may change independent of known seizures, and that interictal rCBF may be normal on some occasions and abnormal on others. For example, in the present study there were 3 patients in whom rCBF was abnormal interictally, and became normal postictally. This is open to at least two interpretations.

1. That the change is due to the seizure, i.e. rCBF has increased from a low level to a normal level because of the metabolic activity associated with the seizure, or the injection has been carried out during an intermediate phase of rCBF changes in a temporal lobe which has just been or is about to be hyperperfused.
2. That the change represents a variability in interictal hypoperfusion that would have taken place in any event, and is nothing to do with the seizure.

The issue of intra-individual variability in rCBF in normals or in patients with focal epilepsy has not been adequately addressed in this work or elsewhere, because of the ethical problems relating to radiation dosage. As discussed in Chapters 1 and 2, those small studies that have been done suggest that interictal hypoperfusion is stable, while there are nonetheless well documented individual examples of variability, even where injections have been EEG controlled to exclude recent or ongoing seizure activity (Shen et al, 1990; Berkovic et al., 1992). Hyperperperfusion is occasionally seen in apparently interictal studies, and is also variable (Duncan et al., 1990a). The question should therefore be addressed of whether ictal and postictal changes are consequent on the seizure or are coincidental.

Hyperperfusion of the whole temporal lobe has never been seen interictally in any study, so is highly likely to be truly associated with the seizure. The same reasoning can be applied to the early postictal (type 2) finding, excepting that this type of abnormality was found interictally in one patient in the present study (see Chapter 2), albeit that no EEG recording was carried out during injection of HMPAO, and subclinical seizure activity could not be ruled out as a cause in that case. There are

no instances of this finding occurring interictally in any study in the literature. It is therefore likely that it is also relatively specific for the postictal (or late ictal) period.

The late postictal (type 3) change consists of hypoperfusion of the whole temporal lobe, which is commonly seen interictally. Even examining numeric and visual data in retrospect, there was no clear distingushing feature between interictal and postictal hypoperfusion (e.g. in the relative degree of mesial and lateral hypoperfusion). There are now many examples of this type of postictal change documented in the literature, but where such changes seen at relatively long time periods after a seizure, their connection with that seizure remains in doubt.

It would be useful to have a range of 'normal' for variability in asymmetry indices. Ethical permission was not sought and would not have been given for repeat studies in normal volunteers. The meaning of normal data based on epileptic patients would be doubtful, since they may show changes in rCBF between one examination and the next which might be of similar magnitude to postictal changes (Berkovic et al., 1992). The number of subjects required would also pose ethical problems.

Timing of Injections

Previous ictal and postictal studies of regional cerebral perfusion have timed the injections of radionuclide with reference to EEG-recorded ictal onsets. In the present study EEG recording was not available, so HMPAO injections were timed with reference to the clinical features of the seizure; a study was labelled 'ictal' if the patient was injected during the 'motionless stare' phase of the seizure. Times of postictal injections are given with respect to the end of this phase. This method has potential inaccuracies, since the end of the stare phase was not always clear cut and, depending on the manifestations of the seizure, was not always clearly observable. While patients were observed as closely as possible, it was not always possible for a nurse or doctor to be present by the end of brief seizures. Although the geography of the ward and situation of the patients within it was such that nursing staff were usually on the scene within 30 seconds of the alarm being given, patient care took precedence over noting and recording times. This is likely to have resulted in some errors, particularly in patients whose seizures included automatisms and florid behavioural disturbances, in which case times were not recorded until the patient's safety had been secured.

In the early phase of the study, the nursing and medical staff were not used to the procedure, and the injections carried out at this time were all late in the postictal period, and times were recorded only to the nearest 30 seconds. As the study

progressed, all injections were carried out either ictally or within the first minute (since the data were used for clinical purposes, and it was already known that injection closer to the seizure was more likely to yield useful localising information, it would not have been ethically acceptable to delay injections for the sake of obtaining a better spread of injection times, or to obtain more late postictal studies with more accurate timing). Even then ward staff were usually not able to record the time of the end of the stare to the nearest second, even when it was reasonably clearcut, and would normally note it to the nearest 10-15 seconds, while taking care of the patient, and record it as soon as other members of staff arrived. In terms of accuracy, this was not ideal but it was felt that the practical problems of patient care did not allow any more elaborate procedure.

Notwithstanding these sources of error, with the exception of two patients, the changes labelled as ictal and postictal in this study were the same as those in the studies of Rowe et al. (1989b; 1991b) and Newton et al. (1992), where EEG timing with reference to seizure onset was used. Allowing for the usual 1-2 minute duration of a temporal lobe complex partial seizure, the timing of postictal changes was also similar, given the different reference points used. Type II change seen within 5 minutes of seizure onset in the studies of Rowe and Newton, and within 2 minutes of the end of the seizure in the present study. To determine the accuracy of clinical timing, one would have to use it in patients who were also EEG monitored, comparing the results. The above figures do, however, suggest that any inaccuracy in timing was not large.

Blinding of observers

The results of this study hinge on the changes in pattern of cerebral perfusion seen in association with a clinical event, i.e. the seizure. Ideally, one would have reported interictal and ictal/postical images separately, and blind to the result of the other scan. However, prior to this study the observers had found by comparing interictal and ictal/postictal images after separate reporting that the latter method resulted in some changes not being detected. It was considered justifiable, therefore, to sacrifice a degree of 'blindness' of reporting for the sake of accuracy, and to report the interictal scan first, then report the ictal/postictal scan with reference to it.

Other issues impinging on the visual analysis of images are discussed in Chapter 2.

Temporal group

Visual analysis of images

Comparison with results of previous studies

The temporal characteristics of HMPAO make it difficult to compare the results of the present study to those using amine type tracers such as HIPDM. The problem is that where the shape or size of an area of alteration of cerebral perfusion is altering rapidly (as during a seizure it appears to do), the long uptake time of HIPDM and the consequent lack of temporal resolution of the images produced, is translated into lack of spatial resolution. Similarly, where an area is hyperperfused at the beginning of the uptake period and becomes hypoperfused before the end of it, the average uptake may be the same as parts of the brain which are normally perfused throughout.

A further difficulty as regards comparison with studies using other methods is compatability of the slices used to view and analyse images. The transaxial slices used in this study were originated by Rowe et al. (1989a; b). They are logically the best for seeing temporal lobe structures, allowing easy differentiation between mesial and lateral temporal cortex, and between mesial cortex and the adjacent frontal lobe. The studies of Lee et al. (1986; 1987a; b; 1988) and Shen et al. (1990) as well as using the tracer HIPDM, used standard orbitomeatal slices, which make it difficult to appreciate temporal lobe anatomy. Such difficulties of anatomy and resolution are reflected in the fact that in these studies abnormalities are reported as *regions* of increased or decreased uptake, rather than as structures. Given these problems, only the studies of Rowe et al. (1989b;1991b) and Newton et al. (1992) are directly comparable with those of the present study.

The ictal and postictal changes seen in other studies are compared with those in the present study in the light of the above factors.

1. Ictal changes

Lee et al. (1986; 1987a; b; 1988) found areas of increased cerebral perfusion in the temporal lobe in 12/14 patients with temporal lobe foci. All their patients were injected during the seizure, so no postictal changes were shown. They comment that 'in a few patients' rCBF was decreased in areas adjacent to the hyperperfused areas, and suggested this might be due to a steal phenomenon. The later study from the same group (Shen et al., 1990) found areas of increased perfusion in the temporal regions of 33/34 patients with temporal lobe foci. In neither of these studies do they comment on the morphology of the areas of increased perfusion, and it

is not clear whether the whole or part of the temporal lobe is involved in all cases. The limitations of their method makes it unlikely that they could make such a distinction clearly (see above). Rowe et al. (1991b) and Newton et al. (1992) found hyperperfusion of the whole temporal lobe on ictal images, as in the present study. They also commented on hypoperfusion of the frontal and parietal lobes ipsilateral to the focus. Hypoperfusion was seen during the ictal phase by Penfield et al. (1939). It was not noted on visual analysis in the present study, but was detected in 2 patients by numeric analysis.

Two patients injected ictally in the present study had hyperperfusion of the hippocampus with lateral hypoperfusion (i.e.) the pattern found more typically in the early postictal period. This would be compatible with the finding of Shen et al. (1990) of hypoperfusion 'adjacent to' ictal hyperperperfusion, given the relatively poor anatomical definition in their study, but given differences in timing methods, it may be that our own patients showing this were actually in the early postictal phase. However, one patient was in the clonic phase of a secondary generalised seizure at the time of injection, and one had EEG coincidentally recorded at the time (showing continuous spike/wave discharge), making inaccurate timing an unlikely explanation in these cases. Both had seizures which were prolonged, so it may be that the 'postictal' pattern of perfusion occurs in the late stage of long periods of seizure activity, as well as after shorter periods.

The studies of Lee et al. (1988), Shen et al. (1990), Rowe et al. (1991) and Newton et al. (1992) detected changes in a total of 54/57 (96%) of patients studied in the ictal phase. Changes were detected in 6 of the 8 ictal images in the present study (both scans showing no change were in the same patient).

In contrast to the above changes, one patient (patient 61) in the present study showed ictal hyperperfusion confined to the hippocampus, with no hypoperfusion. There was no obvious difference between this patient and the others, clinically, interms of EEG findings or in terms of postoperative pathology (Ammon's Horn sclerosis was found). As in all the patients, injection followed the habitual type of seizure, which was of the complex partial type. It is possible that the seizure discharge remained very localised, and that the associated metabolic disturbance was therefore also small in extent, but only depth EEG recordings would be able to establish this, and these were not available.

2. Postictal changes

The only studies comparable with the present one are those of Rowe et al. (1989; 1991) and Newton et al. (1992). Early in the postictal period, these studies found

hyperperfusion in the hippocampus with hypoperfusion of lateral temporal structures, corresponding to the type 2 change found in the present study. In the studies of Rowe et al., and Newton et al., the hypoperfusion sometimes extended into the parietal and occipital regions. In the present study, extensive postictal hypoperfusion extending outside the temporal lobe occurred in most patients, although it was often of a relatively minor degree. The timing the changes relative to the HMPAO injections in the two studies were compatible; Rowe et al. found that hippocampal hyperperfusion resolved 5-8 minutes after the beginning of the seizure, compared to up to 6 minutes after the end of the seizure in this study (according both to visual and numeric analysis of images).

Type 3 change, or hypoperfusion only, was seen up to 15 minutes after the end of the seizure. This has been seen in other studies up to 20 minutes postictally Berkovic et al., 1991) but clearly, given the fact that up to 30% of patients injected later in the postictal period to show no changes in rCBF (Rowe et al., 1989b; 1991b), it is likely that the duration of this phase is highly variable.

Postictal HMPAO SPECT localised the epileptic focus correctly in Rowe's (1989b; 1991b) studies in 72% and 69% of patients, with 1 patient apparently localised incorrectly. In the present study 24/26 (92%) were localised correctly, with no false localisations. It is not clear why relatively few of Rowe's patients showed localising changes, as one would expect changes in perfusion to occur in association with all seizures. Rowe et al. (1989b) did find a tendency for injections closer in time to the seizure to be more likely to show changes in rCBF, as one would expect to be the case. Our injections may have been closer to the seizure than Rowe's (the difference in timing method makes exact comparison impossible), and it may be that the superior resolution of the imager allowed confident reporting of less obvous abnormalities.

Causes of ictal and postictal hyperperfusion and hypoperfusion

It is probable that ictal hyperperfusion is the result of metabolic demand of electrical activity (increased local metabolic rate has been shown in the limited PET studies done during seizures (Engel, 1984; Engel et al., 1983; Franck et al., 1986; Theodore et al., 1984; Theodore et al., 1983), and that hyperperfusion persisting postictally is the result of metabolic debt built up during the seizure as a result of non-oxidative glucose metabolism (Ackerman et al., 1989), and persisting metabolic activity taking place to restore ion gradients, activity which had been shown to persist for several minutes postictally in animal experiments (Leninger & Follett 1984). It seems likely that the area most metabolically active will have the greatest metabolic debt, and that given that the patients had mesial temporal foci, persistence into the postictal period of hyperperfusion in the hippocampus is consistent with seizure origin in that structure.

While ictal hypoperfusion was not noted on visual analysis of images in the present study, numerical analysis shows that hypoperfusion occurred during the seizure in the parietal and frontal lobes in 3 patients, and the phenomenon has been observed in several patients since completing the above study. Hypometabolism surrounding ictal hypermetabolism was noted in one PET study (Engel, 1983), and animal studies of metabolism and blood flow have also shown the same phenomenon (see Chapter 4). It is therefore likely that metabolism as well as perfusion is depressed. The phenomenon may be related to the inhibition seen around epileptic foci in animal models (see Chapter 4; Prince & Wilder, 1967).

Presumably postictal hypoperfusion relates to the same effect. PET studies of metabolic rate in generalised seizures have found postictal depression of metabolism (Engel, 1983a,b; Engel, 1984; Engel et al., 1982b; Engel et al., 1983; Mazziotta & Engel, 1984), so postictal depression of blood flow is also likely to be secondary to depression of metabolism. No attempt was made in this study to relate postictal confusional states to postictal hypoperfusion, but postictal hypoperfusion has been related to the slowing of EEG rhythms which is associated with postictal confusion (Rowe et al., 1991b).

Temporal group

Numerical analysis of images

Ictal changes

In the present study, the largest increase in asymmetry index was found in the lateral temporal cortex in patient 69. The interictal asymmetry index was -41.6, and the ictal index was 18.6, giving an increase in asymmetry index of 60.2. Without knowing absolute rCBF it is not possible to say what percentage increase in perfusion this change represents, as the perfusion in the contralateral side may also have changed in either direction. Assuming it did not, then rCBF in the lateral temporal cortex approximately trebled in this patient, even without allowing for the fact that HMPAO underestimates high flows. Studies of blood flow and metabolism in generalised seizures have shown rises of up to 350% in humans (Engel, 1983;1984; Engel et al., 1982a; Engel et al, 1983; Mazziotta & Engel, 1984) and of up to 900% in rats (Meldrum & Nilsson, 1976). Studies of metabolism using rat models of epilepsy have found rises of 2-300% in seizures originating in the motor cortex (Collins, 1976; 1978) and rises of 30-180% in seizures originating in the limbic system (Blackwood et al., 1981; Collins et al., 1983; Lothman et al., 1985). It appears that the range of changes seen in the present study is consistent with these data.

The 95% confidence interval of the mean ictal change in asymmetry index for the lateral temporal cortex found by Newton et al. (1992) was 21.8-48.4%. The total range in the present study was -10.2-60.2, with a 95% confidence interval of -11.9-34.4. The smaller confidence interval probably reflects the fact that some patients in our series showed ictal hypoperfusion of the lateral cortex. The 95% confidence interval in the study of Newton et al. for the mesial temporal cortex was 22.4-39.2, compared to the present study, where the total (ictal) range was 2.3-57.5, with a 95% confidence range of -1.2-44.8. The difference at the lower end of this range might also be explained by 2 patients showing the typical postictal (Type 2 change) pattern of perfusion (the degree of mesial hyperperfusion was less in these patients, both in the present study and that of Newton et al.), and by 2 patients showing no change. The range of change in the parietal ROI was greater in the present study than in that of Newton et al., at 0.8-48.0 with a 95% confidence interval of -2.7-32.2, the larger range being entirely due to the single patient at its top end. The frontal ROI used by Newton et al. was laterally placed, and not comparable with those found in the present study which was anterior. The frontal changes seen in the present study were more prominently positive (95% confidence intervals of -13.9-2.5 for Newton et al. compared with -3.9-12.3% in the present study). If the negative changes seen by

Newton et al. were due to 'surround hypoperfusion' then the greater proximity of their lateral ROI to the temporal lobe may have been responsible for the greater negativity of the changes seen.

Postictal changes

Changes in asymmetry index in frontal, lateral temporal and parietal ROIs all showed greater negativity from the ictal period on, decreasing in the first minute to around or below zero, suggesting a more or less immediate decrease in perfusion, continuing several minutes into the postictal period. By contrast, the first negative change in the mesial temporal ROI did not appear until 1 minute postictally, and even late into the postictal period mean changes were only slightly negative. This difference reflects the tendency noted on visual inspection of images for mesial temporal structures to remain hyperperfused longer into the postictal period than lateral cortical structures. Obviously in interpreting mean values of postictal changes differences in the size of the time groups should be taken into account; most injections (14) were carried out up to 1 minute postictally, while only 3 were carried out between 2 and 3 minutes postictally.

The greater prominence of hypoperfusion into the postictal period may reflect increasing inhibition; one would expect neuronal exhaustion to recover in the postictal period, rather than worsen. Hypoperfusion tended to affect the lateral temporal ROI most prominently of the lateral ROIs, which one would expect given the abundant connections between the mesial and lateral temporal structures thought to be responsible for rapid propagation of seizure impulses (Van Hoesen, 1982; Van Hoesen et al., 1979).

Compatability of numeric data with the results of visual analysis

There are no control data for ictal or postictal change in asymmetry index. For the purposes of comparison with visual analysis, therefore, the change in rCBF according to numeric analysis was determined by noting which ROIs had asymmetries of 9% or more on interictal scans, and doing the same on the ictal or postictal scan. The change in rCBF was defined as the difference between the two.

There were only 4 scans in which numeric analysis detected abnormalities which visual analysis did not, compared with a total of 9 scans in which there were discrepancies in the other direction. Agreement between the two methods was similar to that in the interictal study (Chapter 2).

Ictal and postictal changes in asymmetry index in the basal ganglia

The changes seen in asymmetry indices in the basal ganglia and thalamus were similar to those seen by Newton et al. (1992). In all the ictal images which showed changes, the direction of the change was the same as that in the temporal lobe. Postictally, while the average change was in the same direction as cortical changes, there were individual patients in whom the direction of change disagreed. There are projections in both directions between limbic structures (particularly the amygdala) and the basal ganglia (Alheid & Heimer, 1988), and one might expect changes in temporal cortical structures to be mirrored in subcortical structures postictally as well as ictally. Why this is not always the case is unclear. It may be that the precise topography of inhibitory discharges in the early postictal period causes depression of function in subcortical structures while the hippocampus remains hyperfunctional.

Extratemporal group

In contrast to the situation in the temporal lobe, where the great majority of seizure foci are in the hippocampus, seizures may originate in a wide variety of locations in the frontal lobe (Bancaud & Talairach, 1992), which is a much larger structure. Patients 6 and 7 both had epileptogenic lesions (manifested as signal changes on MRI) in the frontopolar area, and both showed ispilateral adjacent hyperperfusion with contralateral hypoperfusion, albeit one injection was during a seizure, the other 2 minutes postictally. The 3 patients showing hypoperfusion only had EEG onsets recorded over the hypoperfused frontal lobe, but had no evidence of the location of the focus within the frontal lobe. The patients showing no change had no localisation within the frontal lobe.

One might hypothesise that the different changes in rCBF seen (i.e. hypoperfusion alone c.f. hyperperfusion with contralateral hypoperfusion) were because the location of the foci within the frontal lobe were different. However, the possibility should be considered that the three patients showing hypoperfusion only had a small focus of hyperperfusion in the contralateral frontal lobe, beyond the resolution of the imaging technique (the area of hyperperfusion seen in patient 6 was small, and may well have been missed using an imager of lesser spatial resolution). One study of postictal rCBF including patients with frontal seizures has been published (Stefan et al., 1990), and it included one patient in whom such a finding was false

lateralising. While the side of the hypoperfusion agreed with surface EEG ictal onsets in the patients in the present study, such onsets may be false lateralising (Swartz et al., 1991), and do not exclude the above explanation for there being different findings in these patients. A recent study of rCBF including some patients with frontal lobe seizures (Marks et al., 1992) has shown different changes accoring to site of origin in the frontal lobe.

The observation that hypoperfusion associated with frontal seizures may be contralateral to the focus is in marked contrast to the temporal seizures and the single occipital seizures observed where it was without exception ipsilateral. The observation has been repeated on several occasions since completing this study. One of the patients in this study (patient 6) and one subsequent patient had complete corpus callosum sections, making it unlikely that the effect is mediated by callosal pathways. It may be mediated through bulbocortical pathways and the locus ceruleus or other brainstem structures, known to have cerebrovascular regulatory effects (Lance et al., 1986 others). Whether it is related to postictal slowing or to postictal inhibition is unknown. While conclusions regarding patterns of ictal and postictal rCP cannot really be drawn from these limited data, they were completely different from those seen in the temporal group in the present study. The difference was confirmed by the results of numerical analysis of images, showing that ROI data for the groups as a whole were differed mainly in the mesial temporal ROI, which showed virtually no changes in the extratemporal group.

Comparison of the results of the present study with animal studies

Studies of local cerebral metabolic rate in the rat have some obvious parallels with the ictal and postictal changes in regional cerebral perfusion found in the present study. Studies of focal motor seizures (e.g. using intracortical injection of penicillin) have shown local increases of up to 300%, with secondary activation of the homotopic motor cortex, the cingulate gyrus, the caudate and globus pallidus (Collins, 1976; 1978). Prominent depression of metabolism is seen throughout the rest of the cortex. Rat models of limbic seizures show increases in metabolism of up to 180% in the limbic structures themselves, with lesser increases in the contralateral limbic structures, the substantia nigra, thalamus and septal nucleus (Blackwood et al., 1981; Collins et al., 1983; Lothman et al., 1985). Depression of metabolism has been seen only to a small extent in these studies (Lothman & Collins, 1981).

In rat models of limbic seizures, increases in local metabolic rate and blood flow are seen in the ipsilateral thalamic nuclei and substantia nigra (Blackwood et al.,

1981; Collins et al., 1983; Lothman et al., 1985; Tanaka et al., 1990). Basal ganglia changes seem to be more prominently described in models of focal motor seizures (Collins, 1976a; b; 1978). It is, however, interesting to note that in the present work (see chapter 4) changes in blood flow secondary to focal motor seizures were seen in the thalamus and substantia nigra, but not in the basal ganglia.

Studies in the rat and their relationship to human studies are further discussed in Chapter 4.

Comparison of results of the present study with the observations of Penfield

Penfield (1933; 1937) observed changes in perfusion at the site of the focus starting seconds after seizure onset, and lasting several minutes after the end of the seizure. These changes corresponded well with those seen in the present study. He observed ictal increases in perfusion starting seconds after seizure onset, focal blanching and arterial spasm of the pia during and after the seizure, and showed that ictal perfusion fell at sites distant to the focus. These latter changes are likely to correspond to the ictal 'surround' hypoperfusion, and more widespread postictal hypoperfusion seen in the present study.

Conclusions

1. In seizures originating in the mesial temporal lobe, the whole temporal lobe is hyperperfused during the seizure. The lateral temporal cortex becomes hypoperfused early in the postictal period, while hyperperfusion persists longest in the hippocampus. Such changes were seen in the majority of seizures studied.
2. Postictal hypoperfusion may be very extensive, and may involve the whole hemisphere ipsilateral to the focus.
3. The anatomical correlation with interictal findings was good, but ictal and postictal changes are seen in a higher proportion of patients.
4. Seizures of extratemporal origin showed different patterns of change in rCBF during and after seizures, but numbers of patients were too small for definite conclusions to be drawn. In some patients at least, hypoperfusion may appear ictally or postictally in the hemisphere contralateral to the focus.

Chapter 4

Validation of HMPAO as a tracer of cerebral perfusion during seizures

Introduction

HMPAO

HMPAO (Neirinckx et al., 1987) is hexamethylpropyleneamineoxime. It is a lipophilic compound which can be labelled with ^{99m}Tc to form ^{99m}Tc-HMPAO. When injected intravenously it is distributed throughout the body, with approximately 4% of the dose going to brain in man and animals (Costa et al. 1986; Andersen et al., 1988a). Being lipophilic, it crosses the blood-brain barrier freely. Inside brain tissue it undergoes a chemical change (the precise nature of which remains uncertain (Costa et al., 1989; El Shibirny et al., 1989)), and becomes hydrophilic and therefore unable to cross cellular membranes and the blood brain barrier. Its distribution in brain therefore remains stable for some hours. Studies in the rat (Costa et al 1989) have shown that it distributes largely in the neurones in the neocortex (92%) and in the paleocortex (85%), and to a lesser extent in the cerebellum (70%). The remainder is localised in the glia. Within the neurones, it is concentrated in the lysosomes.

The brain distribution of microspheres and ^{99m}Tc HMPAO correlate well in the dog (Costal et al, 1987), and previous autoradiographic studies using iodoantipyrine (IAP) have also shown good agreement (Lear, 1988; Bullock et al., 1991). Initial uptake in the normal human brain appears to be proportional to rCBF (Lassen et al., 1988), and to correspond well with rCBF as shown by other in vivo methods such as ^{133}Xe (Andersen et al., 1988) and PET (Yonekura et al., 1988: Inugami et al., 1988).

The conversion of HMPAO to a hydrophilic compound takes place with an exponential half life of 40 seconds so, at high flow rates, there is a 'wash out' effect, causing HMPAO uptake to underestimate flow. This can be corrected using the correction factor of Lassen et al. (1988). The expression used to derive the correction relates the corrected HMPAO uptake, hence the true CBF, to the measured HMPAO uptake by the expression;

$$f/fr=\acute{o}xC/Cr)/(1+\acute{o}-Cr)$$

where f is the true CBF, C is the measured HMPAO uptake in the brain area of interest, and fr and Cr are the flow rate and measured ^{99m}Tc HMPAO concentration, respectively, in a reference region of the brain. The constant ó is the ratio of the rate of conversion to the rate of back-diffusion and clearance in the reference region (the reference flow rate in this study is 100ml/100g/min and the value for ó is 2.0 (Igunami et al., 1988)). The function is illustrated in Fig 4.1. HMPAO and its kinetics are further discussed in the Appendix.

This correction has been applied in normal rats and in low flow rodent models of ischemia, but has not so far been applied at flows as high as those seen during seizures in rats and in humans. This study aims to compare HMPAO uptake with rCBF as measured by ^{14}C iodoantipyrine IAP uptake in the normal rat and during focal motor seizures, using the penicillin model of focal epilepsy, to verify that the Lassen correction linearises the relationship at very high flows. A recent publication (Sperling & Lassen, 1993) suggests that HMPAO uptake may be spuriously high in areas reperfused following cerebral infarction, underlining the need to verify the accuracy of the technique in specific pathological situations.

Methods

Ten male Sprague Dawley rats weighing between 375g and 595g (mean 480 ± 21g) were used, 5 for control studies and 5 for seizure studies. The procedure was as follows;

Induction of focal motor seizures using intracortical injection of penicillin

1. The rat was anaesthetised using halothane and nitrous oxide. Anaesthesia was continued during the procedure using a plastic face mask.
2. Cannulae were inserted into both femoral arteries and veins. One arterial catheter was used for monitoring of blood pressure and pulse rate, and for obtaining arterial gases for blood gas estimation.
3. The rat was placed in a plaster of paris hip brace, and secured to lead bricks.
4. An incision was made over the skull, and a 1mm burr hole of sufficient size to expose 0.5mm of dura was made 2mm anterior and lateral to bregma.
5. The skin was resutured.
6. One venous catheter was connected to the syringe pump containing 125uCi/kg of ^{14}C IAP in 1.5ml, the other to a syringe containing 500MBq of ^{99m}Tc HMPAO in 1ml. The remaining arterial catheter was used for sampling during the IAP procedure.
7. Blood pressure and gasses were checked.
8. The skull suture was divided, and the burr hole re-exposed.
9. A fine needle attached to a 500µl microsyringe was inserted into the cortex through the dura to a depth of 1.5mm from the outer dural surface. A volume of 200µmol of penicillin in 200µl of pH-balanced artificial CSF was injected. Control animals were injected with 200µl of artificial CSF.
10. The scalp wound was resutured, and the anaesthesia discontinued.
11. The rat was observed and the first manifestations of seizure timed.

Injection of HMPAO and measurement of rCBF

1. After 7 minutes of seizure activity 200MBq of ^{99m}Tc labelled HMPAO was injected intravenously over 1minute.
2. Two minutes were allowed between the injection of HMPAO and the IAP procedure to allow time for any back-diffusion of HMPAO to occur. After 10 minutes of seizure activity, therefore, the IAP procedure was commenced. The procedure and the method of

calculation of rCBF are described in detail by Sakurada et al. (1978), Tamura et al. (1981), and Gotoh et al. (1986). It is carried out by 3 operators, 1 who collects and times (by speaking into a tape recorder) the arterial samples, 1 who regulates the ramped infusion of ^{14}C iodoantipyrine, and one who monitors the condition of the animal during the 30 seconds of the infusion (in particular to ensure that blood pressure does not drop below the limit of autoregulation during the procedure) and operates the guillotine at the end of the infusion. Just prior to commencing the IAP procedure:

1. The rate of flow through the arterial catheter was regulated to give approximately 50 drops over 30 seconds.

2. Blood gasses, pulse and blood pressure were checked. The experiment proceeded if pCO2 was 60mmHg or less and pO2 was 70mmHg or more. Systolic blood pressures of 100-200mmHg were considered acceptable.

The IAP procedure was then commenced as follows;

1. At the same moment, the arterial catheter was opened and the IAP infusion started.
2. The IAP was injected at a progressive rate, the whole dose being given over 30s.
3. During the period of the injection 15-18 drops were collected from the arterial cannula on pre-weighed 1cm filter paper discs.
4. At the moment the infusion was terminated, the animal was decapitated.
5. The brain quickly dissected out and frozen (to prevent tracer diffusion (Williams et al, 1991) by immersion in isopentane chilled to -42deg.C in dry ice.
6. The blotting paper discs were transferred to pre-weighed scintillation counter vials which were immediately capped to prevent evaporation and re-weighed.
4. Immediately following the procedure, the brain was cut into 20μm coronal sections with a cryostat. Three consecutive sections every 13 were mounted on cover slips. Within 1 hour of decapitation the sections were placed on autoradiographic film (Amersham Hyperfilm) for 4 hours, with a series of 6 standards from 2.5-19.00 μCi/g.
4. IAP was eluted from the arterial samples contained on the blotters. The samples left for 4 days to allow ^{99m}Tc activity to diminish, were placed in a scintillation counter, and counted 3 times and the counts averaged. The concentration of tracer in the blood was calculated from the detected radioactivity and the sample volume.
5. After a gap of 4 days to allow ^{99m}Tc activity to diminish, the sections were then placed on ^{14}C sensitive film (Kodak GRL, Rochester, NY) for 14 days, along with a set of 12 standards from 44-1475nCi/g, to produce the ^{14}C IAP autoradiograph.

6. Quantitative autoradiography was carried out on both films using a Quantimet 970 densitometer (Cambridge Instruments).The structures measured were;

1. the centre (low flow area) of the focus
2. the high flow area of the focus (penumbra) around the injection site
3. lateral frontal cortex adjacent to the focus 4. cingulate cortex
5. subcortical white matter
6. caudate nucleus
7. septal nucleus
8. globus pallidus
9. lateral amygdaloid nucleus
10. lateral habenular nucleus
11. medial habenular nucleus
12. ventral thalamic nucleus
13. dorsomedial thalamic nuclei
14. lateral thalamic nucleus
15. entopeduncular nucleus
16. hypothalamus
17. parietal cortex
18. auditory cortex
19. hippocampus
20. substantia nigra pars reticulata
21. inferior colliculus
22. pontine reticular formation
23. visual cortex
24. cerebellar hemisphere

For control animals, structures 1 and 2 were omitted. Each structure was measured on three adjacent sections, and the measurements were then averaged. Each structure was measured with its contralateral homotopic structure. Structures were measured at the same position on the same section in IAP and HMPAO films. The set of standards on each film were measured before and after the measurement of the structures.

rCBF was calculated as described by Sakurada et al. (1978) from the arterial IAP curve and the local tissue ^{14}C concentration, using a partition coefficient for IAP of 0.78.

Optical density values from HMPAO films were converted to ^{99m}Tc counts using the known standards. The Lassen correction factor was then applied.

Chapter 4

Results

Physiological parameters.

pO2, pCO2, pH, systolic and diastolic blood pressures, and rectal temperatures are given for all 10 animals in Table 4.1. Because the animals were semi-conscious and breathing spontaneously, because of the time frame of the experiments (i.e. rCBF measured within 10 min of withdrawal of anaesthetic), and because of seizure activity in the animals injected with penicillin, physiological variables were difficult to control. In particular, it proved difficult to achieve stable blood gas concentrations. Despite relatively wide variations being accepted, some experiments had to be aborted for this reason. Blood pressure rose sharply during seizures in animals 8,9 and 10. This was accepted since rises in blood pressure appear to contribute to the large rises in rCBF seen during seizures (during generalised seizures, at least (Plum et al., 1968)), and the main aim of the experiment required the production of high blood flows.

Seizures.

Control animals awoke normally 2-3 minutes after withdrawal of anaesthetic, and showed no abnormality of behaviour. Seizure animals exhibited subtle twitching of the right (contralateral to the seizure focus) whiskers from the moment of regaining consciousness. The twitching gradually spread to the muzzle, then to the foreleg, the hindleg and tail. The seizure remained unilateral and affected face, legs and tail in all 5 animals, although the jerking movements were of obviously lesser amplitude in animal 10. EEG recordings showed a high amplitude spike and slow wave discharge of greater amplitude on the left (Fig 4.2).The autoradiographic films showed a similar site and depth of injection in all the animals, and there was no other obvious technical reason for the difference in intensity of seizure activity in animal 10.

Blood flow as determined by the ^{14}C Iodoantipyrine method.

a. Non seizure animals.

Blood flows in non-seizure animals are shown with means and ranges for each structure in Table 4.2. Percentage side to side differences are given in Table 4.3. Cerebellar sections were not obtained for Rat 2. The blood flows for the group as a whole were compatable with those found in normal rats in previous studies using the same methods (McCulloch et al., 1982a; Mohamed et al., 1985; McCulloch et al., 1982b). Inter-animal variability was, however, great; the smallest inter-animal range was 18ml/100g/min (subcortical white matter, left side) and the largest 251ml/100g/min (inferior colliculus, right side).

The pattern of regional cerebral blood flow was similar to that seen in the normal rat, with the exception that in animals 1,3,4 and 5 there was an asymmetry in cortical blood flow (Fig 4.3), the flow on the side of the craniotomy being relatively low. The difference was maximal posteriorly: side to side differences in the parietal cortex in these 4 animals were 84, 55, 76 and 81 ml/100g/min, and in the auditory cortex, 61, 44, 50 and 31 ml/100g/min, respectively. These compare with frontal side-to-side differences of -19, 19,-37 and 1 ml/100g/min. Over the group as a whole, left-right differences were statistically significant only in the parietal cortex and visual cortex ($p=0.019$ and 0.014, respectively; paired Student's t-test).

b. Seizure animals.

Flows in seizure animals are shown with means and ranges for each structure in Table 4.4, with percentage side-to-side differences in Table 4.5. Cerebellar sections were not obtained in Rats 6 and 10. Mean flows were higher in seizure than in control animals in all structures except for the amygdalar and entopeduncular nuclei bilaterally, where flows were slightly higher in the control group (amygdalar nucleus control means 114 and 119 ml/100g/min, seizure means 100 and 109 ml/100g/min; entopeduncular nucleus control means 92 and 89 ml/100g/min, seizure means 98 and 74 ml/100g/min) and for the parietal and auditory cortex on the side of the focus, where flows were lower in seizure animals (left parietal cortex control mean 156 ml/100g/min, seizure mean 110 ml/100g/min; left auditory cortex control mean 138 ml/100g/min, seizure mean 132 ml/100g/min).

The pattern of distribution of rCBF in seizure animals was different from that in the control animals. Side to side differences are assessed using the paired Student's t-test, and differences between the groups using the unpaired Student's t-test.

The needle track could be seen as an axial area of low flow, (mean side to side difference 35ml/100g/min: p=ns), in contrast to control rats where the needle track was difficult to visualise (Fig 4.4). Around this was an area of flow higher than that in the surrounding frontal cortex (mean difference 170ml/100g/min; p=0.035), and higher than the homotopic cortical area (mean difference 110.4ml/100g/min; p=0.049). This area extended over an area of cortex 3-5mm in diameter, and extended into the cingulate cortex bilaterally in animals 8,9 and 10. (Fig 4.5). In animal 10 the septal nucleus showed high flow bilaterally (287 (left) and 216 (right) ml/100g/min) (Fig 4.6). The frontal cortex surrounding the focus tended to have low flow (Fig 4.4) although the difference was relatively small over the group (mean difference 17.2ml/100g/min; p=ns). More posteriorly, however, in the parietal, auditory and visual cortical areas hypoperfusion was more obvious (mean differences 136ml/100g/min; p=0.027, 181.4ml/100g/min; p=0.002, 89.6ml/100g/nim; p=0.046, respectively) (Figs 4.7 and 4.8).

In subcortical structures, the thalamus ipsilateral to the focus was hyperperfused, principally in the dorsomedial nucleus (mean difference 287ml/100g/min, p=0.001), but also in the ventral nucleus (mean difference 142ml/100g/min, p=0.003)(Fig 4.7). There was slight relative hyperperfusion of the contralateral medial thalamus in animals 6,7 and 8, although the difference between seizure and control groups was not significant. In animals 7-10 there was visually apparent hyperperfusion of the substantia nigra pars reticularis, with a mean asymmetry for the group of 78ml/100g/min (p=0.007) (Fig 4.8). Although the differences were not easy to see on visual inspection of the films, increases in flow ipsilateral to the focus were also seen in the medial and lateral habenula (mean differences 56 and 52ml/100g/min, p=0.008 and 0.049, respectively). Significant left-right differences in seizure animals are shown in Fig 4.9.

Percentage side-side differences - control vs seizure animals

Side-side differences were expressed as percentages ((focus side - contralateral)/contralateral x 100), to eliminate inter-animal variability in general levels of blood flow, and are shown in Fig 4.10.

a. Cortical areas

Significant differences between seizure and control groups were seen in the focus penumbra (increase on focus side of 56.7% in seizure rats vs decrease of 3.3% in controls, p=0.028), the adjacent septal nucleus (increase of 19.5%in seizure animals vs decrease of 3.8% in controls, p=0.020) Significant decreases on the focus side were seen in the aditory (decrease of 56.8% in seizure animals vs decrease of 28.9% in controls, p=0.040) and visual (decrease of 39.7% in seizure animals vs decrease of 6.9% in controls, p=0.001) cortices.

b. Subcortical areas

Significant increases on the focus side in seizure animals were seen in the dorsomedial thalamic nucleus (increase of 161.3% in seizure animals vs increase of 7.8% in controls, p=0.004), the ventral thalamic nucleus (increase of 72.0% in seizure animals vs increase of 2.9% in controls, p=0.002), the lateral habenular nucleus (increase of 21.8% in seizure animals vs increase of 2.3% in controls, p=0.042), the medial habenular nucleus (increase of 20.8% in seizure animals vs decrease of 1.7% in controls, p=0.002), and the substantia nigra pars reticulata (increase in 63.2% in seizure animals vs decrease of 0.5% in controls, p=0.004).

Assuming that, for any structure, the difference in asymmetry between control and seizure groups indicates the degree of perfusion changes occurring in association with the seizure, then the above figures show that the magnitude of such changes (whether positive or negative) was greater in in some areas distant from the focus than in the area of the focus itself.

Correlation of ^{14}C IAP and ^{99m}Tc HMPAO uptake.

The main aim of this experiment was to test the correlation between blood flow and HMPAO uptake at very high flows. Overall, the flows seen included 4 areas over 600 ml/100g/min, 13 areas between 400 and 600 ml/100g/min, and 30 areas between 300 and 400 ml/100g/min.

The HMPAO films showed a pattern of uptake identical in detail to that on the IAP

films, with 3 exceptions. Firstly, uptake in the choroid plexus was much higher in the HMPAO films in all 10 animals (Figs 4.3 and 4.7). Secondly, in the rhinal fissure uptake of IAP was higher than in the surrounding cortex, while on the HMPAO films it was lower. There were also some (but not all) areas where sections had been inadvertently folded during preparation where HMPAO uptake was relatively high (Fig 4.5). Thirdly, in animal 8 uptake of HMPAO was relatively high in the supramamillary nucleus (Fig 4.8).

In general there was very little difference in resolution between IAP and HMPAO films, although some showed superior resolution with IAP (Figs 4.3, 4.4, 4.7 and 4.8), and some with HMPAO (Figs 4.5 and 4.6). This relative lack of spatial resolution on some of the HMPAO films included bubble artefacts, which appeared blurred. Bubble artefacts are produced during preparation of sections, and therefore appear at the same location on both types of film (see Figure 4.8 for comparison). In contrast, the spatial resolution of scratches, which are produced after the sections are exposed and developed, but before they are photographed, was the same on both types of film, whether the resolution for anatomic detail was poorer on the HMPAO film (e.g. Figure 4.7) or whether there was no obvious difference between the two (e.g. Figure 4.5).

^{99m}Tc activity for control animals is shown in Tables 4.6 (uncorrected) and 4.7 (corrected), and for seizure animals in Tables 4.8 (uncorrected) and 4.9 (corrected). Figs 4.11-4.20 show the within-animal correlation between rCBF as determined by the IAP method, and ^{99m}Tc activity before (above) and after (below) the Lassen correction is applied. The curves fitted to the data are based on the second order binomial relationships shown on the graphs.

R^2 for these curves are shown on the graphs, and ranged from 0.542-0.847. The uncorrected curves show a tendency for the rise in HMPAO uptake as represented by Tc99m activity to become less at high flows. In Rats 1,6 and 7 the curves fitted to the data acually fall off within the range of flows shown (minimally in the case of Rat 1), although the shape of the data itself suggested a plateau effect, not predictable by a second order binomial fit. Even uncorrected, the relationship between blood flow and ^{99m}Tc activity remained almost linear in most of the animals up to 200ml/100g/min, and in some up to 300ml/100g/min.

The linearity of the relationship was improved by the application of the Lassen correction in all the rats. In Rat 4 the corrected curve was similar to the uncorrected curve, but in the opposite direction. In all the rats, however, a straight line fit gave higher R^2 values than the second order polynomial fit illustrated on the graphs (R^2 0.740-0.944, $p<0.001$ in all rats).

Chapter 4

Illustrations and Tables

Figure 4.1

Graph illustrating the shape of the function defined by the Lassen Correction.

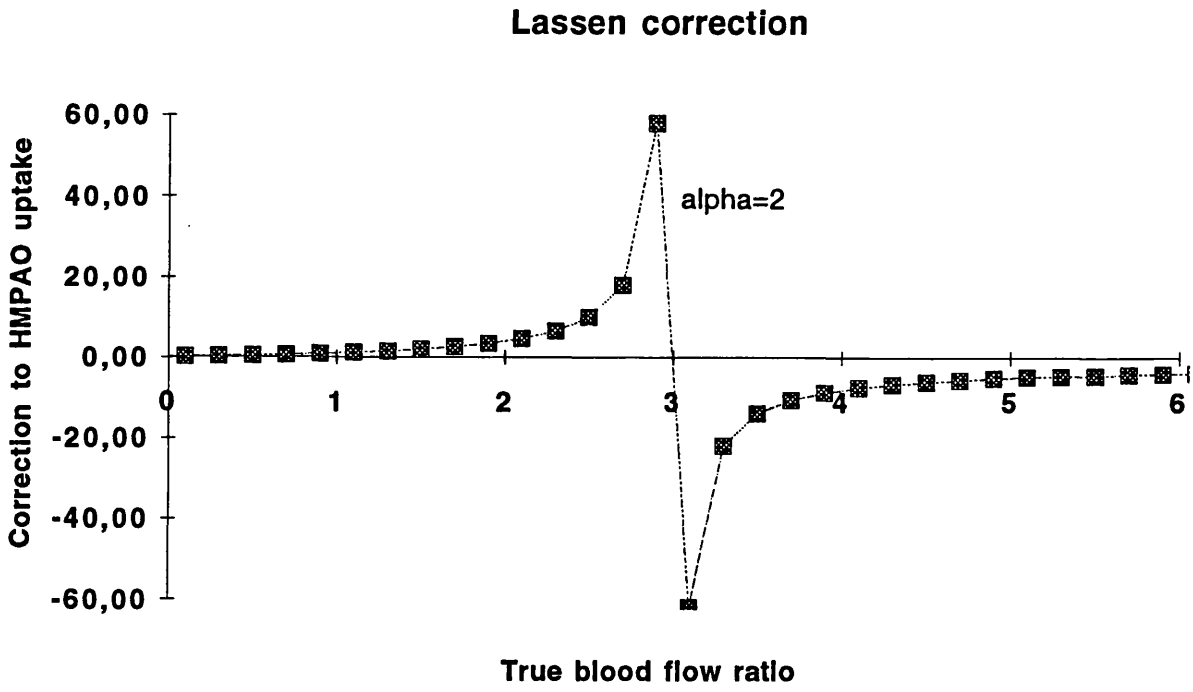

Figure 4.2

Two-channel EEG recording of 3 epochs during right focal motor seizure in animal 6. The lower trace is the left channel. The first (upper left) epoch is early in the seizure when the right whisker and snout are twitching. The second (upper right) is when seizure activity has spread to the forepaw, and the third (lower) when seizure activity involves face and both limbs. The spike-wave discharge typical of the penicillin focus can clearly be seen, at greater amplitude on the left.

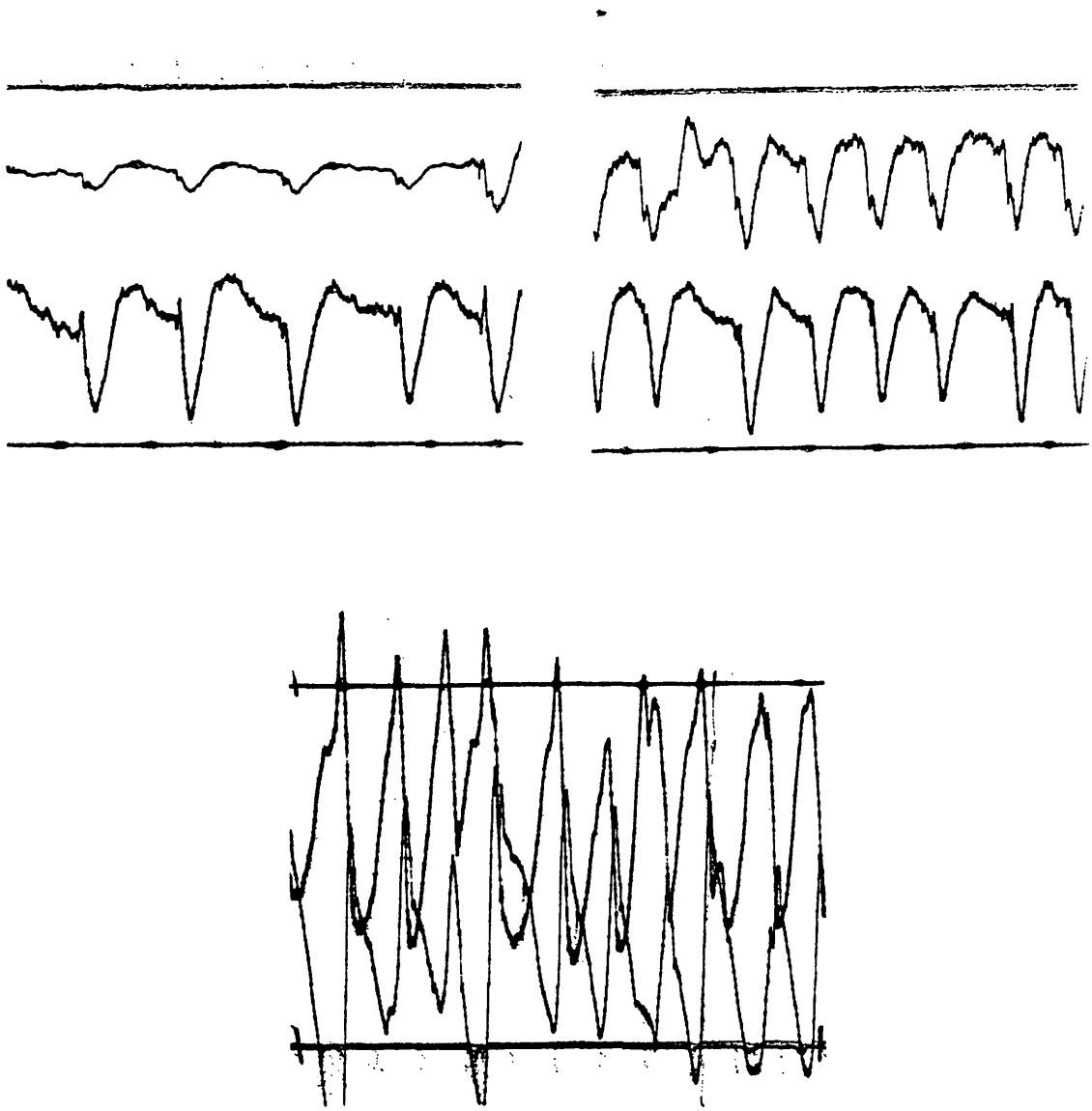

Figure 4.3

IAP (top) and HMPAO (bottom) images of rCBF (section through the frontal lobe and caudate nucleus) in animal 5 showing increased HMPAO uptake in the choroid plexus, and reduced IAP and HMPAO uptake in the left frontal cortex.

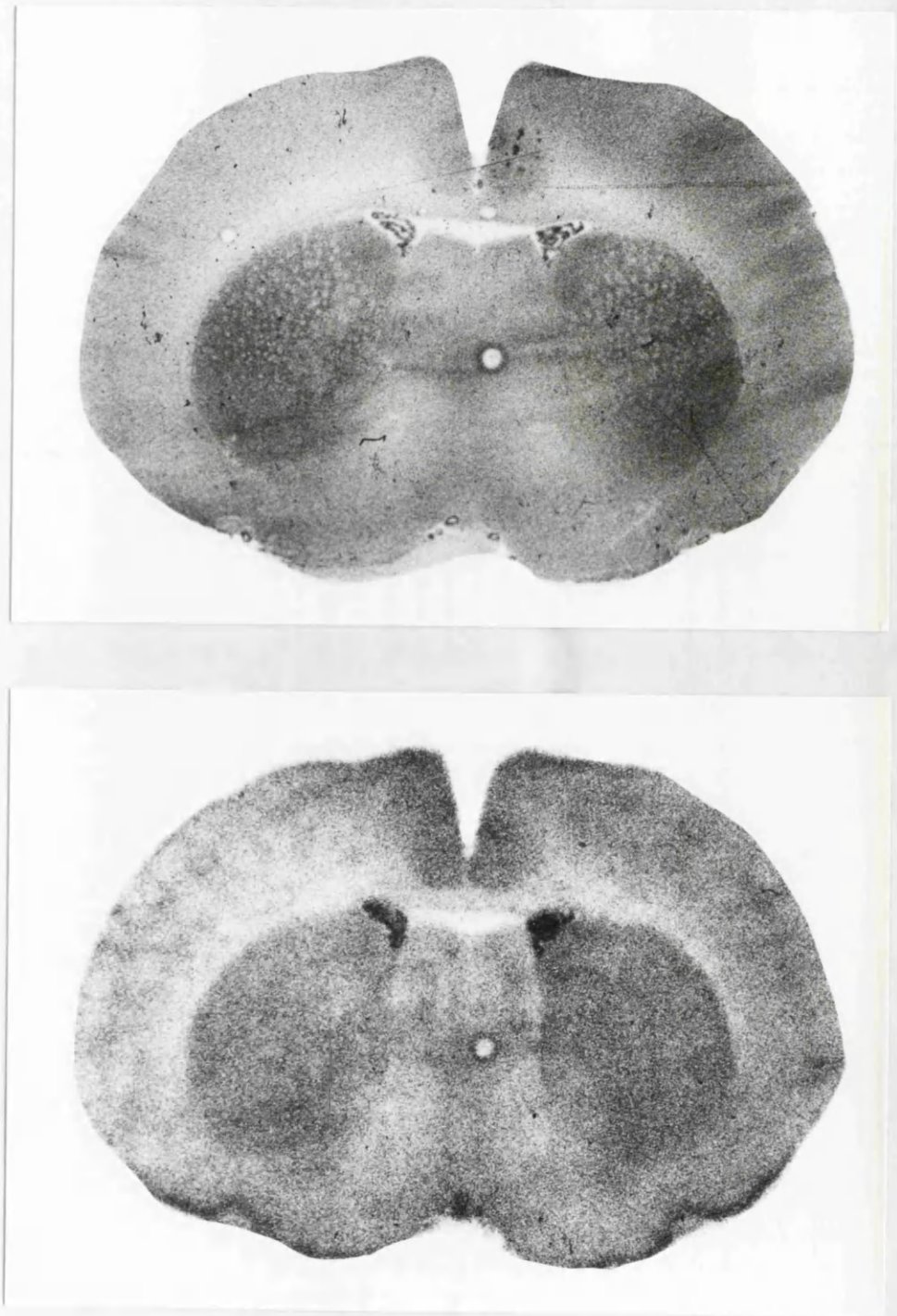

Figure 4.4

IAP (top) and HMPAO (bottom) images of rCBF (section through the frontal lobe in animal 6) showing the seizure focus (left side). There is and area of low HMPAO and IAP uptake in the area of the needle track, which is surrounded by an area of high uptake which also involves the contralateral cingulate cortex. On the IAP film uptake in the rhinal fissure is lower than that in the surrounding cortex, whereas on the HMPAO film it is higher.

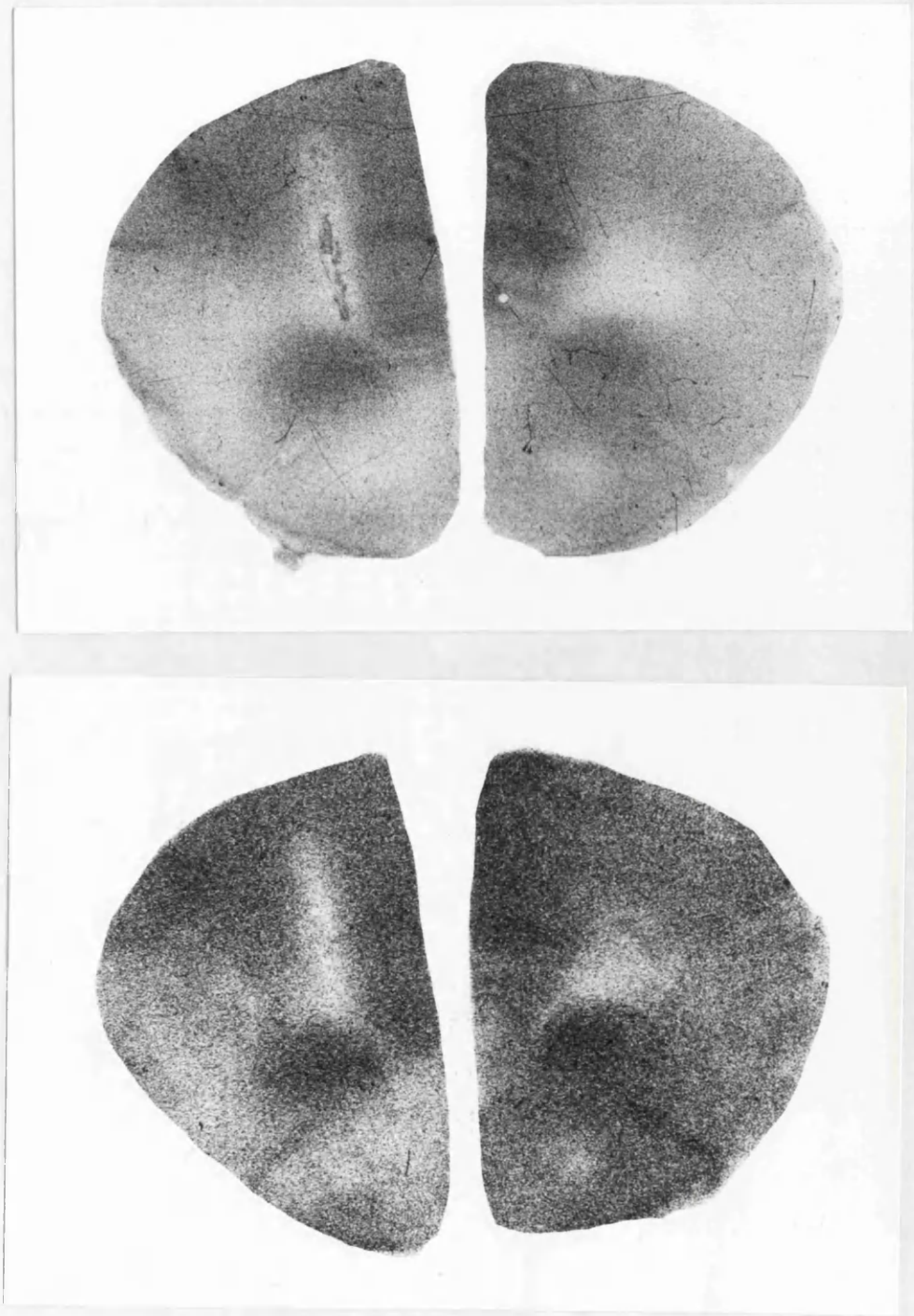

Figure 4.5

IAP (top) and HMPAO (bottom) images of rCBF (section more posteriorly situated in the frontal lobe in animal 6). There is increased uptake of IAP and HMPAO in the area posterior to the focus (left side) and in the cingulate cortex bilaterally. The frontal cortex inferior to the focus shows reduced uptake.

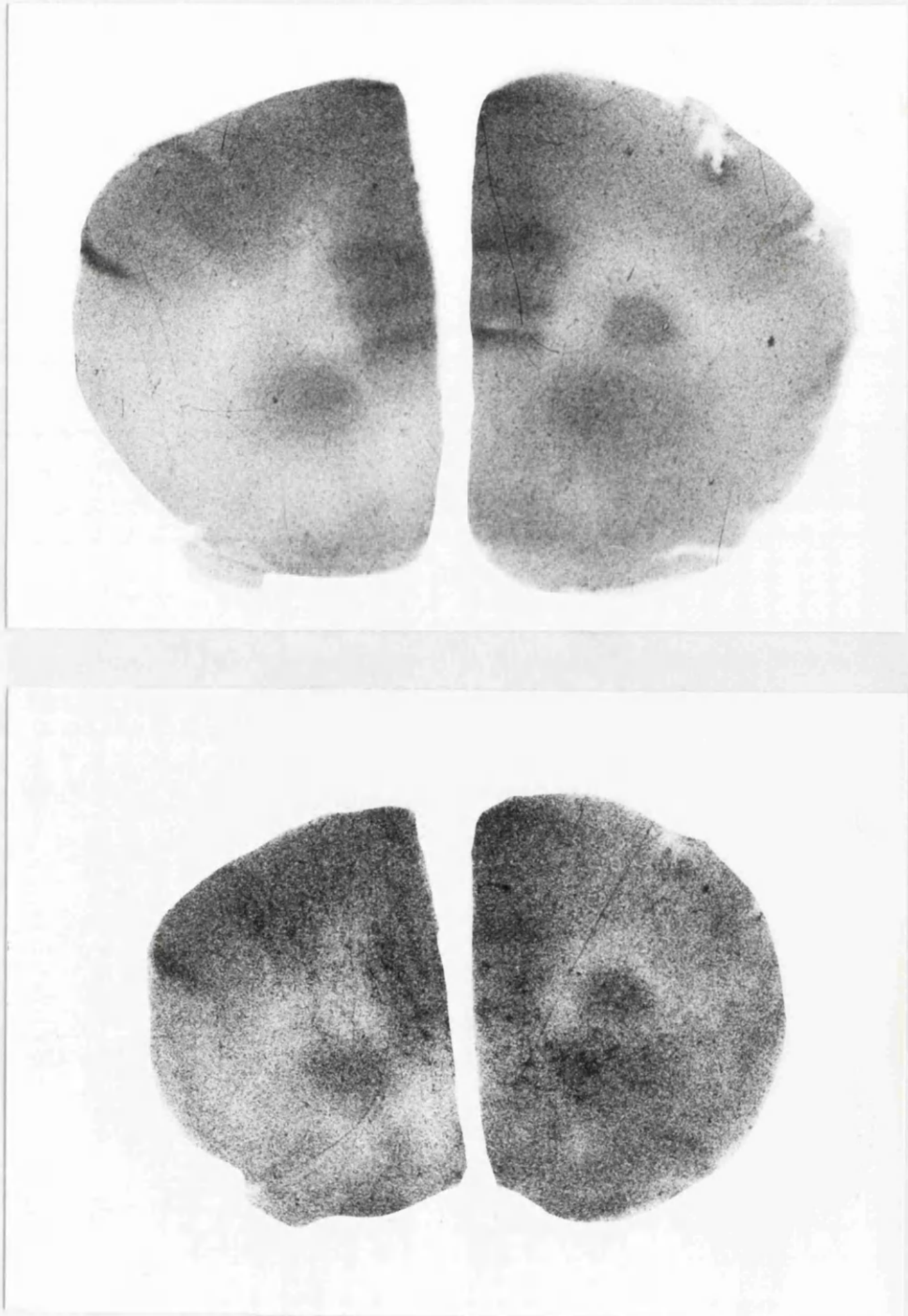

Figure 4.6

IAP (top) and HMPAO (bottom) images of rCBF (section through the frontal lobe in animal 10). There is increased uptake of IAP and HMPAO to a slight degree in the cingulate cortex and more markedly in the septal nucleus bilaterally.

Figure 4.7

IAP (top) and HMPAO (bottom) images of rCBF (section through the thalamus in animal 7) showing increased uptake of IAP and HMPAO in the thalamus ipsilateral to the focus (left) principally affecting the dorsolateral nucleus. There is slightly increased uptake in the contralateral mesial thalamus. There is decreased uptake in the parietal cortex ipsilateral to the focus (left). The HMPAO film shows relatively high uptake in the choroid plexus.

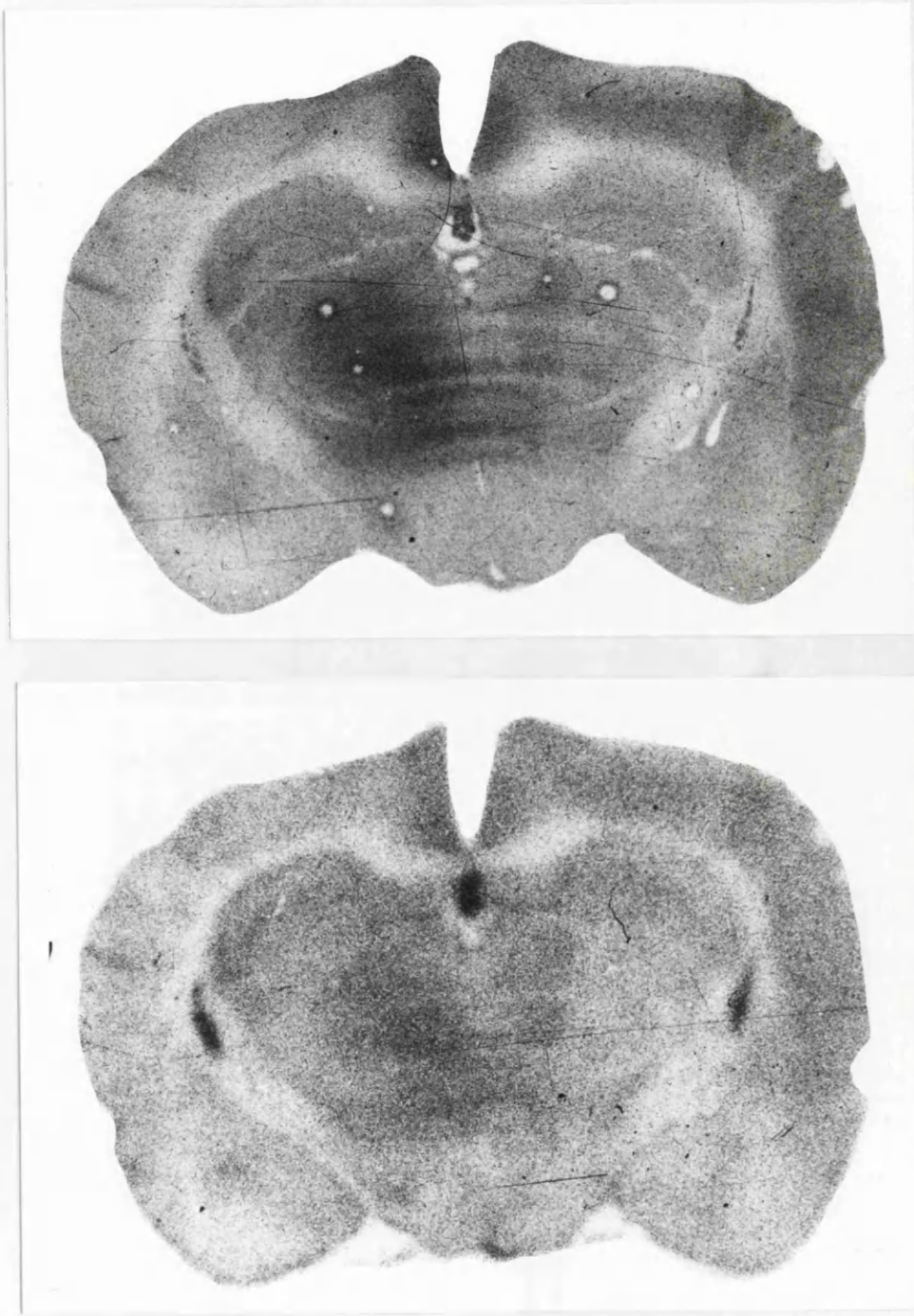

Figure 4.8

IAP (top) and HMPAO (bottom) images of rCBF (section through the hippocampus in animal 8) showing increased IAP and HMPAO uptake in the substantia nigra pars reticultata ipslateral to the focus (left) and decreased uptake in the ipsilateral auditory cortex.

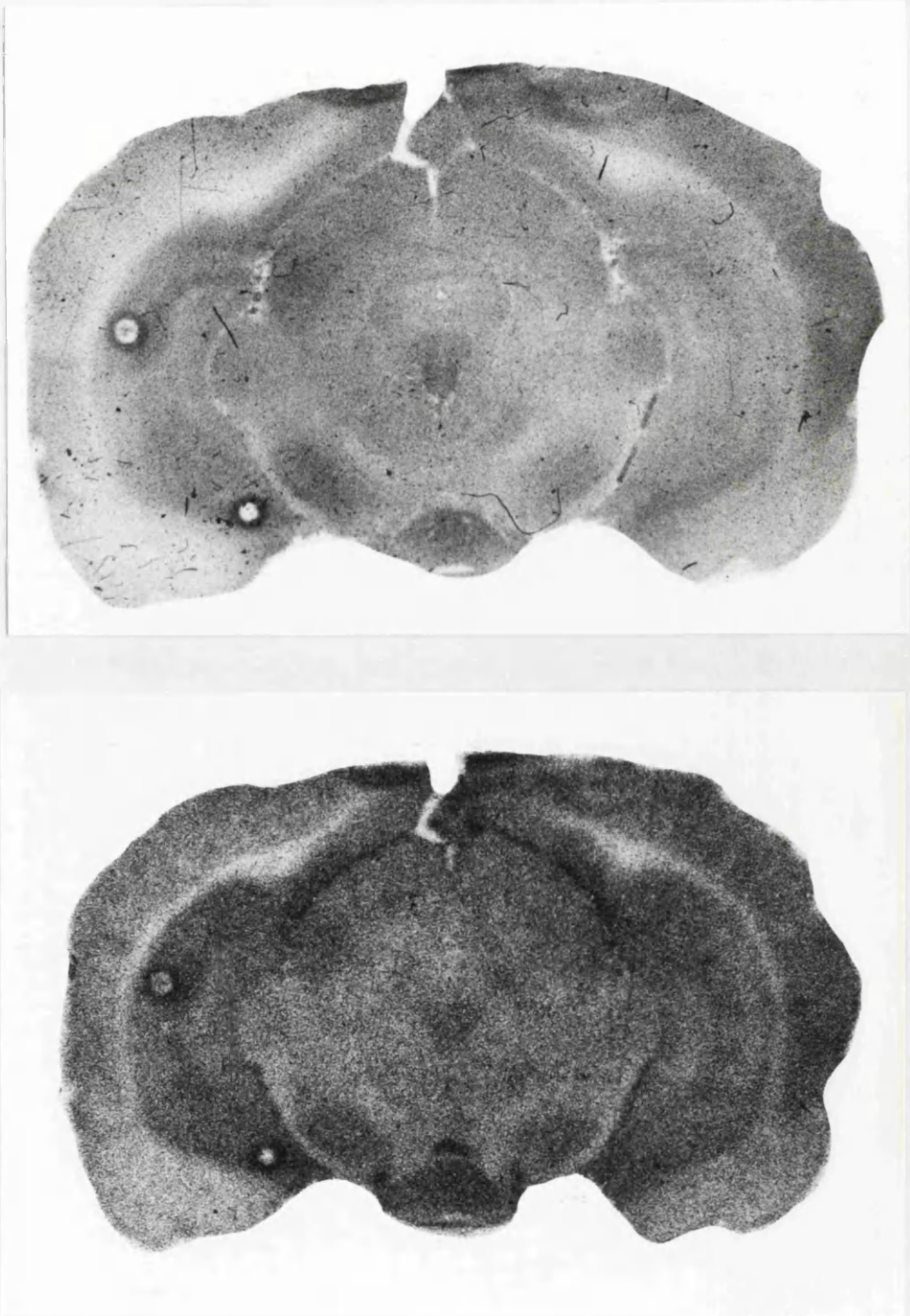

Figure 4.9

Seizure animals: Significant side-side differences in regional cerebral blood flow

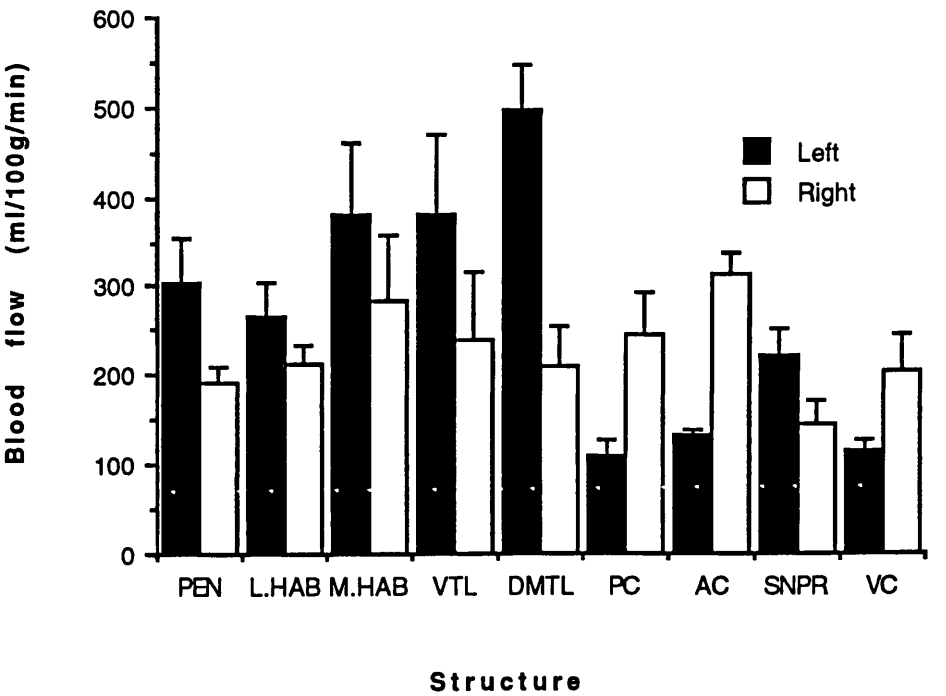

Figure 4.10
Percentage side-side differences in regional cerebral blood flow:- Seizure animals vs. control animals

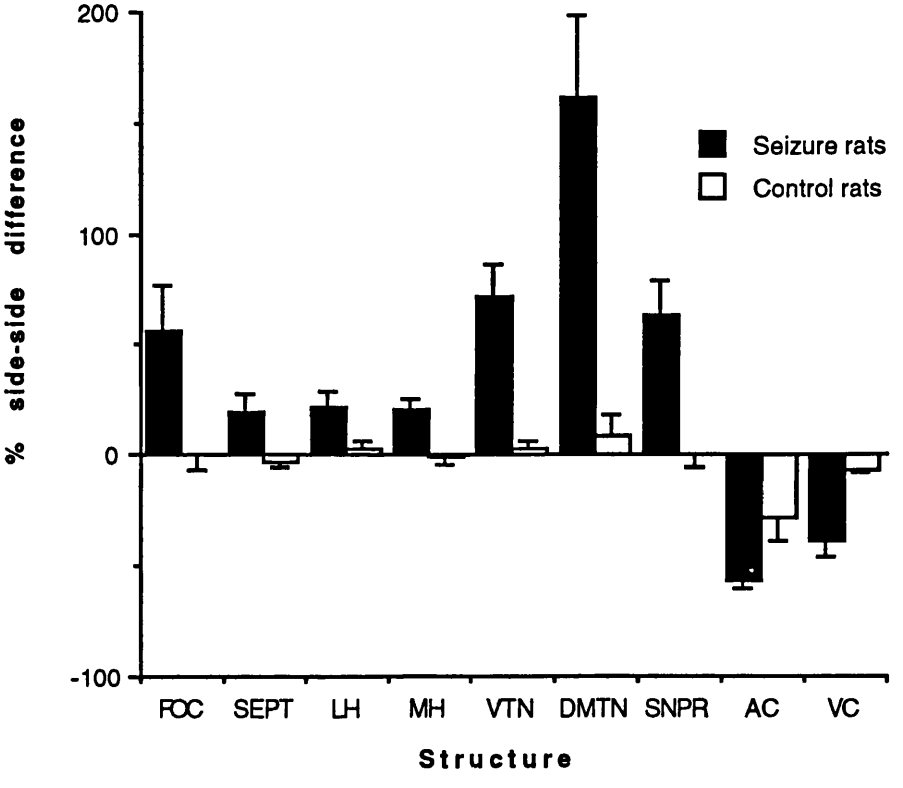

Figure 4.11a: Animal 1
Uncorrected 99mTc activity vs rCBF

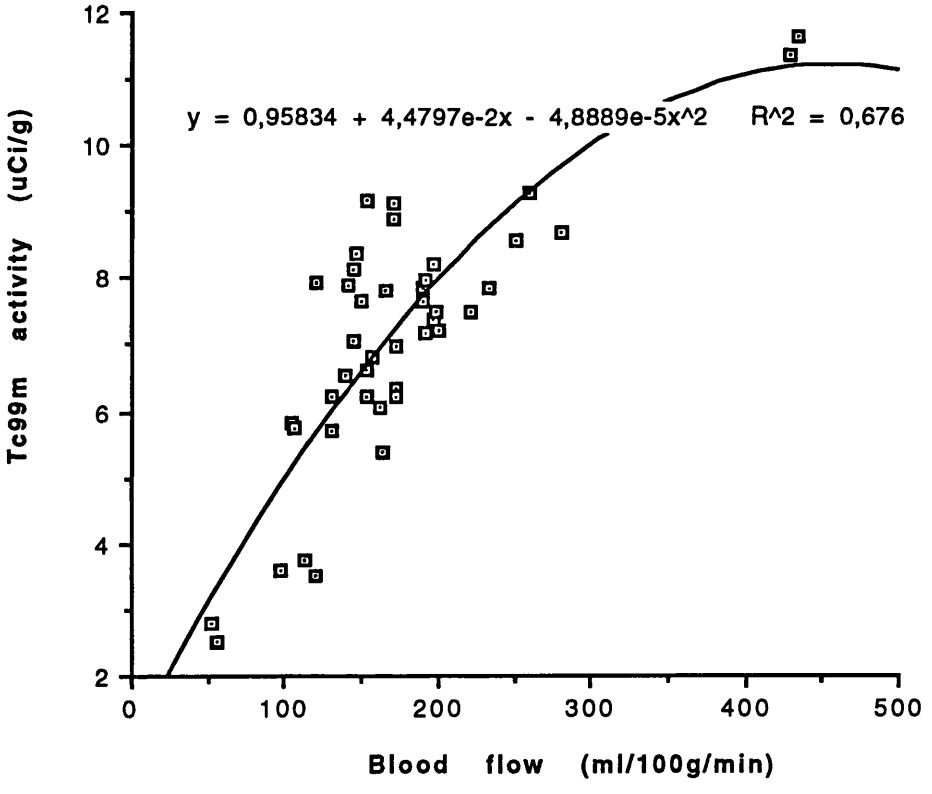

Figure 4.11b: Animal 1
Corrected 99mTc activity vs rCBF

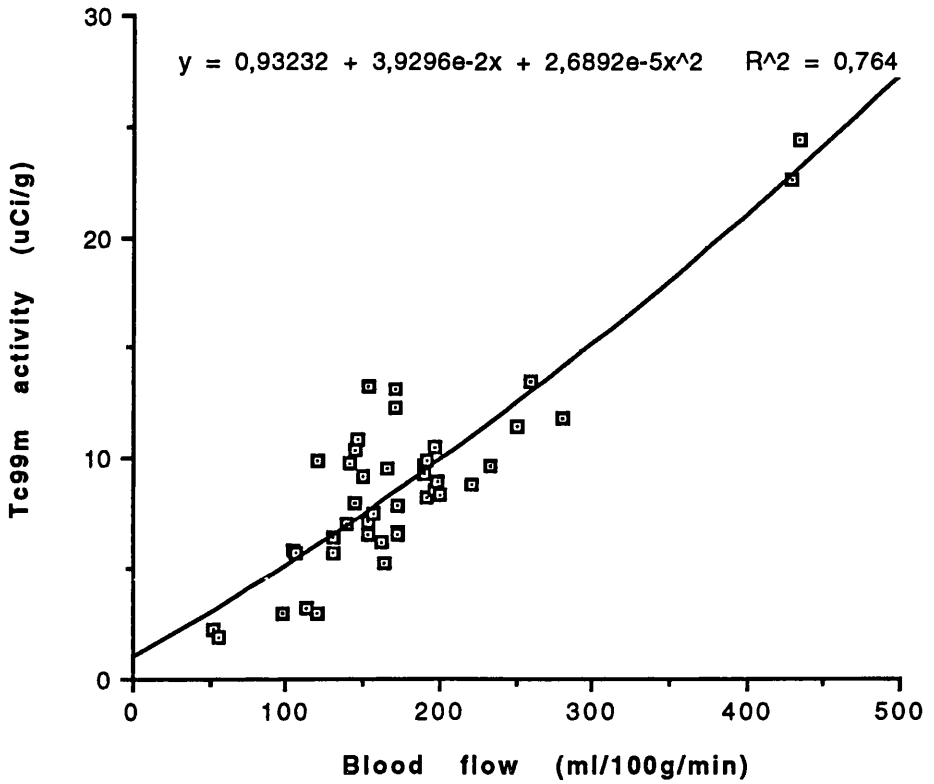

Figure 4.12a: Animal 2
Uncorrected 99mTc activity vs rCBF

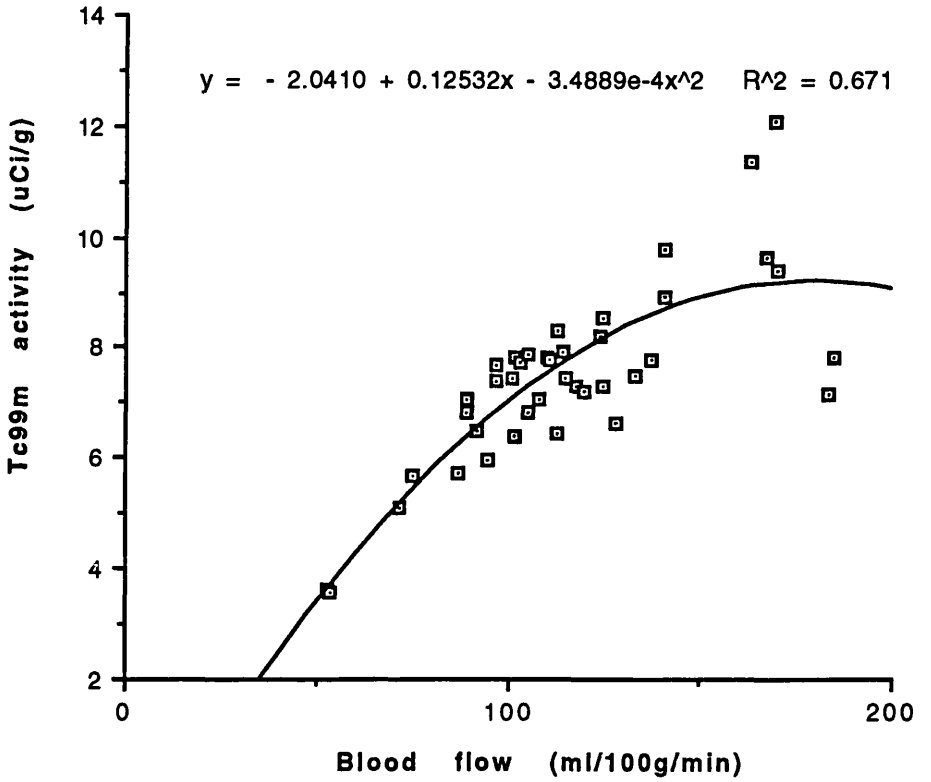

Figure 4.12b: Animal 2
Corrected 99mTc activity vs rCBF

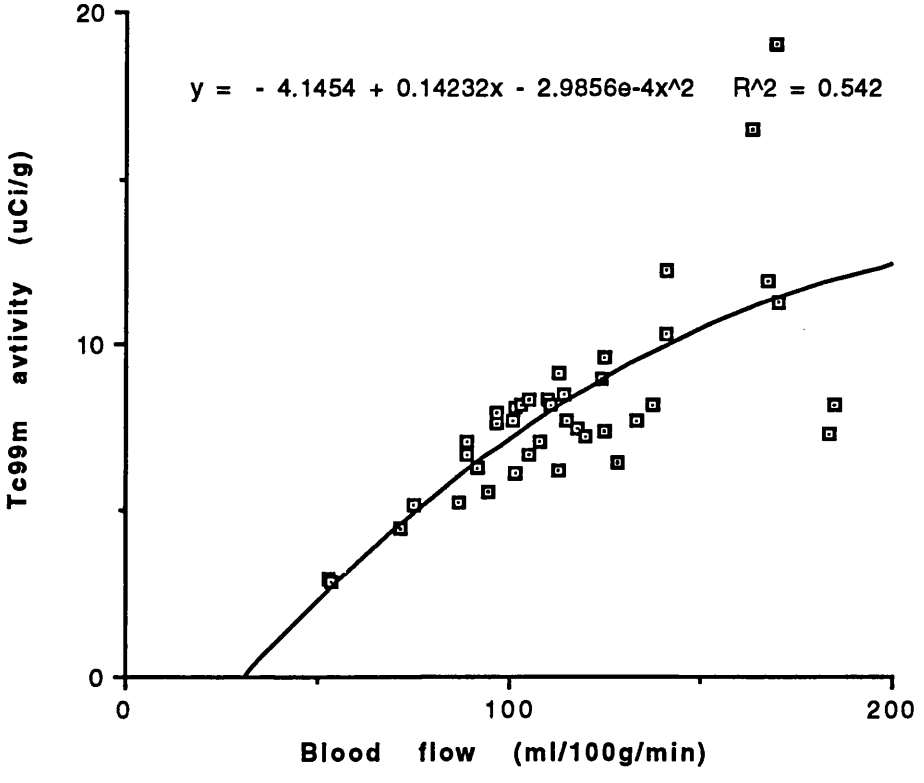

Figure 4.13a: Animal 3
Uncorrected 99mTc activity vs rCBF

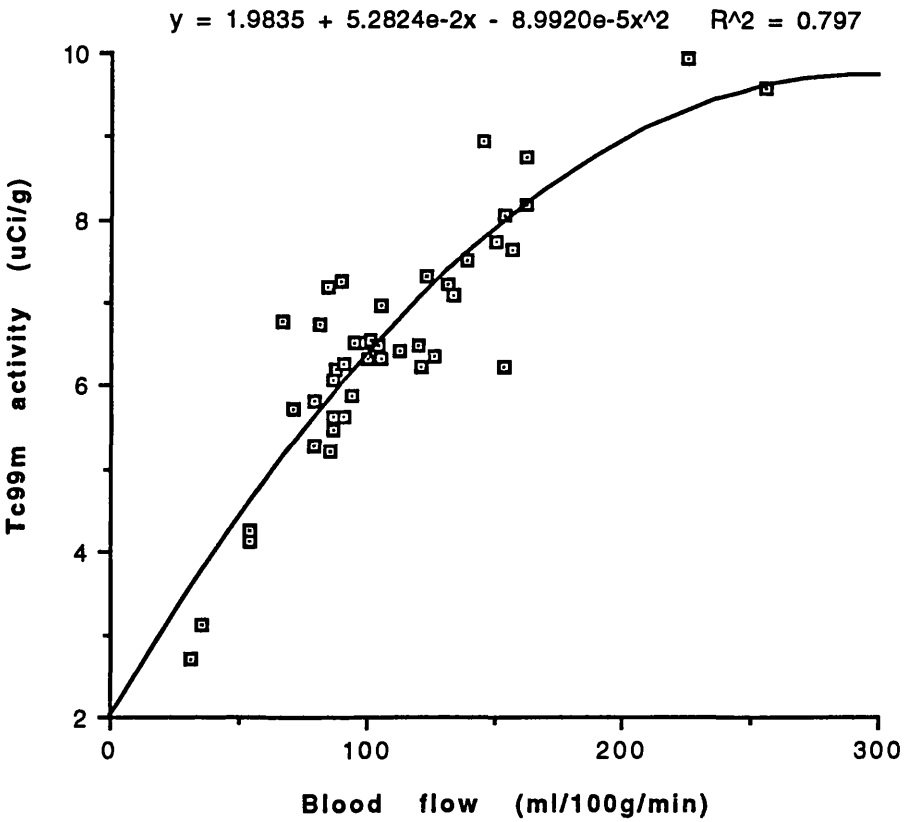

Figure 4.13b: Animal 3
Corrected 99mTc activity vs rCBF

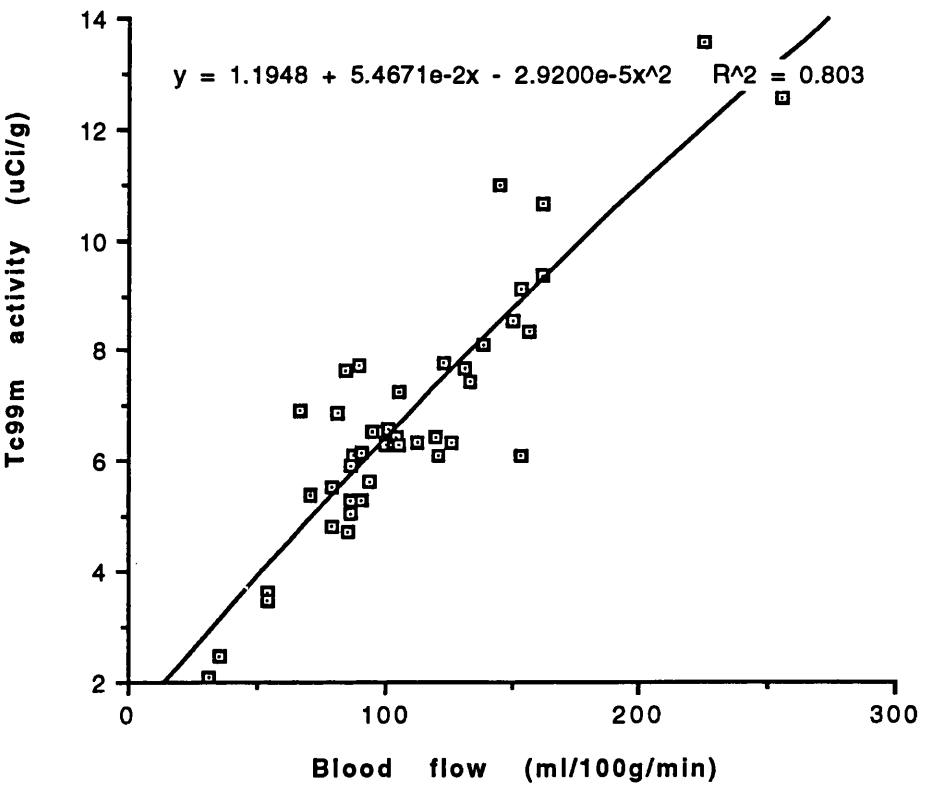

Figure 4.14a: animal 4
Uncorrected 99mTc activity vs rCBF

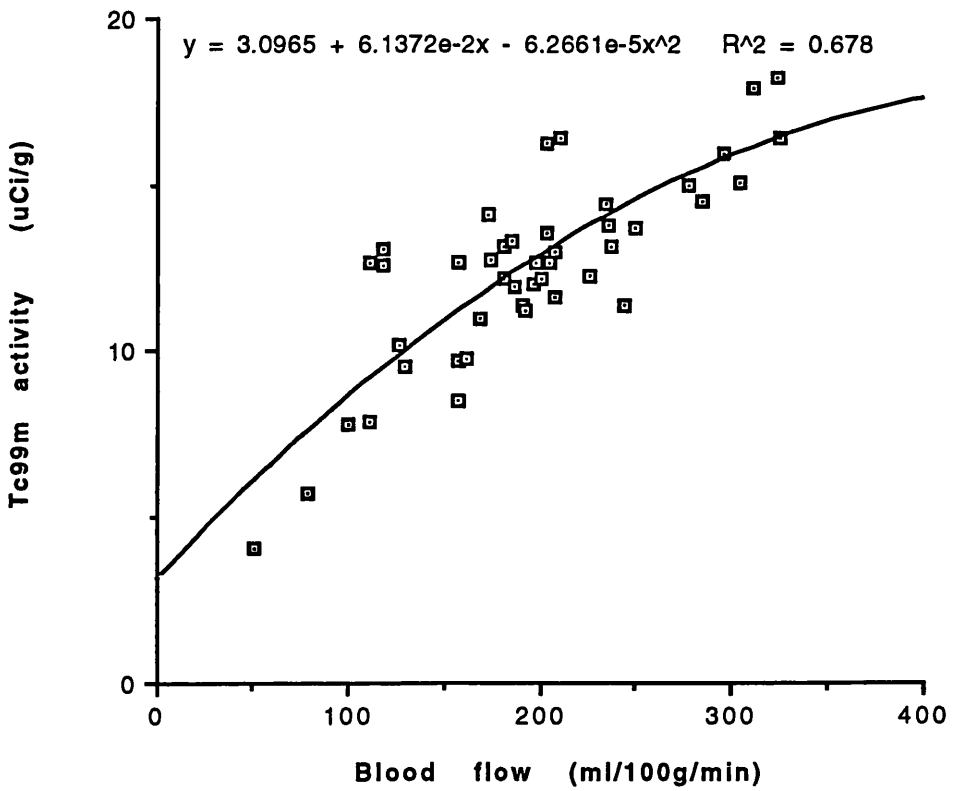

Figure 4.14b: animal 4
Corrected 99mTc activity vs rCBF

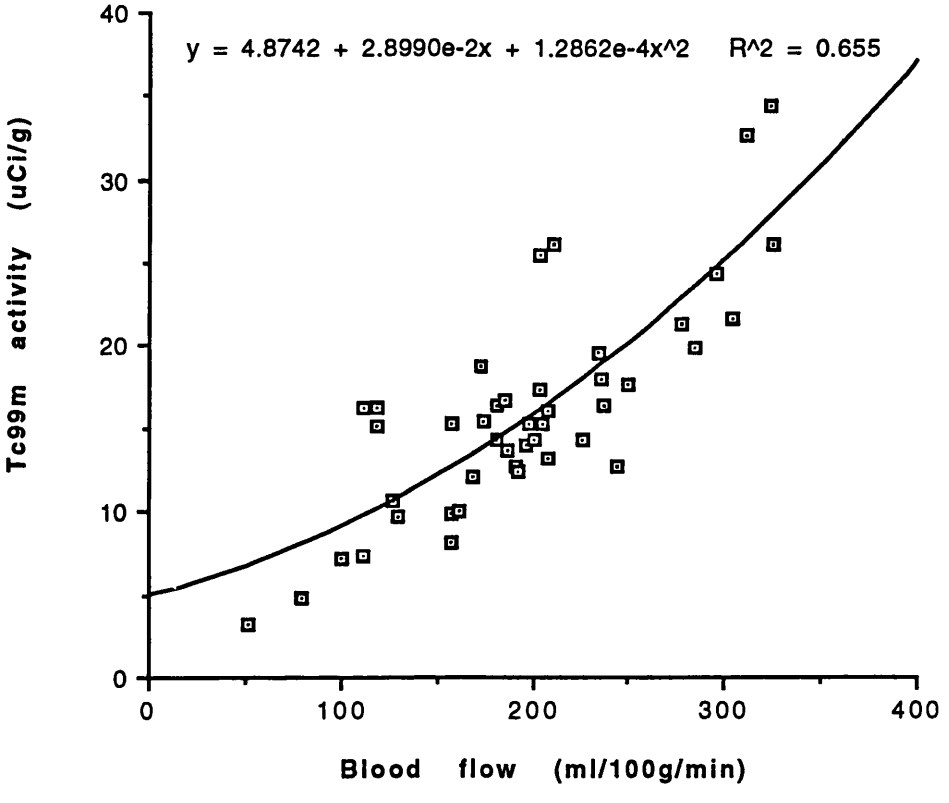

Figure 4.15a: Animal 5
Uncorrected 99mTc activity vs rCBF

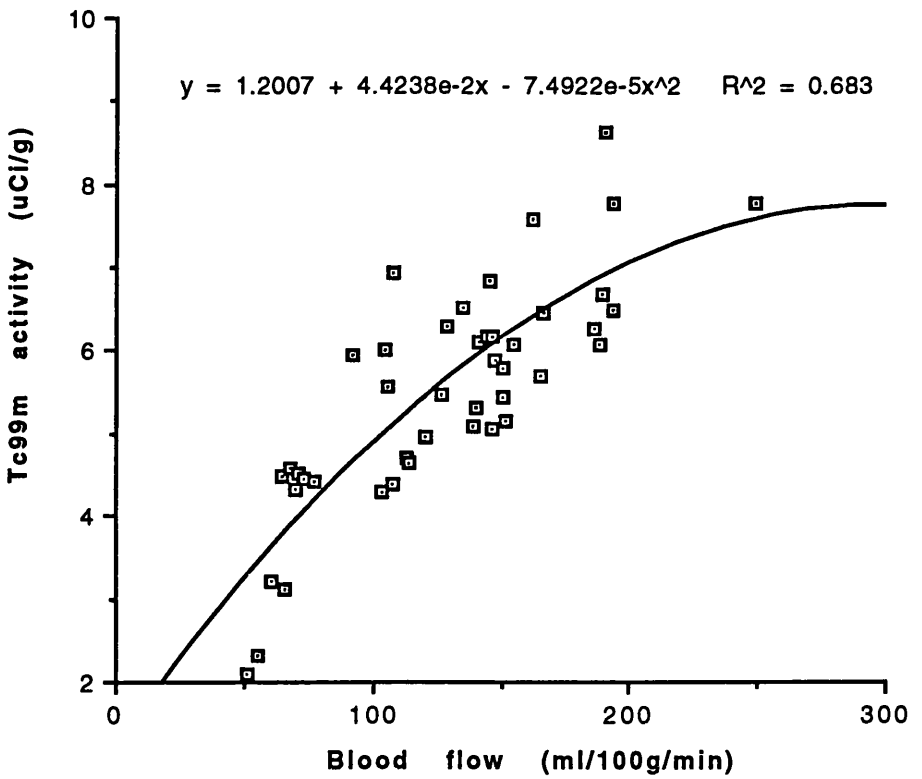

Figure 4.15b: Animal 5
Corrected 99mTc activity vs rCBF

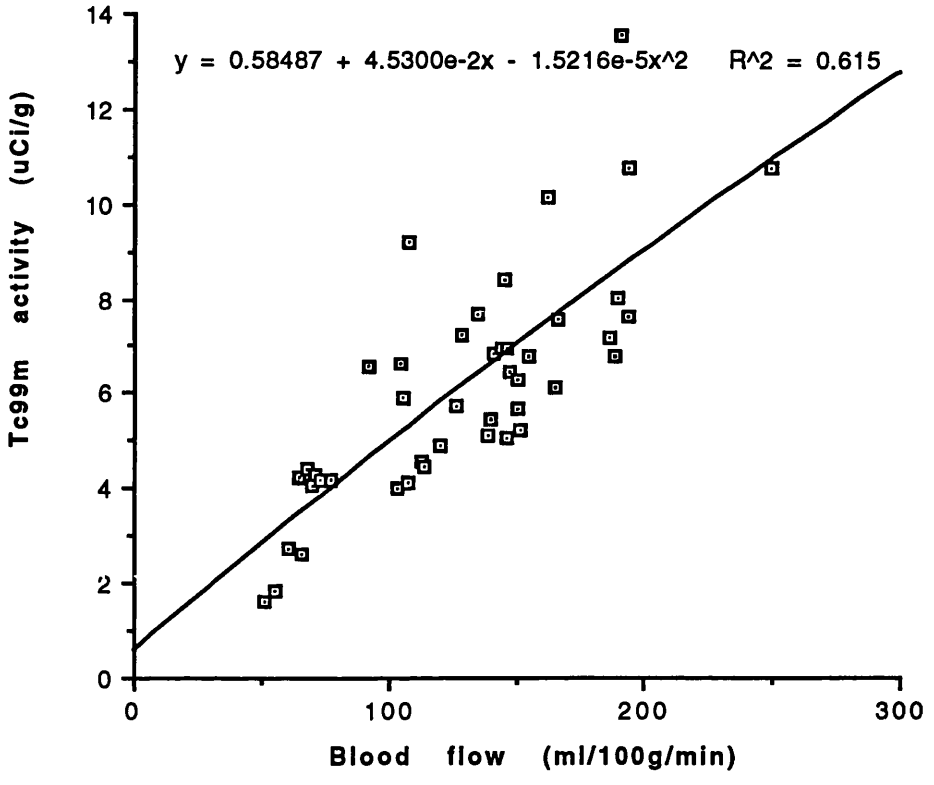

Figure 4.16a: Animal 6
Uncorrected 99mTc activity vs rCBF

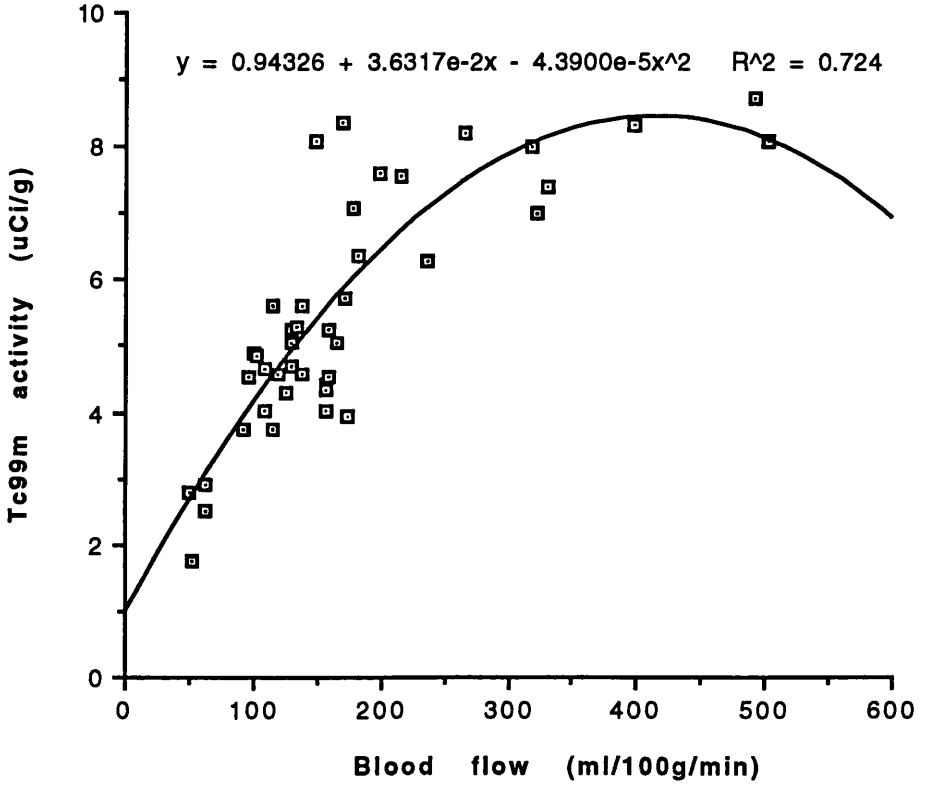

Figure 4.16b: Animal 6
Corrected 99mTc activity vs rCBF

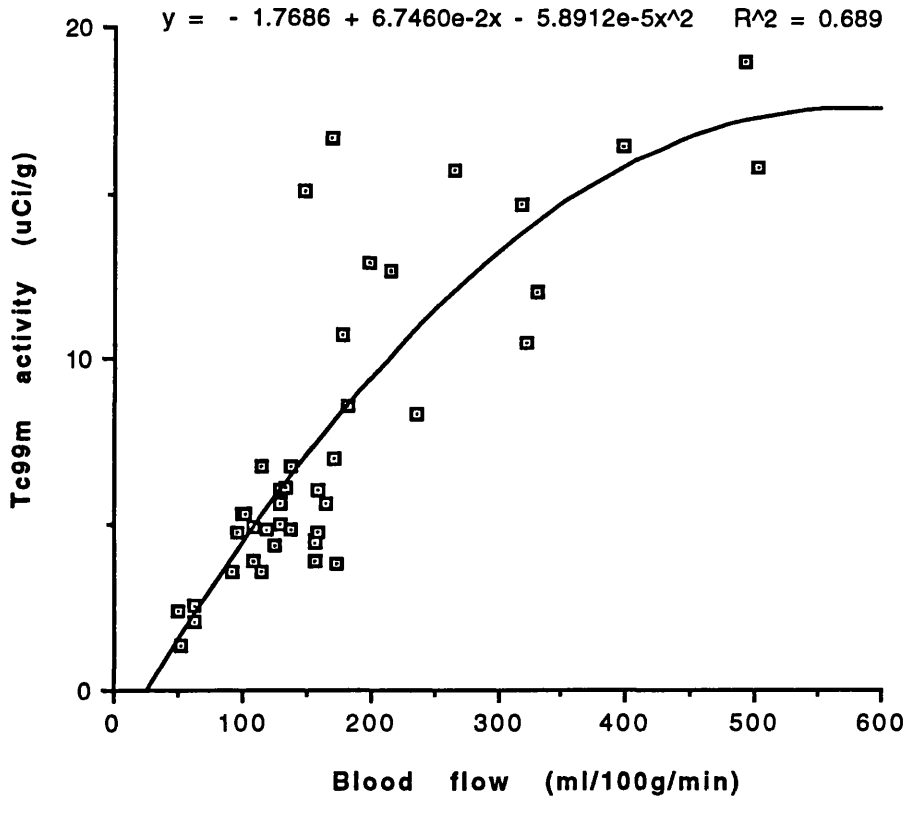

Figure 4.17a: Animal 7
Uncorrected 99mTc activity vs rCBF

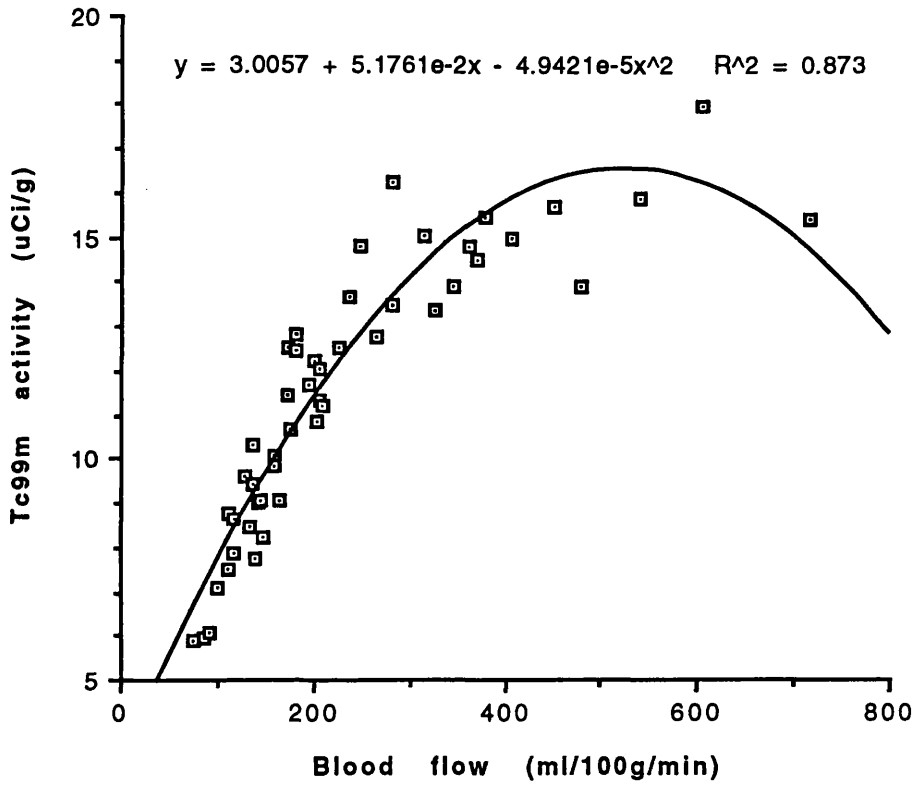

Figure 4.17b: Animal 7
Corrected 99mTc activity vs rCBF

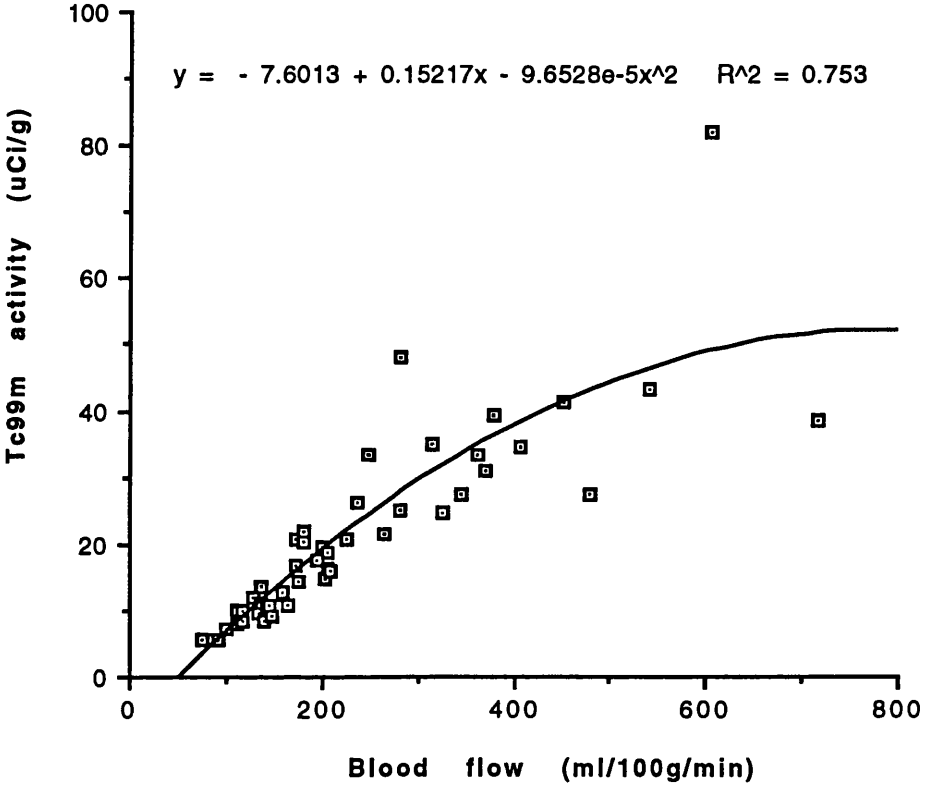

Figure 4.18a: animal 8
Uncorrected 99mTc activity vs rCBF

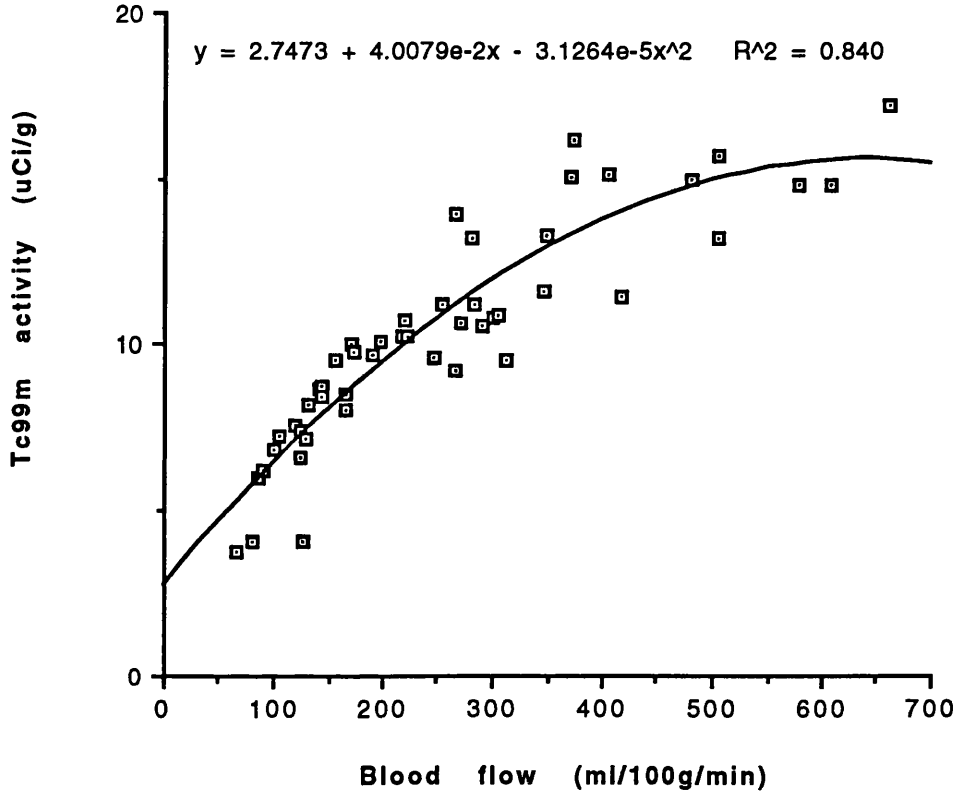

Figure 4.18b: Animal 8
Corrected 99mTc activity vs rCBF

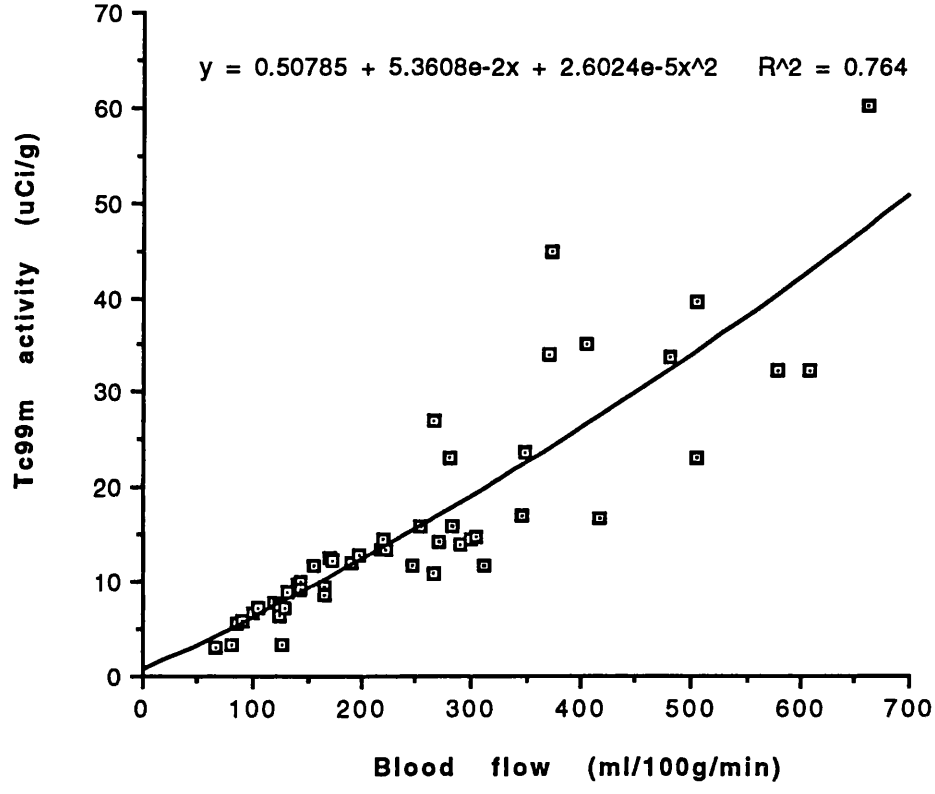

Figure 4.19a: Animal 9
Uncorrected 99mTc activity vs rCBF

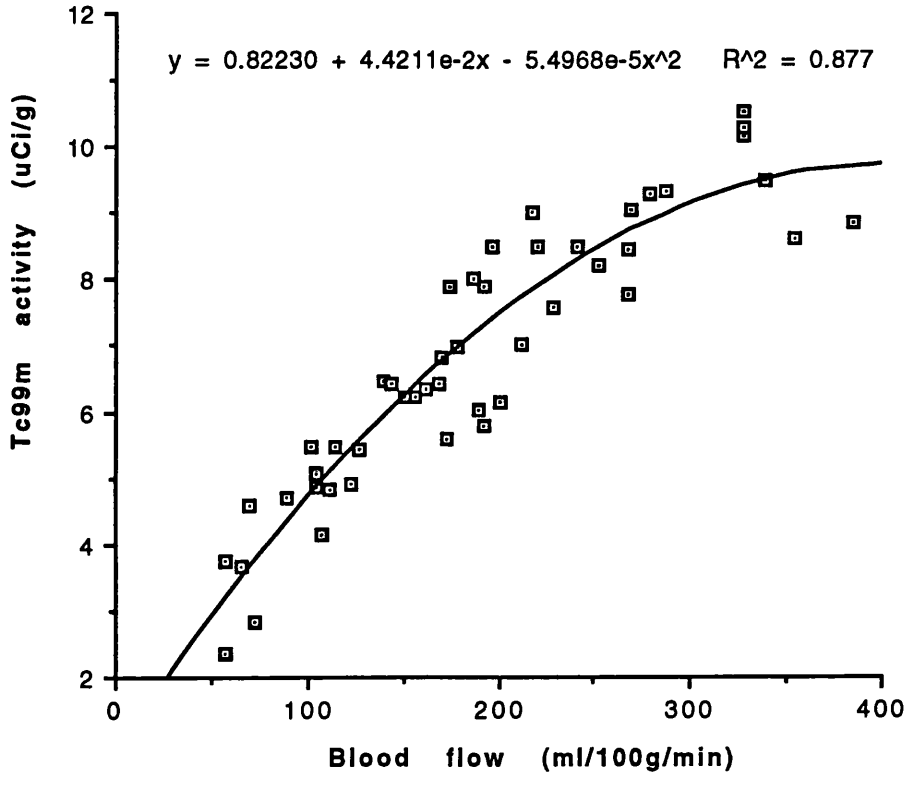

Figure 4.19b: Animal 9
Corrected 99mTc activity vs rCBF

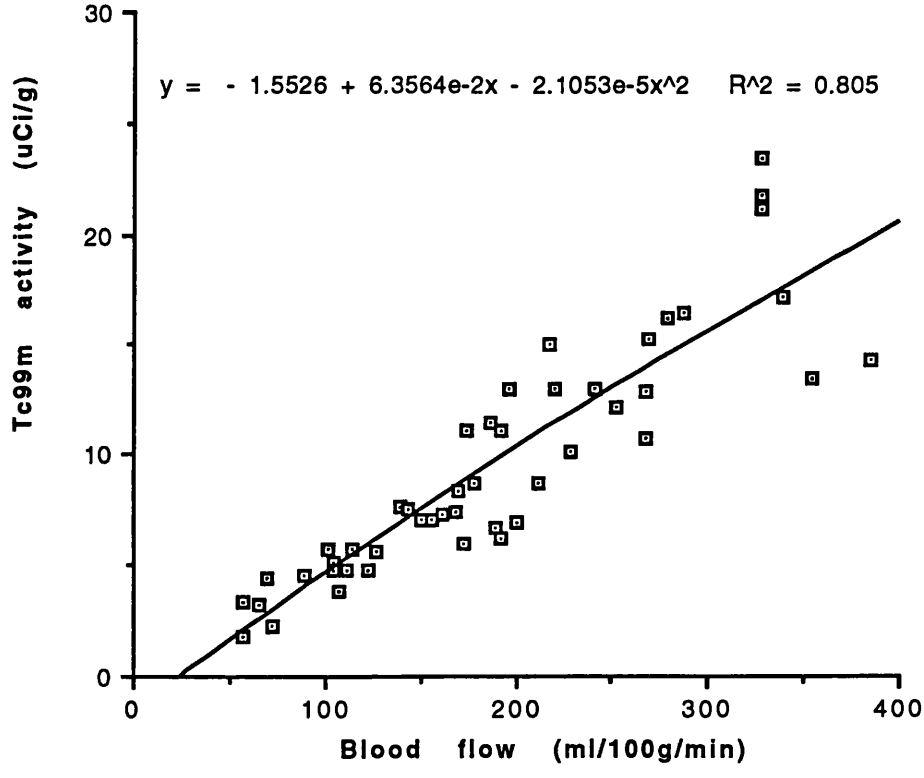

Figure 4.20a: Animal 10
Uncorrected 99mTc activity vs rCBF

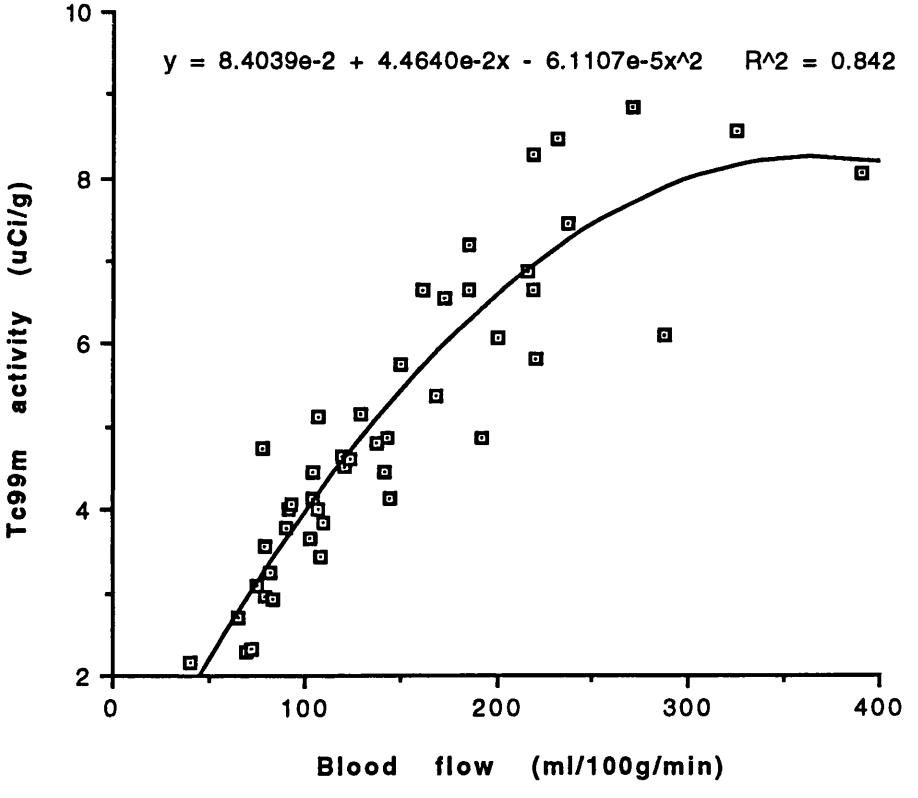

Figure 4.20b: Animal 10
Corrected 99mTc activity vs rCBF

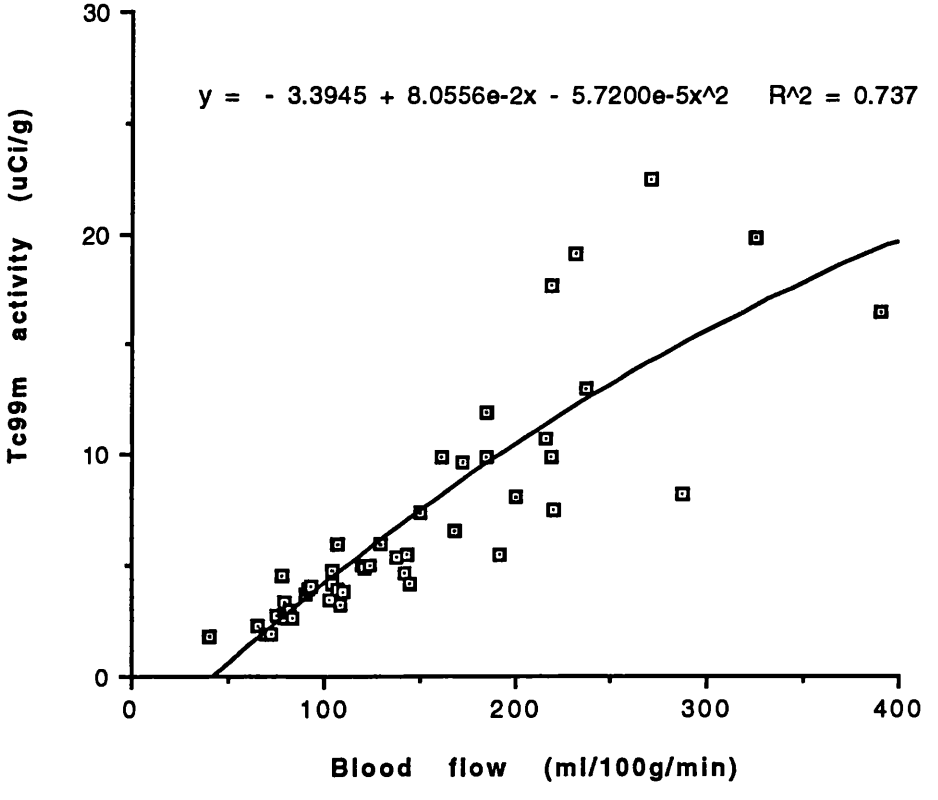

Table 4.1

PHYSIOLOGICAL PARAMETERS

All animals

RAT	WEIGHT (g)	BLOOD PRESSURE (mmHg)	pCO2 (mmHg)	pO2 (mmHg)	pH	TEMPERATURE DEG.C.
1	400	150/120	47,6	79,7	7,39	37,3
2	497	165/100	55	88,2	7,34	39
3	515	165/110	48,6	82,8	7,33	36,4
4	520	135/115	54,6	85,1	7,3	38,1
5	515	125/85	60,3	98,5	7,4	35,9
6	510	135/85	60,5	146,4	7,38	37,2
7	423	125/90	45,7	84,7	7,31	36,4
8	450	195/110	52,5	139,2	7,38	38,2
9	375	195/135	45,9	69,3	7,41	37,7
10	595	200/110	58,8	108,2	7,37	35,8

Table 4.2

REGIONAL CEREBRAL BLOOD FLOW (ml/100g/min)

Control animals

	RAT 1	RAT 2	RAT 3	RAT 4	RAT 5	MEAN	SEM	Max	Min
LEFT (FOCUS)									
FRONTAL CORTEX	191	110	87	244	145	155	28	244	87
CINGULATE CORTEX	154	170	71	157	165	138	18	170	71
SUBCORTICAL WHITE MATTER	53	53	31	52	51	47	4	53	31
CAUDATE NUCLEUS	149	105	106	284	140	157	33	284	105
SEPTAL NUCLEUS	106	108	79	158	114	113	13	158	79
GLOBUS PALLIDUS	120	95	126	296	144	156	36	296	95
AMYGALOID NUCLEUS	97	87	79	201	103	113	22	201	79
LATERAL HABENULA	154	103	162	197	141	151	15	197	103
MEDIAL HABENULA	221	114	157	205	135	166	20	221	114
VENT. THALAMIC NUCLEUS	196	125	154	185	147	161	13	196	125
DORSOMED. THALAMIC NUCLEUS	250	163	132	236	193	195	22	250	132
LATERAL THALAMIC NUCLEUS	192	133	54	208	155	148	27	208	54
ENTOPEDUNCULAR NUCLEUS	121	72	91	111	61	91	11	121	61
HYPOTHALAMUS	173	124	101	112	71	116	17	173	71
PARIETAL CORTEX	196	141	94	158	108	139	18	196	94
AUDITORY CORTEX	198	89	67	173	162	138	25	198	67
HIPPOCAMPUS	147	92	85	210	105	128	23	210	85
SUBSTANTIA NIGRA (PR)	162	115	95	203	65	128	25	203	65
INFERIOR COLLICULUS	429	185	255	325	190	277	46	429	185
PONTINE RETICULAR FORMATION	131	102	86	129	70	104	12	131	70
VISUAL CORTEX	144	97	121	237	120	144	24	237	97
CEREBELLUM	140		105	181	92	130	18	181	92
RIGHT									
FRONTAL CORTEX	172	125	106	207	146	153	18	207	106
CINGULATE CORTEX	190	167	99	169	188	134	17	169	99
SUBCORTICAL WHITE MATTER	56	54	36	79	55	56	7	79	36
CAUDATE NUCLEUS	165	105	104	304	150	166	37	304	104
SEPTAL NUCLEUS	105	120	87	161	113	117	12	161	87
GLOBUS PALLIDUS	163	108	113	191	146	144	16	191	108
AMYGALOID NUCLEUS	114	102	87	187	108	120	17	187	87
LATERAL HABENULA	171	97	145	193	139	149	16	193	97
MEDIAL HABENULA	234	111	154	198	152	170	21	234	111
VENT. THALAMIC NUCLEUS	201	128	134	174	150	157	13	201	128
DORSOMED. THALAMIC NUCLEUS	171	169	123	277	186	185	25	277	123
LATERAL THALAMIC NUCLEUS	190	137	54	118	166	133	23	190	54
ENTOPEDUNCULAR NUCLEUS	121	75	88	100	66	90	10	121	66
HYPOTHALAMUS	172	113	120	118	77	120	15	172	77
PARIETAL CORTEX	280	141	151	234	189	199	26	280	141
AUDITORY CORTEX	259	89	162	323	193	205	40	323	89
HIPPOCAMPUS	141	113	90	203	129	135	19	203	90
SUBSTANTIA NIGRA (PR)	154	118	82	226	73	131	28	226	73
INFERIOR COLLICULUS	433	183	225	311	249	280	43	433	183
PONTINE RETICULAR FORMATION	130	108	91	127	68	105	12	130	68
VISUAL CORTEX	156	101	139	250	126	154	26	250	101
CEREBELLUM	144		100	181	106	133	17	181	100

Table 4.3

SIDE-TO-SIDE DIFFERENCES IN REGIONAL CEREBRAL BLOOD FLOW (%)

Control animals

	RAT 1	RAT 2	RAT 3	RAT 4	RAT 5	MEAN	SEM	MAX	MIN
FRONTAL CORTEX	11,0	-12,0	-17,9	17,9	-0,7	-0,3	6,7	17,9	-17,9
CINGULATE CORTEX	-18,9	1,8	-28,3	-7,1	-12,2	-13,0	5,1	1,8	-28,3
SUBCORTICAL WHITE MATTER	-5,4	-1,9	-13,9	-34,2	-7,3	-12,5	5,8	-1,9	-34,2
CAUDATE NUCLEUS	-9,7	0,0	1,9	-6,6	-6,7	-4,2	2,2	1,9	-9,7
SEPTAL NUCLEUS	1,0	-10,0	-9,2	-1,9	0,9	-3,8	2,4	1,0	-10,0
GLOBUS PALLIDUS	-26,4	-12,0	11,5	55,0	-1,4	5,3	13,9	55,0	-26,4
AMYGALOID NUCLEUS	-14,9	-14,7	-9,2	7,5	-4,6	-7,2	4,1	7,5	-14,9
LATERAL HABENULA	-9,9	6,2	11,7	2,1	1,4	2,3	3,6	11,7	-9,9
MEDIAL HABENULA	-5,6	2,7	1,9	3,5	-11,2	-1,7	2,9	3,5	-11,2
VENT. THALAMIC NUCLEUS	-2,5	-2,3	14,9	6,3	-2,0	2,9	3,4	14,9	-2,5
DORSOMED. THALAMIC NUCLEU	46,2	-3,6	7,3	-14,8	3,8	7,8	10,3	46,2	-14,8
LATERAL THALAMIC NUCLEUS	1,1	-2,9	0,0	76,3	-6,6	13,6	15,7	76,3	-6,6
ENTOPEDUNCULAR NUCLEUS	0,0	-4,0	3,4	11,0	-7,6	0,6	3,2	11,0	-7,6
HYPOTHALAMUS	0,6	9,7	-15,8	-5,1	-7,8	-3,7	4,3	9,7	-15,8
PARIETAL CORTEX	-30,0	0,0	-37,7	-32,5	-42,9	-28,6	7,5	0,0	-42,9
AUDITORY CORTEX	-23,6	0,0	-58,6	-46,4	-16,1	-28,9	10,5	0,0	-58,6
HIPPOCAMPUS	4,3	-18,6	-5,6	3,4	-18,6	-7,0	5,0	4,3	-18,6
SUBSTANTIA NIGRA (PR)	5,2	-2,5	15,9	-10,2	-11,0	-0,5	5,0	15,9	-11,0
INFERIOR COLLICULUS	-0,9	1,1	13,3	4,5	-23,7	-1,1	6,1	13,3	-23,7
PONTINE RETICULAR FORMATIC	0,8	-5,6	-5,5	1,6	2,9	-1,2	1,8	2,9	-5,6
VISUAL CORTEX	-7,7	-4,0	-12,9	-5,2	-4,8	-6,9	1,6	-4,0	-12,9
CEREBELLUM	-2,8		5,0	0,0	-13,2	2,2	1,0	5,0	-13,2

Table 4.4

REGIONAL CEREBRAL BLOOD FLOW (ml/100g/min)

Seizure animals

	RAT 6	RAT 7	RAT 8	RAT 9	RAT 10	MEAN	SEM	Max	Min
LEFT (FOCUS)									
CENTRAL FOCUS	173	206	126	268	109	176	29	268	109
PENUMBRA	321	451	346	252	151	304	50	451	151
FRONTAL CORTEX	156	158	129	143	91	135	12	158	91
CINGULATE CORTEX	114	370	416	279	185	273	56	416	114
SUBCORTICAL WHITE MATTER	52	87	80	72	69	72	6	87	52
CAUDATE NUCLEUS	491	380	300	170	82	285	73	491	82
SEPTAL NUCLEUS	130	137	119	220	287	179	32	287	119
GLOBUS PALLIDUS	317	248	305	156	104	226	42	317	104
AMYGALOID NUCLEUS	97	93	124	107	80	100	7	124	80
LATERAL HABENULA	156	204	371	268	325	265	39	371	156
MEDIAL HABENULA	199	281	661	287	270	340	82	661	199
VENT. THALAMIC NUCLEUS	370	717	265	354	193	380	90	717	193
DORSOMED. THALAMIC NUCLEUS	501	606	608	385	390	498	49	608	385
LATERAL THALAMIC NUCLEUS	148	480	311	193	145	255	64	480	145
ENTOPEDUNCULAR NUCLEUS	62	165	85	66	66	89	19	165	62
HYPOTHALAMUS	102	142	101	104	237	137	26	237	101
PARIETAL CORTEX	93	118	166	69	105	110	16	166	69
AUDITORY CORTEX	108	128	155	139	129	132	8	155	108
HIPPOCAMPUS	130	172	291	241	121	191	33	291	121
SUBSTANTIA NIGRA (PR)	265	282	254	169	138	222	29	282	138
INFERIOR COLLICULUS	441	345	480	327	173	353	53	480	173
PONTINE RETICULAR FORMATION	138	140	143	112	220	151	18	220	112
VISUAL CORTEX	138	111	141	102	78	114	12	141	78
CEREBELLUM		145	170	114		143	13	170	114
RIGHT									
CENTRAL FOCUS	116	175	284	338	144	211	43	338	116
PENUMBRA	171	207	247	192	142	192	18	247	142
FRONTAL CORTEX	159	160	166	174	110	154	11	174	110
CINGULATE CORTEX	159	407	506	197	162	286	72	506	159
SUBCORTICAL WHITE MATTER	63	74	65	57	72	66	3	74	57
CAUDATE NUCLEUS	397	266	265	150	93	234	53	397	93
SEPTAL NUCLEUS	119	111	125	161	216	146	19	216	111
GLOBUS PALLIDUS	216	181	222	179	80	176	25	222	80
AMYGALOID NUCLEUS	109	101	131	127	75	109	10	131	75
LATERAL HABENULA	157	180	280	218	231	213	21	280	157
MEDIAL HABENULA	177	237	577	212	219	284	74	577	177
VENT. THALAMIC NUCLEUS	169	542	173	200	108	238	77	542	108
DORSOMED. THALAMIC NUCLEUS	181	363	216	190	103	211	43	363	103
LATERAL THALAMIC NUCLEUS	166	208	220	173	92	172	22	220	92
ENTOPEDUNCULAR NUCLEUS	50	134	90	57	41	74	17	134	41
HYPOTHALAMUS	101	117	104	105	201	126	19	201	101
PARIETAL CORTEX	237	200	405	269	120	246	47	405	120
AUDITORY CORTEX	331	316	373	327	219	313	25	373	219
HIPPOCAMPUS	133	174	271	228	124	186	28	271	124
SUBSTANTIA NIGRA (PR)	130	226	191	89	84	144	28	226	84
INFERIOR COLLICULUS	451	325	505	328	186	359	56	505	186
PONTINE RETICULAR FORMATION	125	147	144	105	168	138	11	168	105
VISUAL CORTEX	181	194	349	187	107	204	40	349	107
CEREBELLUM		136	197	123		152	18	197	123

Table 4.5

SIDE-TO-SIDE DIFFERENCES IN REGIONAL CEREBRAL BLOOD FLOW (%)

Seizure animals

	RAT 6	RAT 7	RAT 8	RAT 9	RAT 10	MEAN	SEM	MAX	MIN
CENTRAL FOCUS	49,1	17,7	-55,6	-20,7	-24,3	-6,8	18,2	49,1	-55,6
PENUMBRA	87,7	117,9	40,1	31,3	6,3	56,7	20,2	117,9	6,3
FRONTAL CORTEX	-1,9	-1,3	-22,3	-17,8	-17,3	-12,1	4,4	-1,3	-22,3
CINGULATE CORTEX	-28,3	-9,1	-17,8	41,6	14,2	0,1	12,5	41,6	-28,3
SUBCORTICAL WHITE MATTER	-17,5	17,6	23,1	26,3	-4,2	9,1	8,5	26,3	-17,5
CAUDATE NUCLEUS	23,7	42,9	13,2	13,3	-11,8	16,2	8,9	42,9	-11,8
SEPTAL NUCLEUS	9,2	23,4	-4,8	36,6	32,9	19,5	7,7	36,6	-4,8
GLOBUS PALLIDUS	46,8	37,0	37,4	-12,8	30,0	27,7	10,5	46,8	-12,8
AMYGALOID NUCLEUS	-11,0	-7,9	-5,3	-15,7	6,7	-6,7	3,8	6,7	-15,7
LATERAL HABENULA	-0,6	13,3	32,5	22,9	40,7	21,8	7,2	40,7	-0,6
MEDIAL HABENULA	12,4	18,6	14,6	35,4	23,3	20,8	4,1	35,4	12,4
VENT. THALAMIC NUCLEUS	118,9	32,3	53,2	77,0	78,7	72,0	14,5	118,9	32,3
DORSOMED. THALAMIC NUCLEUS	176,8	66,9	181,5	102,6	278,6	161,3	36,6	278,6	66,9
LATERAL THALAMIC NUCLEUS	-10,8	130,8	41,4	11,6	57,6	46,1	24,2	130,8	-10,8
ENTOPEDUNCULAR NUCLEUS	24,0	23,1	-5,6	15,8	61,0	23,7	10,7	61,0	-5,6
HYPOTHALAMUS	1,0	21,4	-2,9	-1,0	17,9	7,3	5,1	21,4	-2,9
PARIETAL CORTEX	-60,8	-41,0	-59,0	-74,3	-12,5	-49,5	10,7	-12,5	-74,3
AUDITORY CORTEX	-67,4	-59,5	-58,4	-57,5	-41,1	-56,8	4,3	-41,1	-67,4
HIPPOCAMPUS	-2,3	-1,1	7,4	5,7	-2,4	1,5	2,1	7,4	-2,4
SUBSTANTIA NIGRA (PR)	103,8	24,8	33,0	89,9	64,3	63,2	15,4	103,8	24,8
INFERIOR COLLICULUS	-2,2	6,2	-5,0	-0,3	-7,0	-1,7	2,3	6,2	-7,0
PONTINE RETICULAR FORMATION	10,4	-4,8	-0,7	6,7	31,0	8,5	6,2	31,0	-4,8
VISUAL CORTEX	-23,8	-42,8	-59,6	-45,5	-27,1	-39,7	6,5	-23,8	-59,6
CEREBELLUM		6,6	-13,7	-7,3		-2,8	-1,25	6,6	-7,3

Table 4.6

UNCORRECTED Tc99m ACTIVITY (uCi/g)

Control animals

LEFT	RAT 1	RAT 2	RAT 3	RAT 4	RAT 5	MEAN	SEM	Max	Min
FRONTAL CORTEX	7,97	7,84	5,73	11,40	6,85	8,23	0,95	11,40	5,73
CINGULATE CORTEX	6,63	9,39	2,71	9,71	5,71	7,11	1,29	9,71	2,71
SUBCORTICAL WHITE MATTER	2,79	3,64	6,35	4,05	2,11	4,21	0,72	6,35	2,11
CAUDATE NUCLEUS	7,64	6,81	5,83	14,50	5,30	8,69	1,67	14,50	5,30
SEPTAL NUCLEUS	5,76	7,07	6,38	8,52	4,65	6,93	0,65	8,52	4,65
GLOBUS PALLIDUS	7,93	5,96	5,27	15,93	6,17	8,77	1,97	15,93	5,27
AMYGALOID NUCLEUS	3,6	5,72	8,17	12,20	4,28	7,42	1,56	12,20	3,60
LATERAL HABENULA	9,19	7,74	7,64	12,06	6,10	9,16	1,01	12,06	6,10
MEDIAL HABENULA	7,48	7,94	6,25	12,63	6,53	8,57	1,16	12,63	6,25
VENT. THALAMIC NUCLEUS	7,38	7,29	7,24	13,27	5,89	8,79	1,29	13,27	5,89
DORSOMED. THALAMIC NUCLEUS	8,56	11,37	4,27	13,77	6,49	9,49	1,69	13,77	4,27
LATERAL THALAMIC NUCLEUS	7,18	7,48	6,28	11,65	6,07	8,15	1,01	11,65	6,07
ENTOPEDUNCULAR NUCLEUS	3,51	5,11	6,55	7,91	3,21	5,77	0,89	7,91	3,21
HYPOTHALAMUS	6,24	8,23	5,89	12,63	4,51	8,25	1,41	12,63	4,51
PARIETAL CORTEX	8,2	8,92	6,78	12,63	6,95	9,13	1,06	12,63	6,78
AUDITORY CORTEX	7,51	6,81	7,21	14,10	7,58	8,91	1,37	14,10	6,81
HIPPOCAMPUS	8,36	6,49	6,51	16,38	6,00	9,44	1,95	16,38	6,00
SUBSTANTIA NIGRA (PR)	6,05	7,45	9,58	13,52	4,48	9,15	1,57	13,52	4,48
INFERIOR COLLICULUS	11,4	7,82	5,21	16,42	8,63	10,20	1,90	16,42	5,21
PONTINE RETICULAR FORMATION	6,21	7,81	6,25	9,57	4,34	7,46	0,88	9,57	4,34
VISUAL CORTEX	8,13	7,71	6,48	13,16	4,95	8,87	1,38	13,16	4,95
CEREBELLUM	6,53		6,21	13,16	5,96	8,63	1,55	13,16	5,96

RIGHT

FRONTAL CORTEX	6,99	8,56	6,98	12,98	5,05	8,88	1,34	12,98	5,05
CINGULATE CORTEX	7,87	9,66	6,51	11,03	6,07	8,77	0,94	11,03	6,07
SUBCORTICAL WHITE MATTER	2,52	3,58	3,12	5,76	2,32	3,74	0,62	5,76	2,32
CAUDATE NUCLEUS	7,8	7,87	6,42	15,08	5,43	9,29	1,70	15,08	5,43
SEPTAL NUCLEUS	5,82	7,19	5,47	9,77	4,71	7,06	0,89	9,77	4,71
GLOBUS PALLIDUS	5,4	7,07	6,42	11,37	6,17	7,57	1,06	11,37	5,40
AMYGALOID NUCLEUS	3,76	6,40	5,63	11,92	4,38	6,93	1,45	11,92	3,76
LATERAL HABENULA	9,15	7,42	8,94	11,20	5,09	9,18	1,02	11,20	5,09
MEDIAL HABENULA	7,84	7,77	8,04	12,63	5,16	9,07	1,21	12,63	5,16
VENT. THALAMIC NUCLEUS	7,21	6,65	7,11	12,73	5,78	8,43	1,23	12,73	5,78
DORSOMED. THALAMIC NUCLEUS	8,89	12,10	7,31	14,97	6,28	10,82	1,60	14,97	6,28
LATERAL THALAMIC NUCLEUS	7,67	7,77	4,14	12,56	6,46	8,04	1,38	12,56	4,14
ENTOPEDUNCULAR NUCLEUS	3,51	5,69	6,22	7,82	3,11	5,81	0,88	7,82	3,11
HYPOTHALAMUS	6,34	8,30	6,48	13,09	4,41	8,55	1,48	13,09	4,41
PARIETAL CORTEX	8,69	9,80	7,74	14,39	6,67	10,16	1,34	14,39	6,67
AUDITORY CORTEX	9,29	7,07	8,77	18,24	7,77	10,84	2,04	18,24	7,07
HIPPOCAMPUS	7,9	6,46	7,27	16,23	6,31	9,47	1,87	16,23	6,31
SUBSTANTIA NIGRA (PR)	6,24	7,32	6,75	12,24	4,44	8,14	1,30	12,24	4,44
INFERIOR COLLICULUS	11,7	7,17	9,95	17,90	7,77	11,67	1,93	17,90	7,17
PONTINE RETICULAR FORMATION	5,72	7,08	5,63	10,18	4,58	7,15	0,97	10,18	4,58
VISUAL CORTEX	6,82	7,44	7,51	13,70	5,47	8,87	1,43	13,70	5,47
CEREBELLUM	7,05		6,35	12,17	5,57	8,52	1,33	12,17	5,57

Table 4.7

CORRECTED Tc99m ACTIVITY (uCi/g)
Control animals

	RAT 1	RAT 2	RAT 3	RAT 4	RAT 5	MEAN	SEM	Max	Min
LEFT									
FRONTAL CORTEX	9,95	8,34	5,90	12,76	8,42	9,24	1,13	12,8	5,9
CINGULATE CORTEX	7,22	11,33	5,41	9,87	6,15	8,46	1,13	11,3	5,41
SUBCORTICAL WHITE MATTER	2,23	2,94	2,10	3,15	1,64	2,41	0,28	3,15	1,64
CAUDATE NUCLEUS	9,21	6,72	6,28	19,88	5,46	9,51	2,67	19,9	5,46
SEPTAL NUCLEUS	5,78	7,10	5,54	8,14	4,49	6,21	0,64	8,14	4,49
GLOBUS PALLIDUS	9,87	5,55	6,33	24,42	6,99	10,6	3,52	24,4	5,55
AMYGALOID NUCLEUS	3,04	5,24	4,82	14,34	3,99	6,29	2,05	14,3	3,04
LATERAL HABENULA	13,2	8,17	9,38	14,06	6,86	10,3	1,41	14,1	6,86
MEDIAL HABENULA	8,86	8,51	8,37	15,24	7,71	9,74	1,39	15,2	7,71
VENT. THALAMIC NUCLEUS	8,65	7,44	6,13	16,70	6,46	9,08	1,96	16,7	6,13
DORSOMED. THALAMIC NUCLEUS	11,4	16,53	7,68	17,94	7,63	12,2	2,16	17,9	7,63
LATERAL THALAMIC NUCLEUS	8,25	7,75	3,64	13,23	6,79	7,93	1,55	13,2	3,64
ENTOPEDUNCULAR NUCLEUS	2,94	4,50	6,18	7,33	2,72	4,73	0,9	7,33	2,72
HYPOTHALAMUS	6,55	9,02	6,57	16,29	4,30	8,55	2,08	16,3	4,3
PARIETAL CORTEX	10,5	10,35	5,63	15,24	9,23	10,2	1,54	15,2	5,63
AUDITORY CORTEX	8,92	6,72	6,93	18,79	10,13	10,3	2,22	18,8	6,72
HIPPOCAMPUS	10,9	6,27	7,62	26,06	6,66	11,5	3,73	26,1	6,27
SUBSTANTIA NIGRA (PR)	6,24	7,70	6,52	17,31	4,26	8,41	2,29	17,3	4,26
INFERIOR COLLICULUS	22,5	8,23	12,55	26,20	13,56	16,6	3,34	26,2	8,23
PONTINE RETICULAR FORMATION	6,5	8,11	4,73	9,66	4,08	6,62	1,04	9,66	4,08
VISUAL CORTEX	10,3	7,97	6,13	16,45	4,93	10,2	2,04	16,5	4,93
CEREBELLUM	7,05		6,47	16,45	6,59	9,99	2,18	16,5	6,47
RIGHT									
FRONTAL CORTEX	7,87	9,63	7,24	16,04	5,08	9,17	1,86	16	5,08
CINGULATE CORTEX	9,72	11,93	6,52	12,07	6,79	9,41	1,2	12,1	6,52
SUBCORTICAL WHITE MATTER	1,97	2,88	2,48	4,83	1,83	2,8	0,54	4,83	1,83
CAUDATE NUCLEUS	9,57	8,39	6,37	21,61	5,68	10,3	2,91	21,6	5,68
SEPTAL NUCLEUS	5,88	7,29	5,06	9,97	4,58	6,56	0,97	9,97	4,58
GLOBUS PALLIDUS	5,27	7,10	6,37	12,70	6,99	7,69	1,3	12,7	5,27
AMYGALOID NUCLEUS	3,21	6,14	5,28	13,77	4,12	6,5	1,88	13,8	3,21
LATERAL HABENULA	13,1	7,65	11,01	12,38	5,13	9,86	1,51	13,1	5,13
MEDIAL HABENULA	9,64	8,23	9,12	15,24	5,24	9,49	1,63	15,2	5,24
VENT. THALAMIC NUCLEUS	8,32	6,49	7,46	15,48	6,28	8,81	1,71	15,5	6,28
DORSOMED. THALAMIC NUCLEUS	12,3	19,05	7,79	21,28	7,20	13,5	2,87	21,3	7,2
LATERAL THALAMIC NUCLEUS	9,28	8,23	3,50	15,09	7,56	8,73	1,87	15,1	3,5
ENTOPEDUNCULAR NUCLEUS	2,94	5,20	6,09	7,21	2,62	4,81	0,89	7,21	2,62
HYPOTHALAMUS	6,71	9,14	6,47	16,28	4,17	8,55	2,09	16,3	4,17
PARIETAL CORTEX	11,8	12,24	8,55	19,58	8,02	12	2,07	19,6	8,02
AUDITORY CORTEX	13,6	7,10	10,63	34,44	10,75	15,3	4,89	34,4	7,1
HIPPOCAMPUS	9,79	6,22	7,73	25,50	7,27	11,3	3,6	25,5	6,22
SUBSTANTIA NIGRA (PR)	6,55	7,49	6,87	14,42	4,21	7,91	1,72	14,4	4,21
INFERIOR COLLICULUS	24,4	7,31	13,55	32,65	10,75	17,7	4,7	32,7	7,31
PONTINE RETICULAR FORMATION	5,74	7,13	5,28	10,61	4,39	6,63	1,09	10,6	4,39
VISUAL CORTEX	7,57	7,75	8,14	17,76	5,74	9,39	2,13	17,8	5,74
CEREBELLUM	8		6,28	14,27	5,91	8,61	1,73	14,3	5,91

Table 4.8

UNCORRECTED Tc99m ACTIVITY (uCi/g)

Seizure animals

LEFT (FOCUS)	RAT 6	RAT 7	RAT 8	RAT 9	RAT 10	MEAN	SEM	Max	Min
CENTRAL FOCUS	3,95	11,32	4,06	7,78	3,42	6,11	1,52	11,32	3,42
PENUMBRA	7,01	15,70	11,63	8,23	5,76	9,67	1,80	15,70	5,76
FRONTAL CORTEX	4,42	9,87	7,20	6,44	3,80	6,35	1,08	9,87	3,80
CINGULATE CORTEX	3,75	14,49	11,51	9,29	6,65	9,14	1,86	14,49	3,75
SUBCORTICAL WHITE MATTER	1,76	5,94	4,09	2,82	2,29	3,38	0,75	5,94	1,76
CAUDATE NUCLEUS	8,73	15,48	10,81	6,81	3,25	9,02	2,04	15,48	3,25
SEPTAL NUCLEUS	4,70	9,40	7,57	8,48	6,10	7,25	0,84	9,40	4,70
GLOBUS PALLIDUS	8,02	14,79	10,89	6,23	4,47	8,88	1,82	14,79	4,47
AMYGALOID NUCLEUS	4,56	6,08	6,64	4,14	2,97	4,88	0,66	6,64	2,97
LATERAL HABENULA	4,36	10,83	15,03	8,45	8,55	9,44	1,74	15,03	4,36
MEDIAL HABENULA	7,62	16,26	17,24	9,33	8,85	11,86	2,02	17,24	7,62
VENT. THALAMIC NUCLEUS	11,21	15,39	13,95	8,61	4,88	10,81	1,88	15,39	4,88
DORSOMED. THALAMIC NUCLEUS	8,10	17,94	14,81	8,84	8,07	11,55	2,03	17,94	8,07
LATERAL THALAMIC NUCLEUS	8,09	13,89	9,60	5,78	4,14	8,30	1,68	13,89	4,14
ENTOPEDUNCULAR NUCLEUS	2,91	9,08	5,94	3,66	2,69	4,86	1,20	9,08	2,69
HYPOTHALAMUS	4,88	9,01	6,86	4,97	7,44	6,63	0,78	9,01	4,88
PARIETAL CORTEX	3,75	8,66	8,54	4,57	4,12	5,93	1,10	8,66	3,75
AUDITORY CORTEX	4,67	9,59	9,60	6,47	5,15	7,10	1,06	9,60	4,67
HIPPOCAMPUS	5,05	12,55	10,56	8,48	4,53	8,23	1,55	12,55	4,53
SUBSTANTIA NIGRA (PR)	8,21	13,51	11,22	6,41	4,79	8,83	1,58	13,51	4,79
INFERIOR COLLICULUS	10,75	13,89	14,99	10,18	6,56	11,27	1,49	14,99	6,56
PONTINE RETICULAR FORMATION	4,60	7,74	8,77	4,83	5,82	6,35	0,82	8,77	4,60
VISUAL CORTEX	5,63	7,52	8,69	5,48	4,75	6,41	0,73	8,69	4,75
CEREBELLUM		9,08	10,04	5,45		8,19	1,08	10,04	5,45

RIGHT

CENTRAL FOCUS	5,63	10,67	11,22	9,49	4,88	8,38	1,31	11,22	4,88
PENUMBRA	5,74	12,05	9,64	7,88	4,44	7,95	1,36	12,05	4,44
FRONTAL CORTEX	5,27	10,07	8,03	7,88	3,85	7,02	1,10	10,07	3,85
CINGULATE CORTEX	4,56	14,96	13,22	8,48	6,65	9,57	1,96	14,96	4,56
SUBCORTICAL WHITE MATTER	2,51	5,87	3,72	2,35	2,31	3,35	0,68	5,87	2,31
CAUDATE NUCLEUS	8,33	12,76	9,24	6,23	4,06	8,12	1,46	12,76	4,06
SEPTAL NUCLEUS	4,60	8,77	7,42	6,35	6,87	6,80	0,68	8,77	4,60
GLOBUS PALLIDUS	7,58	12,47	10,28	6,97	3,57	8,17	1,51	12,47	3,57
AMYGALOID NUCLEUS	4,02	7,07	8,23	5,42	3,08	5,56	0,95	8,23	3,08
LATERAL HABENULA	4,02	12,80	13,22	9,00	8,46	9,50	1,67	13,22	4,02
MEDIAL HABENULA	7,08	13,68	14,81	7,00	8,27	10,17	1,69	14,81	7,00
VENT. THALAMIC NUCLEUS	8,37	15,87	9,84	6,14	4,00	8,84	2,02	15,87	4,00
DORSOMED. THALAMIC NUCLEUS	6,36	14,79	10,28	6,02	3,65	8,22	1,96	14,79	3,65
LATERAL THALAMIC NUCLEUS	5,05	11,19	10,77	5,60	4,00	7,32	1,52	11,19	4,00
ENTOPEDUNCULAR NUCLEUS	2,79	8,47	6,20	3,74	2,15	4,67	1,17	8,47	2,15
HYPOTHALAMUS	4,91	7,89	7,27	4,86	6,07	6,20	0,61	7,89	4,86
PARIETAL CORTEX	6,29	12,26	15,16	9,07	4,65	9,49	1,92	15,16	4,65
AUDITORY CORTEX	7,43	15,01	16,17	10,51	6,65	11,15	1,93	16,17	6,65
HIPPOCAMPUS	5,30	11,44	10,69	7,56	4,62	7,92	1,38	11,44	4,62
SUBSTANTIA NIGRA (PR)	5,27	12,51	9,72	4,71	2,94	7,03	1,77	12,51	2,94
INFERIOR COLLICULUS	10,71	13,39	15,69	10,28	7,19	11,45	1,45	15,69	7,19
PONTINE RETICULAR FORMATION	4,32	8,24	8,42	5,06	5,39	6,29	0,85	8,42	4,32
VISUAL CORTEX	6,36	11,68	13,31	8,01	5,12	8,90	1,56	13,31	5,12
CEREBELLUM		10,31	10,12	4,89		8,44	1,38	10,31	4,89

Table 4.9

CORRECTED Tc99m ACTIVITY (uCi/g)

Seizure animals

LEFT (FOCUS)	RAT 6	RAT 7	RAT 8	RAT 9	RAT 10	MEAN	SEM	Max	Min
CENTRAL FOCUS	3,84	16,36	3,34	10,78	3,19	8,42	2,85	16,36	3,19
PENUMBRA	10,52	41,45	17,08	12,15	7,38	19,52	6,78	41,45	7,38
FRONTAL CORTEX	4,55	12,42	7,25	7,53	3,70	7,73	1,60	12,42	3,70
CINGULATE CORTEX	3,56	31,17	16,68	16,29	9,96	18,53	4,01	31,17	9,96
SUBCORTICAL WHITE MATTER	1,36	5,52	3,37	2,31	1,88	3,27	0,73	5,52	1,88
CAUDATE NUCLEUS	18,96	39,27	14,63	8,32	2,98	16,30	7,17	39,27	2,98
SEPTAL NUCLEUS	5,00	11,34	7,84	13,02	8,26	10,12	1,11	13,02	7,84
GLOBUS PALLIDUS	14,69	33,35	14,86	7,10	4,74	15,01	5,80	33,35	4,74
AMYGALOID NUCLEUS	4,77	5,71	6,43	3,81	2,63	4,65	0,78	6,43	2,63
LATERAL HABENULA	4,44	14,91	34,04	12,91	19,86	20,43	4,26	34,04	12,91
MEDIAL HABENULA	12,87	48,09	60,28	16,44	22,43	36,81	9,31	60,28	16,44
VENT. THALAMIC NUCLEUS	67,99	38,45	26,95	13,49	5,49	21,10	6,52	38,45	5,49
DORSOMED. THALAMIC NUCLEUS	4,49	82,22	32,43	14,35	16,45	36,36	14,14	82,22	14,35
LATERAL THALAMIC NUCLEUS	15,09	27,38	11,65	6,26	4,22	12,38	4,69	27,38	4,22
ENTOPEDUNCULAR NUCLEUS	2,53	10,67	5,49	3,23	2,32	5,43	1,67	10,67	2,32
HYPOTHALAMUS	5,30	10,51	6,75	4,96	13,04	8,82	1,63	13,04	4,96
PARIETAL CORTEX	3,56	9,82	9,50	4,38	4,18	6,97	1,39	9,82	4,18
AUDITORY CORTEX	4,94	11,78	11,65	7,59	6,02	9,26	1,30	11,78	6,02
HIPPOCAMPUS	5,62	20,80	13,97	13,02	4,85	13,16	2,92	20,80	4,85
SUBSTANTIA NIGRA (PR)	15,72	25,27	15,80	7,47	5,32	13,47	4,06	25,27	5,32
INFERIOR COLLICULUS	48,77	27,38	33,71	21,14	9,65	22,97	4,59	33,71	9,65
PONTINE RETICULAR FORMATION	4,83	8,17	9,94	4,75	7,53	7,60	0,96	9,94	4,75
VISUAL CORTEX	6,78	7,80	9,79	5,75	4,55	6,97	1,03	9,79	4,55
CEREBELLUM		10,67	12,66	5,70		9,68	1,60	12,66	5,70

RIGHT

CENTRAL FOCUS	6,78	14,46	15,80	17,23	5,49	13,25	2,37	17,23	5,49
PENUMBRA	7,02	18,86	11,74	11,06	4,70	11,59	2,59	18,86	4,70
FRONTAL CORTEX	6,03	12,90	8,60	11,06	3,78	9,09	1,77	12,90	3,78
CINGULATE CORTEX	4,77	34,70	23,25	13,02	9,96	20,23	5,01	34,70	9,96
SUBCORTICAL WHITE MATTER	2,09	5,43	3,01	1,85	1,91	3,05	0,75	5,43	1,85
CAUDATE NUCLEUS	16,40	21,68	10,88	7,10	4,09	10,94	3,44	21,68	4,09
SEPTAL NUCLEUS	4,83	10,05	7,60	7,34	10,72	8,93	0,76	10,72	7,34
GLOBUS PALLIDUS	12,70	20,46	13,25	8,68	3,38	11,44	3,24	20,46	3,38
AMYGALOID NUCLEUS	3,93	7,10	8,93	5,65	2,77	6,11	1,16	8,93	2,77
LATERAL HABENULA	3,93	21,86	23,25	15,01	19,10	19,81	1,62	23,25	15,01
MEDIAL HABENULA	10,78	26,18	32,43	8,75	17,71	21,27	4,61	32,43	8,75
VENT. THALAMIC NUCLEUS	16,63	43,33	12,19	6,93	4,00	16,61	8,11	43,33	4,00
DORSOMED. THALAMIC NUCLEUS	8,57	33,35	13,25	6,70	3,50	14,20	5,99	33,35	3,50
LATERAL THALAMIC NUCLEUS	5,62	15,98	14,52	5,95	4,00	10,11	2,69	15,98	4,00
ENTOPEDUNCULAR NUCLEUS	2,39	9,45	5,82	3,32	1,75	5,09	1,50	9,45	1,75
HYPOTHALAMUS	5,37	8,43	7,36	4,79	8,18	7,19	0,74	8,43	4,79
PARIETAL CORTEX	8,37	19,64	35,07	15,28	5,05	18,76	5,58	35,07	5,05
AUDITORY CORTEX	12,07	35,05	44,77	23,44	9,96	28,31	6,72	44,77	9,96
HIPPOCAMPUS	6,10	16,75	14,30	10,17	5,00	11,56	2,30	16,75	5,00
SUBSTANTIA NIGRA (PR)	6,03	20,63	11,92	4,58	2,60	9,93	3,66	20,63	2,60
INFERIOR COLLICULUS	47,50	24,62	39,68	21,79	11,94	24,51	5,14	39,68	11,94
PONTINE RETICULAR FORMATION	4,39	9,03	9,28	5,09	6,53	7,48	0,90	9,28	5,09
VISUAL CORTEX	8,57	17,56	23,65	11,44	5,96	14,65	3,42	23,65	5,96
CEREBELLUM		13,50	12,85	4,83		10,39	2,16	13,50	4,83

Chapter 4

Discussion

Choice of model of focal epilepsy

The main aim of the present study was to study the correlation between HMPAO and IAP uptake at very high blood flows. For this purpose, a model of generalised seizures in the rat would have been ideal, for reasons of technical simplicity and the high flows seen in such models (Horton et al., 1980). However, the study had the secondary aim to study the particular flow changes seen in an animal model of focal epilepsy. The penicillin model of focal epilepsy was chosen for its technical simplicity, and the fact that the effects of penicillin induced seizures on regional metabolism had been previously studied, allowing correlation with blood flow changes. In the event, the model proved easy to use and effective in producing high flows. There was no obvious technical reason why one animal had less intense seizures and blood flow changes than the others.

The ^{14}C Iodoantipyrine method

The iodo^{14}C iodoantipyrine method is based on on the equation derived by Kety describing the exchange of an inert gas between blood and tissues (Kety, 1951). The use of gaseous tracers posed technical problems, leading to the development of ^{14}C iodoantipyrine. This tracer was limited by poor diffusibility, tending to give lower values than earlier methods. This problem was overcome with the development of iodo^{14}C antipyrine by Sakurada and colleagues (1978), which gave flow values similar to those given by freely diffusible gas tracers. This has become the accepted method for determining blood flow in discrete structural components of the brain. It has, however, been suggested that diffusion limitation may lead to underestimations of very high flows (Abdul-Rahman et al., 1979). Horton et al. (1980) measured rCBF using both the iodo ^{14}C antipyrine method and microspheres during generalised seizures induced by bicuculline. They found values for regional cerebral blood flow which were in general higher than those found in the present study (see below) and total cerebral blood flows which were comparable with those found using the venous outflow and xenon clearance methods (from Meldrum & Nilsson, 1976) in the same model. In their hands, the IAP

methods gave higher values than microspheres, and they concluded that the latter method had underestimated flow.

The accuracy of the IAP technique depends on operator skill at certain points. Three operators are required; one to regulate the arterial catheter flow rate, collect arterial samples and call out the drop rate, one to regulate the arterial injection of iodoantipyrine and one to operate the guillotine. Coordination between the three must be good. Skill is required to make sure that the timing of arterial samples as recorded on tape during the procedure is transcribed accurately. After decapitation, the brain must be dissected out rapidly to prevent diffusion of iodoantipyrine from high to low concentration areas (Williams et al, 1991) to prevent loss of definition of boundaries between high and low flow areas, underestimation of high flows. This must be done skillfully to avoid structural damage to the brain. The laboratory in which the present study took place has extensive experience of the procedure, and several sham experiments were carried out to familiarise the operators with it.

Control animals

rCBF

The blood flows seen in the non-seizure animals were within the total ranges seen in control animals in previous studies using the same methods (McCulloch et al., 1982a,b; Mohammed et al., 1985). However, the range was larger than that seen in any single one of these studies. This may have been due to the difficulty experienced in controlling physiological parameters, in turn due to the constraints of the experimental protocol.

In the experimental animals, seizures began as soon as the animal began to move on recovery from the anaesthetic, i.e. within 2-3 minutes of its withdrawal. The point of measurement of cerebral perfusion was fixed at 10 minutes after seizure onset; this was the maximum judged acceptable in conscious animals, and the minimum judged sufficient to allow development of a steady state between HMPAO and IAP injections, and to allow the development of the high flows necessary for adequate comparison of the HMPAO and IAP methods. In sham animals, therefore, cerebral perfusion was measured 10 minutes after they began moving on recovery from the anaesthetic. This allowed limited time for post-anaesthetic stabilisation of physiological parameters (see below). In retrospect, a lower dose of penicillin might have given sufficiently intense seizures after a longer time

period, allowing more time for stabilisation of physiological parameters.

Effect on rCBF of anaesthetic agents

Nitrous oxide slightly increases both blood flow and metabolic rate in rat studies, while halothane depresses metabolic rate in a dose dependent way, but increases flow (Edvinsson et al., 1993c). Changes due to halothane are not homogeneous, but preferentially involve structures such as the locus ceruleus and substantia nigra. The changes seen are symmetrical. Changes induced by variable residual effects of halothane could at leasst partially explain the variability seen in absolute flows. It is, however, unlikely that the effect impacted significantly on the main object of the study, that of establishing the relationship between HMPAO and IAP uptake at high flows. With respect to the localised changes seen in seizure animals, any localised but symmetric effects of halothane would be negated in results expressed as percentage asymmetry.

Effect on rCBF of craniotomy

Some sham animals showed reduction in cerebral perfusion in the neocortex ipsilateral to the craniotomy. While this might be due to injection of vehicle into the cortex, the same phenomenon was seen to a marked extent in 2 of 4 animals who had craniotomy only (Fig). These animals were not included in the control group for the study, but did show that craniotomy alone was sufficient to produce neocortical hypoperfusion. In these cases, the craniotomy was carried out rapidly, drilling the hole in 2-3 applications of the drill. In the 2 animals not showing marked hypoperfusion, the craniotomy was carried out very slowly, allowing the bone to cool between short applications of the drill. These results were in accord with the previous experience of the laboratory, and the slow procedure was therefore adopted for the study. Drill applications were not formally timed, so it is possible that even minor variations in the speed of drilling were responsible for some animals showing hypoperfusion and some not.

The craniotomy may also have been responsible for neocortical hypoperfusion seen in experimental animals. However, side-to-side differences were greater in experimental animals (with no difference in craniotomy technique), suggesting a contributary effect of seizures.

Effect on rCBF of injection of vehicle

Although the track of the needle could be discerned in non-seizure animals, there was little or no effect on perfusion in surrounding tissues, nor was there any discernible effect around the point of the needle, where an effect of the injection of vehicle might have been seen. There is therefore no evidence that any of the changes seen in experimental animals was due to injection of vehicle.

Experimental animals

Comparison with previous studies

1. Studies using the penicillin model of focal motor epilepsy

Most autoradiographic studies in rat models of focal epilepsy have centred on the functional anatomy of the seizure, i.e. showing the extent of metabolic activity around the focus, and showing which structures are distantly metabolically activated or depressed during the seizure. These studies have measured the local metabolic rate for glucose, rather than regional perfusion. Those which have used the penicillin model of focal epilepsy (Collins, 1976; Collins, 1978a; b; Collins et al., 1983) have found generally similar patterns of activation to those found in the present study, with increases in metabolism around the focus, in the adjacent and contralateral cingulate gyrus, and in the thalamus and substantia nigra, with decreases in metabolism in cortical areas ipsilateral to the focus. In addition to this, these studies have found increases in metabolism in the contralateral homotopic motor cortex, the caudate, putamen, entopeduncular nucleus, subthalamic nucleus and cerebellum, not seen as increases in rCBF in this study.

The degree of increase in metabolic rate in these studies was in general greater than the equivalent percentage increases in rCBF seen in the present study. For example, Collins et al (1976) found increases (focus side c.f. contralateral homotopic area) of 96% in the motor cortex and 70% in the substantia nigra, Collins (1978a) found increases of 218% in the motor cortex, and Collins (1978b) found increases of 251% in the motor cortex, 300% in the substantia nigra and 291% in the thalamus, compared to control animals. These figures compare with side to side differences in rCBF of 56.7% (-3.3% in controls) for the focus, up to 161.3% (7.8% in controls) in the thalamus, and 63.2% (-0.5% in controls) in the substantia nigra seen in the present study.

Decreases in rCBF in the cortex ipsilateral to the focus in the present study were greater than those seen in studies of local metabolic rate. The decrease in frontal cortex adjacent to the focus found by Collins (1978a) was 6-13%, with a reduction of 5-15% in the occipital cortex and 17-26% in the somatosensory cortex, all compared with . This compares to side to side differences in the present study of -12.1% (-0.3% in controls) in the frontal cortex, -49.5% (-28.6% in controls) in the parietal cortex, -56.8% (-28.9% in controls) in the auditory cortex, and -39.7% (-6.9% in controls) in the visual cortex.

The figures for the present study refer to percentage increases or decreases with reference to the contralateral side, while the past studies quoted compare absolute values for seizure and non-seizure groups. If the percentage difference in control animals (presumably that portin of hypoperfusion due to craniotomy) in the present study is subtracted, then the figures for the present and past studies become comparable.

Possible reasons for differences between the present and previous studies

a. Differences in intensity of seizure activity

It is possible that differing degrees of metabolic disturbance reflect different intensities of seizure activity. In the studies of Collins and Collins et al. mentioned above, various doses of penicillin (ranging from 25-300 units) were injected intracortically. The greater the dose, the greater the frequency of seizure movement, the wider the involvement of cerebral structures and the wider and more intense the metabolic disturbance. For example, Collins (1978) found that injection of 25 units produced mild unilateral seizures with 96% increase in metabolism round the focus, whil injection of 300 units produced seizures with bilateral spread and an increase of 134% in metabolism round the focus. Collins (1978a) found that larger and repeated doses of penicillin increased the size and intensity of the metabolic disturbance, and increased the number of structures distantly activated by the discharges.

Differences in seizure intensity might explain some of the above differences between the present and previous studies. It is certainly the case that activation (not seen in the present study) of such subcortical structures as the extrapyramidal nuclei, globus pallidus and entopeduncular nucleus, or the cerebellar hemisphere were seen only after repeated injections (Collins 1978b) or after larger doses (i.e. 300 units) of penicillin (Collins et al., 1976), both of which resulted in more severe or bilateral seizures.

However, Collins et al. (1976) injected a group of rats with 25 units of penicillin, producing seizures which were descriptively milder than those in the present study i.e. involving the paw, face and head only, while those in the present study (excepting animal 10) also involved the hindleg and tail. Nonetheless, the disturbance in metabolism appears to have been greater than in the present study. It should be remembered that the deoxyglucose method requires that a steady state be achieved. For this reason, the animals in all the above studies had been exhibiting seizure activity for longer (in some cases for a period of days (Collins 1978b) than in the present study, and this may well account for smaller degree of functional disturbance seen.

b. Dissociation of metabolic rate and blood flow

A further possible explanation for differences between the present study and studies of metabolism would be dissociation between metabolism and perfusion. The present study does not address this issue, nor does any study address it using the penicillin model of focal motor epilepsy. One study of kainic acid induced limbic status epilepticus in the rat (Tanaka et al., 1990) has suggested a degree of uncoupling between flow and metabolism, with increases in metabolic rate 2-3 times higher than rises in rCBF in the CA1 and CA3 areas of the hippocampus. However, in that study the two parameters were measured at significantly dfferent time points, in different groups of animals. Other data suggests that the two parameters are coupled (Ingvar, 1986) during seizures.

c. Underestimation of high flows by IAP

It is recognised that very high levels of perfusion may be underestimated by the iodoantipyrine method. The ramped infusion technique produces a rising plasma concentration of iodo ^{14}C antipyrine and thereby prevents diffusion from neurones back into the circulation. Local brain levels of iodo ^{14}C antipyrine at the point of death are determined and maintained by local cerebral blood flow, but when the animal is killed, diffusion from high to low concentration areas is no longer counterbalanced by differences in perfusion, and will continue until the brain is frozen. This effect has been described by Williams et al. (1991). They studied the effects of a delay of 3 minutes on rCBF, finding reductions of up to 50% in some structures. Such reductions were accompanied by marked loss of definition on autoradiographic films. This study of Williams et al. compared

freezing delayed by 3 minutes with immediate immersion of the head in liquid nitrogen and later dissection of the brain. In the present study, the brain was dissected out before freezing, and frozen to -40degC within one minute. No data exists to suggest what the degree of underestimation of high flows resulting from this lesser delay might be.

Theoretically, some index the extent of post-mortem diffusion of IAP can be gained from comparison of the relative definition of IAP and HMPAO films, as diffusion problems affect the two tracers in a different manner. In the period after injection when plasma concentration is falling, but conversion of HMPAO to hydrophilic form is incomplete, some diffusion of the compound from neurones back into the circulation may occur, causing underestimation of high flows. If, as in the present study, the process is allowed to complete and the animal is killed after time has been allowed for all the HMPAO to convert to hydrophilic form, then postmortem redistribution from areas of high to areas of low perfusion will not occur, and neither will loss of definition on autoradiographic films. Any difference in definition between the two films is therefore likely to be due to post-mortem diffusion of IAP. In fact, the definition on IAP films was excellent, and in many cases even superior to that of the corresponding HMPAO film, providing no positive evidence for significant post-mortem diffusion (given possible technical reasons for loss of definition of some of the HMPAO films - see below).

One would expect the effect of post-mortem diffusion on high flow to be greatest at the edge of highly perfused structures, or in small highly perfused structures. In fact, in the smallest structure showing a significant increase, the substantia nigra pars reticulata, the relative increase was 63.2%, which compares with the increase in metabolism in this structure seen by Collins (1978a) after a single seizure of 56%. He found an increase of 80% in the ventral thalamus (a larger structure), compared to 72% in the present study.

It is possible that some very small (in both degree and extent) effects seen in studies of metabolic rate, such as the increases seen in homotopic motor cortex contralateral to the focus, may have been lost due to post mortem diffusion of IAP. There is no reason to believe that they might be lost for this reason on HMPAO films. Nevertheless, even on the most careful inspection, changes in the homotopic cortex could not be discerned.

Ideally one would perform further studies to determine the effect of short postmortem delays in freezing of the brain, but this was beyond the scope of the present study. The above data do, however, suggest that the effect is small, even at high flows, if the brain is dissected out and frozen within 1 minute. This problem is further discussed below with respect to the relationship between IAP and HMPAO uptake.

2. Comparisons with studies using other animal models of epilepsy

The patterns of activation and inhibition seen during focal seizures depend mainly on the structure of origin of the seizure and the anatomical connexions of that structure (see Chapter 1). One would not therefore necessarily expect comparable patterns of change in metabolism or blood flow in different models of epilepsy. However, it is worth making some comparisons with the degree of rise in rCBF and local metabolic rate using expamples from previous studies.

Limbic seizures induced by local amygdalar injection of kainic acid have produced flows of 400% of control values in the hippocampus, of 180% in the sensorimotor cortex, and of up to 185% of control values in the thalamus (Tanaka et al., 1990). Collins et al. (1983) found rises in glucose metabolism of up to 180% of control values in limbic structures in animals with limbic seizures induced by local injections of penicillin and picrotoxin. Lothman & Collins (1981) found increases in glucose metabolism to 440% of control values in the hippocampus, and to 133% of control values in the substantia nigra pars reticulata, in limbic seizures in the rat induced by intravenous injection of kainic acid.

Kindled limbic seizures have shown increases in metabolism to 83% and 173% of control values in the amygdala, to 92% and 224% of controls in the hippocampus and to 230% of controls in the substantia nigra pars reticulata in 2 studies (Lothman et al., 1985; Blackwood et al., 1981).

Studies of rCBF and metabolic rate in bicuculline-induced generalised seizures in the rat have found rises to 173% of control rCBF values in the sensorimotor cortex, to 196% of control values in the thalamus (Ingvar & Siesjo, 1983), of almost 900% of controls in the inferior colliculi and of 860% in the thalamus (Horton et al., 1980).

With the exception of the limbic changes induced by local injection of kainic acid, the above changes in focal seizures are generally comparable in degree to those seen in the present study, e.g., increases to (mean) 113% of control values in the area around the focus, to 158% of control values in the septal nucleus, and to 255% of control values in the thalamus.

3. Comparison with changes in rCBF seen in human focal epilepsy

In a modelof focal motor seizures one might expect to see changes analogous to those found in focal motor seizures in humans, and possibly to seizures originating in the

premotor areas of the frontal lobe. Little work exists to confirm this, but a series of patients with frontal lobe seizures studied ictally with HMPAO SPECT (Duncan et al., J Neurophysiol, 1993, in press) has shown hyperperfusion of the focus, the basal ganglia, the thalamus, and the cerebellum. Hypoperfusion has also been shown but, as in the cases presented in Chapter 3, involving the frontal lobe or hemisphere contralateral to the focus. Possible mechanisms are discussed in Chapter 3. This situation may be contrasted with seizures originating in the mesial temporal lobe, where activation of the basal ganglia is more prominent (see Chapter 3)

Causes of perfusion changes seen in the present study

Given that the perfusion changes seen in the present study have followed the general pattern of metabolic changes seen in similar seizures, then it seems likely that they are simply the result of the circulatory requirements of the metabolic activity required to sustain the electrical activity associated with seizures.

It seems likely that the hypoperfusion seen in association with penicillin induced seizures represents the same phenomenon as hypometabolism in deoxyglucose studies (Collins 1978a), and is therefore simply secondary to reduced metabolic demand. Collins suggested two possible mechanisms. Firstly, inhibition of normal synaptic excitation. He hypothesised that this might occur because of stimulation (by seizure activity (Collins et al., 1976; Schwartzkroin et al., 1975)) of the ventral thalamus, inhibiting or disrupting transmission of sensory data to the cortex. Secondly, an increase in inhibitory firng might also explain the reduced metabolic and circulatory activity. Collins pointed out, however, that inhibitory processes themselves require energy. Nonetheless, in the area around the focus, neurones show reduced firing rates and hyperpolarisation, the phenomenon known as 'surround inhibition' (Prince & Wilder, 1967). The studies of Collins and Colins et al. do show reduced metabolism in these areas, and the present study shows reduced perfusion, suggesting that the net effect of such inhibition (plus or minus any possible effect from lack of normal input) is a reduction in metabolic rate and perfusion. Why the reductions in perfusion and metabolism (both in studies of metabolism and in the present study) are greatest in the posterior cortex rather than around the focus is not clear.

Correlation between IAP and HMPAO distribution

Effect of ^{99m}Tc on IAP films

Contamination of IAP films by ^{99m}Tc activity is very small. Over a period of 4 days ^{99m}Tc(half-life 6 hours) activity will fall to 0.000015 of original levels. By the time the area with the highest ^{99m}Tcactivity seen in this study was exposed on ^{14}C film, its activity was 0.00027uCi/g, a figure which continued to fall by half every 6 hours during the 2 weeks of exposure of ^{14}C films. This would result in a maximium of 0.12% contamination of the the low-flow area on an IAP film mentioned above.

Effect of ^{14}C activity on ^{99m}Tcfilms

If the concentration of ^{99m}Tc HMPAO is high in a given structure, and the ^{14}C IAP concentration low, then contamination will be small: maximal contamination will occur when the concentration of HMPAO is low and the concentration of IAP high. The maximum activity seen on the IAP films in the present study was 1130nCi/g, or 1.13μCi/g. The lowest activity seen on HMPAO fims was just over 2μCi/g. If the activities had been seen in the same structure, then ^{14}C contamination would have been responsible for 56.5% of the optic density of that area of the HMPAO film. In this event, the original discrepancy in uptake between the films would have remained obvious. In fact, the equivalent structure on HMPAO film to that with the highest activity on IAP films had an activity of 17.94μCi/g. The ^{14}C contamination of the HMPAO film in this structure was therefore 6.3%. In an area of low flow (left subcortical white matter in rat 2), the ^{14}C activity was 0.195μCi/g, and the ^{99m}Tc activity 3.64μCi/G. Contamination in this instance was 5.4%. One one would expect this to be the approximate level of contamination in all the animals in the present study, where the distribution of IAP and HMPAO was similar, with slightly lower figures at low flows resulting from relative underestimation of high flows by uncorrected ^{99m}Tc activities.

Pattern of HMPAO vs IAP distribution

The distribution of HMPAO as indicated by the autoradiographs was almost identical to that of IAP. The relatively high uptake seen in the choroid plexus was also described by

Bullock et al. (1991), who suggested it might be due either to the unusual absorption characteristics of the choroid or to an underestimation of blood flow by IAP. The fact that uptake of HMPAO also appeared to be relatively high where the section included 2 layers of pia suggests that increased uptake and/or retention in the pia was responsible. There is no obvious explanation for the difference seen in the supramammillary nucleus, but the difference in timing of the two measurements during an experiment during which little time was allowed for achievement of steady state might also be responsible for some differences between IAP and HMPAO films.

The relatively poor spatial resolution of some HMPAO films may have a technical explanation. From the difference in resolution of bubble artefact, it is clear that whatever factor was responsible operated after the preparation of the sections, i.e. post mortem. Since resolution of scratches was the same in both types of film, it is likely that the responsible factor operated before the stage of photography, suggesting either that redistribution of HMPAO carried on during exposure of the section (which seems unlikely) or a that there was a technical problem with the film itself or with the development process. The ^{3}H sensitive film used for HMPAO is more grainy than the film used for ^{14}C, and this may have contributed to the effect.

Correlation between blood flow as calculated by the IAP method and HMPAO concentration

The main aim of this series of experiments was to test the correspondence between IAP-determined cerebral perfusion and HMPAO concentration at the high flows seen during seizures. The penicillin model produced some very high flows indeed in individual rats. In all the animals, the linearity of the relationship between rCBF and HMPAO (as indicated by ^{99m}Tc activity) was improved, in most cases to a relationship approximating to a straight line. In 2 animals (4 and 8) the statistical programme produced a hyperbolic curve, although the degree of curve was relatively small, and the relationship did not deviate significantly from a straight line.

The uncorrected curve fitted to the data for rats 1,6 and 7 were parabolic, showing fall off above flows of 250, 400 and 450ml/100g/min, respectively. Were this to be a real phenomenon, it would have serious implications on the use of HMPAO as a cerebral perfusion tracer. As flow increases the concentration of HMPAO trapped in brain tissue after bolus injection will peak, and then fall as flow increases further. The same tissue concentration of HMPAO will therefore appear at two points on the curve, and may be indicative of either of two levels of perfusion. However, examination of the data points in

the uncorrected curves for rats 1,6 and 7 show no evidence of fall off, rather showing a flattening of the rate of rise, which the second order polynomial curve fitted by the statistical software used cannot accomodate.

The results therefore show that even without the Lassen correction, HMPAO concentrations increase with blood flow, even at flows of over 600ml/100g/min, albeit in a non linear fashion. After correction, the linearity of the relationship was preserved, even at the highest flows seen.

The closeness of the correlation is less than that found in a previous study. Bullock et al. (1991) found R^2 values of 0.84-0.93 using pooled data for a total of 11 rats, correlating flow as measured by IAP and HMPAO uptake in acute focal ischemia. Flows of up to just over 300ml/100g/min were seen. This compares with the range of R^2 0.74-0.94 for individual animals in the present study, where the range of flows was two times greater. The range of flows may have some bearing on this difference, as in most of the rats the spread of data became greater at high flows. This probably had two causes; the Lassen correction and the calculation of flow from IAP activity both tend to magnify small errors in densitometry as flows increase (Horton et al., 1980). The effect of the Lassen correction at high flows can clearly be seen by comparing uncorrected and corrected correlations with rCBF. Only in Rat 3, where relatively few high flows and Tc99m activities were seen, was the scatter of the data not increased (and R^2 reduced) by the application of the Lassen correction. This effect is exacerbated by the fact that the correction only operates over a limited range. The main determinant of this range is the reference value for blood flow that is chosen (see formula for the Lassen correction, introduction to this chapter). In this study, however, some seizure animals showed a very high range of flow, and the correction calculated by the function became vary large or negative. The function defined by the correction is plotted in Figure 4.1, and illustrates the effect.

The difference in timing of the two techniques may also be responsible. Although the rats were clinically in approximate steady state during the three minutes between HMPAO injection (necessary to allow completion of trapping, and therefore any washout effect) and the performance of the IAP procedure, it is possible that flows in some structures changed during this period. Perfusion changes during seizures take place over a time scale of seconds (Penfield, 1933; 1937; , Gibbs et al., 1946), and it is possible that such changes were of sufficient magnitude to affect the correlation between IAP and HMPAO uptake. Moreover, both groups of animals were recovering from anaesthetic during this period, and it is possible that changes in flow due to changing plasma and brain concentrations af anaesthetic agents may have occurred (see above).

Densitometry was performed on the same slices in IAP and HMPAO films. The point in each strucure at which the region of interest was placed was the same in each film (e.g. in the caudate nucleus 2/3 of the way laterally along a line bisecting the structure horizontally). Each structure was measured on three consecutive sections. These measures were designed to minimise the chance of any discrepancy between IAP and HMPAO films due to differences in region of interest positioning. In relatively large and homogenous structures such as the caudate nucleus, small changes in position of the region of interest will have had minimal effect. In very small structures such as the habenular nuclei, an effect of ROI positioning is difficult to rule out, and may have contributed to poor correlation between HMPAO and IAP uptake.

The uncorrected scatter diagrams were examined, and obvious outliers identified as follows:

Rat 1 amygdalar nucleus (L & R)
substantia nigra (R)

Rat 3 ventral thalamic nucleus (L)

Rat 4 hypothalamus (L & R)
hippocampus (L & R)

Rat 6 ventral thalamic nucleus (R)
lateral thalamic nucleus (L)

These outliers are all in relatively large structures, and mostly in non-seizure rats. Six of the 8 outliers in non-seizures rats were pairs of homotopic structures, suggesting a possible real change in perfusion of the structure between HMPAO and IAP injection, or some other structure-specific factor leading to a difference in uptake, in these cases at least.

If practice effects were responsible for scatter in the data, one would expect later experiments to show less scatter. There may be some effect of this. In chronological order, the R^2 values for the uncorrected data were 0.64, 0.67, 0.79, 0.67, 0.72, 0.87, 0.68, 0.84, 0.87, 0.84. There is some trend toward improvement in later experiments. Such an effect might operate at the stage of animal preparation (earlier animals took longer to cannulate and prepare, and it was more difficult to control their physiological parameters,

allowing variation between the HMPAO and IAP injections), performance of the IAP procedure (e.g. error in the timing of arterial samples), performance of the densitometry (e.g. error in positioning of regions of interest).

Conclusions

1. The pattern of change in cerebral perfusion seen in association with penicillin induced seizures is similar to the pattern of change seen in studies of local metabolic rate for glucose.
2. HMPAO and IAP distribute in the same manner in rats during penicillin seizures, with the exception that HMPAO is taken up into the choroid plexus and possibly in the pia mater to a greater degree.
3. ^{99m}Tc and ^{14}C activities correlate well, even in structures where blood flow is very high. Although uncorrected data showed a fall off in the rate of rise of ^{99m}Tc uptake vs IAP uptake, there was no evidence of reduction in HMPAO uptake at high flows. The results of this study therefore support the use of HMPAO as a cerebral perfusion tracer during seizures.
4. The Lassen correction improved the linearity of the relationship between HMPAO and IAP uptake in this study. Where the range of flow is high, however, small changes in optic density produce large and sometimes negative corrections, limiting the utility of the correction.

Appendix

Methods

^{99m}Tc as a radioisotopic marker

^{99m}Tc has a physical half life of 6 hours. It is produced as a pertechnetate from the decay of ^{99}Mo in commercially available generators. Because of its easy availability, and its predominant energy peak at 140keV in the gamma range, it is widely used for radioisotope imaging. The pertechenetate form does not pass the blood-brain barrier, and cannot therefore be used for imaging regional cerebral blood flow.

HMPAO as a radiochemical tracer of rCBF

HMPAO (hexamethylpropyleneamine oxime) is the result of an effort to develop a convenient tracer of rCBF which could be used with conventional rotating gamma cameras. The relatively long acquisition time of these instruments means that the ideal tracer for use with them should be lipophilic, with a high first-pass extraction across the blood brain barrier, and should be retained in the first pass pattern, in much the same way as microemboli. ^{123}I labelled tracers such as IMP and HIPDM (Holman et al., 1984) were originally developed, but these compounds had a relatively long uptake phase, and were unstable in the brain, allowing a degree of washout. ^{123}I, moreover, is costly and requires a cyclotron, limiting availability. Suitable ^{99m}Tc labelled compounds were therefore sought.

HMPAO was developed from PnAO, a lipophilic compound which distributed in brain according to rCBF with a high first-pass extraction, but which was not retained. HMPAO was produced by alkylating PnAO. The structure of the HMPAO molecule is shown in Fig 1. It is a neutral and lipophilic molecule, with meso and d,l diastereoisomeric forms, the *d,l* form being a recemic mixture of *d* and *l* enantiomers. The *d,l* form is less stable, and has a higher brain uptake and lower washout rate (Sharp et al 1986). The mechanism of the change from lipophilic to hydrophilic form remains uncertain, but may be related to interaction between the oxime groups of the HMPAO molecule and intracellular reducing agents such as glutathione. Neirinckx et al. (1988) showed that incubation with glutathione rapidly converted lipophilic HMPAO to the hydrophilic form, and that depletion of glutathione in brain homogenates reduced the rate of conversion. They also showed that *in vivo* retention of HMPAO in the brain, heart and liver matched well with retention predicted by glutathione concentrations, although measured and predicted values in the

lung matched less well. El Shibirny et al. (1989), however, found no correlation between glutathione concentration and HMPAO uptake in the rat.

^{99m}Tc HMPAO is obtained simply by mixing up to 1000MBq of ^{99m}Tc pertechnetate diluted in 5ml of saline with 0.5g of freeze dried *d,l* HMPAO (stored in a nitrogen-filled vial), and shaking for a few seconds. The percentage of total radioactivity in the lipophilic form (or radiochemical purity) is 88-92% immediately after reconstitution. The compound is unstable in the vial: conversion to hydrophilic forms takes place with a $T_{1/2}$ of 2-4 hours, so it is recommended that it is injected within 1 hour of mixing (in the present study, HMPAO was injected within 30 minutes of mixing). Radiochemical purity changes rapidly in saline and in blood: Lear (1988) found that this occurred so rapidly that by the time blood samples could be prepared for chromatography, most of the HMPAO was in hydrophilic form. The time curve of the conversion in blood appears to be complex, and may differ for *d* and *l* forms (Lassen et al., 1988). Because of this change in radiochemical purity, the *in vivo* curve for total reactivity and that for activity in the lipophilic fraction after IV injection are different. Andersen et al. (1988b) measured arterial input of lipophilic tracer to the brain using rapid octanol extraction of the lipophilic fraction, and found that while the lipophilic fraction constituted 75% of the total counts at the peak of the curve, it constituted only 23% 15s later. Despite the use of the rapid octanol technique for separating and measuring the lipophilic fraction, difficulty in determining the quantity of lipophilic HMPAO delivered to brain has remained a major problem in the development of a practical method for quantitating rCBF using HMPAO (absolute CBF for the whole brain has been measured (Andersen et al., 1988), but problems in measuring regional CBF include the variation in HMPAO extraction with flow, and scatter effects inherent in the SPECT method).

After intravenous injection HMPAO is distributed widely in body tissues, approximately 4% of the injected dose reaching the brain (Sharp et al., 1986; Neirinckx et al., 1988). In the head, there is uptake in the thyroid, nasal and oral mucosa, lacrymal glands and temporalis muscles (Andersen, 1989), all of which may be seen on brain SPECT images . Peak first-pass extraction of HMPAO was found to be 0.81 by Andersen et al. (1988a). Andersen et al. (1988c) measured the time course of externally detected head counts (Fig 4), finding at peak at 50s after IV injection. There was a (decay corrected) 20% decrease in activity over the subsequent 24 hours.

The kinetics of HMPAO can be described using the four compartment model (Fig 2) proposed by Neirinckx et al. (1988), and Lassen et al. (1988). A represents the amount of freely diffusible (lipophilic) HMPAO in blood, B represents the amount of freely diffusible (lipophilic) HMPAO in tissue, C represents the amount of trapped (hydrophilic) HMPAO in tissue, and D represents the amount of trapped (hydrophilic)

HMPAO in blood. The first-order rate constants k3 and k5 describe the conversion rate from lipophilic to hydrophilic HMPAO. The conversion is complete and irreversible, so effectively k4 and k6 = 0. K1 describes the clearance of HMPAO from blood to tissue. K1=EF, where F is blood flow (ml/g/min) and E is the first pass extraction from blood to brain. k2=K1/l=EF/l, where l is the tissue-blood partition coefficient of Kety.

Lassen et al. (1988) studied the comparison of rCBF, as measured using the Xe-133 intracarotid injection method, and counts recorded after intracarotid bolus injections ^{99m}Tc HMPAO in human volunteers. They used a three compartment model (Fig 3) to analyse the diffusion of HMPAO across the blood brain barrier, its uptake into brain tissue, its retention and its back-diffusion into blood. Compartment 1 is the lipophilic tracer in blood (measurements of radiochemical purity of the injected HMPAO were made using rapid thin layer chromatography - as the time between injection and arrival in brain was short, the activity peaking at 3-5s, it was assumed that it did not change significantly before arriving in brain), compartment 2 is the lipophilic tracer inside brain tissue, and compartment 3 is the hydrophilic HMPAO retained in brain. They found a steady state extraction (i.e. retention) of 0.38 $\pm$ 0.05, the plateau being reached after a rapid decline phase of 10-12s, followed by a slow decline phase of 2-4 min, to 40-50% of peak values. Decay-corrected losses after steady state had been reached were 0.5%/hour in 2 human subjects. They found that the retained fraction of HMPAO decreased linearly with increasing rCBF (R=-0.18F+0.5, where R is the retained fraction of lipophilic HMPAO and F is flow). From their data, they derived an equation to linearise the relationship between rCBF and ^{99m}TcHMPAO uptake :

$$f/fr=óxC/Cr)/(1+ó-Cr)$$

where f is the true CBF, C is the measured HMPAO uptake in the brain area of interest, and fr and Cr are the flow rate and measured ^{99m}Tc HMPAO concentration, respectively, in a reference region of the brain. The constant ó is the ratio of the rate of conversion to the rate of back-diffusion and clearance in the reference region Applied to images, the correction has the effect of slightly increasing the contrast between high and low flow regions, (Yonekura et al., 1988). The correction was not applied to images in this study. Since a non-linear colour scale was used for visual interpretation, the application of a linearising correction to images was considered spurious. It is likely that the effects of the non-linear relationship between rCBF and HMPAO uptake are seen to some degree in the ictal and postictal work presented in Chapter 3, where the ictal high-flow abnormalities seen may have been underestimated. Given that the relationship remains almost linear at flows of up to

200ml/100g/min (see Chapter 4), it is unlikely that the data in Chapter 2 (where almost exclusively low-flow abnormalities were identified) was significantly affected.

Single photon emission Tomography

The aim of emission tomography is to determine the three-dimensional distribution in space of a gamma-emitting radioisotope. For medical purposes, the space usually contains all or part of the body, and the information is usually produced as a visual image, generally of a slice of the structure imaged, of a given thickness in a given plane. This three-dimensional information is reconstructed by computer from a series of planar images taken from different angles by the imager. The mathematical principles used in this process have been known for a long time (Radon, 1917), but in practice, account has to be taken of the finite sampling and other physical characteristics of the devices used (Budinger, 1980). Kuhl et al., (1963) made the first attempts to produce tomographic cross sections of the body using radionuclides, and single rotating gamma camera systems were in use for brain imaging by the late seventies (Kuhl et al., 1975).

The SPECT imager usually consists of a large flat detector, behind a parallel-hole collimator (the 'head'). Very fine collimators improve spatial resolution, but reduce sensitivity. Multi-head instruments acquire more information during an acquisition of a given duration, allowing the use of a finer collimator without loss of sensitivity. This therefore produces images of better spatial resolution and contrast. Instruments with ring detectors and rotating annular collimators are also available. The majority of SPECT systems are single headed gamma cameras. The camera rotates around the head (Fig 5), stopping every few degrees, taking a series of images. The images are planar, and are of the sum of activity coming from the full thickness of brain, distributed in the plane of the detector. There are two types of technique for reconstructing a three-dimentsional data set from these series of planar images images; filtered back-projection and iterative reconstruction (Herman, 1980; Williams, 1985). The former technique is based on the projection of of pixel data onto the reconstruction image plane, followed by a filtering process to compensate for the blurring effect of back-projection, and statistical counting errors. The latter technique involves an initial estimate of the distribution of the data, followed by repeated back-projection and comparison with the previous estimate. The process stops when the differences between estimate and real data are within defined limits. Iterative techniques offer advantages where data is less complete and in image smoothness, although they require more computational power.

The SPECT imaging system used in the present study is dedicated to the imaging of the brain. Rather than producing the three-dimensional reconstruction from a series of planar images, it acquires a series of axial slices one after the other (Stoddart & Stoddart, 1979). The device comprises 12 large sodium iodide detectors spaced 30° apart in a ring round the head. Each detector has a point-focused collimator. The detector and collimator move rectilinearly (in 3 dimensions) during the acquisition of each slice (Fig 6), so that the focal point of the collimator scans through half the field of view, the opposite detector scanning the other half simultaneously. Each detector takes 128 measurements along 6 or 9 lines in its field of view, which is an 8x4xZ inch cube (Z being the axial dimentsion, which is adjustable)(Fig 7). The field of view of the entire system is taken to be a cylinder 8 inches in diameter, of variable height, and is therefore scanned by the focal points of the 12 detectors with 6-fold redundancy.

The system uses an iterative reconstruction algorithm (Stoddart & Stoddart, 1979; Moore & Mueller, 1986), which has to take into account the fact that photons coming from a direction described by any line passing through the focal point at an angle within the angular field of the collimator, will be included in the acquired information, and will contribute to image blurring (see point spread function of the detector, Fig 7). The algorithm can be simply summarised as follows:

1. Deblur raw data to determine the boundary ellipse (of the slice) to be used in the estimation and correction of attenuation (i.e. attenuation of radiation as it passes through tissue) effects.
2. Deblur again using filtration and attenuation correction derived from 1.
3. Reblur in a simulated scan, using the difference between the simulated and raw data to determine the error in the ability of the image to reproduce the raw data.
4. Repeat 2.

Usually 1-4 iterations are required before the raw data can be reproduced with acceptable accuracy from the simulated image.

The head is scanned in the axial plane for practical reasons. Slice thickness is 12mm, and sufficient contiguous 12mm slices are acquired to include the whole brain. These slices are then integrated into a three-dimensional representation of rCBF which can be sliced in any plane, with any degree of tilt. The FWHM of the system is 8.1mm at the centre of the field and 8.7mm 8cm from the centre.

Spatial resolution, contrast and partial volume effects

The spatial resolution of a SPECT system is empirically determined by placing a small diameter line source in the fields of the detector(s). The source is ideally infinitely small, but in practice should be small enough (commonly <1mm) as to appear as a point. A signal profile is drawn through the line source at right angles, and a Gaussian curve is obtained. The distance between the arms of the curve at half maximum signal (full width at half maximum - FWHM) is defined as the system spatial resolution. This distance defines the ability of the system to distinguish two point sources of the same signal strength, and to produce images with appropriate contrast and sharp boundaries between neighbouring structures of different signal. A structure of interest can be reconstructed if its size is greater than twice FWHM, assuming it is of similar signal to the surrounding tissues (structures with activity higher than the surrounding tissue are better distinguished - even a point source will be distinguished if it is of sufficiently high activity, albeit that its size will be overestimated). If the structure in question is smaller than 2 x FWHM, then the reconstructed volume will be different from the true volume (larger or smaller depending on whether its signal strength is higher or lower than surrounding tissues), and the difference between the activity concentration of the structure and its surroundings will be underestimated. This is termed the 'partial volume effect'.

The effect of scatter of emitted photons

A proportion of the photons emitted by a radioisotope will collide with particles in the matter through which it is travelling, and will be scattered. Such photons give false directional information, causing a loss of contrast. They have lower energy than their non-scattered counterparts, but filtration methods, including the use of asymmetric energy windows, are not yet adequate to compensate. Improvements in image quality have been reported using information acquired using a scatter energy window simultaneously with that acquired using a standard peak window. A proportion of the scatter data is subtracted from the peak window data (Koral et al., 1990). Systems incorporating scatter corrections are now becoming available, although their effectiveness has still to be shown, and scatter remains one of the problems with quantification of SPECT images.

Visual analysis of HMPAO SPECT images

Visual analysis of images is of necessity subjective. Where images are non-quantitative, estimates of normality or otherwise of the pattern of signal are based on the previous experience of the observers of both normal and abnormal images, and are made in the light of cerebral anatomy in general and of individual anatomy where it is known to be abnormal. In the present study, the SPECT images were all of sufficient spatial resolution to allow the observers to infer the anatomic location of parts of the image of interest from the known normal or individual anatomy, and the known normal pattern of rCBF. The reported localisation of abnormalities of rCBF in the present study is based on this type of inference. Reporting entailed the assumption that if the brain were divided into two areas, each with a different signal level, then it was the smaller area that was likely to be abnormal: e.g. when one temporal lobe had lower signal than the rest of the brain, it was assumed that it was the temporal lobe that was abnormal, not the rest of the brain.

As regards the presence or absence of abnormality (and its degree), three questions were asked;

1. Is the signal in a given area of the image the same as that in the homologous contralateral area, or is there a significant asymmetry?
2. Is the signal in a given area of the image in normal relationship to the signal levels in homolateral areas?
3. Can any abnormality seen be accounted for simply by the anatomy?

The question of limits of normal (in numeric terms) has been addressed in series of normal patients (see Chapter 2, p35). To gauge the practice of visual analysis adopted in the present study, the exercise described in Chapter 2 was carried out (see Chapter 2 Discussion, p71 & Fig 2.16). This experiment showed that, using the colour scale adopted in this study, the observers reported asymmetries of more that 8% as abnormal. However, factors other than simple asymmetry were taken into account by the observers: if an area of $2cm^2$ of the lateral temporal cortex had a signal level 5% less than the homotopic structure, and less than the surrounding cortex, then numeric analysis would regard the difference as being within normal limits. However, if the area had a sharply (taking account of the spatial resolution of the imager) delineated boundary, then the observer is likely to notice and report the feature as abnormal. In this event, the answer to Question 2 (above) is no. There is at present no generally available system of numeric analysis which can take this type of factor into account. This is probably why the experiment described in Chapter 2, in which the observers were asked to judge symmetry of signal only, yielded a limit of

normal close to that derived numerically in other studies, with almost no discrepant observations, whereas there were in practice a number of discrepancies between visual and numeric analysis in the present study.

As discussed in Chapter 2, the practice of reporting images by independent observers, followed by consensus conference when reports disagree is an accepted method of producing visual reports of images for scientific studies. Knowing only the diagnosis of epilepsy, each observer looks at the image and notes his interpretation of it. Once all the images have been seen by both observers, the reports are compared. Where reports agree, they are recorded as the result of visual analysis of the scan. Where reports disagree, the two obsevers then re-analyse the images together and produce a consensus report. The method has been largely used in SPECT studies in epilepsy (Rowe et al., 1989a;b;1991a;b; Newton et al., 1992; Lee et al., 1986; 1987a;b;1988; Shen et al., 1990). In the present work, 139 SPECT studies were reported. The blinded visual reports disagreed in 18 cases, in all of which the two observers had disagreed over whether an asymmetry was or was not within normal limits. All but one were finally reported as normal.

Numerical analysis of HMPAO SPECT images

In the present study, regions of interest were determined and measured as follows:

1. The anatomic structures of interest were identified on normal MRI images.

2. Using a normal image of rCBF acquired by the device used in the present study, the correspondence of these anatomic structures of interest with normal cortical and subcortical patterns of rCBF was established (the correspondence is close, and has been illustrated elsewhere (George et al., 1991)).

3. Regions of interest were drawn on those SPECT slices which displayed the anatomy of the structures to be analysed most clearly, and allowed a reasonably large ROI to be used so as to have the largest sample volume possible (in practice, transaxial temporal lobe slices in the case of temporal lobe ROIs, and orbitomeatal slices for other ROIs). ROIs were drawn such that as much of the structure as possible was included, but that the ROIs were sufficiently within the boundaries of that structure to minimise partial volume effects. To further increase sample size, double thickness slices were used.

4. The ROIs were placed on corresponding double thickness slices on patient images, according to the pattern of rCBF. ROI placement was symmetric, except where structural imaging had shown anatomic asymmetry, in which case the ROIs were placed with reference to the individual's structural image.

5. The counts for the defined volume of brain were measured, and were averaged over the area (and therefore the volume) of the ROI. This figure was used to calculate an asymmetry index as described in Chapter 2, Methods section.

This method of ROI placement with maximal sample size was designed to minimise variations in asymmetry index due to 'small volume' variations in rCBF and to variations in ROI placement. Smaller and more numerous ROIs might have detected changes in smaller volumes of brain, but would have produced data which was much more intrinsically variable. In addition, the procedure used for image analysis was time consuming - the inclusion of a large number of ROIs would have precluded a study including such a large number of patients, a fundamental requirement of the aims of the interictal study described in Chapter 2.

The variability of asymmetry index due to variations in ROI placement was studied by the author (who carried out all the numerical image analysis in this work). Two HMPAO SPECT studies (of patients who were not among those studied in this work) were selected, one of high quality and one of relatively poor quality, with a large low flow area (so that the effect on ROI placement of difficulty in perceiving cortical paterns of flow could be studied). The two scans were analysed using the same procedure as in the Chapters 2 and 3 on five separate occasions separated by one week. The results are shown in Table 1, with means, standard deviations, ranges and 95% confidence limits for each ROI.

Standard deviations and 95% confidence limits were larger for the poorer quality scan in all ROIs with the exception of the frontal ROI. Nonetheless, standard deviations were within 1% (i.e. one percentage unit of the asymmetry index) on both scans for all structures except the basal ganglia and thalamic ROIs. This was not surprising, as these were the smallest of the ROIs, and both areas were surrounded by areas of lower flow (particularly in the case of the basal ganglia ROI which was adjacent to periventricular white matter) so that one would expect small variations in placement to result in relatively larger variations in asymmetry index. With the exceptions of the basal ganglia and thalamic ROIs, 95% confidence limits of the measurements were within 5% in the first scan, and within 3% in the second. Rowe et al. (1991) measured five scans on 2 occasions separated by 2 weeks. They found that the asymmetry measurements differed by 1.5% $\pm$ 1.8% in the mesial temporal cortex, by 3.1% $\pm$ 5.9% in the anterolateral temporal cortex, and by 0.2% $\pm$ 2.5%

in the posterolateral temporal cortex. Repeating several analyses on only two occasions is probably not the most informative way to study variablity in ROI placement, nonetheless the figures presented here probably compare favourably rather than otherwise with those of Rowe et al. This may be because of the larger ROIs used in the present study, and the superior spatial resolution of the imager used (allowing more accurate and consistent placement of ROIs with respect to the anatomy as inferred from blood flow patterns).

The above exercise was carried one year after the image analysis in the main study. The operator had not used the same method of ROI placement in the meantime, so it is unlikely that a practice effect falsely improved the results of repeat analysis of SPECT images.

Figure 1

The chemical structure of ^{99m}Tc PnAO and ^{99m}Tc HMPAO (reproduced from Neirinckx et al., 1988)

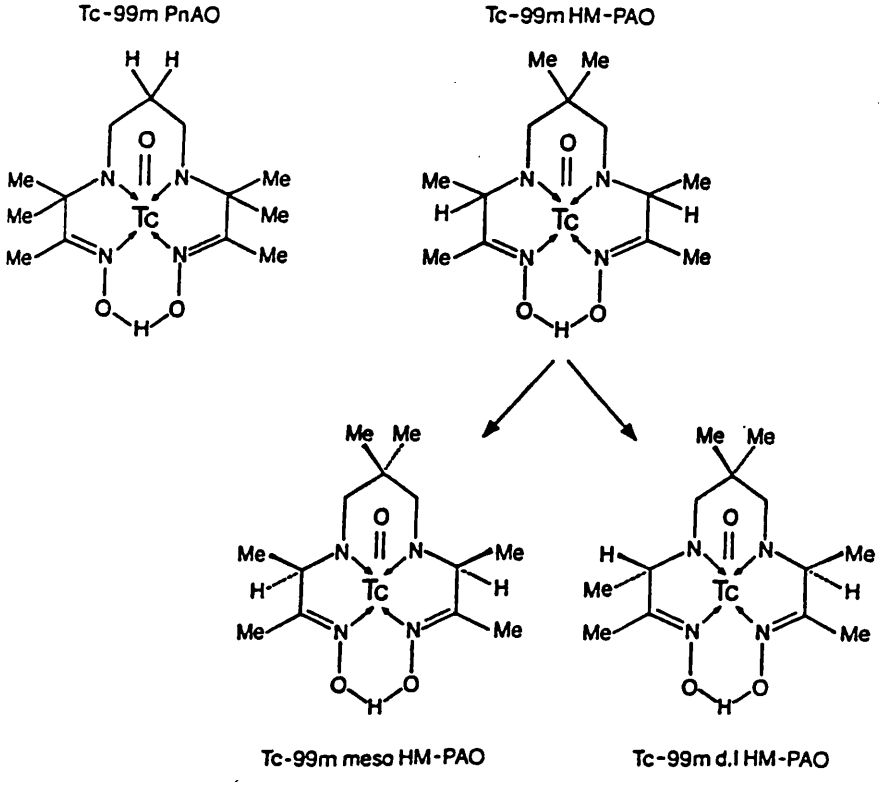

Figure 2

Four-compartmental model describing in vivo kinetics of ^{99m}Tc HMPAO, as proposed by Neirinckx et al., (1988) and Lassen et al. (1988)(reproduced from Neirinckx et al., 1988).

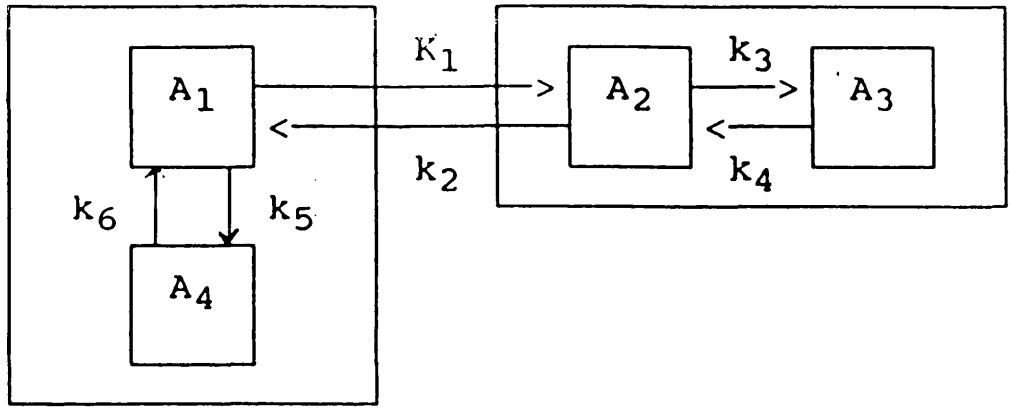

A = freely diffusible lipophilic complex in blood; B = freely diffusible lipophilic complex in tissue; C = nondiffusible, hydrophilic complex in tissue; D = nondiffusible hydrophilic complex in blood; K_1 = transfer of ^{99m}Tc from blood to tissue; K_2-K_6 = first order rate constants for the transfer of ^{99m}Tc HMPAO between compartments.

Figure 3

Three-compartment model used by Lassen et al. (1988) to describe the kinetics of ^{99m}Tc HMPAO after intracarotid bolus injection.

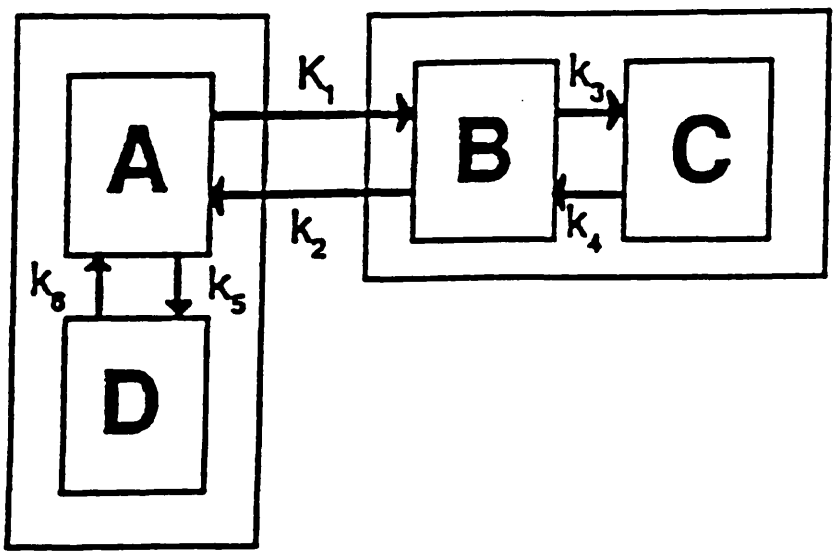

A1 = lipophilic ^{99m}Tc HMPAO in blood; A2 = lipophilic ^{99m}Tc HMPAO in brain tissue; A3 = hydrophilic ^{99m}Tc HMPAO retained in brain

Figure 4

Time course of 99mTc HMPAO uptake into brain after intravenous injection as assessed by externally detected head counts in man (reproduced from Andersen et al., 1988).

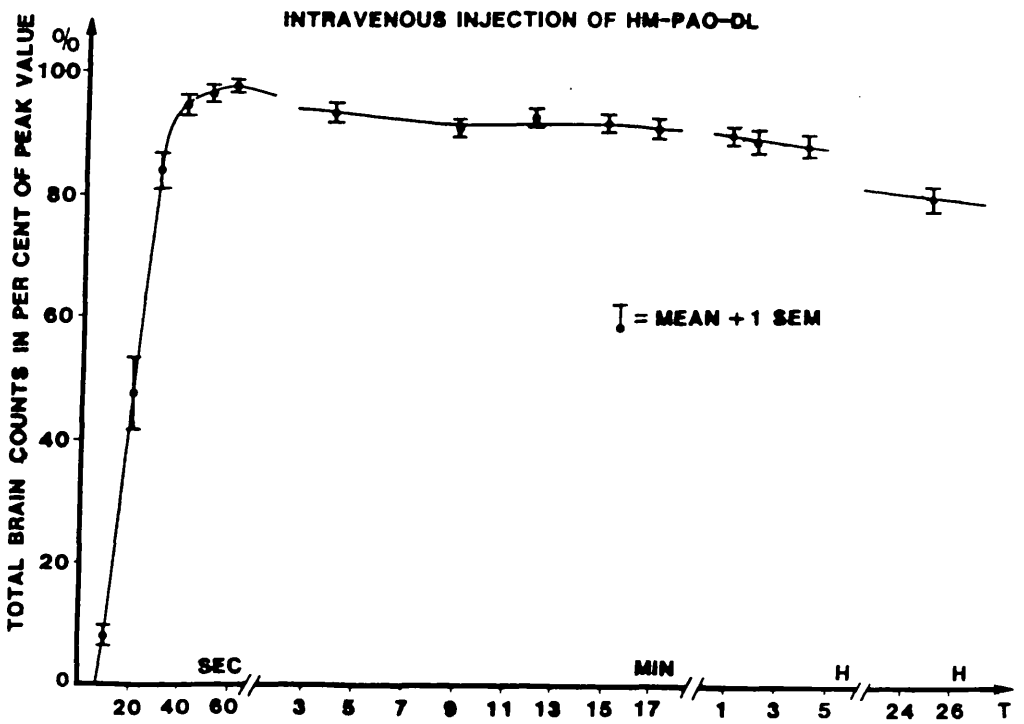

Figure 5

The functioning of a single head rotating gamma camera. In practice, commonly used acquisition protocols involve 64 images per study, with 30s acquisition time per image, and therefore a total acquisition time of 32 minutes. The entire study is acquired as a single unit.

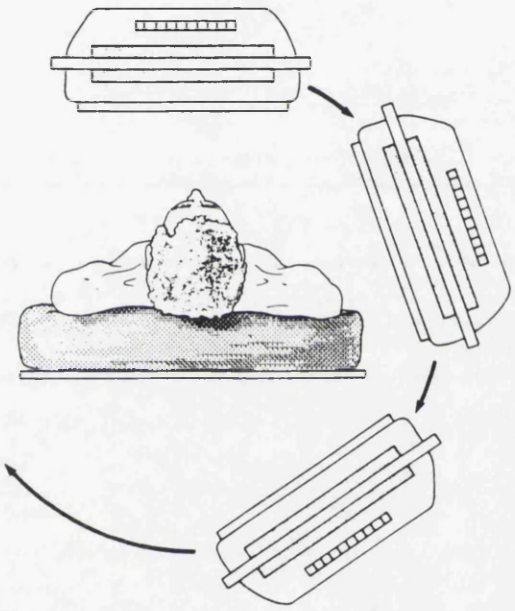

Figure 6

The functioning of the SME 810 mutidetector SPECT system. The detectors can scan 3, 6 or 9 lines during the 3 minute acquisition of each slice. The acquisition time varies from 30-60 minutes, depending on the protocol used. The study is acquired slice by slice, the patient being physically moved downward with respect to the plane of the detectors each time a slice is completed. The slices are combined to make up an image of the whole brain.

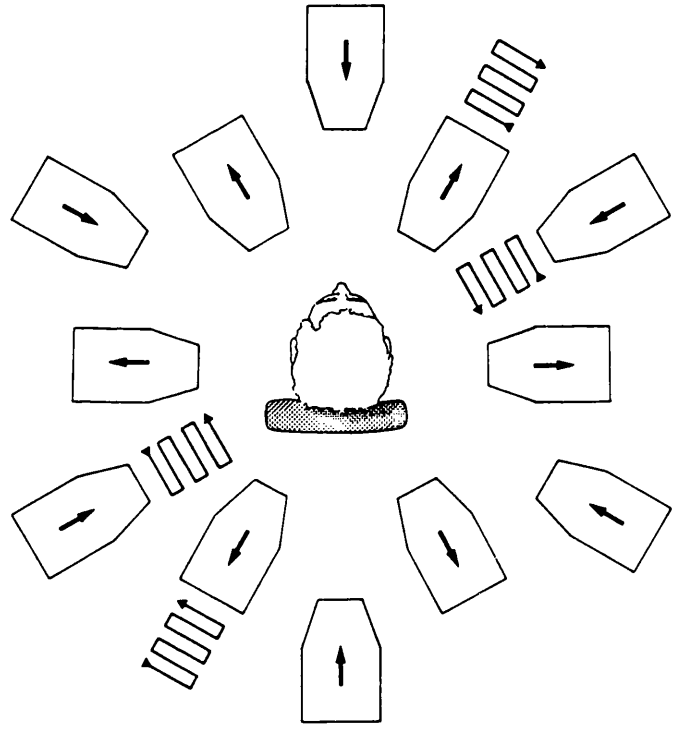

Figure 7

Diagramme of a detector and collimator from the imager used in the present study. The point spread function (PSF) is the volume taken into account by the reconstruction process (analogous to the optical concept of 'depth of focus' of a lens). The axial projection of the scan pattern of the detector is shown (u,v scan pattern) (reproduced from Stoddart & Stoddart, 1979).

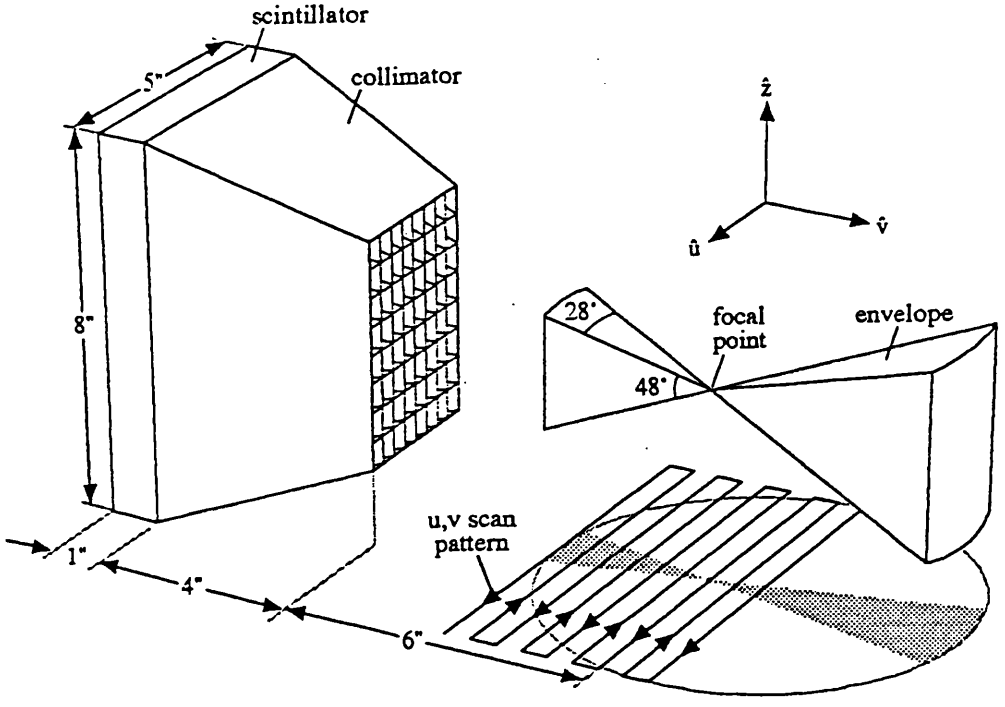

Appendix Table 1

Results of measurement of ROIs placed on 5 occasions 1 week apart

ROI Scan 1	Mean of 5 measurements (asymmetry index)	SD	Min	Max	95%CL+	95%CL-
Lat Temp	-32,15	0,81	-33,10	-30,98	-30,12	-34,186
Mes Temp	13,16	0,57	12,49	13,97	14,59	11,73
Occipital	-6,11	0,67	-6,99	-5,32	-4,45	-7,7804
Frontal	-11,84	0,26	-12,18	-11,54	-11,18	-12,492
Bas Gang	0,94	1,22	-0,79	2,31	4,00	-2,1127
Thalamus	4,33	1,28	2,50	6,04	7,52	1,1414
Parietal	-7,65	0,64	-8,37	-6,90	-6,04	-9,265
Scan 2						
Lat Temp	12,69	0,44	12,26	13,24	13,79	11,583
Mes Temp	-1,09	0,16	-1,31	-0,87	-0,70	-1,4851
Occipital	-0,73	0,43	-1,25	-0,10	0,38	-1,8394
Frontal	4,60	0,44	4,09	5,10	5,70	3,5095
Bas Gang	-10,24	1,15	-10,34	-7,33	-7,36	-13,115
Thalamus	12,89	1,33	10,88	14,13	16,23	9,5616
Parietal	10,69	0,39	10,34	11,29	11,67	9,7069

References

Abou Khalil BW, Siegel GJ, Sackellares JC, Gilman S, Hichwa R & Marshall R (1987)
Positron emission tomography studies of cerebral glucose metabolism in chronic partial epilepsy
Annals of Neurology, **22**, 480-486

Ackerman RF & Lear JL (1989)
Glycolysis induced discordance between glucose metabolic rates measured with radiolabelled fluorodeoxyglucose and glucose
Journal of Cerebral Blood Flow and Metabolism, **9**, 774-785

Alheid GF & Heimer L (1988)
New perspectives in basal forebrain organisation of special relevance for neuropsychiatric disorders: the striatopallidal, amygdaloid and corticopetal components of the substantia innominata
Neuroscience, **27**, 1039

Andersen AR, Friberg H, Knudsen GM (1988a)
Extraction of Tc99m D,L-HMPAO across the blood brain barrier
Journal of Cerebral Blood Flow and Metabolism, **8** (Suppl 1), S44-51

Andersen AR, Friberg H, Lassen NA, Kristensen K, Neirinckx R (1988b)
Assessment of the artererial input curve for Tc99m D,L-HMPAO by rapid octanol extraction
Journal of Cerebral Blood Flow and Metabolism, **8** (Suppl 1), S23-30

Andersen AR, Friberg H, Schmidt JF, Hasselbalch SG (1988c)
Quantitative measurements of cerebral blood flow using SPECT and Tc99m D,L-HMPAO compared to xenon-133
Journal of Cerebral Blood Flow and Metabolism, **8** (Suppl 1), S69-81

Andersen AR (1989)
^{99m}Tc-D,L-Hexamethylene-propyleneamine Oxime (^{99m}Tc-HMPAO): a basic kinetic studies of a tracer of cerebral blood flow
Cerebrovascular and Brain Metabolism Reviews, **1**, 288-318

Anonymous (1988)
Surgery for temporal lobe epilepsy
Lancet, **II**, 1115-1116

Armstead WM, Mirro R, Busija DW & Leffler CW (1989a)
Permissive role of prostanoids in acetylcholine induced cerebral cerebral vasoconstriction
Journal of Pharmacology and Experimental Therapeutics, **251**, 1012-1019

Armstead WM, Mirro R, Leffler CW & Busija DW (1989b)
Influence of endothelin on piglet cerebral microcirculation
American Journal of Physiology, **257**, H707-710

Ayala GF, Matsumoto H & Gumnit RJ (1970)
Excitability changes and inhibitory mechanisms in neocortical neurons during seizures
Journal of Neurophysiol, **33**, 73-85

Babb TL & Brown WJ (1986)
Neuronal dendritic and vascular profiles of human temporal lobe epilepsy correlated with cellular physiology in vivo
In: Basic mechanisms of the epilepsies; AV Delgado Escueta, AA Ward, DM Woodbury Eds.
Raven, New York

Baldy-Moulinier M (1990)
Partial epilepsy: ictal and interictal.
In: Handbook of Clinical Neurophysiology, vol 4, pp 291-310. Ed JA Wada
Elsevier, Amsterdam

Bancaud J & Talairach J (1992)
In:P Chauvel, AV Delgado Escueta, E Halgren, JournalBancaud, eds. Frontal lobe epilepsies and seizures. Advances in neurology, Vol 57, pp3-58.
New York, Raven

Berkovic SF, Newton MR & Rowe CC (1991)
In: Epilepsy surgery, pp 251-256. Ed. H Luders
Raven Press, New York

Bernardi S, Trimble MR, Frackowiak RSJ, Wise RJS & Jones T (1983)
An interictal study of partial epilepsy using positron emission tomography and the oxygen-15 inhalation technique
Journal of Neurology Neurosurgery and Psychiatry,**46**, 473-477

Bevan JA (1987)
A comparison of the contractile response of the rabbit pulmonary and basilar arteries to sympathomimetic agonists. Further evidence for variation in vascular adrenoceptor characteristics
Journal of Pharmacology and Experimental Therapeutics, **216**, 83-89

Biersack HJ, Stefan H & Reichman K (1986)
Brain imaging with 99mTc-HMPAO SPECT, CT and NMR - results in epilepsy
Journal of Nuclear Medicine **27**, 1028

Binnie CD (1990)
Generalised epilepsy: ictal and interictal.
In: JA Wada, ed., Handbook of Clinical Neurophysiology, vol 4.
Elsevier, Amsterdam: pp263-290

Blackwood DHR, Kapoor V & Martin MJ (1981)
Regional changes in cerebral glucose utilization associated with amygdaloid kindling and electroshock in the rat
Brain Research, **224**, 204-208

Bonte FJ, Devous MD, Stokely EM & Homan RW (1983)
Single photon tomographic determination of regional cerebral blood flow in epilepsy
American Journal of Neuroradiology, **4**, 544-546

Bonte FJ, Stokely EM, Devous MD & Homan RW (1983)
Single photon tomographic study of regional cerebral blood flow in epilepsy. A preliminary report
Archives of Neurology, **40**, 267-270

Brodersen P, Paulson OB, Bolvig TG, Rogon ZE, Rafaelson OJ & Lassen NA (1973)
Cerebral hyperemia in electrically induced epileptic seizures
Archives of Neurology, **8**, 334-338

Budinger TF (1980)
Physical attributes of single-photon tomography
Journal of Nuclear Medicine, **21**, 579-592

Bullock R, Patterson J & Park C (1991)
Evaluation of 99mTc-hexamethylpropyleneamine Oxime cerebral blood flow mapping after acute focal ischaemia in rats
Stroke, **22**, 1284-1290

Collins RC (1976)
Metabolic response to focal penicilin seizures in rat: spike discharge vs. afterdischarge
Journal of Neurochemistry, **27**, 1473-1482

Collins RC (1978a)
Use of cortical circuits during focal penicillin seizures: an autoradiographic study with (14C) deoxyglucose
Brain Research, **150**, 487-501

Collins RC (1978b)
Kindling of neuroanatomic pathways during recurrent focal penicillin seizures
Brain Research, **150**, 503-517

Collins RC, Kennedy C, Sokoloff L & Plum F (1976)
Metabolic anatomy of focal motor seizures
Archives of Neurology, **33**, 536-542

Collins RC, Tearse RG & Lothman EW (1983)
Functional anatomy of limbic seizures: focal discharges from medial entorrhinal cortex in rat
Brain Research, **280**, 25-40

Cooper A (1836)
Some experiments and observations on tying the carotid and vertebral arteries, and the pheumogastric, phrenic and sympathetic nerves
Guys Hospital Report, **1**, 457

Corsellis JAN & Meldrum BS (1976)
The pathology of epilepsy
In: Greenfields Neuropathology, 3d Ed., Eds. W Blackwood & JAN Corsellis, pp771-795
London, Arnold

Costa DC, Ell PJ, Cullum ID & Jarrett PH (1986)
The in vivo distribution of 99Tcm HMPAO in normal man
Nuclear Medicine Communication, **7**, 647-658

Costa DC, Jones BE, Steiner TJ, Aspey BS, Ell PJ, Cullum ID & Jewkes RF (1987)
Relative 99mTc HMPAO and 113Sn microspheres distribution in dog brain
Nuklearmedizin, suppl 23:498-500

Costa DC, Lui D, Sinha AK, Jarritt PH & Ell PJ (1989)
Intracellular localisation of 99Tcm-d,l-HMPAO and 201Tl-DDC in rat brain
Nuclear Medicine Communications, **10**, 459-466

Davies PW & Remond A (1947)
Oxygen consumption of the cat during metrazol convulsions in the dog
Research Publication of the Association of Nervous and Mental Disease, **26**, 184

Davis EW, McCulloch WS & Roseman E (1944)
Rapid changes in the O2 tension of cerebral cortex during induced convulsions
American Journal of Psychiatry, **100**, 825

Delgado-Escuate AV & Greenberg D (1984)
The search for epilepsies ideal for clinical and molecular genetic studies
Annals of Neurology,**16** (suppl), S1-11

DiChiro G & Brooks, RA (1988)
PET quantitation: blessing and curse
Journal of Nuclear Medicine, **29**, 1603-1604

Duckles SP & Said SI (1982)
Vasoactive intestinal peptide as a neurotransmitter in the cerebral circulation Eur Journal of Pharmacology, **78**, 371-374

Duncan R, Patterson J, Bone I, Wyper DJ & McGeorge AP (1990a)
Tc99m HMPAO single photon emission computed tomography in temporal lobe epilepsy
Acta Neurologica Scandinavica, **81**, 287-293

Duncan R, Patterson J, Hadley DM & Bone I (1990b)
Unilateral cerebellar atrophy in focal epilepsy
Journal of Neurology Neurosurgery and Psychiatry, **53**, 436-437

Duncan R, Patterson J, Hadley DM, Bone I & Wyper D (1990c)
SPECT in temporal lobe epilepsy: ictal and interictal studies
In: Eds Baldy Moulinier M, Lassen N, Engel J, Askienazy S. Current problems in epilepsy, Vol 6, pp79-96
London:Libbey

Duncan R, Patterson J, Hadley DM, Macpherson P, Brodie MJ, Bone I, McGeorge AP & Wyper DJ (1990d)
CT, MR and SPECT imaging in temporal lobe epilepsy
Journal of Neurology Neurosurgery and Psychiatry, **53**, 11-15

Duncan S, Gillan J, Duncan R & Brodie M (1992)
Interictal HMPAO SPECT: a routine investigation in medically intractable complex partial epilepsy?
Epilepsy Research, **13**, 83-87

Dymond AM & Crandall PH (1976)
Oxygen availablility and blood flow in the temporal lobe during spotaneous epileptic seizures in man
Brain Research, **103**, 191-196

Edvinsson L (1975)
Neurogenic mechanisms in the cerebral circulation
Acta Physiolica Scandinavica, **427** (suppl), 1-35

Edvinsson L, Copeland JR, Emson PC, McCulloch J & Uddman R (1987)
Nerve fibres containing neuropeptide Y in the crrebrovascular bed:
immunocytochemistry, radioimmunoassay, and vasomotor effects.
Journal of Cerebral Blood Flow and Metabolism, **7**, 45-47

Edvinsson L, Fahrenkrug J, Hanko J, Owman C, Sundler F & Uddman R (1980)
VIP (vasoactive intestinal polypeptide)-containing nerves of intracranial arteries in mammals
Cell and Tissue Research, **208**, 135-142

Edvinsson L, MacKenzie ET & McCulloch J (1993a)
Energy generation in the central nervous system. In: Cerebral blood flow and metabolism, pp153-158.
New York: Raven Press

Edvinsson L, MacKenzie ET & McCulloch J (1993b)
Arterial gas tensions. In: Cerebral blood flow and metabolism, pp524-552.
New York: Raven Press

Edvinsson L, MacKenzie ET & McCulloch J (1993c)
Anaesthetic agents. In: Cerebral blood flow and metabolism, pp403-420.
New York: Raven Press

Edvinnson L, Owman C & West KA (1971)
Changes in continuously recorded inracranial pressure of conscious rabbits at different time periods after superior cervical sympathectomy
Acta Physiolica Scandinavica, **83**, 42-50

El-Shibirny AM, Sadel S, Owunwanne A, Yacoub T Suresh L & Abdel-Dayem HM (1989)
Is 99mTc HMPAO uptake in tissues related to glutathione cellular content?
Nucl Med Commun, **10**, 905-911

Engel J (1984)
The use of positron emission tomographic scanning in epilepsy
Annals of Neurology, **15** (suppl), S180-191

Engel J (1983)
Metabolic patterns of human epilepsy: possible physiological correlates of clinical aberrations
In: Eds. Baldy Moulinier M, Ingvar DH, Meldrum BS. Current problems in epilepsy pp6-18.
London: John Libbey

Engel J, Brown WJ, Kuhl DE, Phelps ME, Mazziotta JC & Crandall PH (1982a)
Pathological findings underlying focal temporal lobe hypometabolism in partial epilepsy
Annals of Neurology, **12**, 518-528

Engel J, Henry TR, Risinger MW, Mazziotta JC, Sutherling WW & Phelps ME (1990)
Presurgical evaluation for partial epilepsy: relative contributions of chronic depth electrode recordings versus FDG-PET and scalp-sphenoidal ictal EEG
Neurology, **40**, 1670-1677

Engel J, Kuhl D & Phelps ME (1982b)
Patterns of human local cerebral glucose metabolism during epileptic seizures
Science, **218**, 64-66

Engel J, Kuhl DE & Phelps ME (1983)
Regional brain metabolism during seizures in humans
In: Advances in neurology, pp 141-148. Vol 34. Eds. Delgado-Escueta AV, Wasterlain CG, Treiman EM and Porter RJ
New York: Raven Press

Engel J, Kuhl DE, Phelps ME & Crandall PH (1982c)
Comparative localisation of epileptic foci in partial epilepsy by PCT and EEG
Annals of Neurology, **12**, 529-537

Engel J, Kuhl DE, Phelps ME & Mazziotta JC (1982d)
Interictal cerebral glucose metabolism an partial epilepsy and its relation to EEG changes
Annals of Neurology, **12**, 510-517

Engel J, Lubens P, Kuhl DE & Phelps ME (1985)
Local cerebral metabolic rate for glucose during petit mal absences
Annals of Neurology, **17**, 121-128

Evans MC & Meldrum BS (1984)
Regional brain glucose metabolism in chemically induced seizures in the rat
Brain Research, **297**, 235-245

Faraci FM (1989)
Effects of endothelin and vasopressin on cerebral blood vessels
American Journal of Physiology, **257**, H1511-1517

Fish DR, Lewis TT, Brooks DJ, Zilkha E, Wise RJS & Kendall BE (1987)
Regional cerebral blood flow of patients with focal epilepsy studied using xenon enhanced CT brain scanning
Journal of Neurology Neurosurgery and Psychiatry, **50**, 1584-1588

Folkow B (1964)
Description of the myogenic hypothesis
Circulation Research, **15** (suppl 1), 279-287

Fox PT & Raichle ME (1986)
Focal physiological uncoupling of cerebral blood flow and oxidative metabolism during somatosensory stimulation in human subjects
Proceedings of the National Academy of Sciences, **83**, 1140-1144

Franck G, Sadzot B & Salmon E (1986)
Regional cerebral blood flow and metabolic rates in human focal epilepsy and status epilepticus
In: Delgado-Escueta et al., eds. Advances in neurology pp 935-948.
New York: Raven Press

Furchgott RF, Cherry PD, Zawadski JV & Jothianandan D (1984)
Endothelial cells as mediators of vasodilatation in arteries
Journal of Cardiovascular Pharmacology, **6** (suppl 2), S336-343

George MS, Ring H, Costa DC, Ell PJ, Kouris K, Jarritt PH (1991)
In: Neuroactivation and neuroimaging with SPET
Springer-Verlag, London: pp51-57

Gibbs EL, Gibbs FA, Hayne R & Maxwell H (1946)
Cerebral blood flow in epilepsy
Association for Research Nervous and Mental Disease Proceedings, **26**, 131

Gibbs FA, Lennnox WG & Gibbs EL (1934)
Cerebral blood flow preceding and accompanying seizures in man
Archives of Neurology and Psychiatry, **32**, 257-272

Goadsby PJ & Duckworth JW (1987)
Effect of stimulation of trigeminal ganglion on regional cerebral blood flow in cats
American Journal of Physiology, **253**, R270-274

Goldstein LH & Polkey CE (1993)
Short term cognitive changes after unilateral temporal lobectomy or
amygdalohippocampectomy for the relief of temporal lobe epilepsy
Journal of Neurology Neurosurgery and Psychiatry, **56**, 135-140

Gotman J (1991)
Relationship between interictal spiking and seizures: human and experimental evidence
Canadian Journal of Neurological Science, **18**, 573-576

Grant FC, Spitz EB, Shenkin HA, Schmidt CF & Kety SS (1947)
The cerebral blood flow and metabolism in idiopathic epilepsy
Transactions of the American Neurological Association, **72**, 82-87

Grasso E, Ambrogio L, Cognazzo A, Gerbino-Promis PC, Zagnoni P, Cammuzzini GF, Papaleo A, Acchiardi F & Perno G (1989)
Single photon emission computed tomography with 99mTc HMPAO in the study of focal epilepsy
Italian Journal of Neurological Science, **10**, 175-179

Greenamyre JT (1986)
The role of glutamate in neurotransmission and in neurologic disease
Archives of Neurology, **43**, 1058-1063

Gumnit RJ & Takahashi T (1975)
Changes in direct current activity during experimental focal seizures
Electroencephalography and Clinical Neurophysiology, **19**, 63-74

Gurdjian ES, Webster JE & Stone WE (1947)
Cerebral metabolism in metrazol convulsion in the dog
Research Publication of the Association for Nervous and Mental Disease, **26**, 184-204

Hara H, Hamill GS & Jacobovitz DM (1985)
Origin of cholinergic nerves to the rat major cerebral arteries: coexistence with vasoactive intestinal polypeptide
Brain Research Bulletin, **14**, 179-188

Harder DR (1984)
Pressure-dependent membrane depolarisation in cat middle cerebral artery
Circulation Research, **55**, 197-202

Harder DR & Lombard JM (1985)
Voltage dependant mechanisms of receptor stimulation in cerebral arterial muscle
In: Bevan JA, Godfraind T, Maxwell RA, Stoclet JA, Worcel M, eds. Vascular neuroeffector mechanisms pp181-186.
Amsterdam: Elsevier

Harper AM, Desmuckh VD, Rowan JO & Jeanett WB (1972)
The influence of sympathetic nervous activity on cerebral blood flow
Archives of Neurology, **27**, 1-6

Hauser WA & Kurland LT (1975)
The epidemiology of epilepsy in Rochester Minnesota, 1935 through 1967
Epilepsia, **16**, 1-66

Heiss WD, Herholz K, Podreka I, Neubauer I & Pietryzyk U (1990)
Comparison of [99mTc] HMPAO SPECT with [18F]Fluoromethane PET in cerebraovascular disease
Journal of Cerebral Blood Flow and Metabolism, **10**, 687-697

Henry TR, Mazziotta JC, Engel J, Christensen PD, Zhang JX, Phelps ME & Kuhl DE (1990)
Quantifying interictal metabolic activity in human temporal lobe epilepsy
Journal of Cerebral Blood Flow and Metabolism, **10**, 748-757

Herman GT (1980)
Image reconstruction from projections: the fundamentals of computerised tomography
Academic Press, London

Holman BL, Lee RGL, Hill TC, Lovett RD & Lister-James J (1984)
A comparison of two cerebral perfusion tracers. N-Isopropyl I-123 piodoamphetamine and I-123 HIPDM, in the human
Journal of Nuclear Medicine, **25**, 25-30

Homan RW, Paulman RG, Devous MD, Walker P, Jennings LW & Bonte FJ (1989)
Cognitive function and regional cerebral blood flow in partial seizures
Archives of Neurology, **46**, 964-970

Horton RW, Meldrum BS, Pedley TA & McWilliam JR (1980)
Regional cerebral blood flow in the rat during prolonged seizure activity
Brain Research, **192**, 399-412

Hougaard K, Oikawa T, Sveinsdottir E, Skinhoj E, Ingvar DH & Lassen NA (1976)
Regional cerebral blood flow in focal cortical epilepsy
Archives of Neurology, **33**, 527-535

Iadecola C, Nakai M, Arbit E & Reis DJ (1983)
Global cerebral vasodilatation elicited by focal electrical stimulation within the dorsal medullary reticular formation in anaesthetised rat
Journal of Cerebral Blood Flow and Metabolism, **3**, 270-279

Ingvar M (1986)
Cerebral blood flow and metabolic rate during seizures
Annals of the New York Academy of Science, **462**, 194-206

Ingvar M & Siesjo BK (1983)
Local blood flow and glucose consumption in the rat brain during sustained bicuculine induced seizures
Acta Neurologica Scandinavica, **68**, 129-144

Ingvar M, Soderfeldt B, Folbergrova J, Kalimo H, Olsson Y & Siesjo BJ (1984)
Metabolic, circulatory and structural alterations in the rat brain induced by sustained pentylenetetrazol seizures
Epilepsia, **25**, 191-204

Inugami A, Kanno I, Uemura K, Shishido F, Murakami M, Tomura N, Fijita H & Higano S (1988)
Linearisation correction of 99m Tc labelled HMPAO image in terms of regionalCBF distribution: Comparison to C15 O2 inhalation steady state method measured by positron emission tomography.
Journal of Cerebral Blood Flow and Metabolism, **8**, S52-S60

Ishitsuka T, Underwood MD, Iadecola C & Reis DJ (1984)
Bilateral lesions of nucleus tractus solitarii abolishes cerebral vascular autoregulation independently of associated hypertension
Federation Proceedings, **43**, 305

Jackson JH (1890)
The Lumleian lectures on convulsive seizures
British Medical Journal, **1**, 765-771

Jasper H & Erickson TC (1941)
Cerebral blood flow and pH in excessive cortical discharge induced by metrazol and electrical stimulation
Journal of Neurophysiology, **4**, 333-347

Jibiki I, Kubota T, Fujimoto K, Yamaguchi N, Matsuda H, Tsuji S & Hisada K (1990)
High reproducibility of regional abnormalities on interictal 123I-IMP SPECT brain scans on patients with partial epilepsy
European Archives of Psychiatric and Neurological Sciences, **240**, 5-8

Johnston D & Brown TH (1984)
The synaptic nature of the paroxysmal depolarisation shift in hippocampal neurones
Annals of Neurology, **16** (suppl), S65-71

Kennedy C, Anderson W & Sokoloff L (1958)
Cerebral blood flow in epileptic children during the interseizure period
Neurology, **1**, 100-105

Kety SS (1951)
The theory and applications of the exchange of inert gas at the lungs and tissues
Pharmacological Reviews, **3**, 1-4

Kety SS, Woodford RB, Harmel MH, Freyham FA, Appel KE & Schmidt CF (1948)
Cerebral blood flow and metabolism in schitzophrenia. The effects of barbiturate semi-narcosis, insulin coma and electroshock
American Journal of Psychiatry, **104**, 765-770

Koral KF, Swailem FM, Buchbinder etal (1990)
SPECT dual-energy window Compton correction: scatter multiplier required for quantification
Journal of Nuclear Medicine, **31**, 90-98

Kuchinsky W (1987)
Coupling of function, metabolism and blood flow in the brain
Physiological Reviews, **2**, 217-220

Kuchinsky W & Wahl M (1978)
Local chemical and neurogenic regulation of cerebral vascular resistence
Physiological Reviews, **58**, 656-689

Kuhl DE, Alavi A, Reivich M (1975) et al
Computerised emission transaxial tomography and determination of local brain function
In: DeBlanc HJ, Sorensen JA (eds) Noninvasive brain imaging.
Society of Nuclear Medicine, New York: pp 67-79

Kuhl DE, Edwards RQ (1963)
Image separation in radioisotope scanning
Radiology, **80**, 653-661

Kuhl DE, Engel J, Phelps ME & Selin C (1980)
Epileptic patterns of locla cerebral metabolism and perfusion in humans determined by emission compiuted tomography of 18FDG and 13NH3
Annals of Neurology, **8**, 348-360

Lance JW, Adams RW & Lambert GA (1986)
Bulbo-cortical pathways and their possible relevance to migraine and epilepsy
Functional Neurology, **1**, 357-361

Lassen NA, Andersen AR, Friberg L, Paulson OB (1988)
The retention of [^{99m}Tc]-*d,l*-HM-PAO in the human brain after intracarotid bolus injection: a kinetic analysis
Journal of Cerebral Blood Flow and Metabolism, **8** (Suppl 1), S13-22

Lassen NA, Andersen AR, Freiberg L & Paulson OB (1988)
The retention of 99m Tc/DL HMPAO in human brain after intracarotid bolus injection: A kinetic analysis
Journal of Cerebral Blood Flow and Metabolism, **8**, S13-S22

Latack JT, Abou-Khalil BW, Siegel GJ, Sackellares JC, Gabrielsen T & Aisen AM (1986)
Patients with partial seizures: evaluation by MR, CT and PET imaging
Radiology, **159**, 159-163

Lavy S, Melamed E, Portnoy Z & Carmon A (1976)
Interictal regional cerebral blood flow in patients with partial seizures
Neurology, **26**, 418-422

Lear JL (1988a)
Quantitative local blood flow measurements with 99m Tc HMPAO: evaluation using multiple radionuclide digital quantitative autoradiography
Journal of Nuclear Medicine, **29**, 1387-1392

Lear JL (1988b)
Initial cerebral HM-PAO distribution compared to LCBF: use of a model which considers cerebral HM-PAO trapping kinetics
Journal of Cerebral Blood Flow and Metabolism, **8** (Suppl 1), S31-37

Lee BI, Markand ON, Siddiqui AR, Park HM, Mock B, Wellman HN, Worth RM & Edwards MD (1986)
Single photon emission computed tomography (SPECT) brain imaging using N,N,N'-trimethyl-N'-(2 hydroxy-3-methyl-5-123I-iodobenzyl)-1,3-propanediamine 2 HCl (HIPDM): intractable complex partial seizures
Neurology, **36**, 1471-147

Lee BI, Markand ON, Wellman HN, Siddiqui AR, Park HM, Mock B, Krepshaw J & Kung H (1987a)
HIPDM single photon emission computed tomography brain imaging in partial onset secondary generalised tonic-clonic seizures
Epilepsia, **28**, 305-311

Lee BI, Markand ON, Wellman HN, Siddiqui AR, Park HM, Mock B, Krepshaw J & Kung H (1987b)
HIPDM single photon emission computed tomography brain imaging in
partial onset secondary generalised tonic-clonic seizures
Epilepsia, **28**, 305-311

Lee BI, Markand ON, Wellman HN, Siddiqui AR, Park HM, Mock B, Worth RM, Edwards MK & Krepshaw J (1988)
HIPDM SPECT in patients with medically intractable complex partial seizures
Archives of Neurology, **45**, 397-402

Leib JP, Engel J, Gevins A & Crandall PH (1981)
Surface and deep EEG correlates of surgical outcome in temporal lobe epilepsy
Epilepsia, **22**, 515-538

Leiderman D, Balish M, Bromfield E, Sato S & Theodore WH (1989)
Comparison of interictal FDG and ^{15}O H_2O PET scanning in aptients with uncontrolled complex partial seizures
Neurology, **39** (suppl 1), 301

Leifer D, Cole DG & Kowall NW (1991)
Neuropathological asymmetries in the brain of a patient with unilateral
status epilepticus
Journal of Neurolological Science, **103**, 127-135

Leninger-Follett E (1984)
Mechanisms of regulation of cerebral microflow during bicuculine induced seizures in anaesthetised cats
Journal of Cerebral Blood Flow and Metabolism, 4, 150-165

Lothman EW & Collins RC (1981)
Kainic acid induced limbic seizures: metabolic, behavioural, electroencephalographic and neuropathological correlates
Brain Research, **218**, 299-318

Lothman EW, Hatlelid JM & Zorumski CF (1985)
Functional mapping of limbic seizures originating in the hippocampus: a combined deoxyglucose and electrophysiologic study
Brain Research, **360**, 92-100

Lou HC, Edvinsson L & MacKenzie ET (1987)
The concept of coupling blood flow to, brain function: revision required?
Annals of Neurology, **22**, 289-297

Margerison JH & Corsellis JAN (1966)
Epilepsy and the temporal lobes: a clinicalm electroencephalographic and neuropathological study of the brain in epilepsy, with particular reference to the temporal lobes
Brain, **89**, 499-530

Marks DA, Katz A, Hoffer P & Spencer SS (1992)
Localisation of extratemporal epileptic foci during ictal single photon emission computed tomography
Annals of Neurology, **31**, 250-255

Marshall JJ & Kontos HA (1990)
Endothelium-derived relaxing factors. A perspective from in vivo data.
Hypertension, **16**, 371-386

Mazziotta JC & Engel J (1984)
The use and impact of positron computed tomography scanning in epilepsy
Epilepsia, **25** (suppl. 2), S86-104

McCulloch J, Kelly PAT & Ford I (1982a)
Effect of apomorphine on the relationship between local cerebral glucose utilisation and local cerebral blood flow (with an appendix on its statistical analysis
Journal of Cerebral Blood Flow and Metabolism, **2**, 487-499

McCulloch J, Kelly PAT, Grome JJ & Pickard JD (1982b)
Local cerebral circulatory and metabolic effects of indomethacin
American Journal of Physiology, **243**, H416-H423

McHenry JL, West JW, Cooper ES, Goldberg HI & Jaffe ME (1974)
Cerebral autoregulation in man
Stroke, **5**, 695-705

McKee JC, Denn MJ & Stone HL (1976)
Neurogenic cerebral vasodilatation from electrical stimulation of the cerebellum in the monkey
Stroke, **7**, 179-186

MacKenzie ET, Farrar JK, Fitch W, Graham DI, Gregory PC & Harper AM (1979a)
Effects of hemorrhagic hypotension on the cerebral circulation. 1. Cerebral blood flow and pial arteriolar calibre
Stroke, **10**, 711-718

MacKenzie ET, McGeorge AP, Graham DI, Fitch W, Edvinsson L & Harper AM (1979b)
Effects of oncreasing arteriolar pressure on cerebral blood flow in the baboon: influence of the sympathetic nervous system
Pflugers Archive, **378**, 189-195

MacKenzie ET, Strandgaard S, Graham DI, Fitch W, Edvinsson L & Harper AM (1976)
Effect of acutely induced hypertension in cats on pial arteriolar caliber, local cerebral blood flow and the blood-brain barrier
Circulation Research, **39**, 33-41

McNamara JO (1984)
Kindling: an animal model of complex partial epilepsy
Annals of Neurology, **16** (suppl), S75

Meldrum BS, Corsellis JAN (1984)
Epilepsy. In: Greenfields neuropathology, JAN Corsellis & LW Duchen , eds. pp 921-950
Wiley, New York

Meldrum BS & Nilsson B (1976
Cerebral blood flow and metabolic rate early and late in prolonged
epileptic seizures induced in rats by bicuculine
Brain, **99**, 523-542

Meyer JS, Gotoh F & Favale E (1965)
Cerebral metabolism during epileptic seizures in man
Electroencephalography and Clinical Neurophysiology, **21**, 10-22

Mohamed AA, Mendelow AD, Teasdale GM, Harper AM & McCulloch J (1985)
Effect of the calcium antagonist nimodipine on local cerebral blood flow and
metabolic coupling
Journal of Cerebral Blood Flow and Metabolism, **5**, 26-33

Moore SC, Mueller SP (1986)
Inversion of the 3D Radon transform for a mutidetector, point focussed SPECT brain scanner
Physics in Medicine and Biology, **31**, 207-221

Mosier JM, White P, Grant P, Fisher JE & Taylor R (1957)
Cerebraoautonomic and myographic changes accompanying induced seizures
Neurology, **7**, 204-210

Nakai M, Iadecola C, Ruggerio DA, Tucker LW & Reis DJ (1983)
Electrical stimulation of of cerebellar fastigial nucleus increases cerebrocortical blood flow without change in local metabolism: Evidence for an intrinsic system in brain for primary vasodilatation
Brain Research, **260**, 35-49

Neirinckx RD, Burke FJ, Harrison RC, Forster AM, Andersen AR, Lassen NA (1988)
The retention mechanism of Technetium-(99m-HMPAO: Intracellular Reaction with Glutathione
Journal of Cerebral Blood Flow and Metabolism, **8** (Suppl 1), S4-12

Neirinckx, RD, Canning, LR, Piper, IM, Nowotnik, DP, Pickett, RD, Holmes, RA, Volkert, WA, Forster, AM, Weisner, PS, Marriott, JA & Chaplin, SR (1987)
Technetium 99m d,l-HM-PAO: a new radiopharmaceutical for SPECT imaging of regional cerebral blood perfusion
Journal of Nuclear Medicine, **28**, 191-202

Nelson KB & Ellenberg JH (1976)
Predictors of epilepsy in children who have experienced febrile seizures
New England Journal of Medicine, **295**, 1029-1033

Newton MR, Bercovik SF, Austin MC, Rowe CC, McKay WJ & Bladin PF (1992)
Postictal switch in blood flow distribution and temporal lobe seizures
Journal of Neurology Neurosurgery and Psychiatry, **55**, 891-894

Noebels JL (1984)
Isolating single genes of the inherited epilepsies
Annals of Neurology, **16** (suppl), S18-21

Norman RM (1964)
The neuropathology of status epilepticus
Medicine Science and Law, **4**, 46-51

Ochs RF, Gloor P, Tyler JL, Wolfson T, Worsley K, Andermann F, Diksic M, Meyer E & Evans A (1987)
Effect of generalised spike and wave discharge on glucose metabolism measured by positron emission tomography
Annals of Neurology, **21**, 458-464

Pearce WJ, Screming OU, Sonneschein RR & Rubinstien EH (1981)
The electroencephalogram, blood flow, and oxygen uptake in rabbit cerebrum
Journal of Cerebral Blood Flow and Metabolism, **1**, 419-428

Penfield W (1933)
The evidence for a cerebral vascular mechanism in epilepsy
Annals of Internal Medicine, **7**, 303-310

Penfield W (1937)
The circulation of the epileptic brain
Research Publication of the Association for Nervous and Mental Diseases, **18**, 605-737

Penfield W, von Santha K & Cipriani A (1939)
Cerebral blood flow during induced epileptiform seizures in animals and man
Journal of Neurophysiology, **2**, 257-267

Plum F, Posner JB & Troy B (1968)
Cerebral metabolic and circulatory response to induced convulsions in animals
Archives of Neurology, **18**, 1-13

Podreka I, Lang W, Suess E, Wimberger D, Steiner M, Gradner W, Zeitlhofer J, Pelzl G, Mamoli B & Deecke L (1988)
Hexamethyl-propylene-amine-oxime (HMPAO) single photon emission computed tomography (SPECT) in epilepsy
Brain topography, **1**, 55-60

Posner JB, Plum F & Van Poznak A (1969)
Cerebral metabolism during electrically induced seizures in man
Archives of Neurology, **20**, 388-395

Prince DA & Wilder BJ (1967)
Control mechanisms in cortical epileptogenic foci, 'surround' inhibition.
Archives of Neurology, **16**, 194-202

Quesney LF (1986)
Clinical and EEG features of complex partial seizures of temporal lobe origin
Epilepsia, **27** (suppl 2), S27-S45

Radon, J (1917)
On the determination of functions and their integrals along certain manifolds
Sitzungberichte der Bayerische Akademie der Wissenshafte. Mathematische-physikalische Classe, **69**, 262-277

Rausch R, Walsh GO (1984)
Right hemisphere language dominance in right handed epileptic patients
Archives of Neurology, **41**, 1077-1080

Robitaille Y, Rasmussen T, Dubeau F, Tampieri D & Kemball K (1992)
Histopathology of nonneoplastic lesions in frontal lobe epilepsy
In:P Chauvel, AV Delgado Escueta, E Halgren, JournalBancaud, eds. Frontal lobe epilepsies and seizures. Advances in neurology Vol 57, pp499-513
New York, Raven

Rosenblum WI (1986)
Endothelial-dependent relaxation demonstrated in vivo in cerebral arterioles
Stroke, **17**, 494-497

Rowe CC, Berkovic SF, Austin M, McKay WJ & Bladin PF (1989a)
Postictal SPET in epilepsy
Lancet, **1**, 389-390

Rowe CC, Berkovic SF, Sia STB, Austin M, McKay WJ, Kalnins RM & Bladin PF (1989b)
Localisation of epileptic foci with postictal single photon emission computed tomography
Annals of Neurology, **26**, 660-668

Rowe CC, Berkovic SF, Austin MC, Saling M, Kalnins RM, McKay WJ & Bladin PF (1991a)
Visual and quantitative analysis of interictal SPECT with Tc99m HMPAO in temporal lobe epilepsy
Journal of Nuclear Medicine , **32**, 1688-1694

Rowe CC, Berkovic SF, Sia STB & Bladin PF (1991b)
Patterns of postictal blood flow in temporal lobe epilepsy: qualitative and quantitative findings
Neurology, **41**, 1096-1003

Roy CW & Sherrington CS (1890)
On the regulation of the blood supply of the brain
Journal of Physiology, **11**, 85-108

Rubanyi GM, Romero JC & Vanhoutte PM (1986)
Flow induced release of endothelium-derived relaxing factor
American Journal of Physiology, **250**, H1145-1149

Ryding E, Rosen I, Elmqvist D & Ingvar DH (1988)
SPECT measurements with 99Tc HMPAO in focal epilepsy
Journal of Cerebral Blood Flow and Metabolism, **8**, S95-S100

Sackellares JC, Siegel JG, Abou-Khalil BW, Hood TW, Gilman S, McKeever PE, Hichwa RD & Hutchins GD (1990)
Differences between lateral and mesial temporal metabolism interictally in epilepsy of mesial temporal origin
Neurology, **40**, 1420-1426

Sagar HJ & Oxbury JM (1987)
Hippocampal neuron loss in temporal lobe epilepsy: correlation with early childhood convulsions
Annals of Neurology, **22**, 334-340

Sakadura O, Kennedy C, Jehle J, Brown JD, Carbin GL & Sokoloff L (1978)
Measurement of local cerebral blood flow with iodo (14C) antipyrene
American Journal of Physiology, **234**, H59-H66

Sakai F, Meyer JS, Naritomi H & Hsu M-C (1978)
Regional cerebral blood flow and EEG in patients with epilepsy
Archives of Neurology, **35**, 648-657

Sanchez-Ferrer CF & Marin J (1990)
Endothelium-derived contractile factors
General Pharmacology, **21**, 589-613

Schmidt CF, Kety SS & Pennes HH (1945)
The gaseous metabolism of the brain of the monkey
American Journal of Physiology, **143**, 33-52

Schwartzkroin PA, Mutani R & Prince DA (1975)
Orthodromic and antidromic effects of a cortical epileptiform focus on ventrolateral nucleus of the cat
Journal of Neurophysiology, **38**, 795-811

Seylaz J, Hara H, Pinard E, Mraovich S, MacKenzie ET & Edvinsson L (1988)
Effect of stimulation of the sphenopalatine ganglion on cortical blood flow in the rat
Journal of Cerebral Blood Flow and Metabolism, **8**, 875-878

Sharp PF, Smith FW, Gemmel HG, Lyall HD, Evans NTS, Gvozdanovic D, Davidson J, Tyrell DA, Pickett RD, Neirinckx RD (1986)
[^{99m}Tc]-HM-PAO stereoisomers for imaging regional cerebral blood flow
Journal of Nuclear Medicine, **27**, 171-177

Shen W, Lee BI, Park HM, Siddiqui AR, Wellman HH, Worth RM & Markand OM (1990)
HIPDM-SPECT brain imaging in the presurgical evaluation of patients with intractable seizures
Journal of Nuclear Medicine , **31**, 1280-1284

Skinhoj E & Paulson OB (1969)
Carbon dioxide and cerebral circulatory control. Evidence of nonfocal site of action of carbon dioxide on cerebral circulation
Archives of Neurology, **20**, 249-252

Skinhoj E & Strandgaard S (1973)
Pathogenesis of hypertensive encephalopathy
Lancet, **1**, 461-462

Sloviter RS (1991)
Permanently altered hippocampal structure, excitability and inhibition after experimental status epilepticus in the rat: the 'dormant basket cell' hypothesis and its possible relevance to temporal lobe epilepsy
Hippocampus, **1**, 41-66

Sokoloff L & Kety SS (1960)
Regulation of cerebral circulation
Physiological Reviews, **40** (suppl 4), 38-44

Sommer W (1880)
Erkrankung des Ammonshorns als Actiologisches Moment der Epilepsie
Archiv für Psychiatrie und Nervenkrankenheiten, **10**, 631-675

Spencer SS, Williamson PD, Spencer DD & Matson RH (1987)
Human hippocampal seizure spread by depth and subdural recording the hippocampal commisure
Epilepsia, **28**, 479-489

Sperling B & Lassen NA (1993)
Hyperfixation of HMPAO in subacute ischaemic stroke leading to spuriously high estimates of cerebral blood flow by SPECT
Stroke, **24**, 193-194

Sperling MR, Gur RC, Alavi A, Gur RE, Resnick S, O'Connor MJ & Reivich M (1990)
Subcortical metabolic alterations in partial epilepsy
Epilepsia, **31**, 145-155

Sperling MR, Wilson G, Engel J, Babb TL, Phelps M & Bradley W (1986)
Magnetic resonance imaging in intractable partial epilepsy: correlative studies
Annals of Neurology, **20**, 57-62

Stefan H, Bauer J, Feistel H, Schulemann H, Neubauer U, Wenzel B, Wolff F, Neundorfer B & Huk WJ (1990)
Regional cerebral blood flow during focal seizures of temporal and fronto central onset
Annals of Neurology, **27**, 162-166

Stefan H, Pawlik G, Bocher-Schwartz HG, Biersack HJ, Burr W, Penin H & Heiss WD (1987)
Functional and morphological abnormalities in temporal lobe epilepsy: a comparison of interictal and ictal EEG, CT, MRI, SPECT and PET
Journal of Neurology, **234**, 377-384

Stoddart HF, Stoddart HA (1979)
A new development in single gamma transaxial tomography. Union Carbide focussed collimator scanner
IEEE Transactions on Nuclear Science, **26**, 2710-2712

Stone WE, Marshall C & Nims LF (1941)
Chemical changes in the brain produced by injury and by anoxia
American Journal of Physiology, **132**, 770

Swartz BE, Walsh GO, Delgado-Escueta AV & Zolo P (1991)
Surface ictal electroencephalographic patterns in frontal vs temporal lobe epilepsy
Canadian Journal of Neurological Sciences, **18**, 649-662

Tamura A, Graham, DI, McCulloch J & Teasedale GM (1981)
Focal cerebral ischemia in the rat: 1 Description of technique and early neuropathological consequences following middle cerebral artery occlusion.
Journal of Cerebral Blood Flow and Metabolism, **1**, 53-60

Tanaka S, Sako K, Tanaka T Nishihara I & Yonemasu Y (1990)
Uncoupling of local blood flow and metabolism in the hippocampal CA3 in kainic acid induced limbic seizures
Neuroscience, **36**, 339-348

Theodore WH, Bairamian D & Newmark ME (1986a)
The effect of phenytoin on human cerebral glucose metabolism
Journal of Cerebral Blood Flow and Metabolism, **6**, 315-320

Theodore WH, Brooks R, Margolin R, Patronas N, Sato S, Porter RJ, Mansi L Bairamian D & DiChiro G (1985)
Positron emission tomography in generalised seizures
Neurology, **35**, 684-690

Theodore WH, Brooks R, Susumu S, Patronas N, Margolin R, DiChiro G & Porter RJ (1984)
The role of positron emission tomography in the evaluation of seizure disorders
Annals of Neurology **15** (suppl), S176-S179

Theodore WH, DiChiro G & Margolin R (1986b)
Barbiturates reduce human cerebral glucose metabolism
Neurology, **36**, 60-64

Theodore WH, Dorwart RH, Holmes MD, Porter RJ & DiChiro G (1986)
Neuroimaging in refractory partial seizures. Comparison of PET, CT and MRI
Neurology, **36**, 750-759

Theodore WH, Fishbeinn D & Dubinsky R (1988)
Patterns of cerebral glucose metabolism in patients with partial seizures
Neurology, **38**, 1201-1206

Theodore WH, Holmes MD, Dorwart RH, Porter RJ, DiChiro G, Susumu S & Rose D (1986d)
Complex partial seizures: cerebral structure and cerebral function
Epilepsia, **27**, 576-582

Theodore WH, Ito B, Porter RG & Jacobs G (1987)
Carbamazepine and cerebral glucose metabolism
Neurology, **37** (suppl), 327

Theodore WH, Katz D, Kufta C, Sato S, Patronas N, Smothers P & Bromfield E (1990)
Pathology of temporal lobe foci: correlation with CT, MRI and PET
Neurology **40**, 797-803

Theodore WH, Newmark ME & Sato S (1983)
[18F]Fluorodeoxyglucose positron emission tomography in refractory complex partial seizures
Annals of Neurology **14**, 429-437

Touchon J, Valmier J & Baldy-Moulinier M (1983)
Regional cerebral blood flow in temporal lobe epilepsy: interictal studies
In Current problems in epilepsy, pp33-43. Eds, Baldy-Moulinier M, Ingvar DH, Meldrum BS
London:Libbey

Touchon J, Valmier J, Baldy Moulinier M & Cadilhac J (1986)
Regional cerebral blood flow during interictal state: differences between temporal lobe epilepsy and primary generalised epilepsy
European Neurology **25**, 43-52

Uddman R & Edvinsson L (1989)
Neuropeptides in the cerebral circulation Cerebrovasc
Brain Metabolism Reviews, **1**, 230-252

Uren RF, Magistretti PL, Royal HD, Parker JA, Front D, Hill TC, Holman BL, Jones AG & Kolodny GM (1983)
Single photon emission computed tomography. A method of measuring cerebral. blood flow in threee dimensions (preliminary results in epilepsy and stroke)
Medical Journal of Australia, **1**, 411-413

Valmier J, Touchon J & Baldy Moulinier M (1989)
Interictal regional cerebral blood flow during non specific activation test in partial epilepsy
Journal of Neurology Neurosurgery and Psychiatry, **52**, 364-371

Valmier J, Touchon J & Blaylac JP (1990)
Initiation of carbamazepine therapy in partial epilepsy: a regional blood flow study
Epilepsy Research ,**5**, 229-234

Valmier J, Touchon J, Daures P, Zanca M & Baldy Moulinier M (1987)
Correlations between cerebral blood flow variations and clinical parameters in temporal lobe epilepsy: an interictal study
Journal of Neurology Neurosurgery and Psychiatry, **50**, 1306-1311

Van Hoesen GW (1982)
The parahippocampal gyrus: new observations regarding its connections in the monkey
Trends in Neuroscience, **5**, 345-350

Van Hoesen GW, Rosene DC & Mesulam MM (1979)
Subicular input from temporal cortex in the rhesus monkey
Science, **205**, 608-610

Walters BB, Gillespie SA & Moskowitz MA (1986)
Cerebrovascular projections from the sphenopalatine and otic ganglia to the middle cerebral artery of the rat
Stroke, **17**, 488-494

Wang W, Paulson OB & Lassen NA (1992)
Is autoregulation of cerebral blood flow in rats influenced by nitro-L-arginine, a blocker of the synthesis of nitric oxide
Acta Physiologica Scandinavica, **145**, 297-298

Wei EP, Kontos HA & Said SI (1980)
Mechanisms of action of vasoactive intestinal polypeptide on cerebral arteries
American Journal of Physiology, **239**, H765-768

Wei EP & Kontos HA (1984)
Increased venous pressure causes myogenic constriction of cerebral arterioles during local hyperoxia
Circulation Research, **55**, 249-252

White PT, Grant P, Mosier G & Craig A (1961)
Changes in cerebral dynamics associated with seizures
Neurology **11**, 354-361

Wieser HG (1983)
Electroclinical features of the psychomotor seizure
Gustav Fischer-Butterworths, Stuttgart-London

Williams ED (1985)
An introduction to emission computed tomography
Report No 44, The Institute of Physical Sciences in Medicine, London

Williams JL, Shea M, Furlan AJ, Little JR & Jones SC (1991)
Importance of freezing time when iodoantipyrene is used for measurement of cerebral blood flow
American Journal of Physiology, **261**, H252-H256

Williamson PD, Wieser HG & Delgado Escueta AV (1987)
Clinical characteristics of partial seizures. In: Engel J, ed. Surgical treatment of the epilepsies pp 101-120.
New York: Raven Press

Woods SJ, Hegeman IM, Zubal IG, Krystal JH, Koster K, Smith EO, Heninger GR & Hoffer PB (1991)
Visual stimulation increases Technetium-99m-HMPAO distribution in human visual cortex
Journal of Nuclear Medicine , **32**, 210-215

Yamamoto YL, Ochs R & Gloor P (1983)
Patterns of rCBF and focal energy metabolic changes in relation to electroencephalographic abnormality in the interictal phase of partial epilepsy
In: Baldy Moulinier M, Ingvar DH, Meldrum BS, eds. Cuirrent problems in epilepsy, Vol 1 pp51-62
London: John Libbey

Yonekura Y, Nishizawa S, Mukai T, Fujita T, Fukuyama H, Ishikawa M, Kikuchi H, Konishi J, Andersen AR & Lassen NA (1988)
SPECT with 99m Tc HMPAO compared with regional cerebral blood flow measured by PET: effects of linearisation
Journal of Cerebral Blood Flow and Metabolism, **8**, S82-S89